US 20240321457A1

(19) **United States**

(12) **Patent Application Publication** (10) **Pub. No.: US 2024/0321457 A1**

KROGAN (43) **Pub. Date: Sep. 26, 2024**

(54) **SYSTEMS FOR AND METHODS OF TREATMENT SELECTION**

(71) Applicant: **THE REGENTS OF THE UNIVERSITY OF CALIFORNIA**, Oakland, CA (US)

(72) Inventor: **Nevan J. KROGAN**, San Francisco, CA (US)

(21) Appl. No.: **18/032,153**

(22) PCT Filed: **Oct. 14, 2021**

(86) PCT No.: **PCT/US21/55100**

§ 371 (c)(1),
(2) Date: **Apr. 14, 2023**

Related U.S. Application Data

(60) Provisional application No. 63/091,924, filed on Oct. 14, 2020.

Publication Classification

(51) **Int. Cl.**

G16H 50/30	(2006.01)
G01N 33/574	(2006.01)
G01N 33/68	(2006.01)
G16H 10/20	(2006.01)
G16H 10/40	(2006.01)
G16H 20/10	(2006.01)

(52) **U.S. Cl.**

CPC ***G16H 50/30*** (2018.01); ***G01N 33/57484*** (2013.01); ***G01N 33/6848*** (2013.01); ***G16H 10/20*** (2018.01); ***G16H 10/40*** (2018.01); ***G16H 20/10*** (2018.01)

(57) **ABSTRACT**

The disclosure relates to a system comprising software that identifies drug targets and predicts responsiveness of cancer subjects to certain disease modifying drugs. Embodiments of the disclosure include methods comprising calculating a differential interaction score (DIS), correlating the DIS with the likelihood that a dysfunctional protein-protein interaction is the causal agent of a hyperproliferative disorder, identifying a drug target based on the causal agent, evaluating a therapeutic specific to the drug target, thereby restoring and/or alleviating dysfunction within the protein network, identifying a subject responsive to a hyperproliferative disorder treatment based upon the causal agent, and monitoring the subject's response to the hyperproliferative disorder treatment.

Specification includes a Sequence Listing.

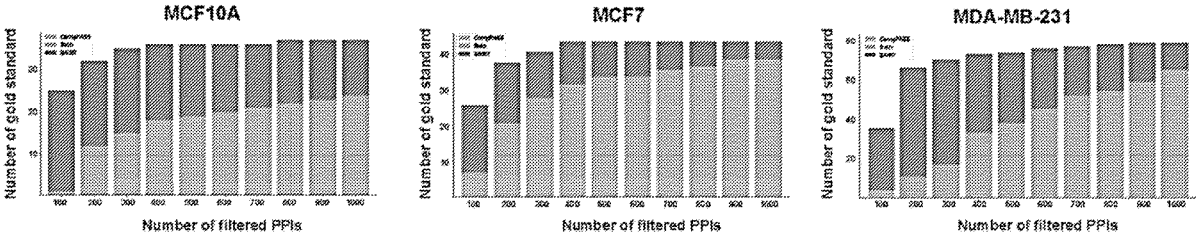

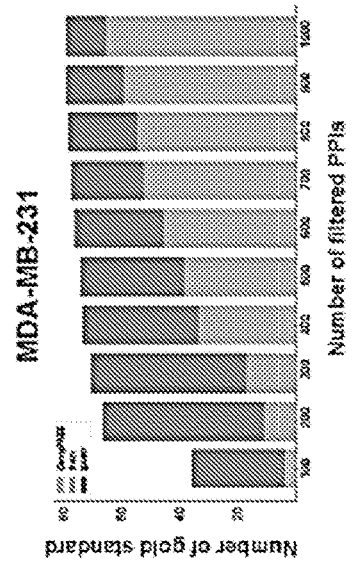
MDA-MB-231
Number of filtered PPIs
Number of gold standard

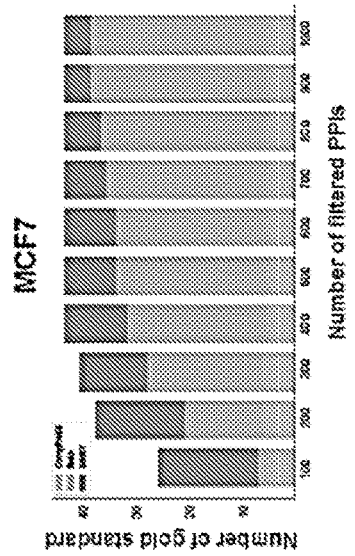
MCF7
Number of filtered PPIs
Number of gold standard

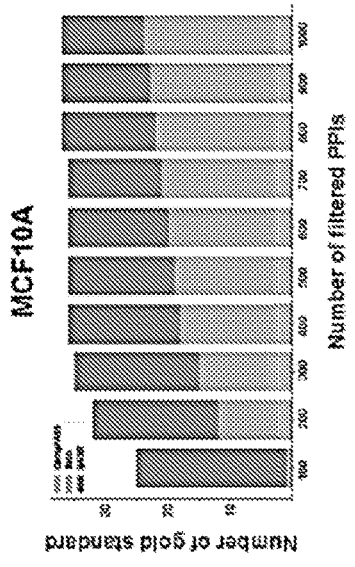
MCF10A
Number of filtered PPIs
Number of gold standard

FIG. 1A

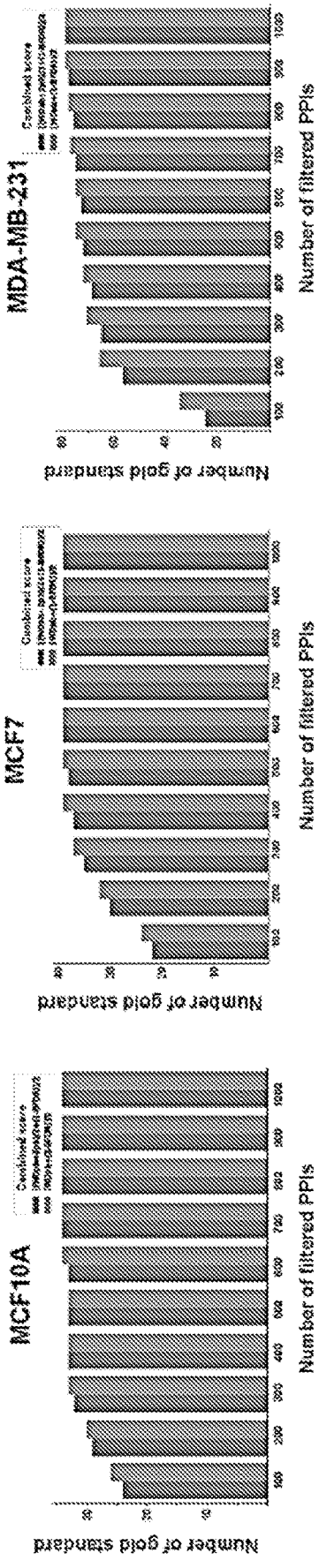
MCF10A
MCF7
MDA-MB-231
Number of filtered PPIs
Number of gold standard

FIG. 1B

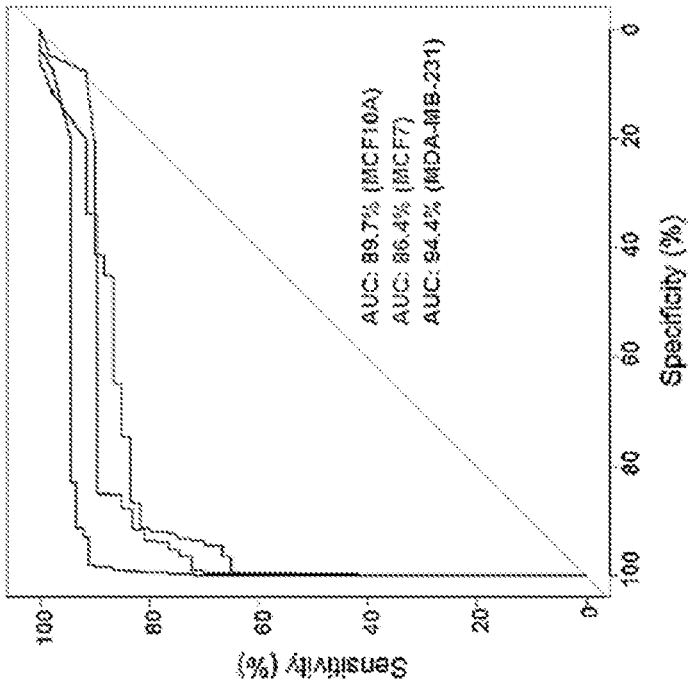
AUC: 89.7% (MCF10A)
AUC: 86.4% (MCF7)
AUC: 94.4% (MDA-MB-231)
Sensitivity (%)
Specificity (%)
0
20
40
60
80
100

FIG. 2A

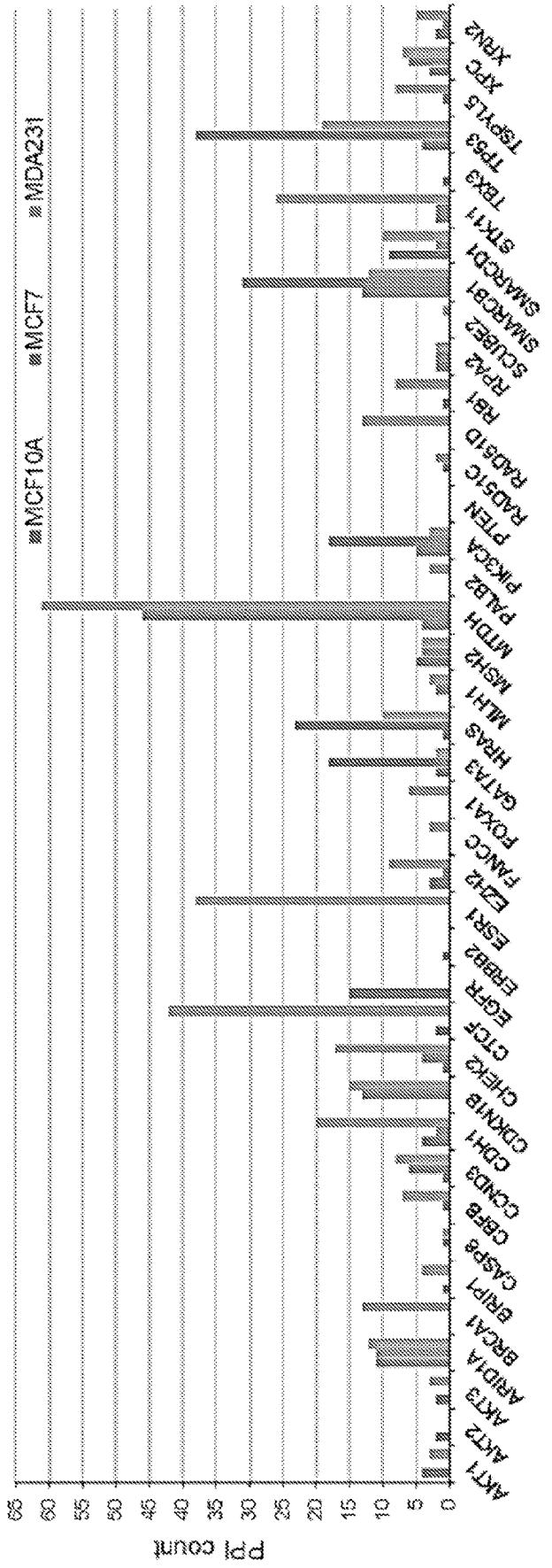
MCF10A
MCF7
MDA231
PPI count
0
5
10
15
20
25
30
35
40
45
50
55
60
65
AKT1
AKT2
AKT3
ARID1A
BRCA1
BRIP1
CASP8
CBFB
CCND3
CDH1
CDKN1B
CHEK2
CTCF
EGFR
ERBB2
ESR1
EZH2
FANCC
FOXA1
GATA3
HRAS
MLH1
MSH2
MTDH
PALB2
PIK3CA
PTEN
RAD51C
RAD51D
RB1
RPA2
SCUBE2
SMARCB1
SMARCD1
STK11
TBX3
TP53
TSPYL5
XPC
XRN2

FIG. 2B

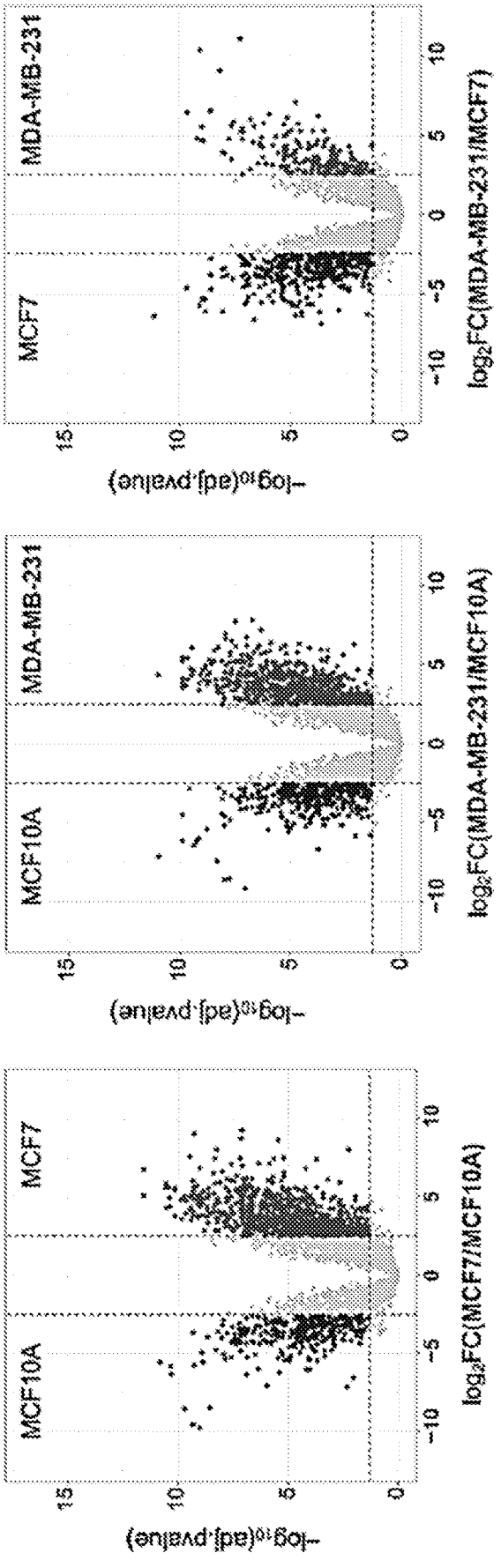
MDA-MB-231
MCF7
log2FC(MDA-MB-231/MCF7)
−log10(adj.pvalue)
MDA-MB-231
MCF10A
log2FC(MDA-MB-231/MCF10A)
−log10(adj.pvalue)
MCF7
MCF10A
log2FC(MCF7/MCF10A)
−log10(adj.pvalue)

FIG. 2C

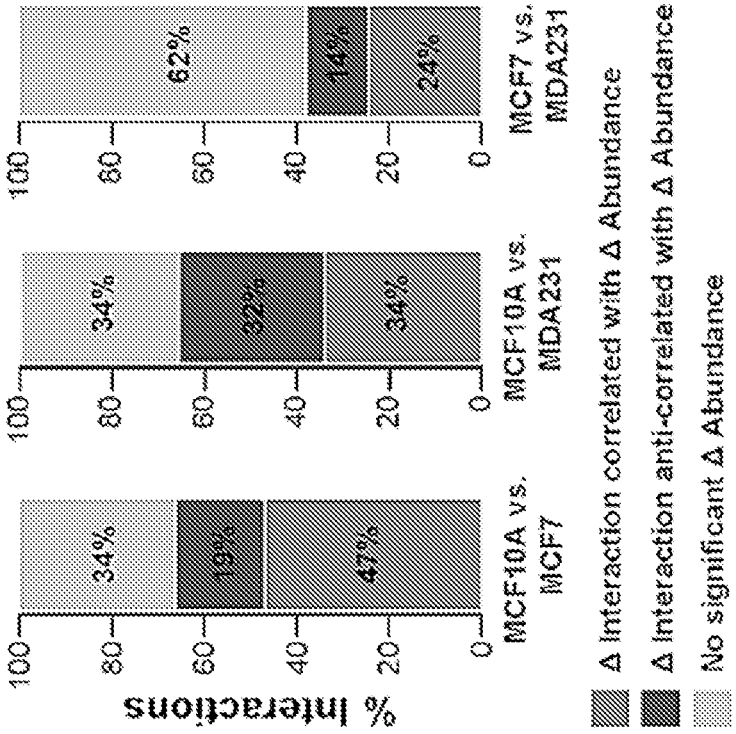
% Interactions
100
80
60
40
20
0
34%
19%
47%
MCF10A vs. MCF7
34%
32%
34%
MCF10A vs. MDA231
62%
14%
24%
MCF7 vs. MDA231
Δ Interaction correlated with Δ Abundance
Δ Interaction anti-correlated with Δ Abundance
No significant Δ Abundance

FIG. 2D

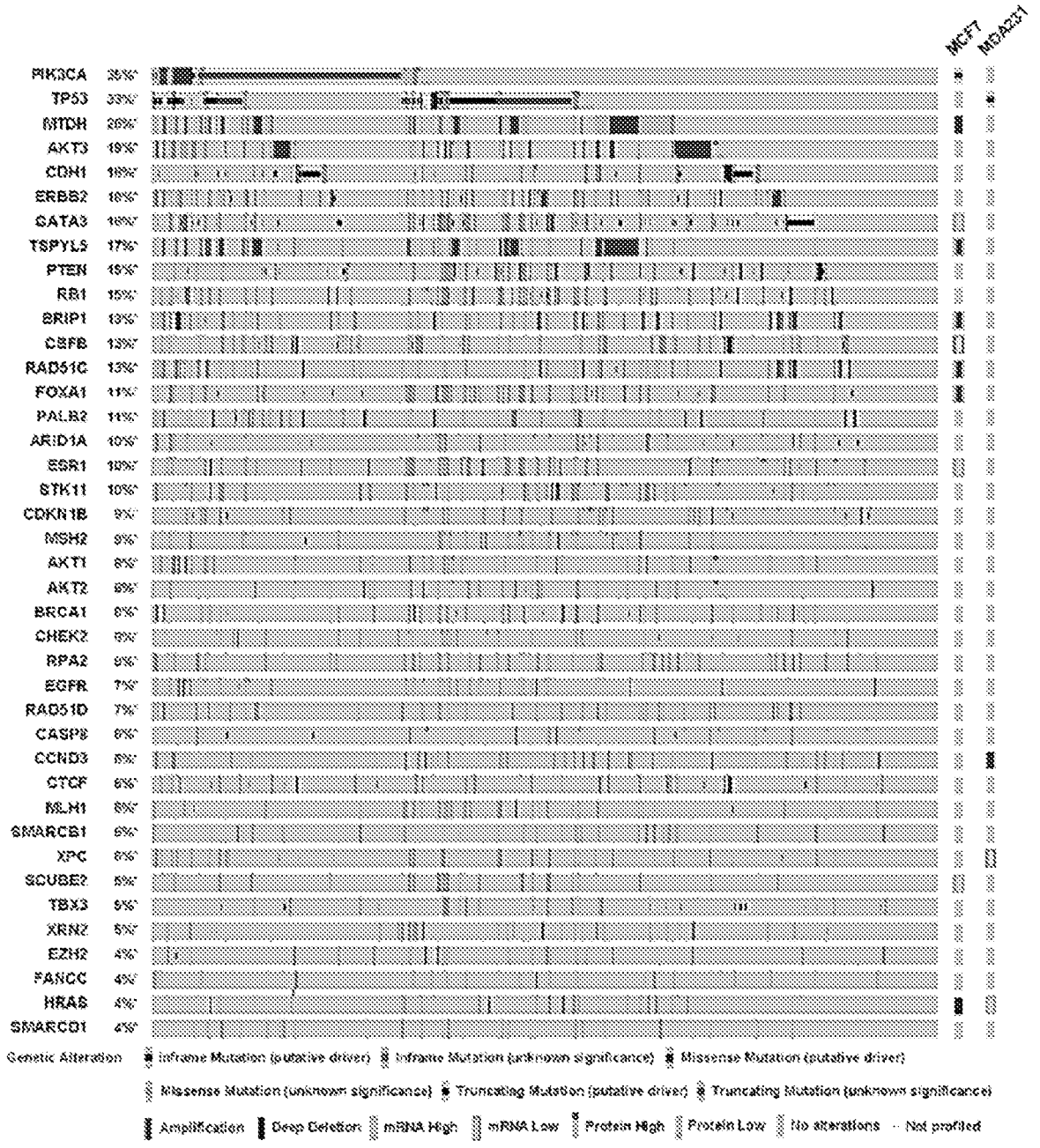
MCF7
MDA231
PIK3CA 35%
TP53 33%
MTDH 20%
AKT3 19%
CDH1 18%
ERBB2 18%
GATA3 18%
TSPYL5 17%
PTEN 16%
RB1 15%
BRIP1 13%
CBFB 13%
RAD51C 13%
FOXA1 11%
PALB2 11%
ARID1A 10%
ESR1 10%
STK11 10%
CDKN1B 9%
MSH2 9%
AKT1 8%
AKT2 8%
BRCA1 8%
CHEK2 8%
RPA2 8%
EGFR 7%
RAD51D 7%
CASP8 6%
CCND3 6%
CTCF 6%
MLH1 6%
SMARCB1 6%
XPC 6%
SCUBE2 5%
TBX3 5%
XRN2 5%
EZH2 4%
FANCC 4%
HRAS 4%
SMARCD1 4%
Genetic Alteration
Inframe Mutation (putative driver)
Inframe Mutation (unknown significance)
Missense Mutation (putative driver)
Missense Mutation (unknown significance)
Truncating Mutation (putative driver)
Truncating Mutation (unknown significance)
Amplification
Deep Deletion
mRNA High
mRNA Low
Protein High
Protein Low
No alterations
Not profiled

FIG. 3A

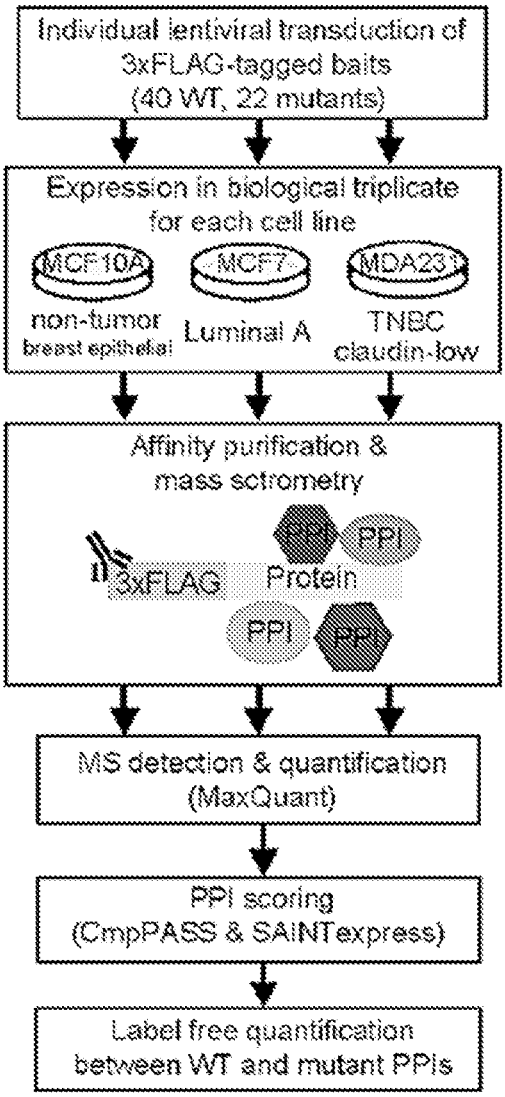
Individual lentiviral transduction of 3xFLAG-tagged baits (40 WT, 22 mutants)
Expression in biological triplicate for each cell line
MCF10A
MCF7
MDA231
non-tumor breast epithelial
Luminal A
TNBC claudin-low
Affinity purification & mass sctrometry
PPI
PPI
3xFLAG
Protein
PPI
PPI
MS detection & quantification (MaxQuant)
PPI scoring (CmpPASS & SAINTexpress)
Label free quantification between WT and mutant PPIs

FIG. 3B

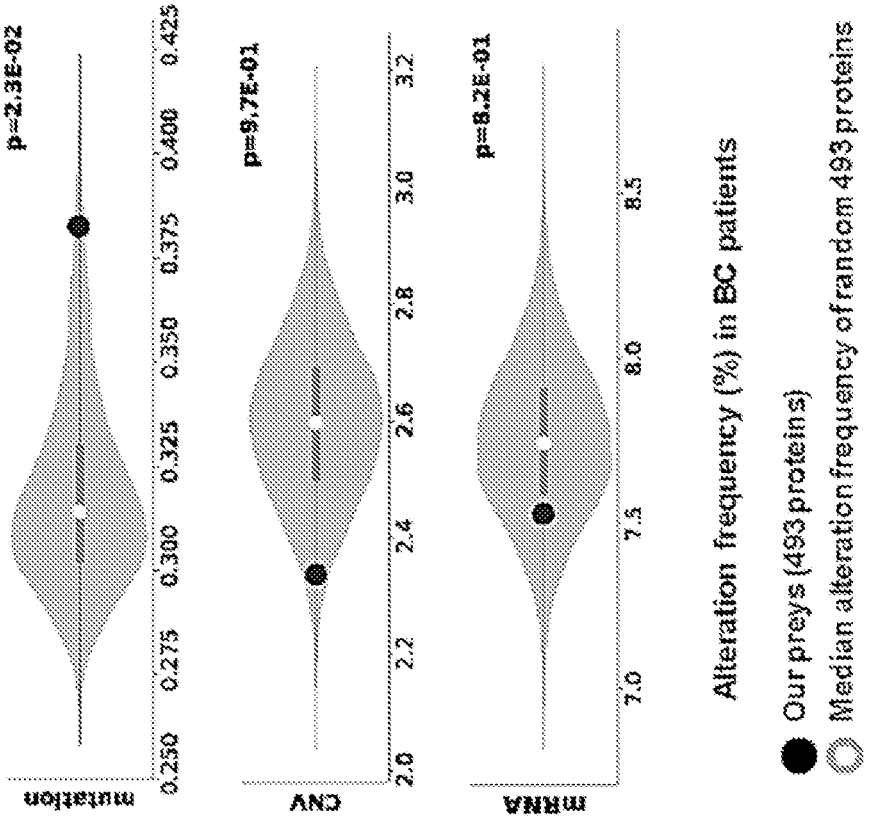
p=2.3E-02
p=9.7E-01
p=8.2E-01
mutation
CNV
mRNA
0.250
0.275
0.300
0.325
0.350
0.375
0.400
0.425
2.0
2.2
2.4
2.6
2.8
3.0
3.2
7.0
7.5
8.0
8.5
Alteration frequency (%) in BC patients
Our preys (493 proteins)
Median alteration frequency of random 493 proteins

FIG. 3D

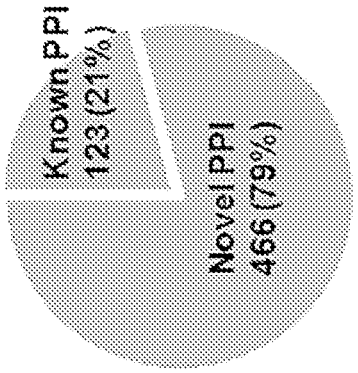
Known PPI
123 (21%)
Novel PPI
466 (79%)

FIG. 3C

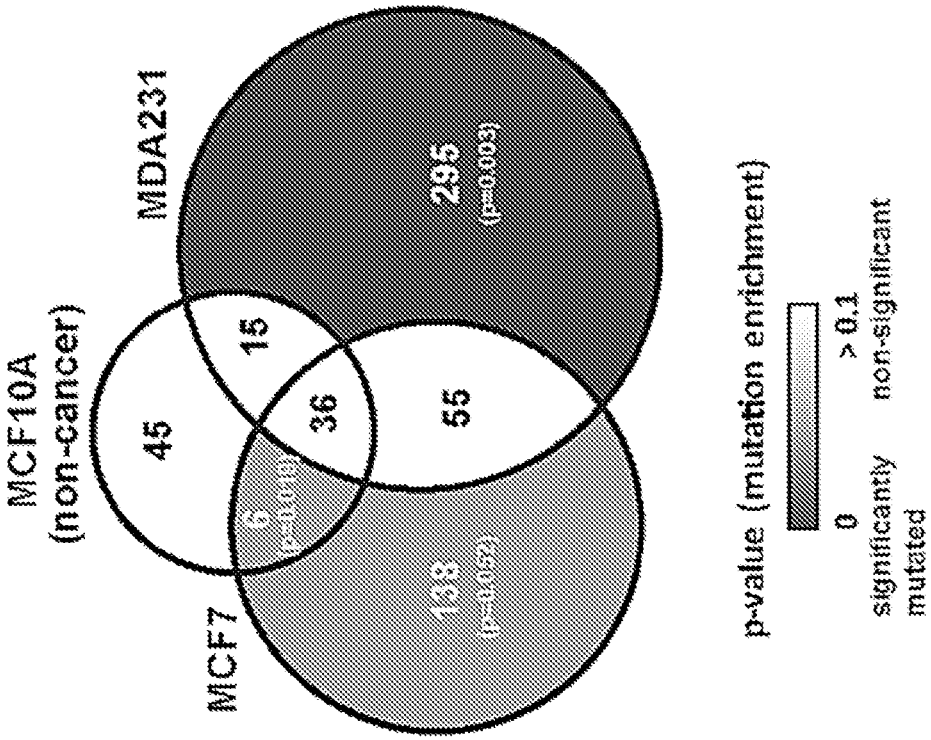
MCF10A
(non-cancer)
MDA231
MCF7
45
15
36
55
295
(p=0.003)
p-value (mutation enrichment)
0
significantly mutated
> 0.1
non-significant

FIG. 3E

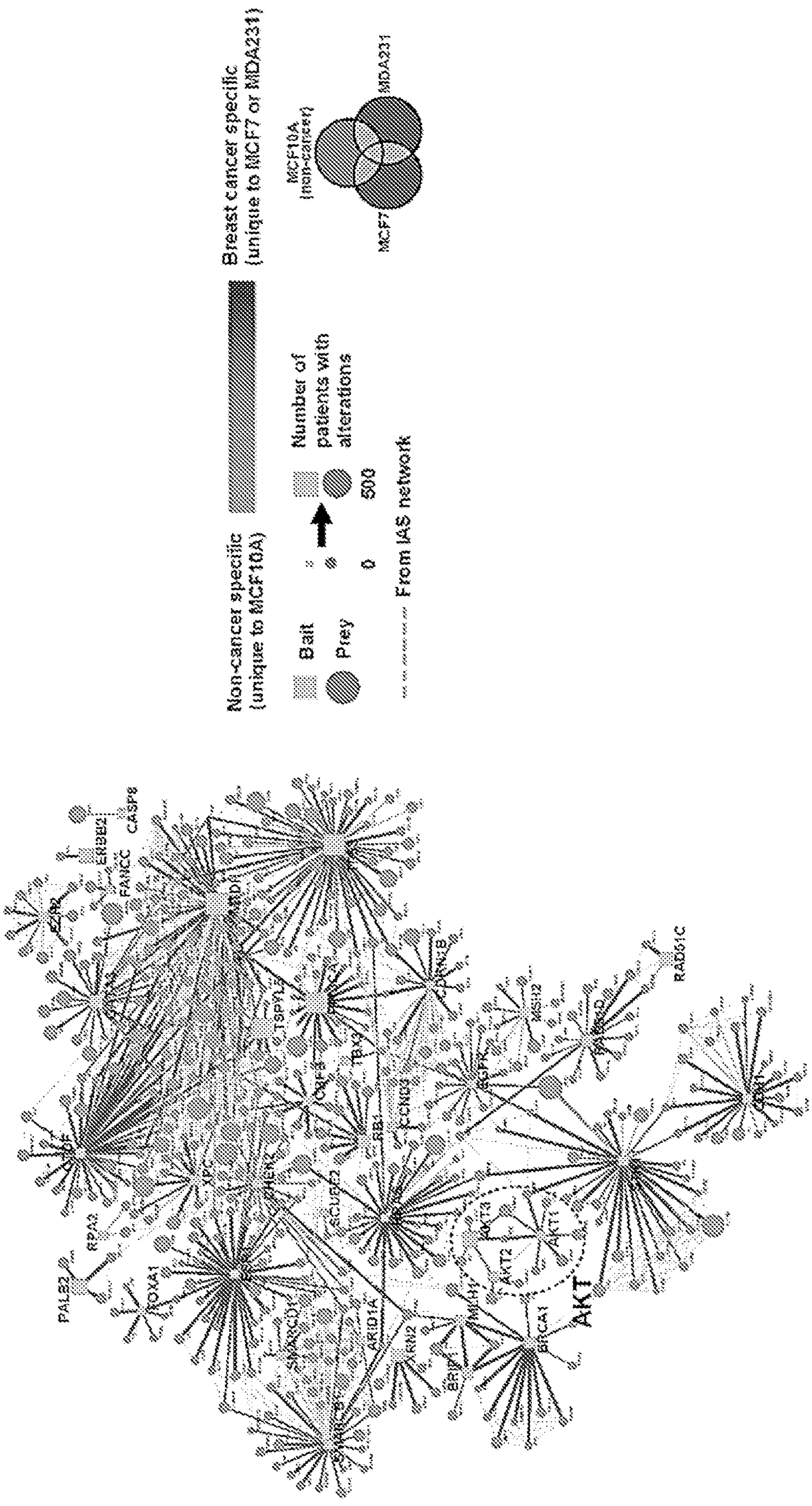

PALB2
RPA3
FOXA1
SMARCD1
ARID1A
SMARCB1
BRIP1
MLH1
BRCA1
AKT
AKT1
AKT2
AKT3
XPC
SCUBE2
RB1
CCND3
TBX3
TSPYL2
EZH2
ERBB2
FANCC
CASP8
CDKN1B
MSH2
RAD51D
RAD51C
Non-cancer specific
(unique to MCF10A)
Breast cancer specific
(unique to MCF7 or MDA231)
Bait
Prey
0
500
Number of
patients with
alterations
From IAS network
MCF10A
(non-cancer)
MCF7
MDA231

FIG. 4A

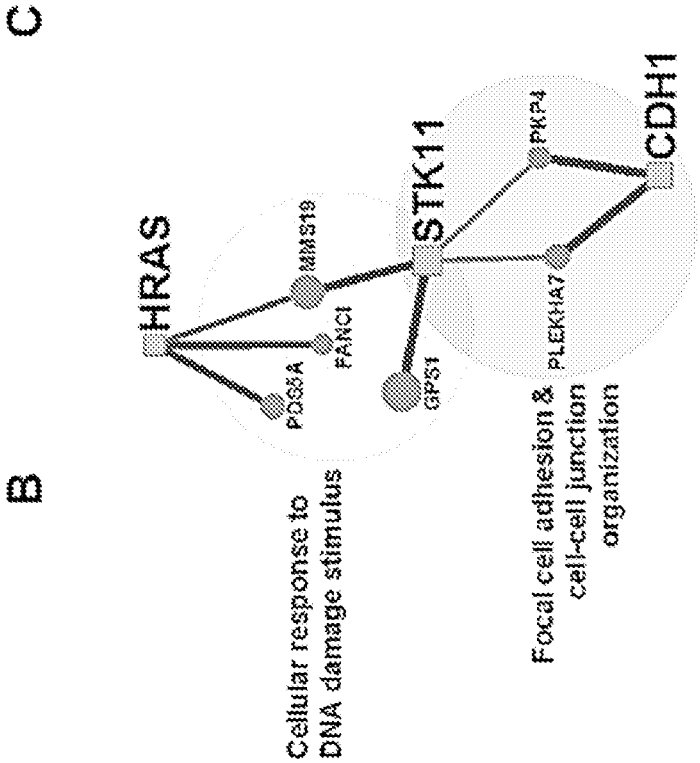
B
HRAS
PDE5A
FANCI
MMS19
STK11
GPS1
PKP4
PLEKHA7
CDH1
Cellular response to DNA damage stimulus
Focal cell adhesion & cell-cell junction organization

FIG. 4B

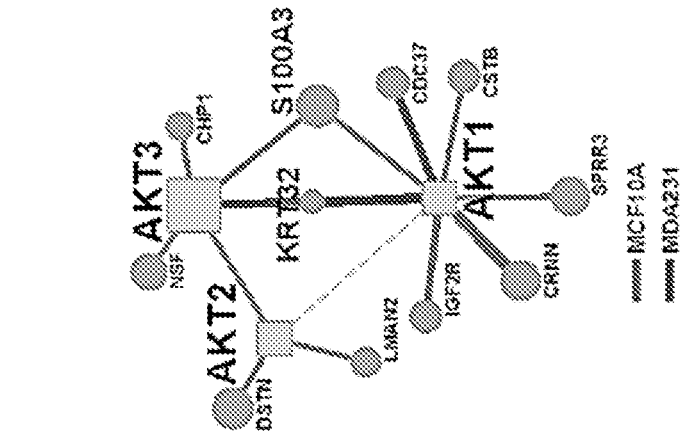
C
AKT3
NSF
CHP1
AKT2
DSTN
S100A3
KRT32
LMAN2
CDC37
IGF2R
AKT1
CSTB
SPRR3
CRNN
MCF10A
MDA231

FIG. 4C

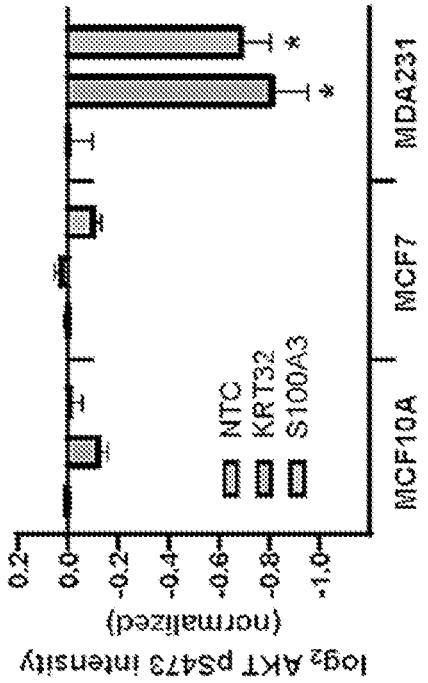
log2 AKT pS473 intensity
(normalized)
0.2
0.0
-0.2
-0.4
-0.6
-0.8
-1.0
NTC
KRT32
S100A3
*
*
MCF10A
MCF7
MDA231

FIG. 4D

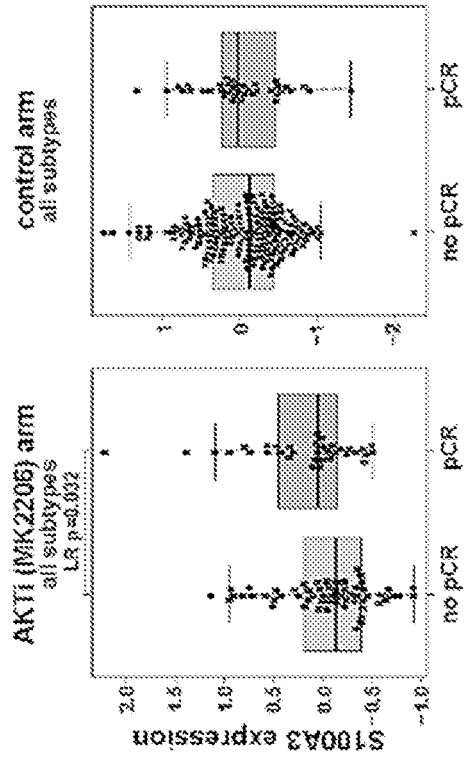
S100A3 expression
2.0
1.5
1.0
0.5
0.0
-0.5
-1.0
AKTi (MK2206) arm
all subtypes
LR p=0.032
no pCR
pCR
control arm
all subtypes
no pCR
pCR

FIG. 4E

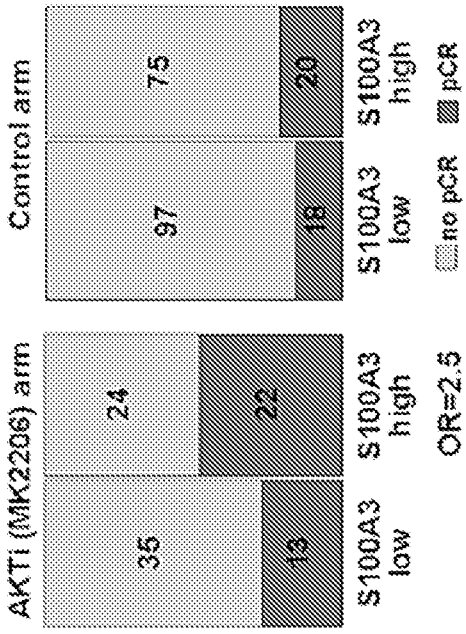
AKTi (MK2206) arm
Control arm
35
13
24
22
97
18
75
20
S100A3 low
S100A3 high
S100A3 low
S100A3 high
OR=2.5
no pCR
pCR

FIG. 4F

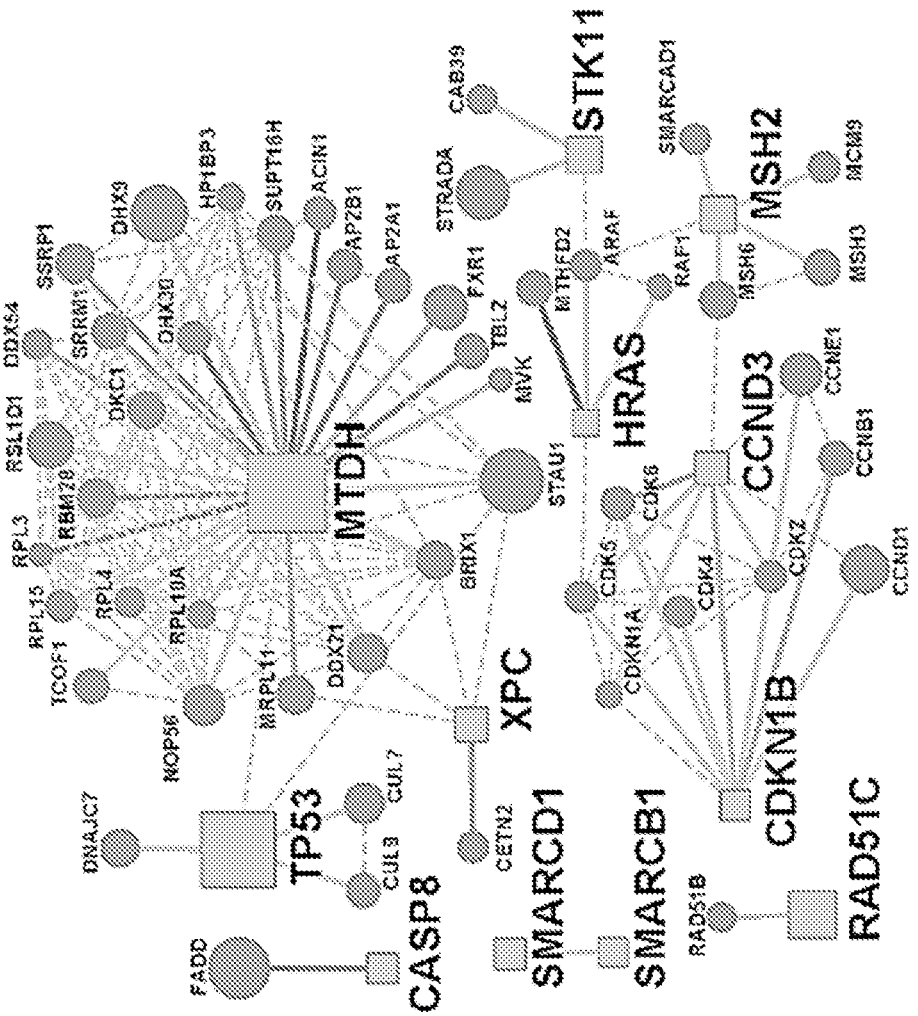
MTDH
TP53
CASP8
XPC
SMARCD1
SMARCB1
RAD51C
CDKN1B
CCND3
HRAS
STK11
MSH2
DDX54
SSRP1
DHX9
HP1BP3
SUPT16H
ACIN1
AP2B1
AP2A1
STRADA
CAB39
SMARCAD1
MCM9
MSH3
MSH6
RAF1
ARAF
MTMR2
FXR1
TBL2
MVK
STAU1
BRD1
DDX21
MRPL11
NOP56
RPL10A
RPL4
RPL15
TCOF1
RPL3
RBM28
RSL1D1
SRRM1
DKC1
DHX30
CUL3
CUL7
DNAJC7
FADD
CETN2
CDK6
CDK5
CDKN1A
CDK4
CDK2
CCNE1
CCNB1
CCND1
RAD51B

FIG. 4G

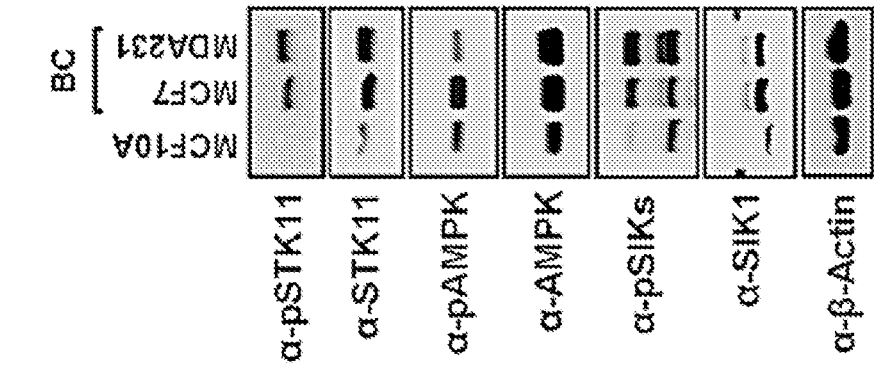
I
BC
MCF10A
MCF7
MDA231
α-pSTK11
α-STK11
α-pAMPK
α-AMPK
α-pSIKs
α-SIK1
α-β-Actin

FIG. 4I

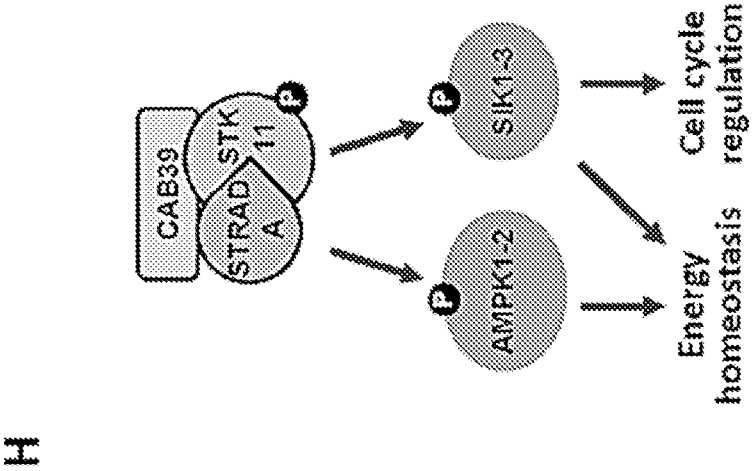
H
CAB39
STRAD A
STK 11
P
SIK1-3
AMPK1-2
Energy homeostasis
Cell cycle regulation

FIG. 4H

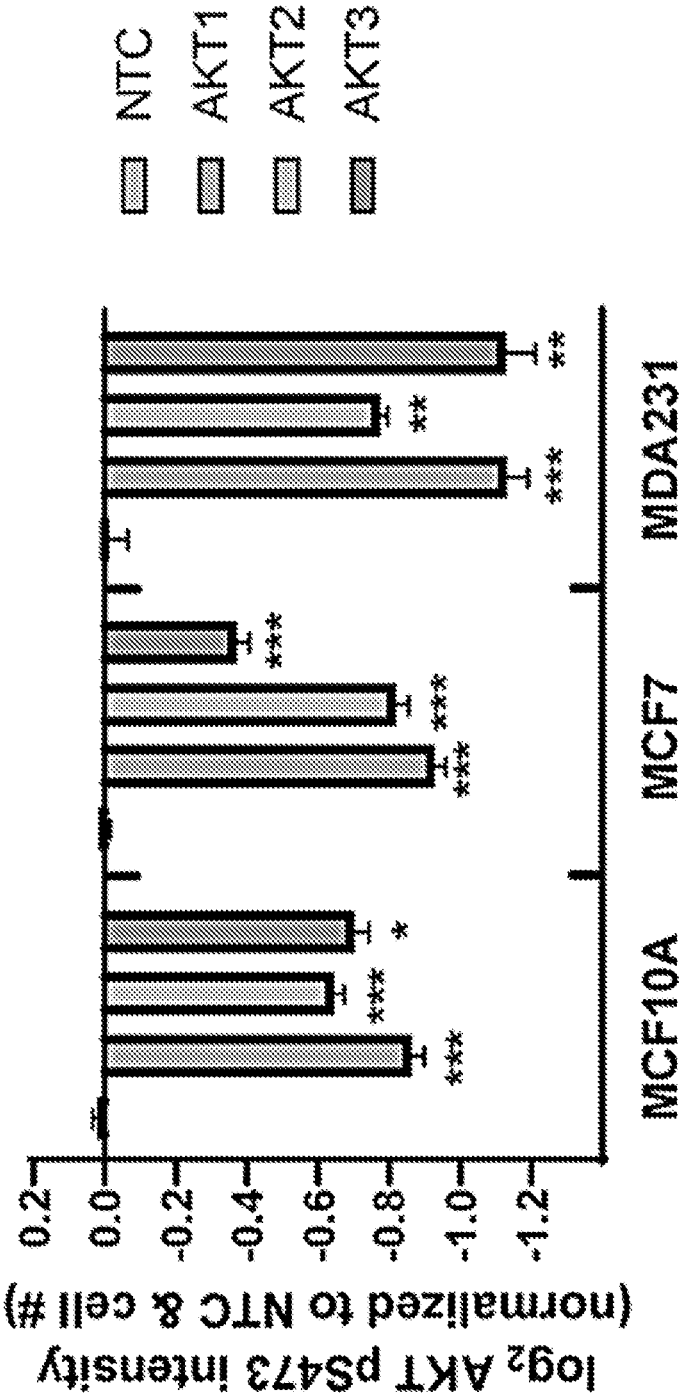
NTC
AKT1
AKT2
AKT3
MCF10A
MCF7
MDA231
0.2
0.0
-0.2
-0.4
-0.6
-0.8
-1.0
-1.2
log2 AKT pS473 intensity
(normalized to NTC & cell #)

FIG. 5

Protein	Mutations
AKT1	E17K
AKT3	E17K
BRCA1	I16A, C61G, R71G, Δexon11, S1655F, 5382insC, M1775R
BRIP1	A745T
CDH1	E243K
CHEK2	1100delC, K373E
HRAS	G12D
MTDH	A78S
PALB2	E837K
PIK3CA	E545K, M1043V, H1047R
TP53	R175H, R248W R273H

FIG. 6A

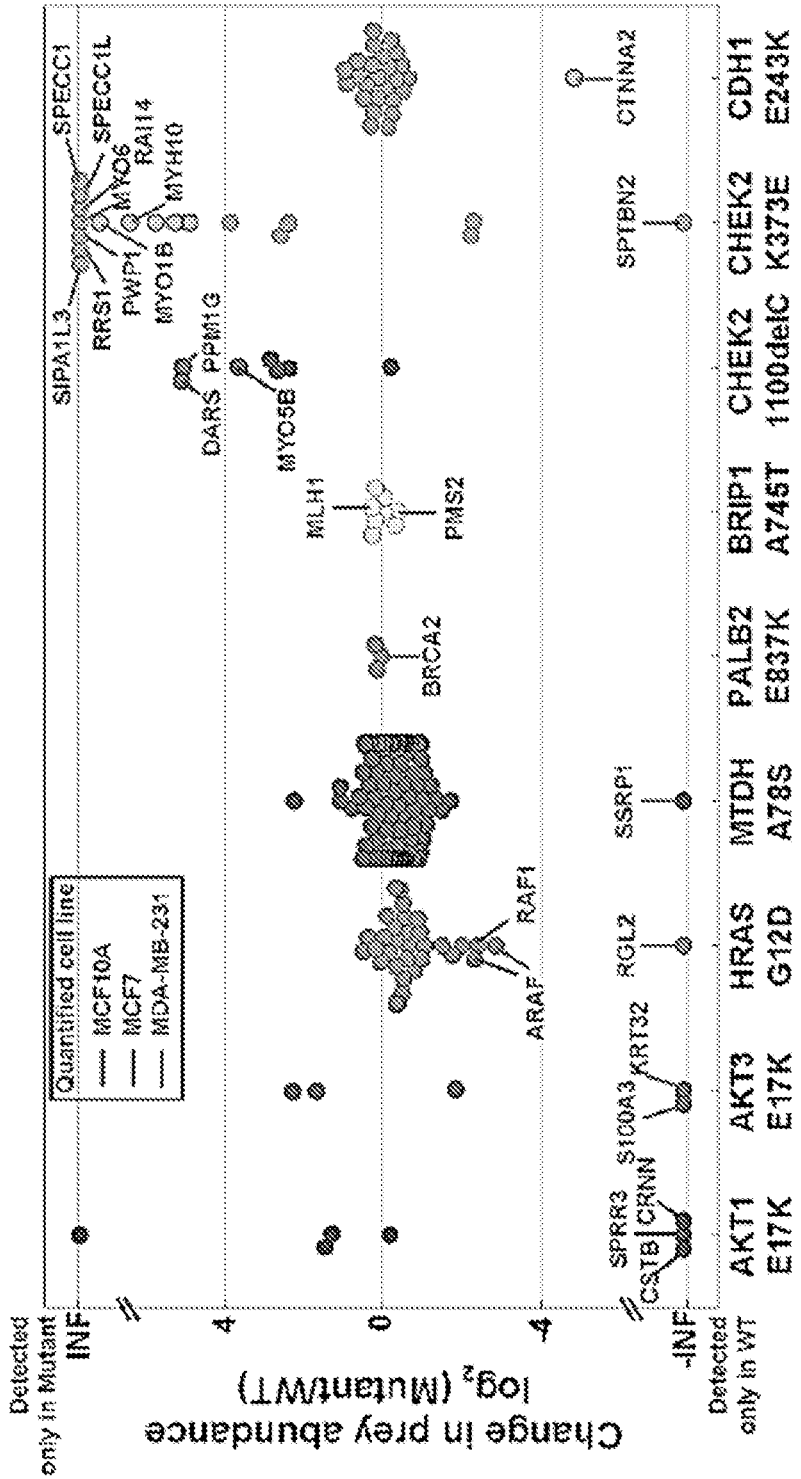
Change in prey abundance
log2 (Mutant/WT)
Detected only in Mutant
Detected only in WT
INF
4
0
-4
-INF
Quantified cell line
MCF10A
MCF7
MDA-MB-231
AKT1 E17K
AKT3 E17K
HRAS G12D
MTDH A78S
PALB2 E837K
BRIP1 A745T
CHEK2 1100delC
CHEK2 K373E
CDH1 E243K
SIPA1L3
SPECC1
SPECC1L
RRS1
MYO5
PWP1
RAI14
MYO1B
MYH10
DARS
PPM1G
MYO5B
MLH1
PMS2
BRCA2
RAF1
ARAF
RGL2
SSRP1
SPTBN2
CTNNA2
SPRR3
CSTB
CRNN
S100A3
KRT32

FIG. 6B

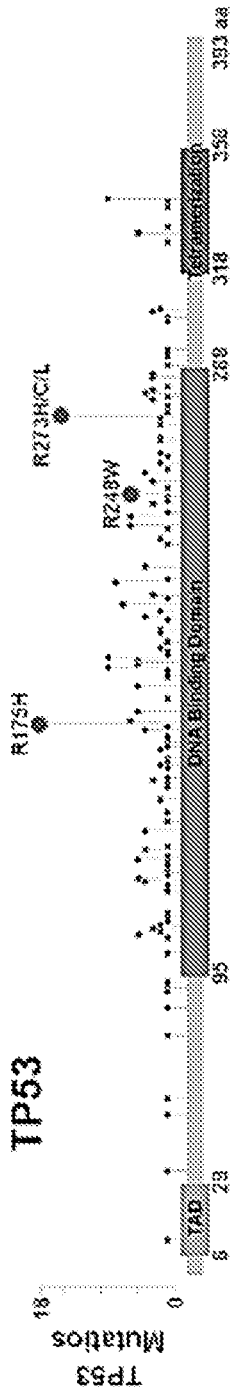
TP53
TP53 Mutations
18
0
TAD
8
23
95
DNA Binding Domain
269
318
Tetramerization
356
393 aa
R175H
R248W
R273H/C/L

FIG. 6C

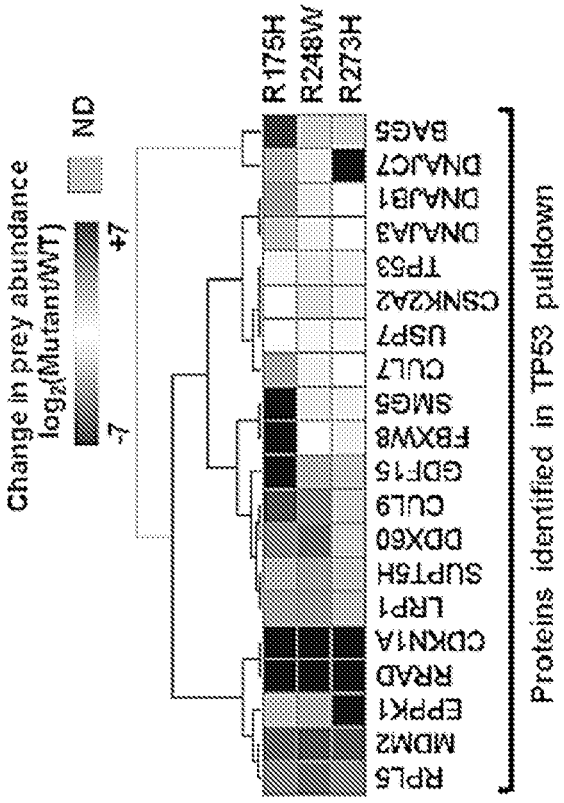
R175H
R248W
R273H
BAG5
DNAJC7
DNAJB1
DNAJA3
TP53
CSNK2A2
USP7
CUL7
SMG5
FBXW8
GDF15
CUL9
DDX60
SUPT5H
LRP1
CDKN1A
RRAD
EPPK1
MDM2
RPL5
Proteins identified in TP53 pulldown
Change in prey abundance
log2(Mutant/WT)
+7
-7
ND

FIG. 6D

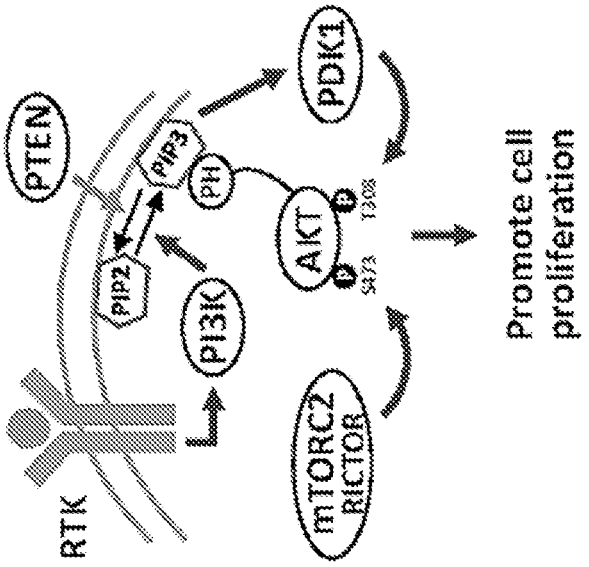
PTEN
PIP3
PH
PDK1
PIP2
PI3K
AKT
S473
T308
RTK
mTORC2
RICTOR
Promote cell proliferation

FIG. 6E

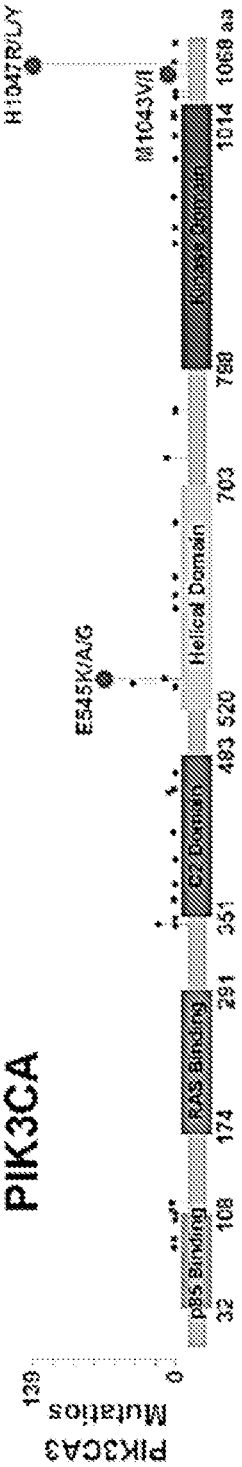
PIK3CA
PIK3CA3 Mutations
120
0
p85 binding
32
108
RAS Binding
174
291
C2 Domain
351
483
520
Helical Domain
703
788
1014
1068 aa
E545K/A/G
H1047R/L/Y
M1043V/I

FIG. 6F

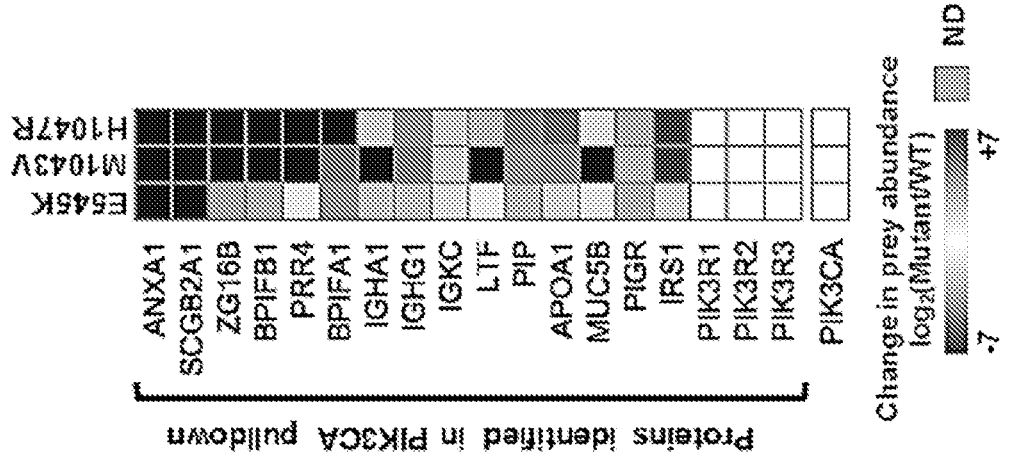
E545K
M1043V
H1047R
ANXA1
SCGB2A1
ZG16B
BPIFB1
PRR4
BPIFA1
IGHA1
IGHG1
IGKC
LTF
PIP
APOA1
MUC5B
PIGR
IRS1
PIK3R1
PIK3R2
PIK3R3
PIK3CA
Proteins identified in PIK3CA pulldown
Change in prey abundance
log2(Mutant/WT)
-7
+7
ND

FIG. 6G

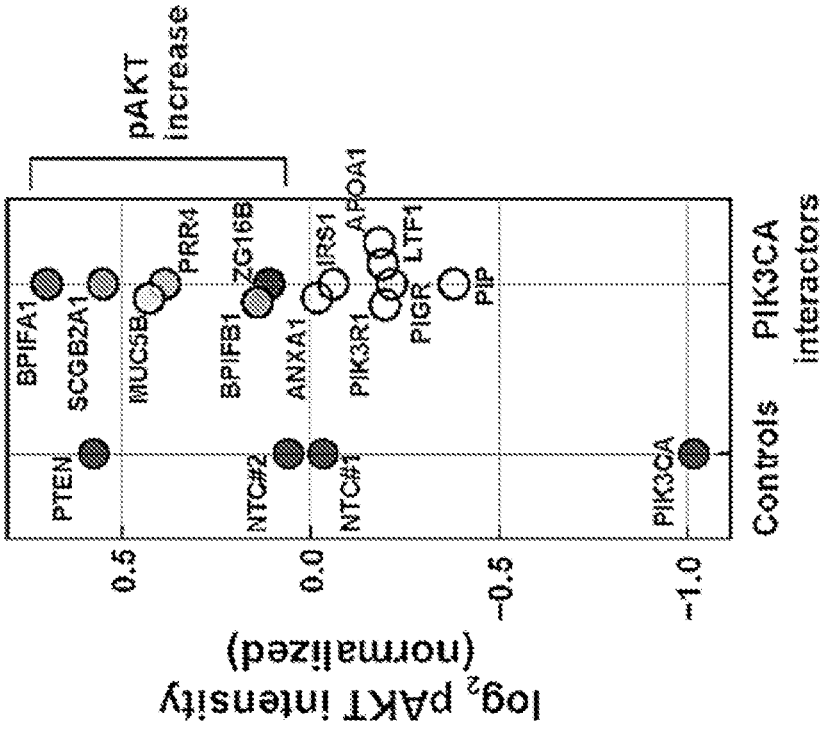
pAKT increase
log2 pAKT intensity (normalized)
0.5
0.0
−0.5
−1.0
PTEN
SCGB2A1
BPIFA1
MUC5B
PRR4
BPIFB1
ZG16B
NTC#2
ANXA1
NTC#1
IRS1
PIK3R1
APOA1
LTF1
PIGR
PIP
PIK3CA
Controls
PIK3CA interactors

FIG. 6H

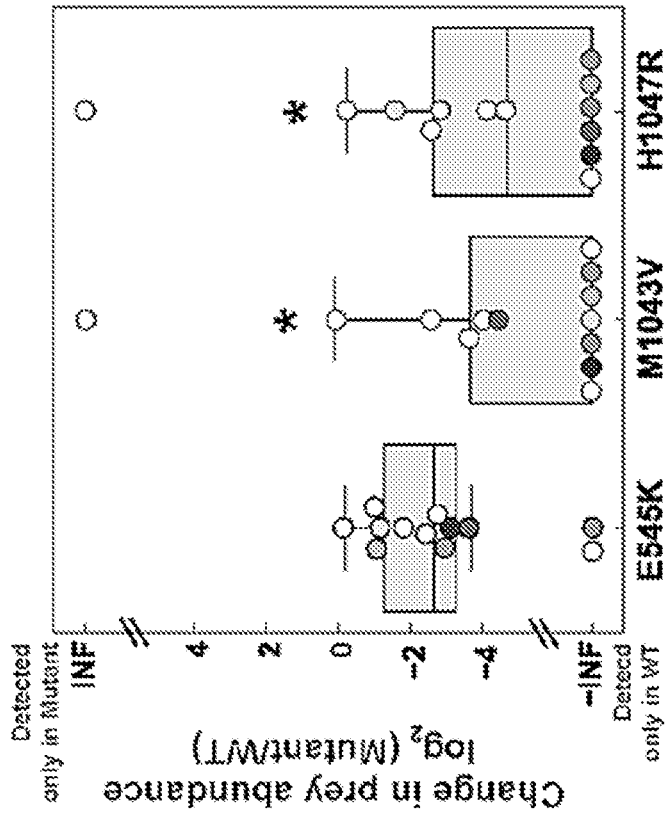
Change in prey abundance
log2 (Mutant/WT)
Detected only in Mutant
Detected only in WT
INF
4
2
0
-2
-4
-INF
E545K
M1043V
H1047R
*
*

FIG. 6I

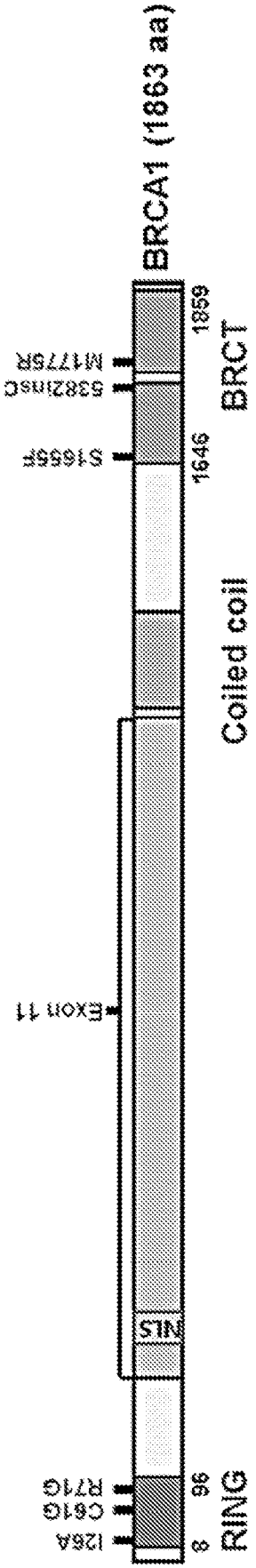
BRCA1 (1863 aa)
1859
BRCT
M1775R
5382insC
S1655F
1646
Coiled coil
Exon 11
NLS
96
R71G
C61G
I26A
8
RING

FIG. 7A

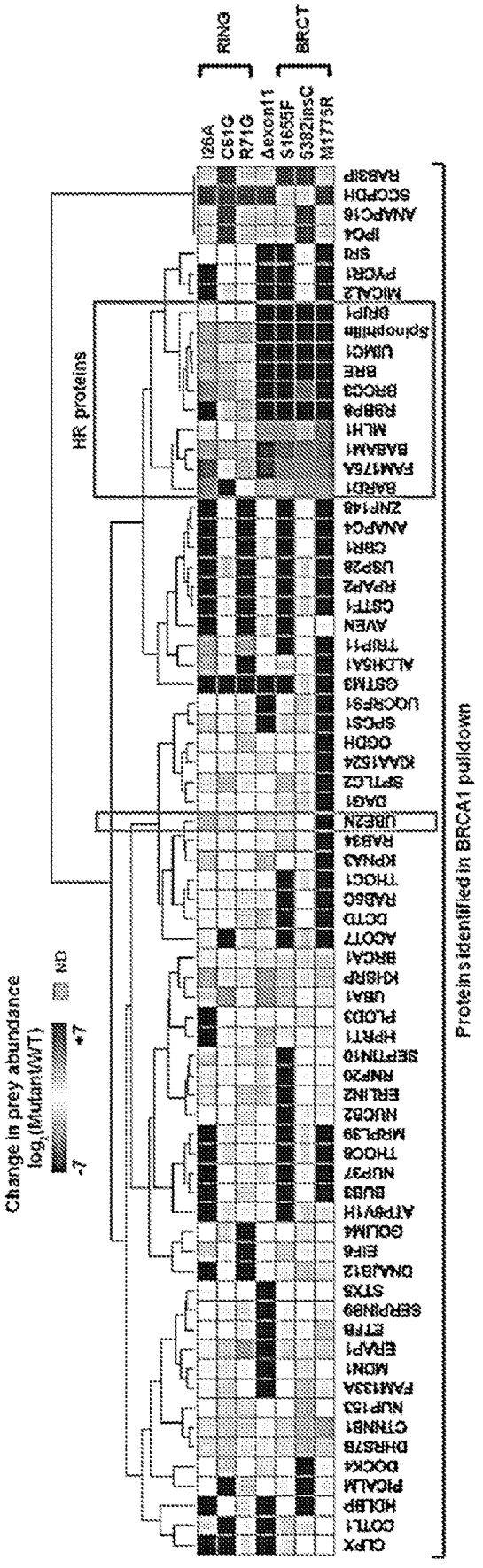
I26A
C61G
R71G
Δexon11
S1655F
S382insC
M1775R
RING
BRCT
HR proteins
Proteins identified in BRCA1 pulldown
Change in prey abundance
log2(Mutant/WT)
+7
-7
ND

FIG. 7B

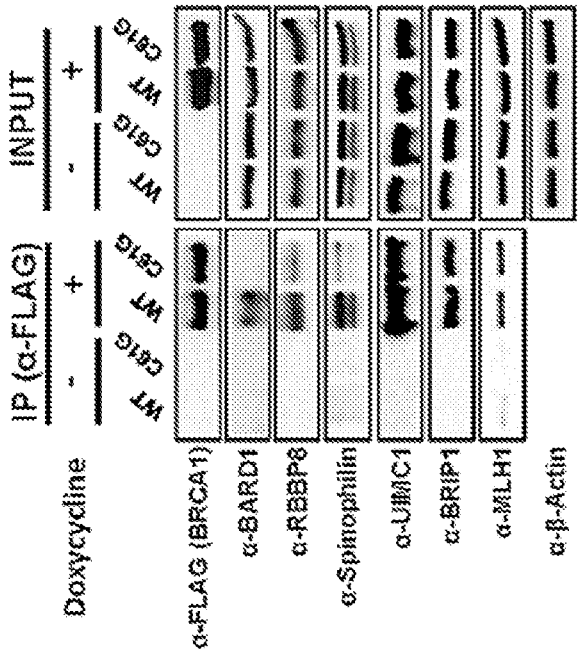
IP (α-FLAG)
INPUT
Doxycycline
-
+
-
+
WT
C61G
WT
C61G
WT
C61G
WT
C61G
α-FLAG (BRCA1)
α-BARD1
α-RBBP8
α-Spinophilin
α-UIMC1
α-BRIP1
α-MLH1
α-β-Actin

FIG. 7C

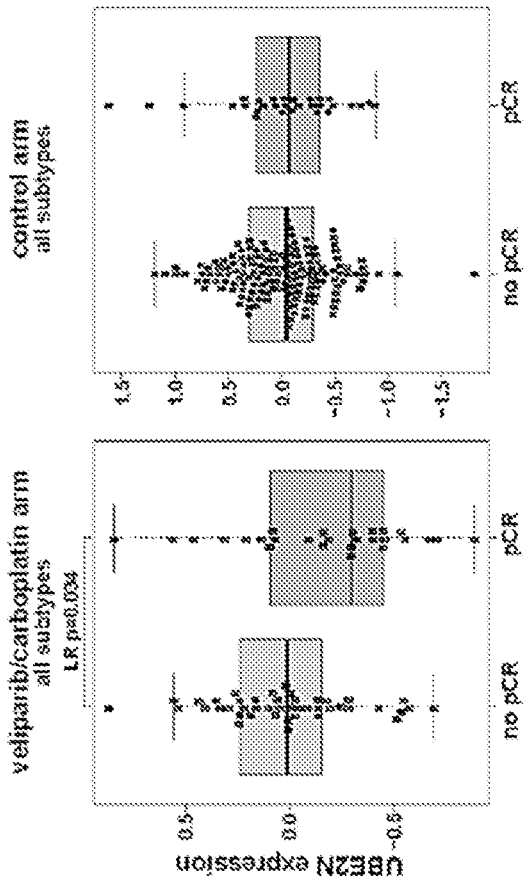
UBE2N expression
0.5
0.0
-0.5
veliparib/carboplatin arm
all subtypes
LR p=0.034
no pCR
pCR
control arm
all subtypes
1.5
1.0
0.5
0.0
-0.5
-1.0
-1.5
no pCR
pCR

FIG. 7D

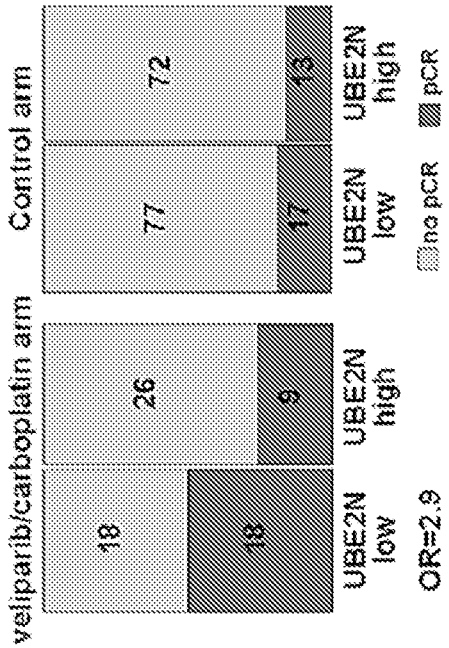
veliparib/carboplatin arm
Control arm
18
13
26
9
77
17
72
13
UBE2N low
UBE2N high
UBE2N low
UBE2N high
OR=2.9
no pCR
pCR

FIG. 7E

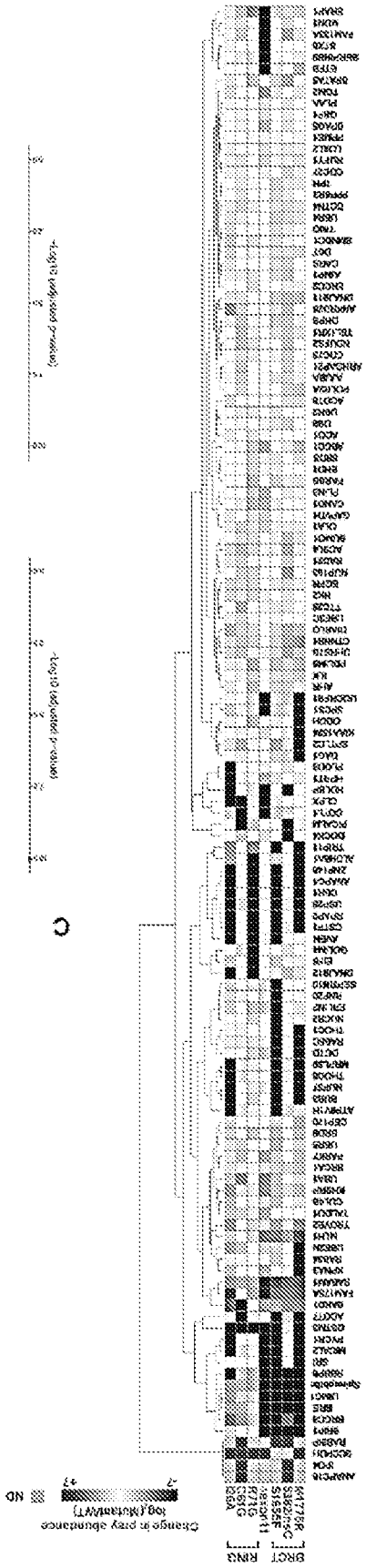
BRCT
RING
Change in prey abundance
log2(MutantMWT)
NS
-log10 adjusted p-value
-log10 adjusted p-value

FIG. 8A

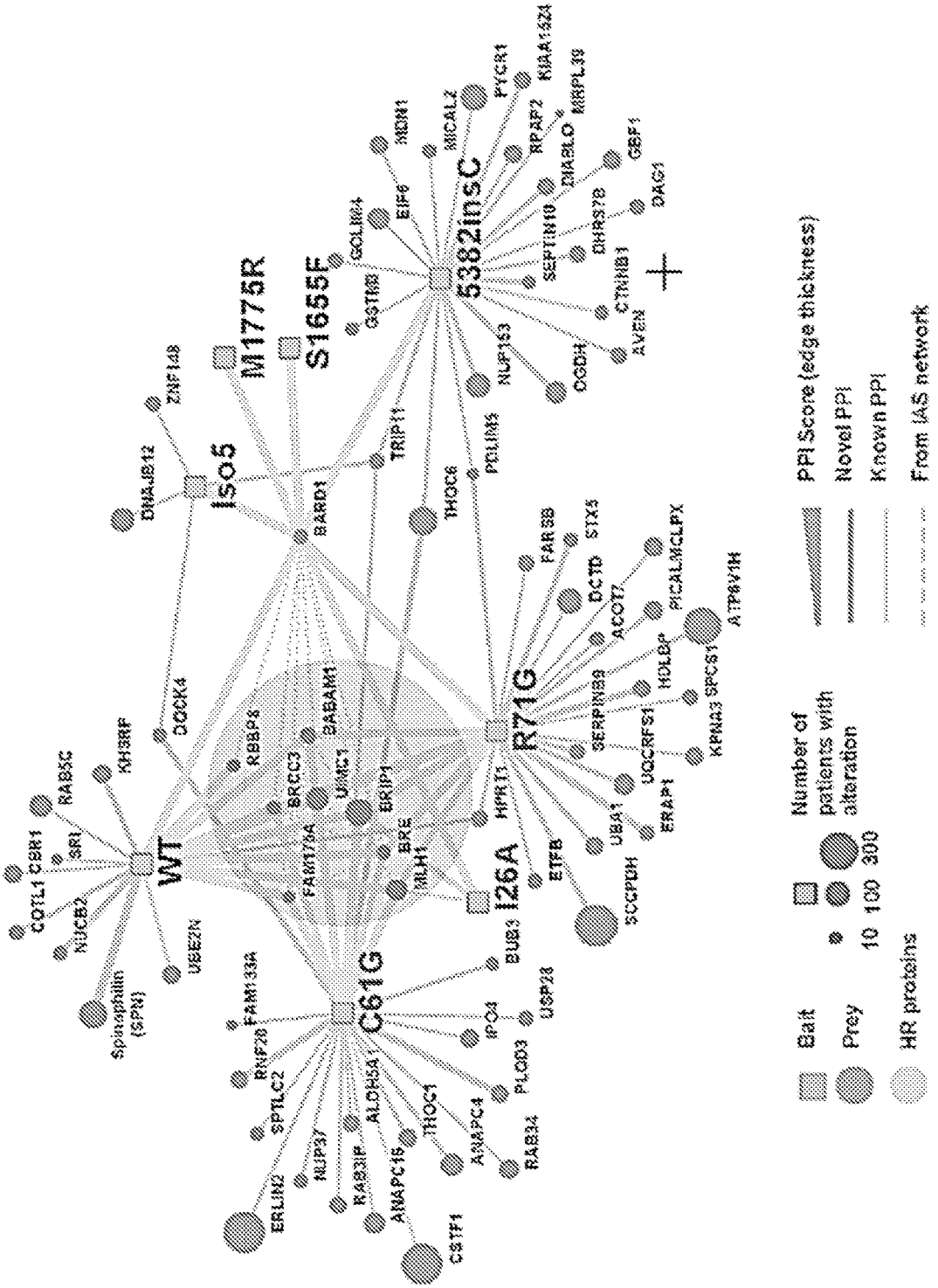
WT
Iso5
M175R
S165F
5382insC
R71G
I26A
C61G
Bait
Prey
HR proteins
Number of patients with alteration
10 100 300
PPI Score (edge thickness)
Novel PPI
Known PPI
From IAS network

FIG. 8B

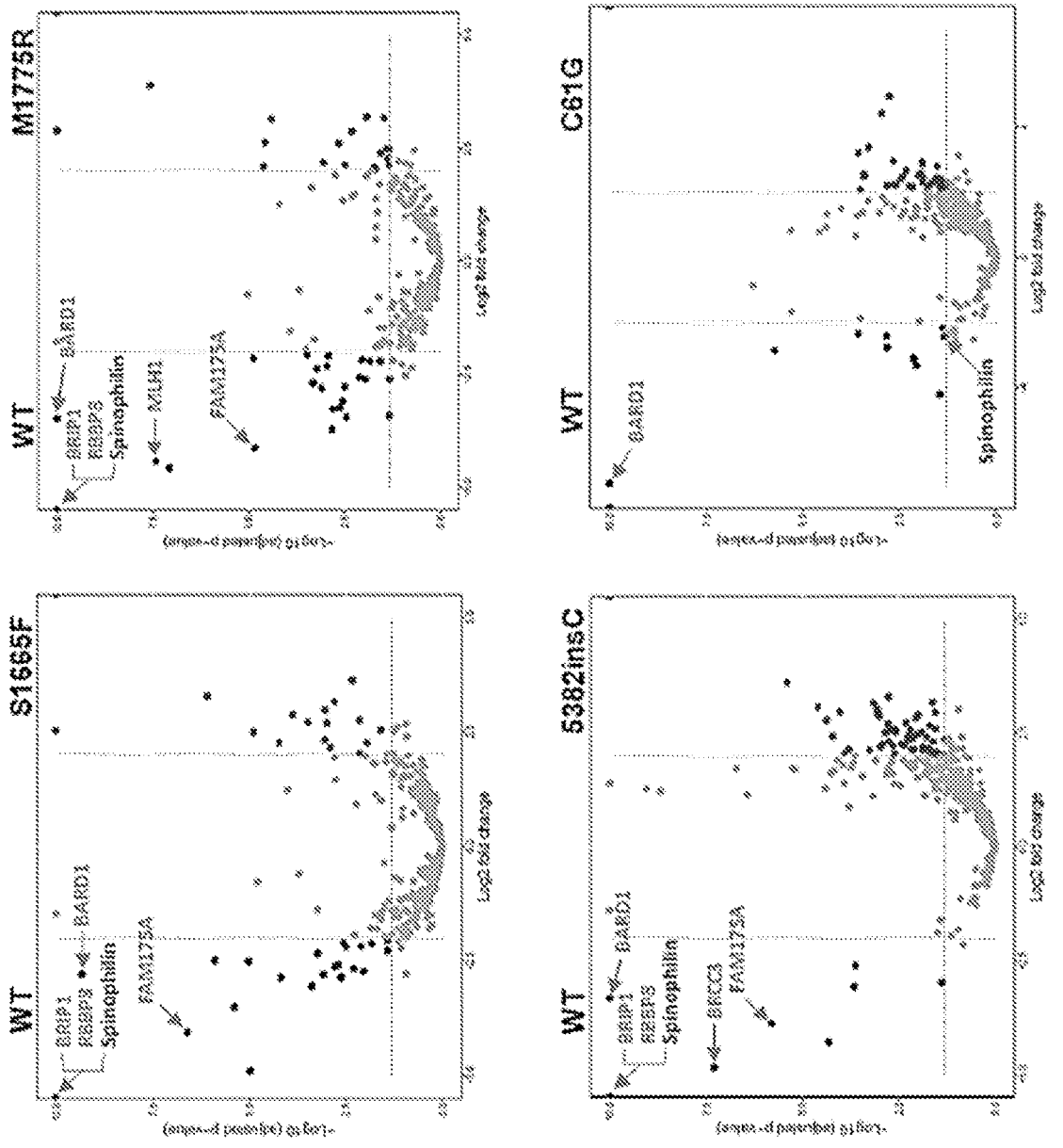
WT
M1775R
S1665F
C61G
5382insC
BARD1
BRIP1
RBBP8
Spinophilin
MLH1
FAM175A
BRCC3
-Log10 (adjusted p-value)
Log2 fold change

FIG. 8C

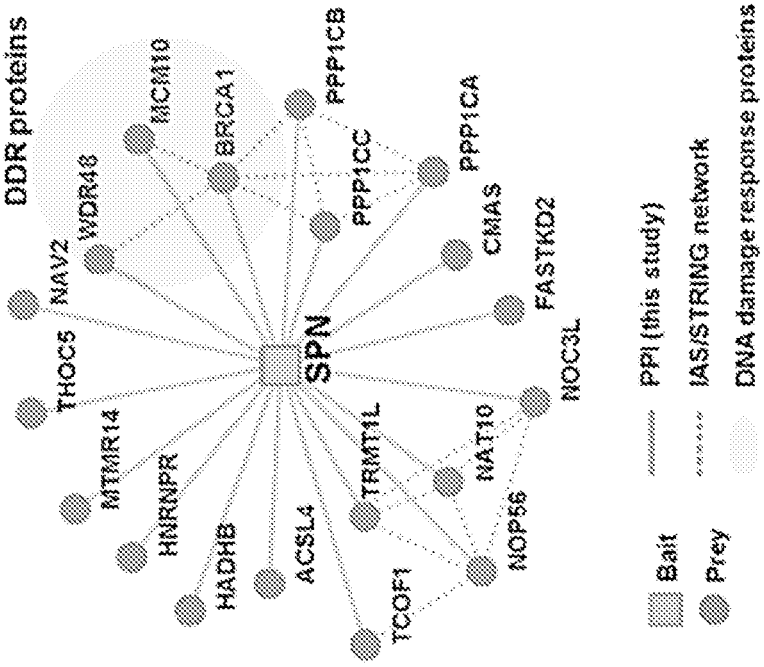
DDR proteins
NAV2
WDR48
MCM10
BRCA1
PPP1CB
PPP1CC
PPP1CA
CMAS
FASTKD2
NOC3L
NOP56
MAT10
TRMT1L
TCOF1
ACSL4
HADHB
HNRNPR
MTMR14
THOC5
SPN
Bait
Prey
PPI (this study)
IAS/STRING network
DNA damage response proteins

FIG. 9A

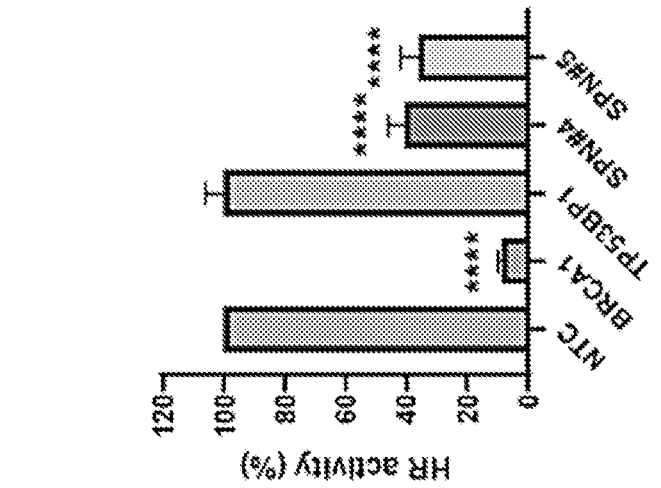
C
HR activity (%)
120
100
80
60
40
20
0
NTC
BRCA1
TP53BP1
SPN#4
SPN#5
****
****
****

FIG. 9C

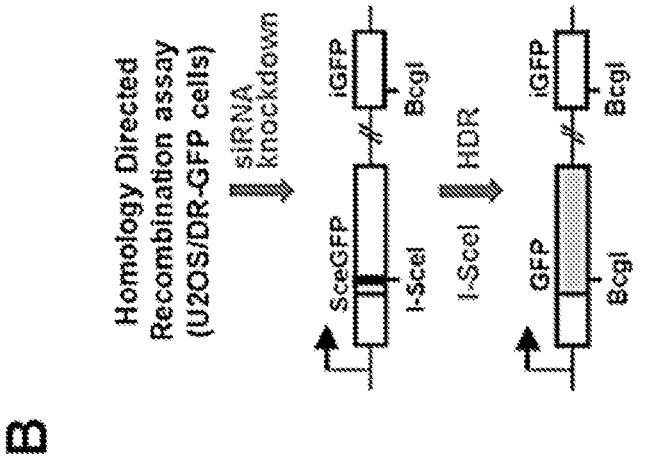
B
Homology Directed
Recombination assay
(U2OS/DR-GFP cells)
siRNA
knockdown
SceGFP
I-SceI
iGFP
BcgI
I-SceI
HDR
GFP
BcgI
iGFP
BcgI

FIG. 9B

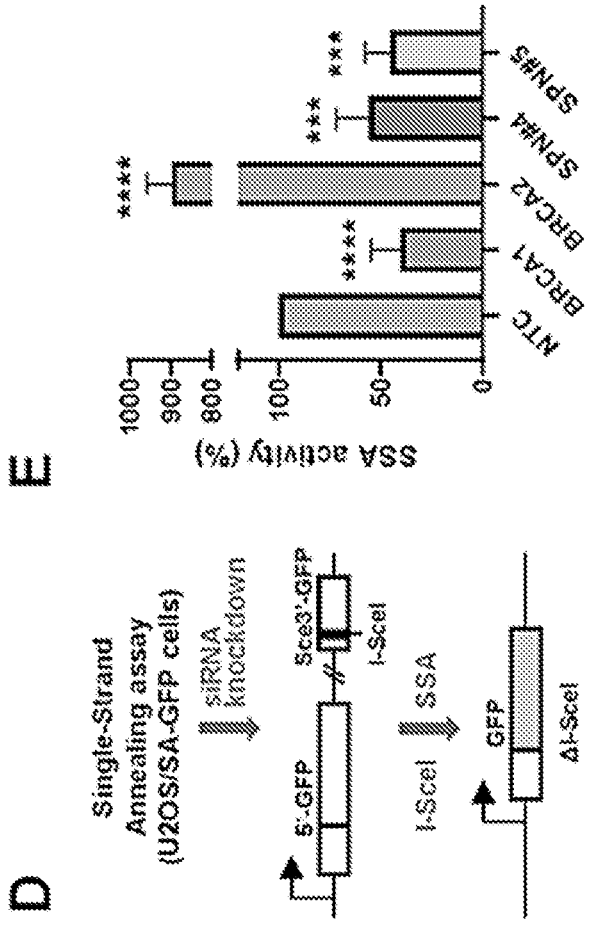
D
Single-Strand
Annealing assay
(U2OS/SA-GFP cells)
siRNA
knockdown
5'-GFP
Sce3'-GFP
I-SceI
I-SceI
SSA
GFP
A-SceI
E
SSA activity (%)
1000
900
800
100
50
0
NTC
BRCA1
BRCA2
SPN#4
SPN#5
****
****
***
***

FIG. 9D

FIG. 9E

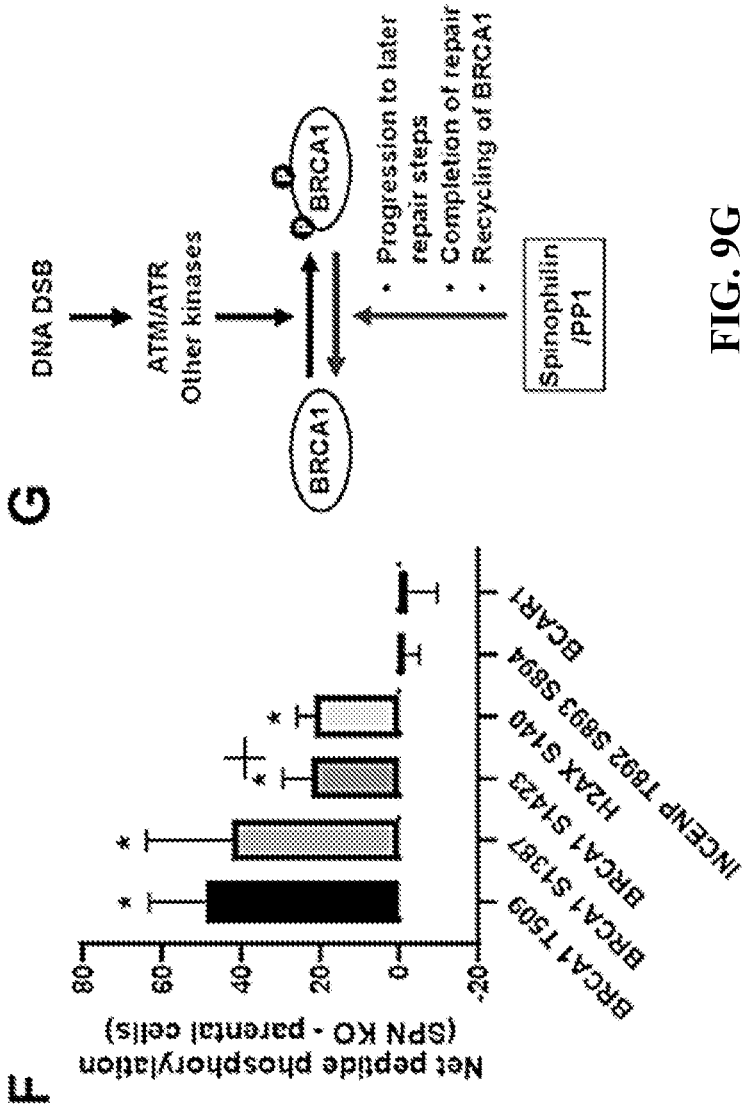
F
Net peptide phosphorylation
(SPN KO - parental cells)
80
60
40
20
0
-20
*
*
*
*
BRCA1 T509
BRCA1 S1387
BRCA1 S1423
H2AX S140
INCENP T892 S893 S894
BCAR1

FIG. 9F

G
DNA DSB
ATM/ATR
Other kinases
BRCA1
P
BRCA1
• Progression to later repair steps
• Completion of repair
• Recycling of BRCA1
Spinophilin
/PP1

FIG. 9G

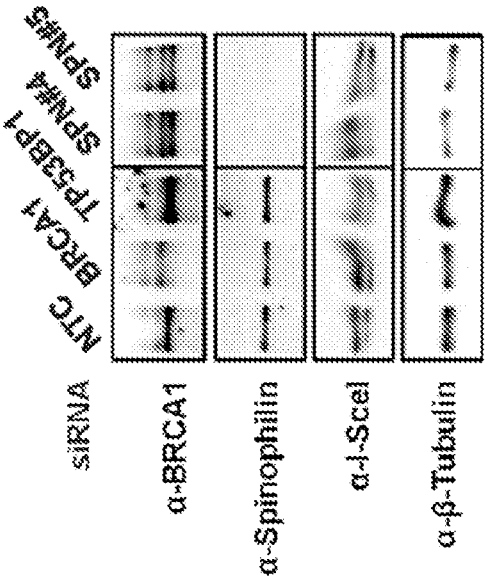
siRNA
NTC
BRCA1
TP53BP1
SPNA4
SPNA5
α-BRCA1
α-Spinophilin
α-I-SceI
α-β-Tubulin

FIG. 10A

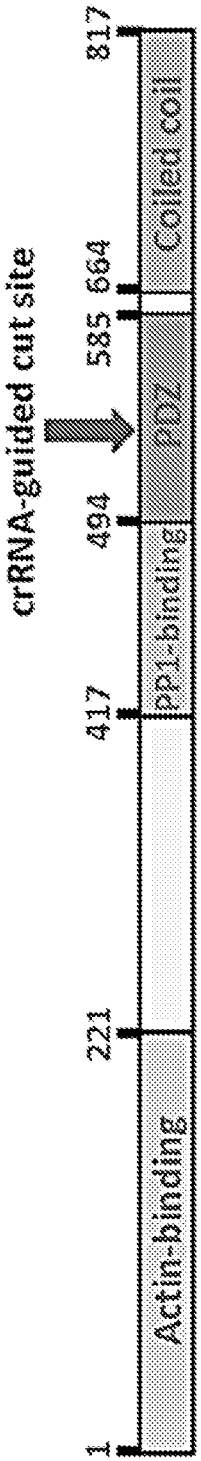
crRNA-guided cut site
1
221
417
494
585
664
817
Actin-binding
PP1-binding
PDZ
Coiled coil

FIG. 10B

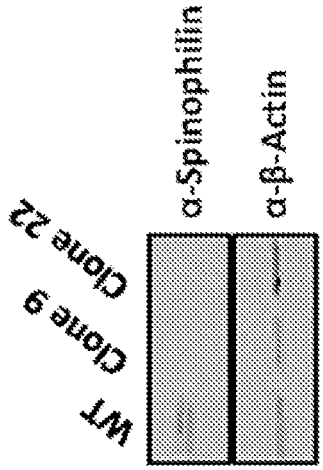

FIG. 10C

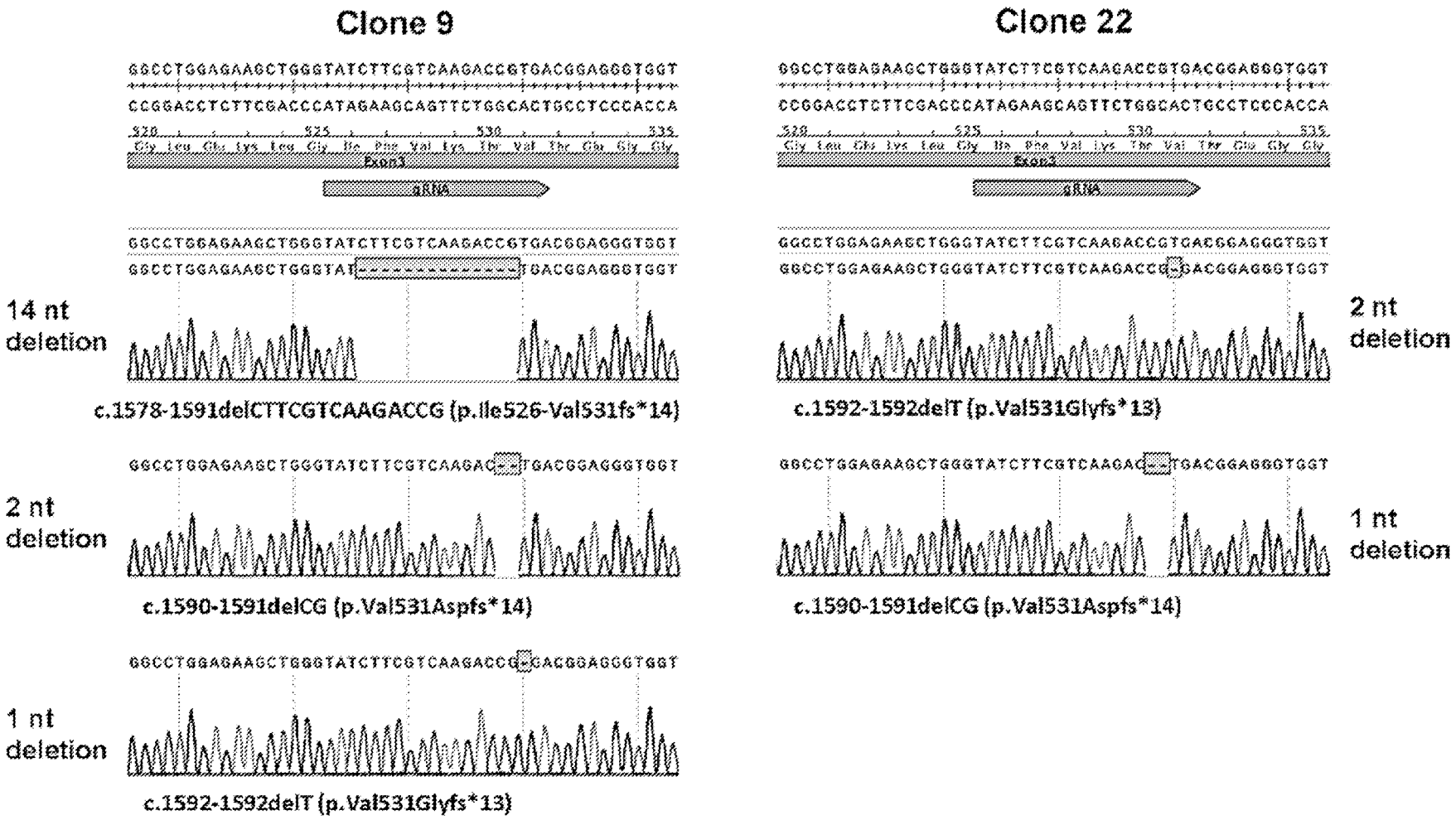
Clone 9
Clone 22
14 nt deletion
2 nt deletion
2 nt deletion
1 nt deletion
1 nt deletion
c.1578-1591delCTTCGTCAAGACCG (p.Ile526-Val531fs*14)
c.1592-1592delT (p.Val531Glyfs*13)
c.1590-1591delCG (p.Val531Aspfs*14)
c.1590-1591delCG (p.Val531Aspfs*14)
c.1592-1592delT (p.Val531Glyfs*13)

FIG. 10D

Peptide substrate	Residue	Known kinase	Parental Run#1	Parental Run#2	SPN KO Run#1	SPN KO Run#2	Net peptide phosphorylation	p-value
LIMK2	T526	CDC42BPA; ROCK1	-68.96	-32.55	33.76	67.75	101.50	0.028
MYC	T58	GSK3B; CSNK2A1; CSNK2A2	-38.18	-34.70	29.57	43.31	72.88	0.005
FOXO1	S256	AKT1; PAK1	-45.54	-14.37	21.30	38.61	59.91	0.039
RPS6KA1	S221	PDPK1	-33.41	-23.59	10.24	46.76	57.00	0.047
CRK	Y221	ABL1; ABL2; EGFR; IGF1R	-34.43	-16.64	21.07	30.00	51.07	0.018
JAK1	Y1034	JAK3; JAK1	-9.68	-40.25	30.84	19.09	49.93	0.046
BRCA1	T509	AKT1	-33.87	-14.94	25.03	23.77	48.81	0.018
BRCA1	S1387	ATM; ATR	-19.34	-22.99	7.79	34.54	42.33	0.044
MTOR	S2481	MTOR	-23.23	-14.87	28.31	9.79	38.10	0.032
AKT1 / AKT2 / AKT3	T308 / T309 / T305	CAMKK1; IKBKE; PDK1; PDPK1; PRKCA; PRKCB; PRKCZ	-29.56	-5.81	17.30	18.07	35.37	0.048
NFKB1	S923	CHUK; IKBKB	-11.10	-24.24	9.64	25.70	35.34	0.038
NFKBIB	S23	CHUK; IKBKB	-21.37	-11.25	10.53	22.09	32.62	0.026
MTOR	T2446	AKT1; AKT3; RPS6KB1	-20.21	-7.76	8.56	19.41	27.97	0.039
MAP2K1 / MAP2K2	S222 / S226	ARAF; BRAF; RAF1; MAP3K1; MAP3K8; PDPK1	-21.33	-6.54	8.95	18.93	27.88	0.044
BRCA1	S1423	ATM; ATR	-8.74	-13.36	8.20	13.90	22.09	0.013
H2AX	S140	ATM	-7.84	-13.64	10.59	10.89	21.48	0.009
SMAD2	S250	MAPK1; MAPK3	-7.83	-12.52	11.32	9.04	20.36	0.008
CDKN1A	T145	AKT1; DAPK3; PIM1	-4.37	-15.55	6.86	13.06	19.92	0.045
TP53	T55,E56K	MAPK1	-12.11	-6.61	11.41	7.31	18.72	0.016
RAF1	Y341	SRC; JAK2	-6.34	-11.65	6.27	11.73	18.00	0.021
INCENP	T892,S893,S894	AURKB	2.72	-1.47	-1.31	0.05	-1.25	0.313
BCAR1	Y234	SRC	3.86	-1.66	-3.53	1.34	-2.19	0.306

FIG. 10E

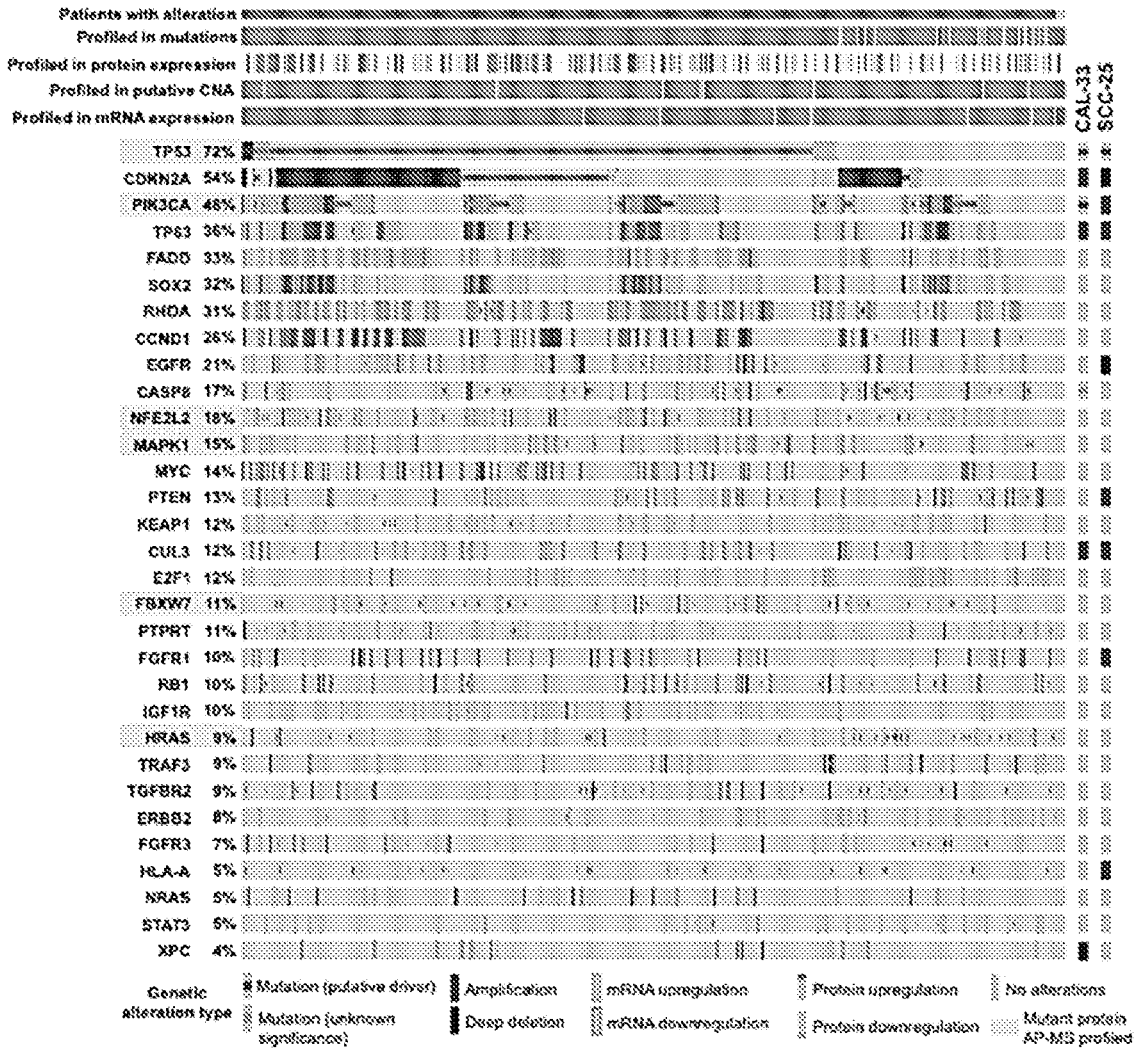
Patients with alteration
Profiled in mutations
Profiled in protein expression
Profiled in putative CNA
Profiled in mRNA expression
CAL-33
SCC-25
TP53 72%
CDKN2A 54%
PIK3CA 48%
TP63 36%
FADD 33%
SOX2 32%
RHOA 31%
CCND1 26%
EGFR 21%
CASP8 17%
NFE2L2 16%
MAPK1 15%
MYC 14%
PTEN 13%
KEAP1 12%
CUL3 12%
E2F1 12%
FBXW7 11%
PTPRT 11%
FGFR1 10%
RB1 10%
IGF1R 10%
HRAS 9%
TRAF3 9%
TGFBR2 9%
ERBB2 8%
FGFR3 7%
HLA-A 5%
NRAS 5%
STAT3 5%
XPC 4%
Genetic alteration type
Mutation (putative driver)
Mutation (unknown significance)
Amplification
Deep deletion
mRNA upregulation
mRNA downregulation
Protein upregulation
Protein downregulation
No alterations
Mutant protein AP-MS profiled

FIG. 11A

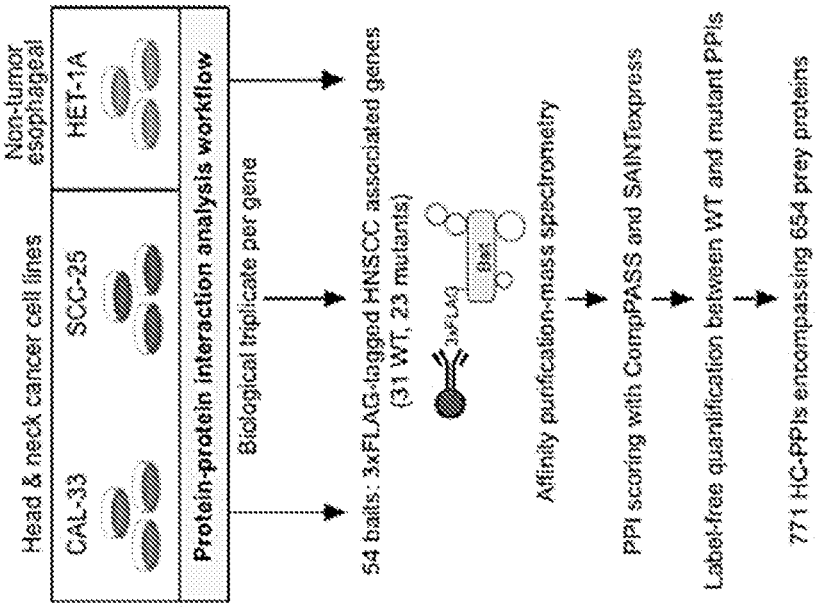
Head & neck cancer cell lines
CAL-33
SCC-25
Non-tumor esophageal
HET-1A
Protein-protein interaction analysis workflow
Biological triplicate per gene
54 baits: 3xFLAG-tagged HNSCC associated genes (31 WT, 23 mutants)
3xFLAG
Affinity purification-mass spectrometry
PPI scoring with CompPASS and SAINTexpress
Label-free quantification between WT and mutant PPIs
771 HC-PPIs encompassing 654 prey proteins

FIG. 11B

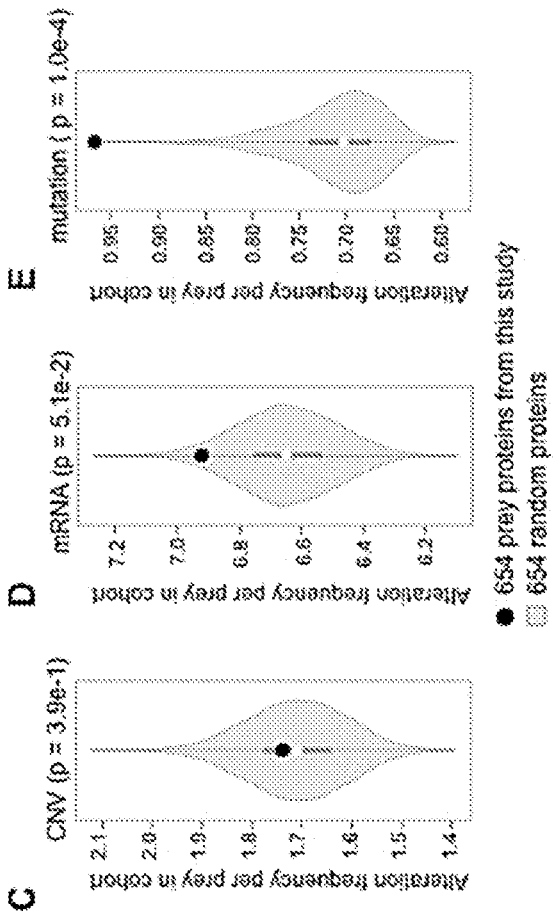

FIG. 11C FIG. 11D FIG. 11E

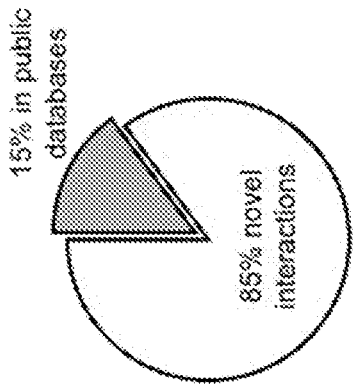

FIG. 11F

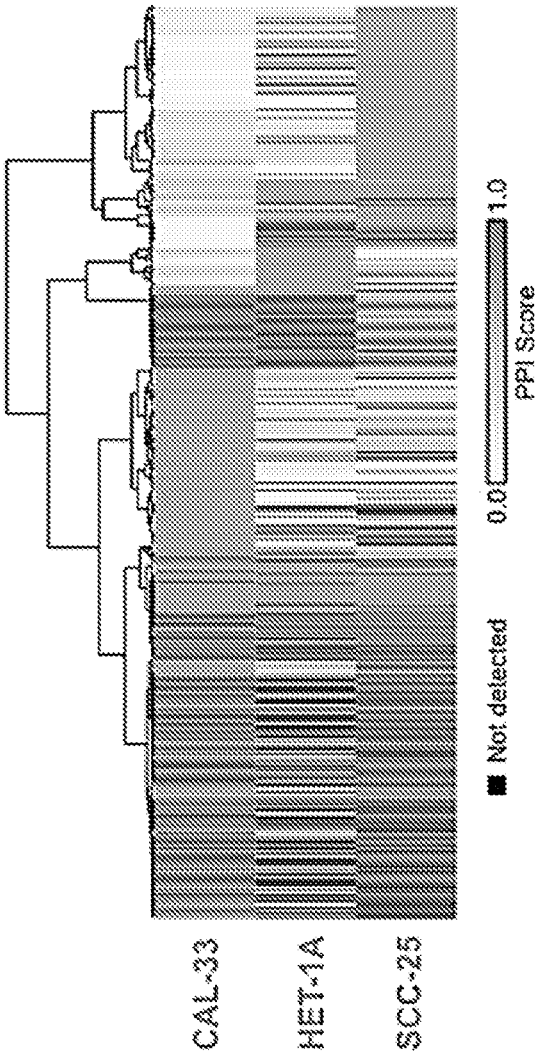

FIG. 11G

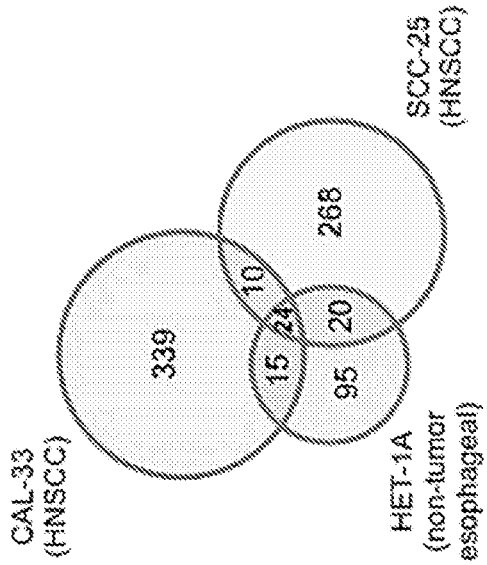
CAL-33
(HNSCC)
SCC-25
(HNSCC)
HET-1A
(non-tumor
esophageal)
339
10
268
15
24
20
95

FIG. 11H

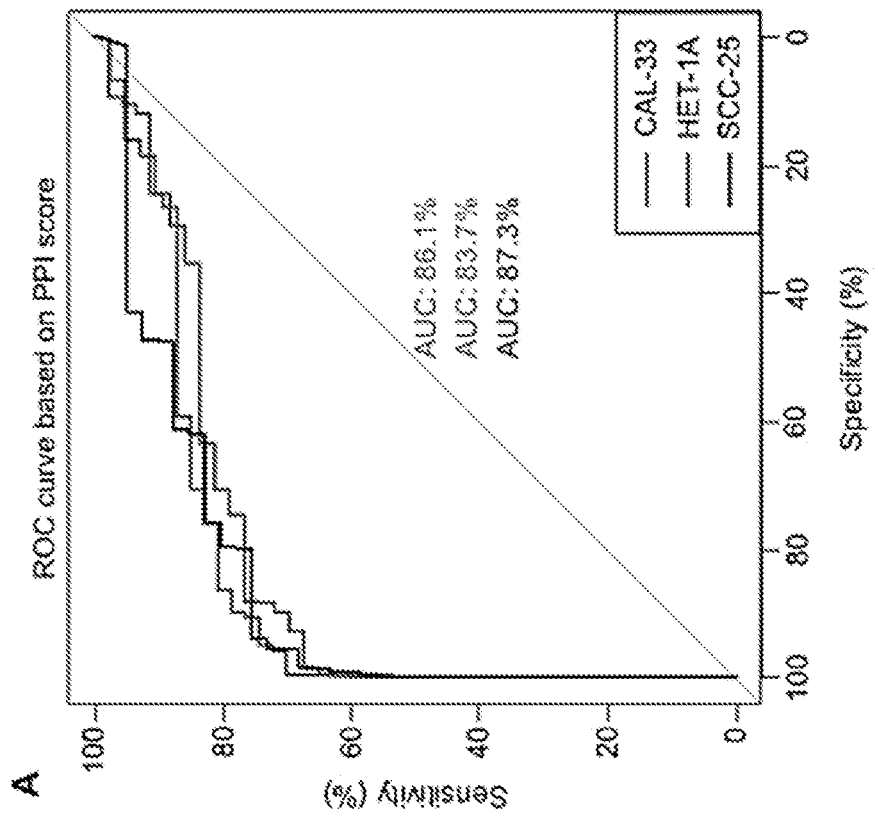
A
ROC curve based on PPI score
Sensitivity (%)
Specificity (%)
0
20
40
60
80
100
CAL-33
HET-1A
SCC-25
AUC: 86.1%
AUC: 83.7%
AUC: 87.3%

FIG. 12A

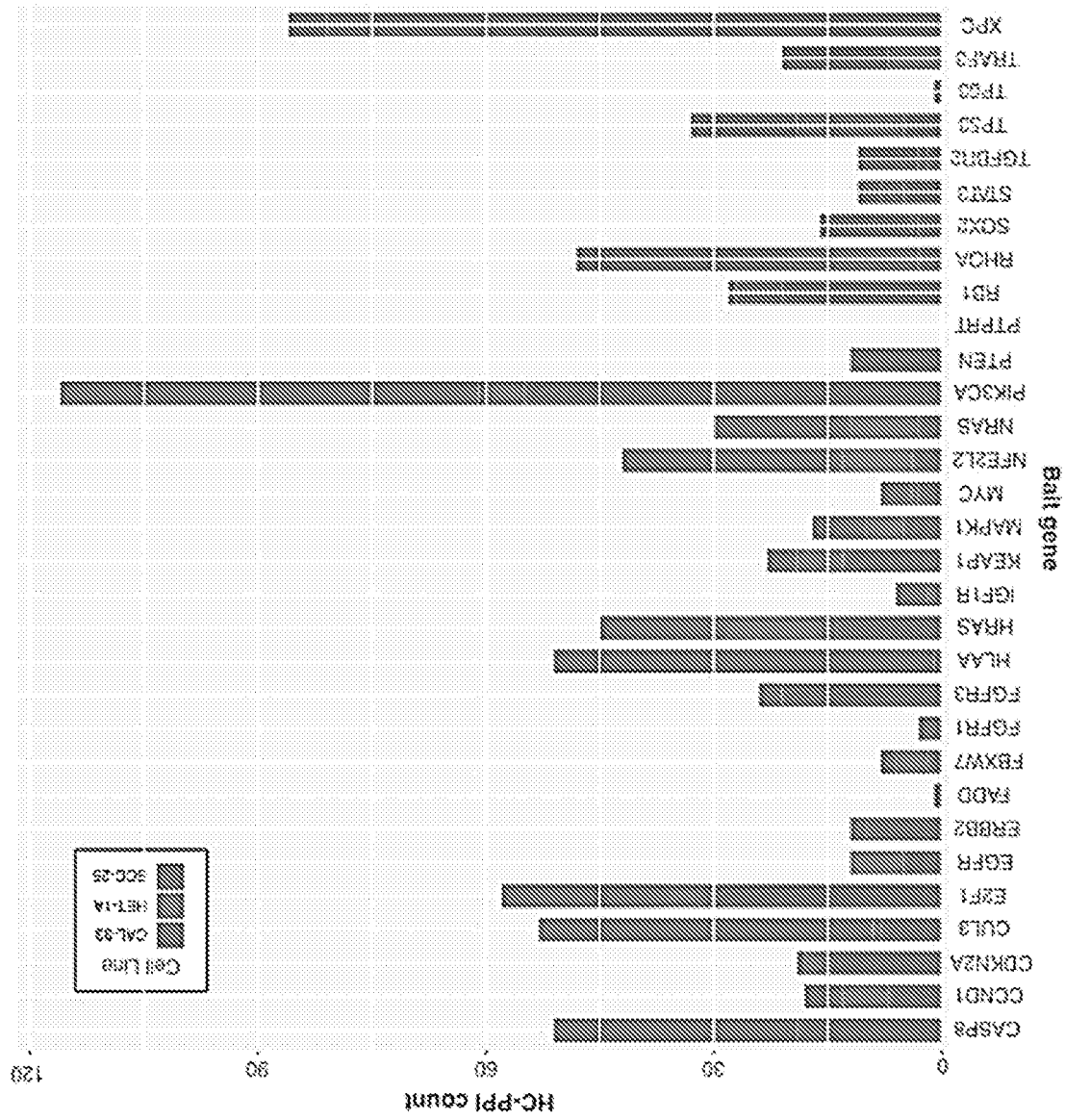
CASP8
CCND1
CDKN2A
CUL3
ERF1
EGFR
ERBB2
FADD
FBXW7
FGFR1
FGFR3
HLAA
HRAS
IGF1R
KEAP1
MAPK1
MYC
NFE2L2
NRAS
PIK3CA
PTEN
PTPRT
RB1
RHOA
SOX2
STK11
TGFBR2
TP53
TP63
TRAF3
XPC
Bait gene
0
30
60
90
120
HC-PPI count
Cell Line
CAL-33
NET-1A
SCC-25

FIG. 12B

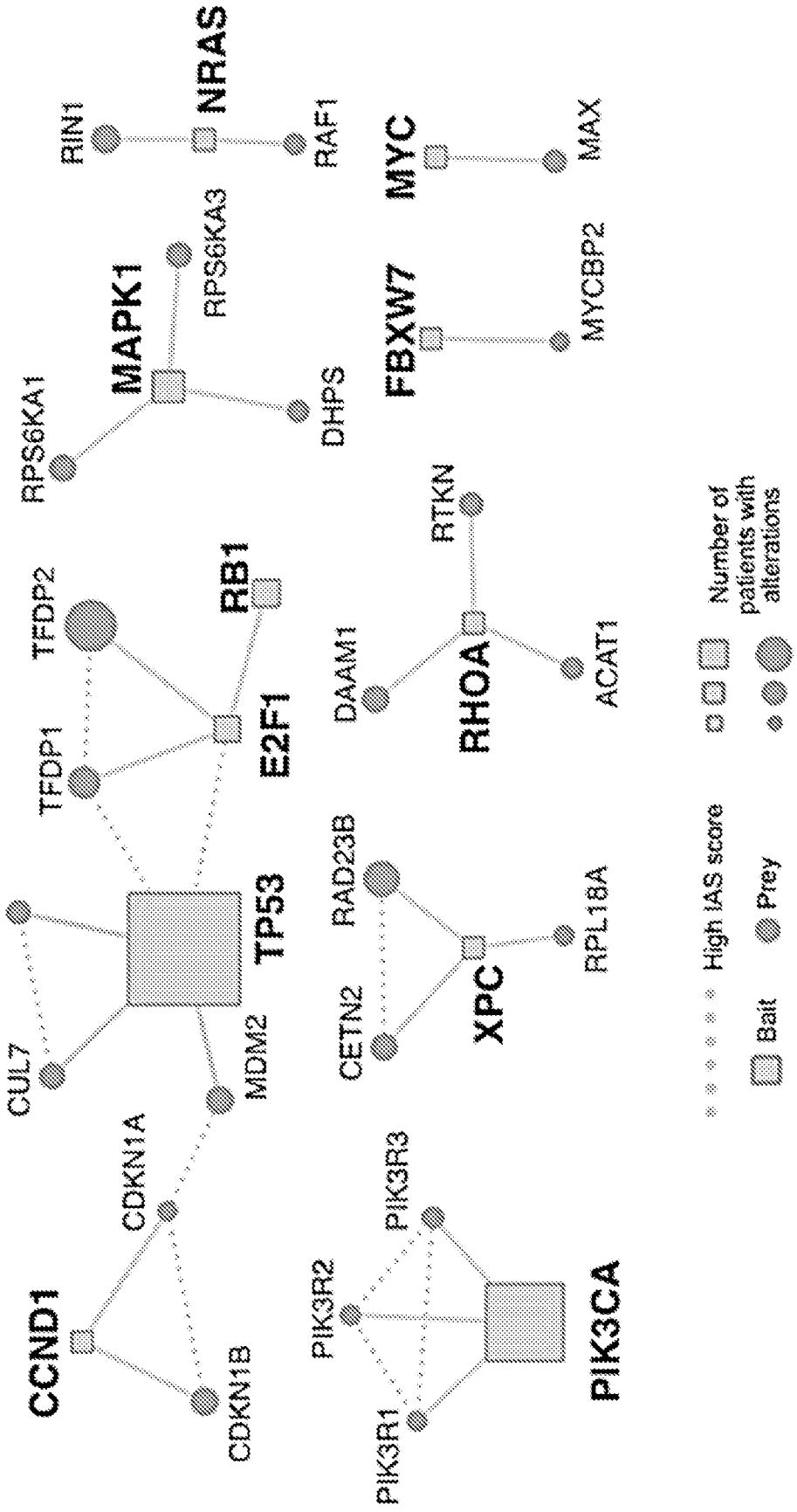
CCND1
CDKN1A
CDKN1B
CUL9
CUL7
TP53
MDM2
TFDP2
TFDP1
E2F1
RB1
PIK3R2
PIK3R3
PIK3R1
PIK3CA
RAD23B
CETN2
XPC
RPL18A
DAAM1
RTKN
RHOA
ACAT1
RPS6KA1
MAPK1
RPS6KA3
DHPS
RIN1
NRAS
RAF1
FBXW7
MYCBP2
MYC
MAX
High IAS score
Prey
Bait
Number of patients with alterations

FIG. 12C

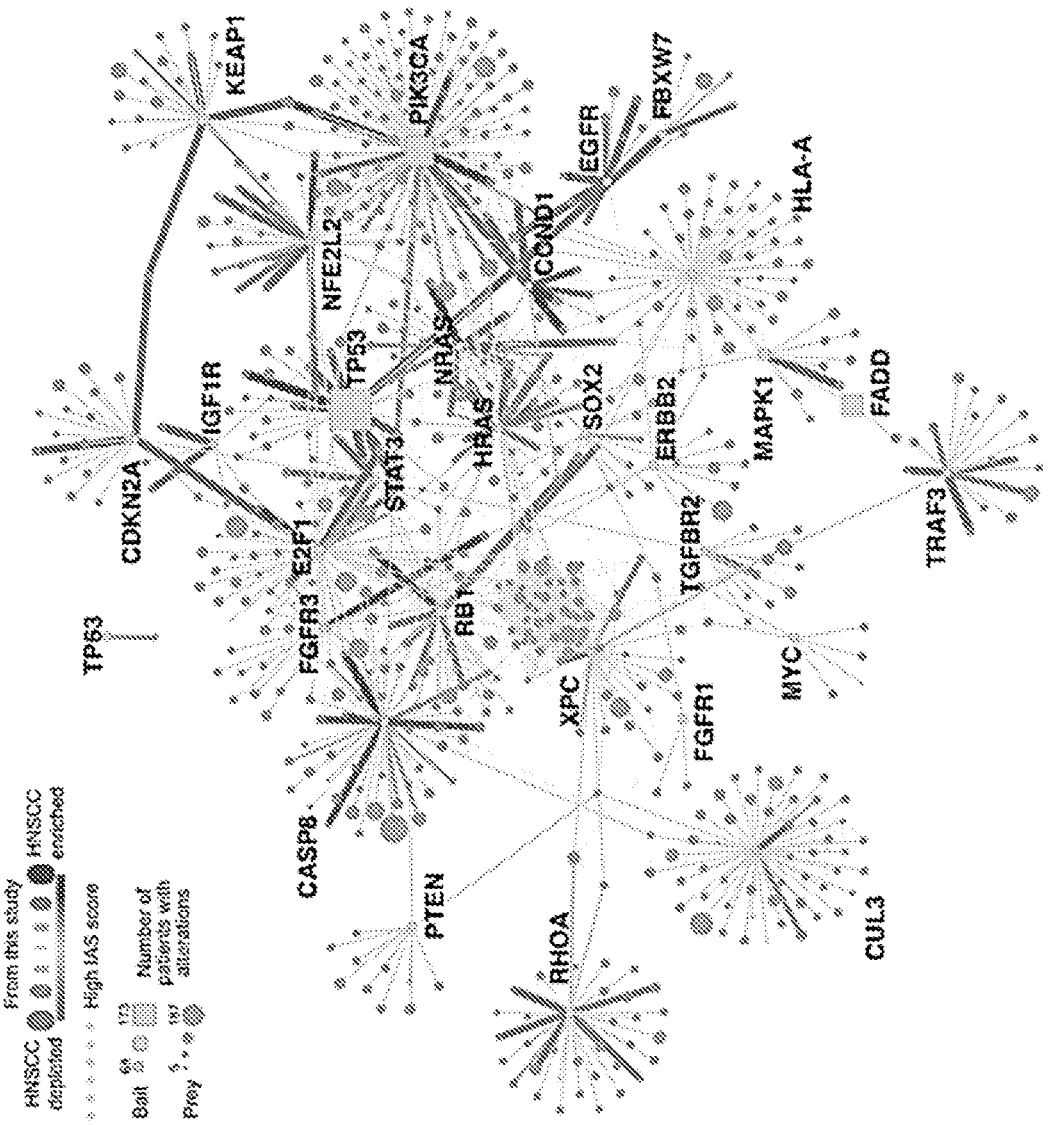
From this study
HNSCC mutated
HNSCC enriched
High IAS score
Bait
Prey
Number of patients with alterations
KEAP1
PIK3CA
NFE2L2
EGFR
FBXW7
HLA-A
CCND1
TP53
NRAS
IGF1R
CDKN2A
HRAS
SOX2
ERBB2
MAPK1
FADD
STAT3
E2F1
FGFR3
RB1
TGFBR2
TRAF3
TP63
XPC
FGFR1
MYC
CASP8
PTEN
RHOA
CUL3

FIG. 13A

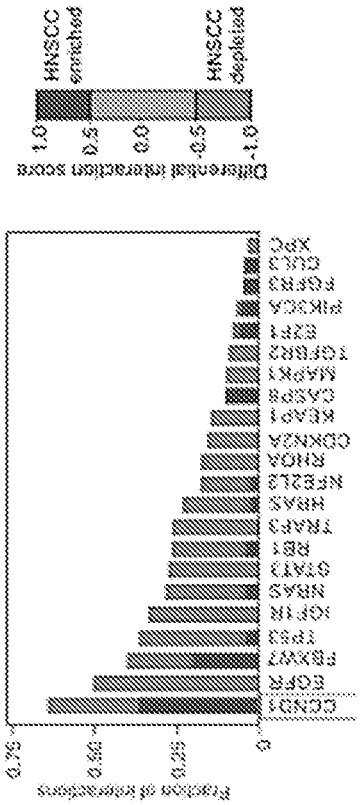
HNSCC enriched
HNSCC depleted
1.0
0.5
0.0
-0.5
-1.0
Differential interaction score
Fraction of interactions
0.75
0.50
0.25
0
CCND1
EGFR
FGFR3
IRS2
IGF1R
NRAS
STAT3
RB1
TRAF3
HRAS
NFE2L2
RHOA
CDKN2A
KEAP1
CASP8
MAPK1
TGFBR2
EZH1
PIK3CA
FGFR3
CUL3
XPC

FIG. 13B

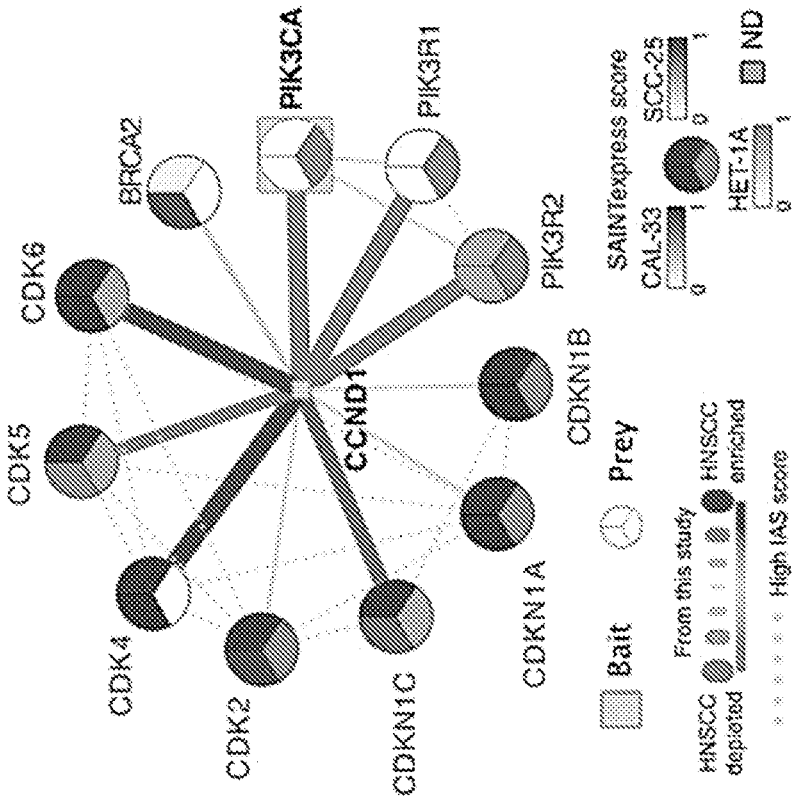
CDK6
BRCA2
PIK3CA
PIK3R1
CDK5
CCND1
PIK3R2
CDKN1B
CDK4
CDKN1A
CDK2
CDKN1C
Bait
Prey
SAINTexpress score
CAL-33
SCC-25
HET-1A
ND
From this study
HNSCC depleted
HNSCC enriched
High IAS score

FIG. 13C

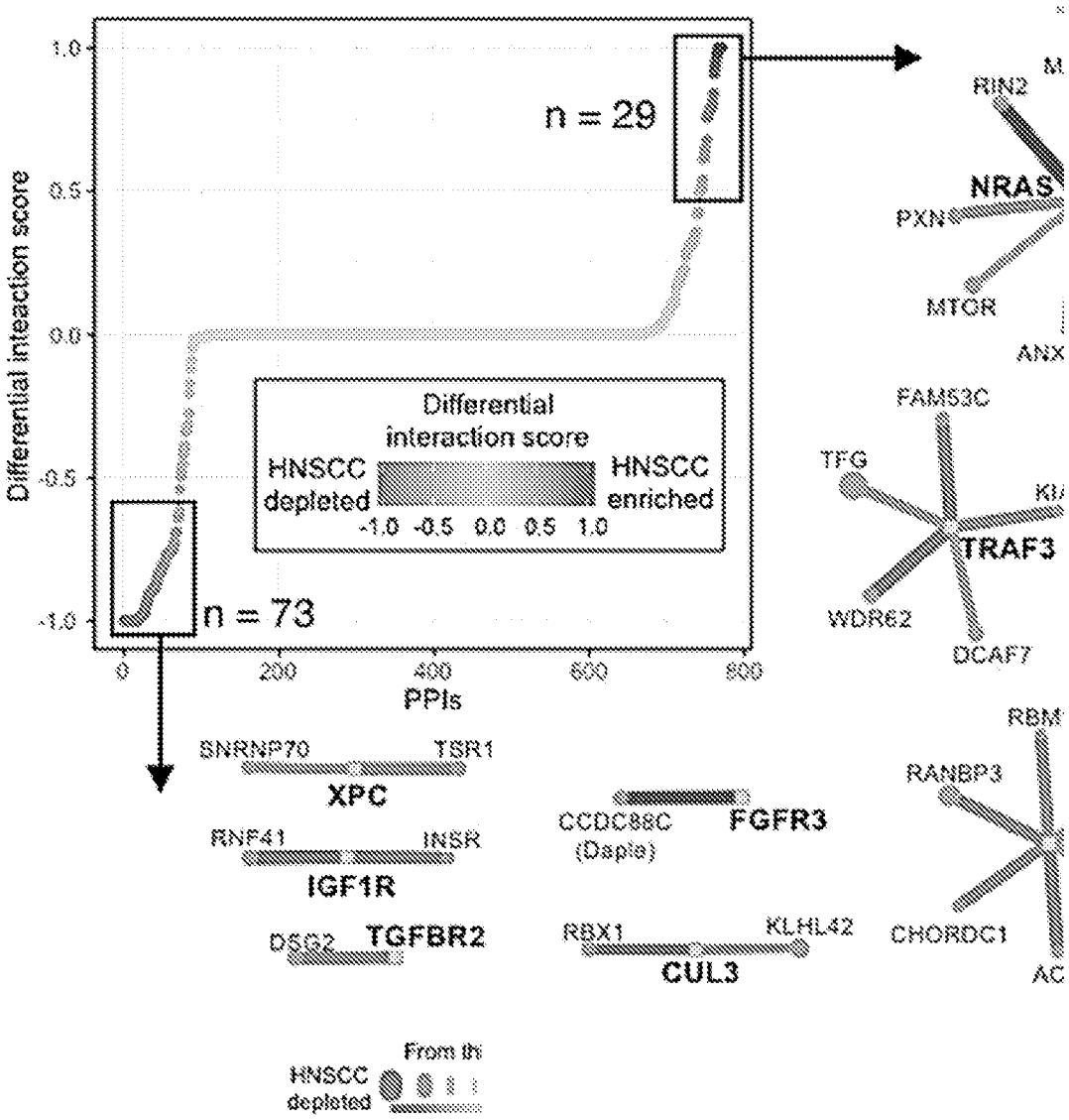
Differential inteaction score
1.0
0.5
0.0
-0.5
-1.0
n = 29
n = 73
Differential interaction score
HNSCC depleted
HNSCC enriched
-1.0 -0.5 0.0 0.5 1.0
0
200
400
600
800
PPIs
RIN2
NRAS
PXN
MTOR
FAM53C
TFG
TRAF3
WDR62
DCAF7
SNRNP70
TSR1
XPC
RNF41
INSR
IGF1R
DSG2
TGFBR2
CCDC88C
(Daple)
FGFR3
RBX1
KLHL42
CUL3
RANBP3
CHORDC1
HNSCC depleted

FIG. 13D

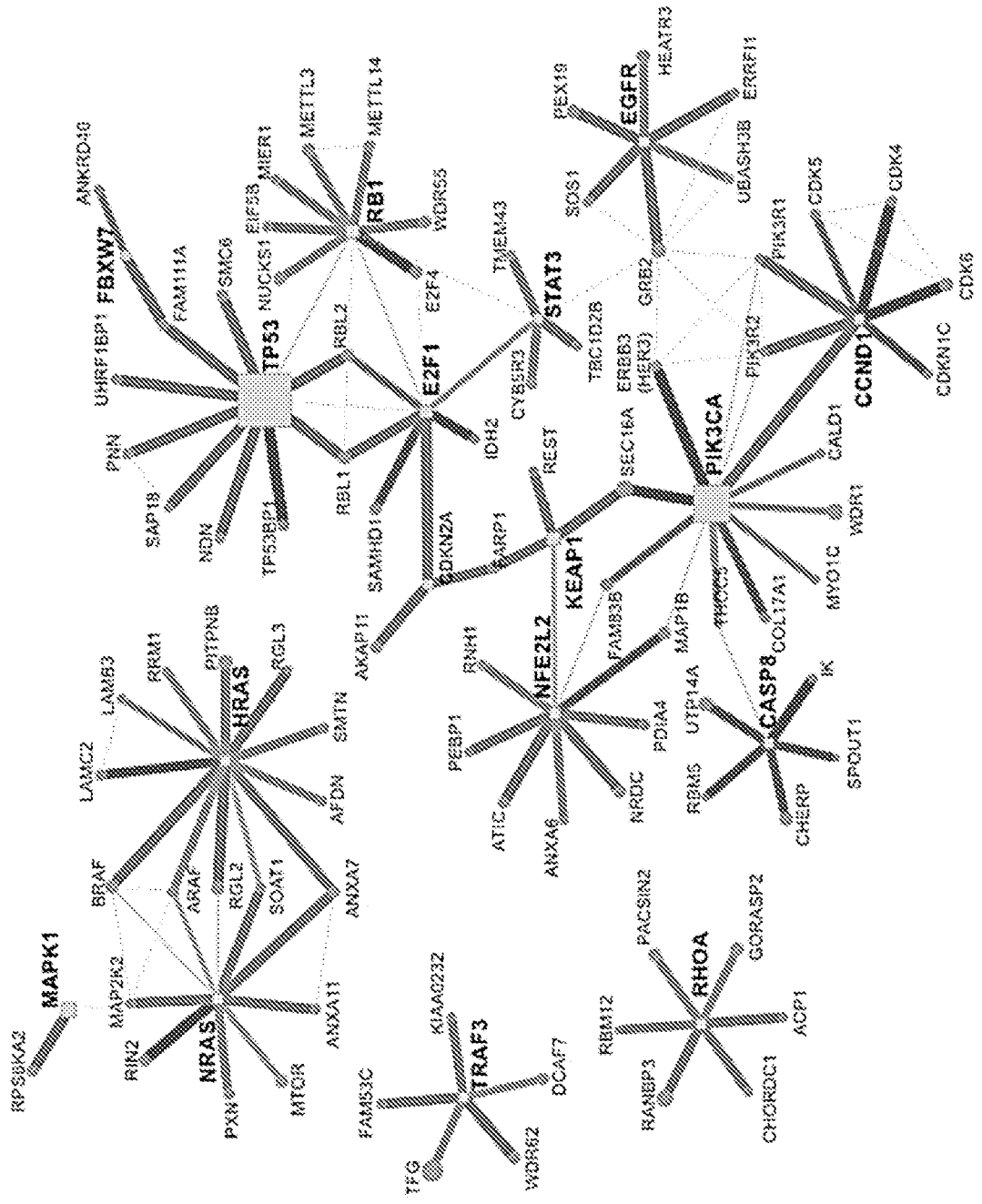
MAPK1
RPS6KA3
MAP2K2
BRAF
ARAF
RGL2
SOAT1
ANXA7
ANXA11
AFDN
SMTN
RGL3
PTPN13
RRM1
LAMB3
LAMC2
NRAS
HRAS
RIN2
PXN
MTOR
TRAF3
KIAA0232
FAM53C
TFG
WDR62
DCAF7
RHOA
PACSIN2
RBM12
RANBP3
GORASP2
CHORDC1
ACP1
NFE2L2
KEAP1
PEBP1
RNH1
ATIC
ANXA6
NRDC
PDIA4
FAM83B
MAP1B
UTP14A
RRM2
CASP8
CHERP
IK
SPOUT1
COL17A1
MYO1C
WDR1
CALD1
PIK3CA
PIK3R2
SEC16A
ERBB3 (HER3)
TBC1D2B
GRB2
EGFR
HEATR3
ERRFI1
UBASH3B
PIK3R1
CDK5
CDK4
CDK6
CDKN1C
CCND1
SOS1
PEX19
STAT3
TMEM43
CYB5R3
E2F1
E2F4
IDH2
RB1
WDR55
METTL14
METTL3
MIER1
EIF3B
NUCKS1
TP53
SMC6
FAM111A
FBXW7
ANKRD36
UHRF1BP1
PNN
SAP18
NDN
TP53BP1
RBL1
RBL2
SAMMD1
CDKN2A
ARP1
REST
AKAP11

FIG. 13E

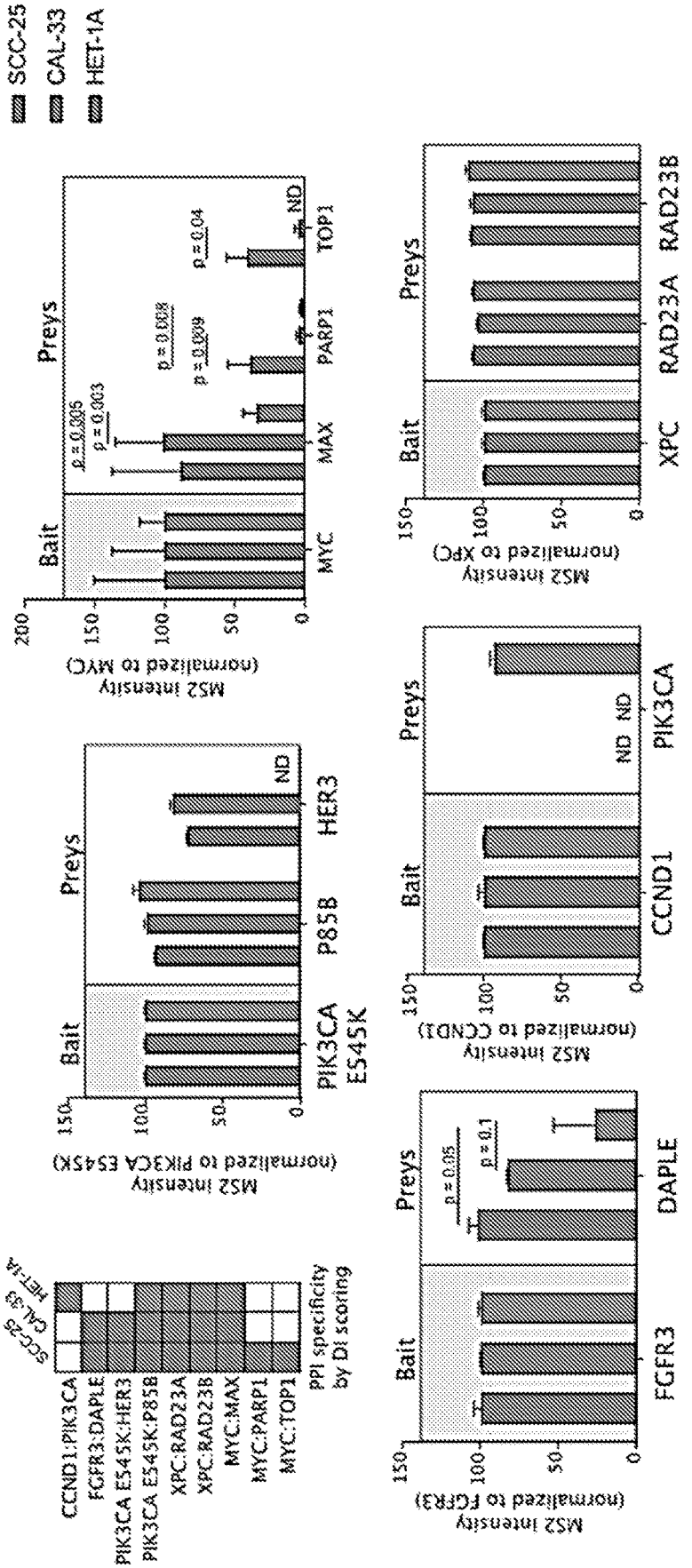
SCC-25
CAL-33
HET-1A
MS2 intensity (normalized to MYC)
Bait
Preys
MYC
MAX
PARP1
TOP1
p = 0.005
p = 0.003
p = 0.008
p = 0.009
p = 0.04
ND
MS2 intensity (normalized to XPC)
XPC
RAD23A
RAD23B
MS2 intensity (normalized to PIK3CA E545K)
PIK3CA E545K
P85B
HER3
MS2 intensity (normalized to CCND1)
CCND1
PIK3CA
ND ND
MS2 intensity (normalized to FGFR3)
FGFR3
DAPLE
p = 0.05
p = 0.1
CCND1:PIK3CA
FGFR3:DAPLE
PIK3CA E545K:HER3
PIK3CA E545K:P85B
XPC:RAD23A
XPC:RAD23B
MYC:MAX
MYC:PARP1
MYC:TOP1
PPI specificity by DI scoring

FIG. 14

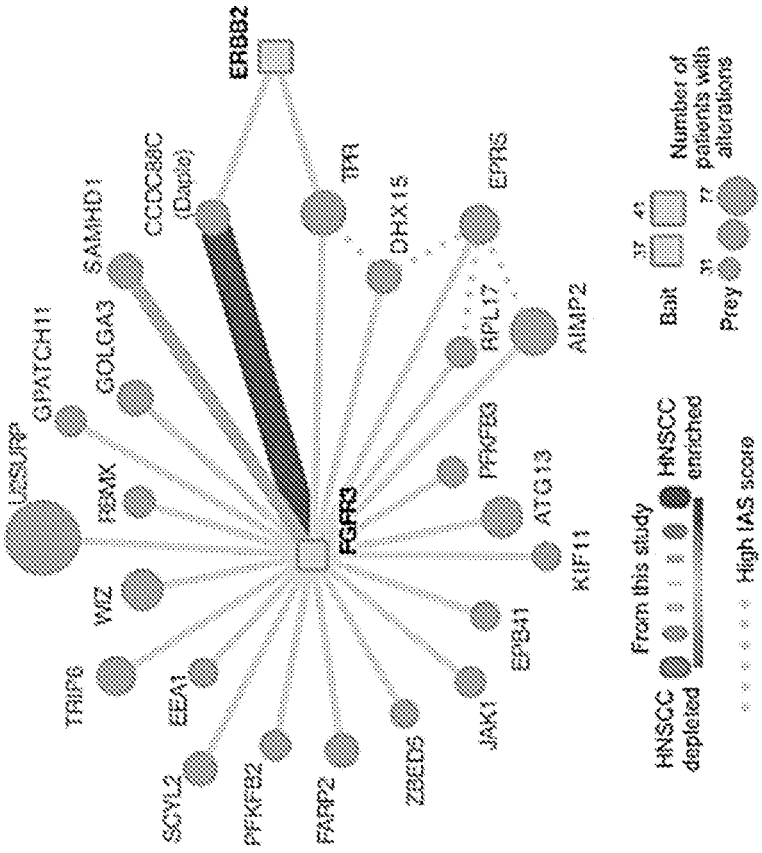
ERBB2
TPR
CCDC88C (Oncite)
SAMHD1
GOLGA3
GPATCH11
LRSAM1
FBXW
WIZ
TRIP6
EEA1
SCYL2
PFKFB2
FARP2
ZBED5
JAK1
EPB41
KIF11
ATG13
PFKFB3
RPL17
AIMP2
EPRS
CHX15
FGFR3
Bait
Prey
Number of patients with alterations
From this study
HNSCC enriched
HNSCC depleted
High IAS score

FIG. 15A

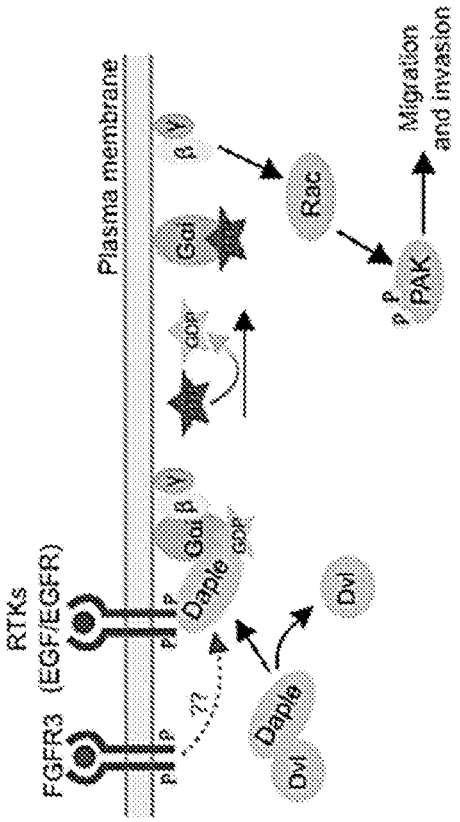
RTKs
FGFR3 (EGF/EGFR)
Plasma membrane
Dapla
Dvl
Gαi
Rac
PAK
Migration and invasion

FIG. 15B

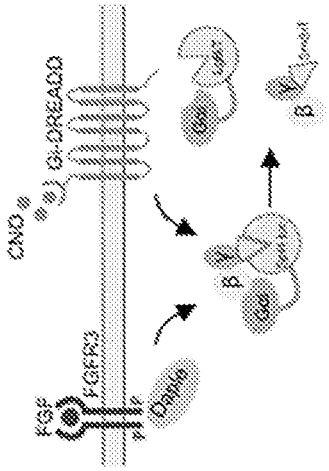

FIG. 15C

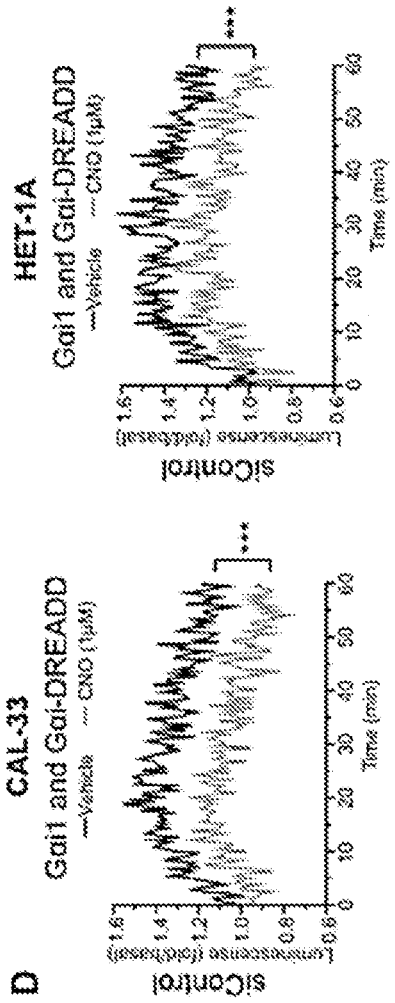
D
CAL-33
Gαi1 and Gαi-DREADD
—Vehicle — CNO (1μM)
siControl
Luminescence (Fold change)
Time (min)
***
HET-1A
Gαi1 and Gαi-DREADD
—Vehicle — CNO (1μM)
siControl
Luminescence (Fold change)
Time (min)
***

FIG. 15D

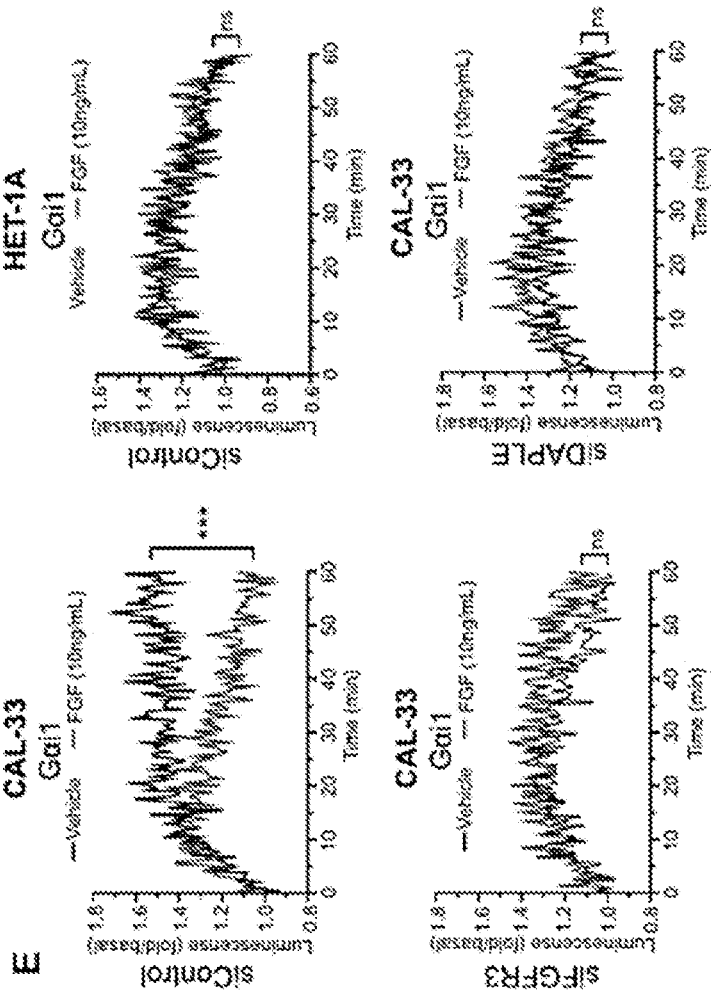
E
CAL-33
Gαi1
Vehicle
FGF (10ng/mL)
siControl
siFGFR3
HET-1A
siDAPLE
Luminescence (fold/basal)
Time (min)
***
ns

FIG. 15E

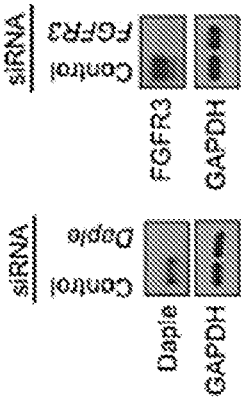
siRNA
Control
Dapk
Dapk
GAPDH
siRNA
Control
FGFR3
FGFR3
GAPDH

FIG. 15F

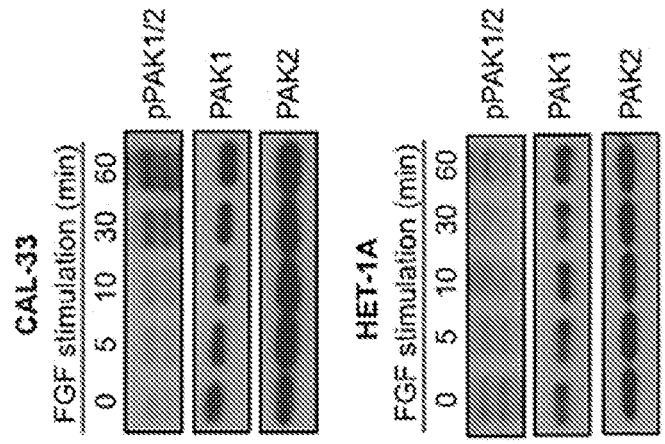
CAL-33
FGF stimulation (min)
0 5 10 30 60
pPAK1/2
PAK1
PAK2
HET-1A
FGF stimulation (min)
0 5 10 30 60
pPAK1/2
PAK1
PAK2

FIG. 15G

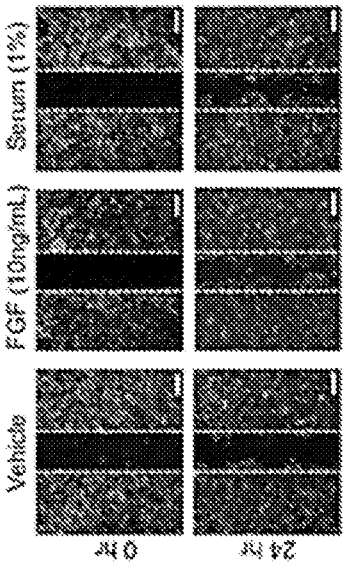

FIG. 15H

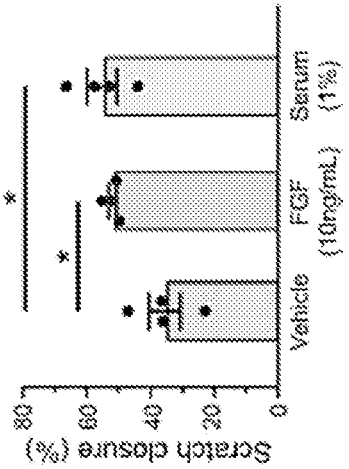

FIG. 15I

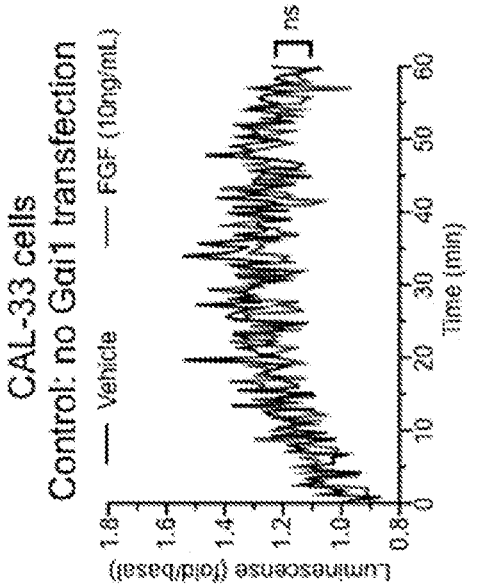
CAL-33 cells
Control: no Gαi1 transfection
Vehicle
FGF (10ng/mL)
ns
Luminescense (fold/basal)
1.8
1.6
1.4
1.2
1.0
0.8
0
10
20
30
40
50
60
Time (min)

FIG. 16A

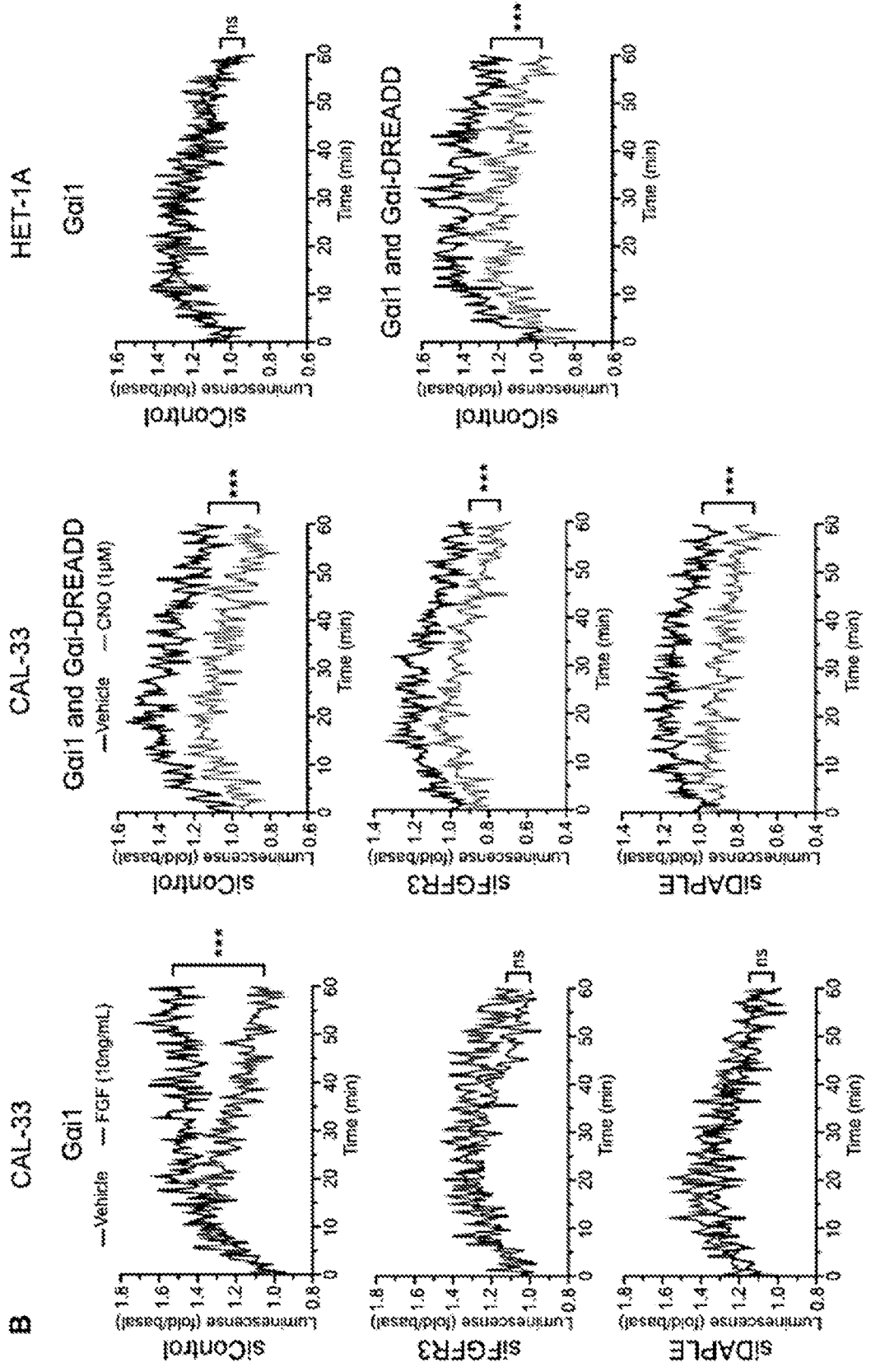
B
CAL-33
Gαi1
Vehicle
FGF (10ng/mL)
siControl
siFGFR3
siDAPLE
***
ns
CAL-33
Gαi1 and Gαi-DREADD
Vehicle
CNO (1μM)
HET-1A
Gαi1
Gαi1 and Gαi-DREADD
Luminescense (fold/basal)
Time (min)

FIG. 16B

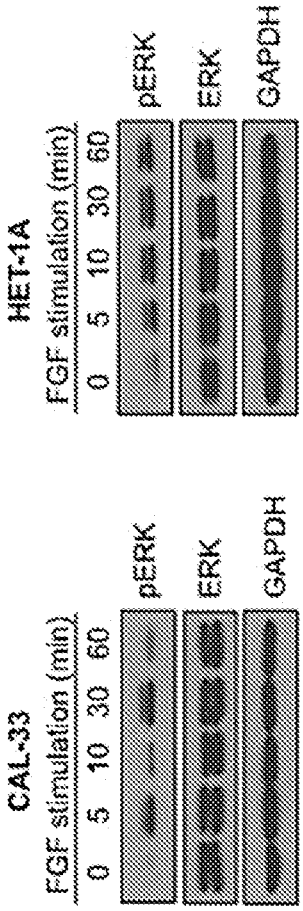
CAL-33
FGF stimulation (min)
0 5 10 30 60
pERK
ERK
GAPDH
HET-1A
FGF stimulation (min)
0 5 10 30 60
pERK
ERK
GAPDH

FIG. 16C

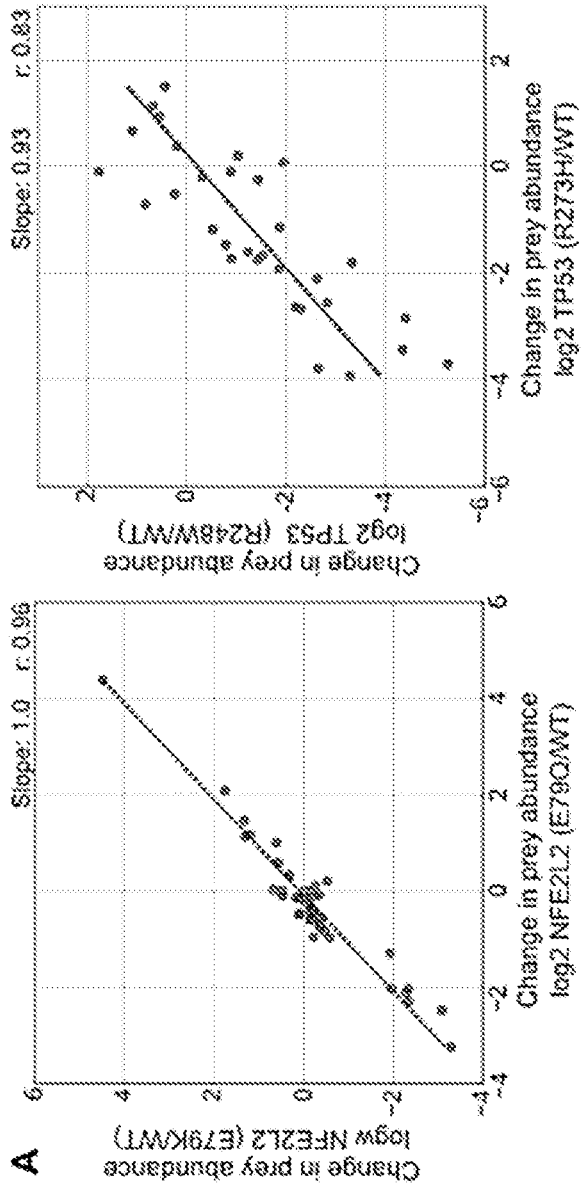
A
Change in prey abundance log2 NFE2L2 (E79K/WT)
Slope: 1.0 r: 0.96
Change in prey abundance log2 NFE2L2 (E79Q/WT)
Change in prey abundance log2 TP53 (R248W/WT)
Slope: 0.93 r: 0.89
Change in prey abundance log2 TP53 (R273H/WT)

FIG. 17A

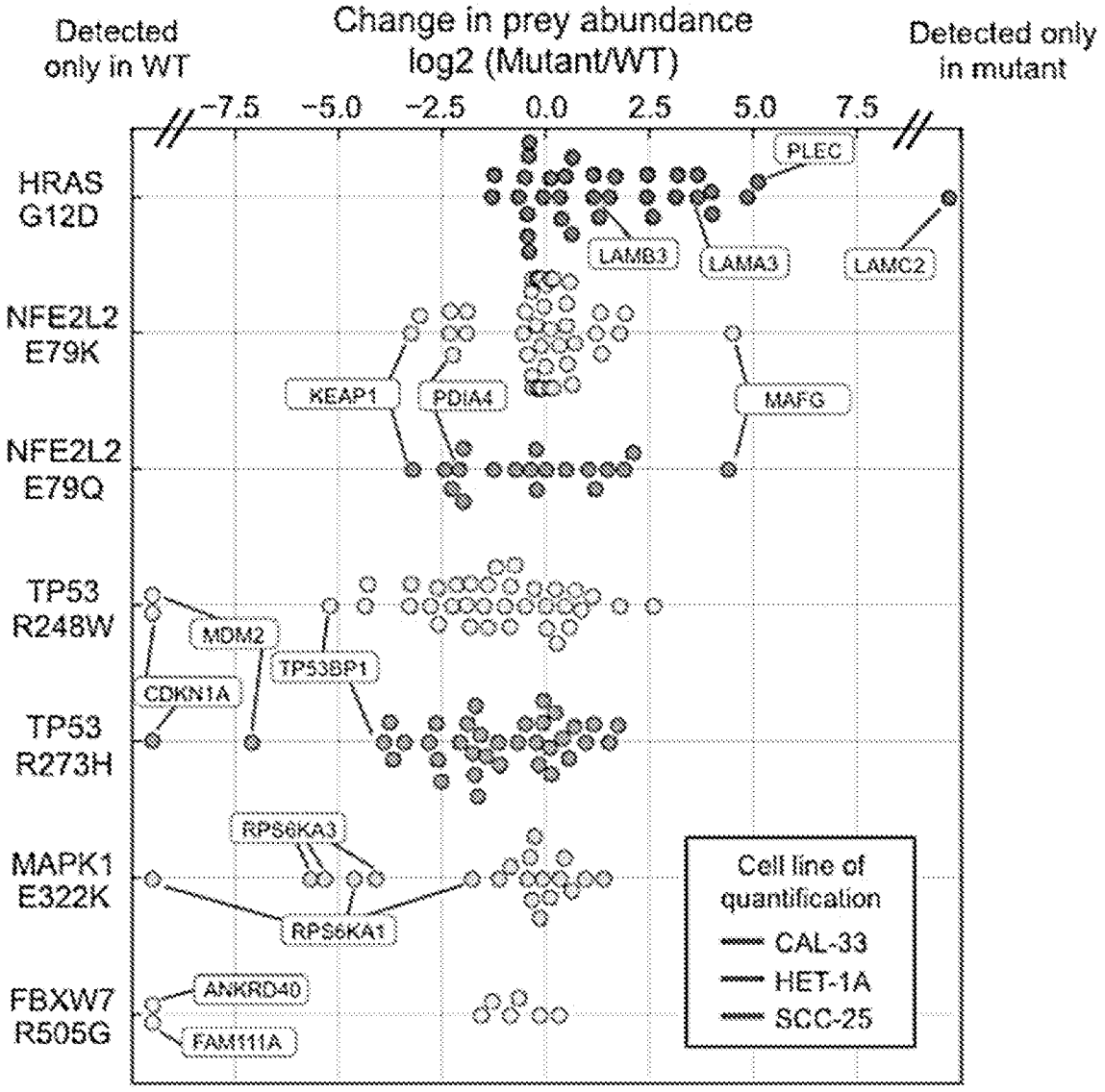
Detected only in WT
Change in prey abundance log2 (Mutant/WT)
Detected only in mutant
−7.5
−5.0
−2.5
0.0
2.5
5.0
7.5
HRAS G12D
NFE2L2 E79K
NFE2L2 E79Q
TP53 R248W
TP53 R273H
MAPK1 E322K
FBXW7 R505G
PLEC
LAMB3
LAMA3
LAMC2
KEAP1
PDIA4
MAFG
MDM2
TP53BP1
CDKN1A
RPS6KA3
RPS6KA1
ANKRD40
FAM111A
Cell line of quantification
CAL-33
HET-1A
SCC-25

FIG. 17B

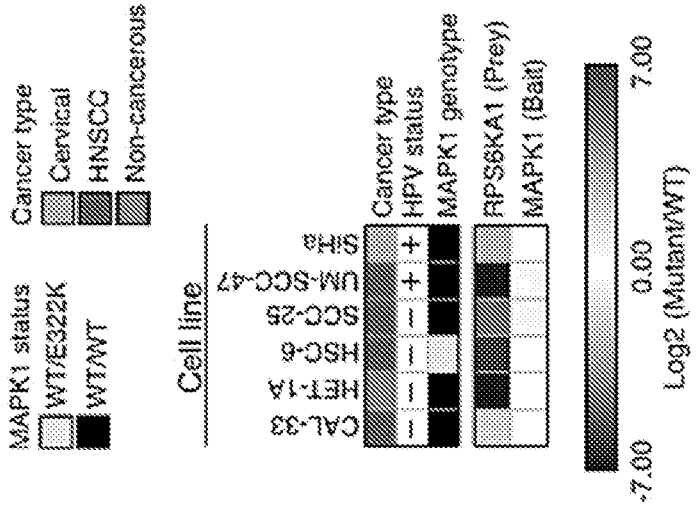
MAPK1 status
WT/E322K
WT/WT
Cancer type
Cervical
HNSCC
Non-cancerous
Cell line
SiHa
UM-SCC-47
SCC-25
HSC-6
HET-1A
CAL-33
Cancer type
HPV status
MAPK1 genotype
RPS6KA1 (Prey)
MAPK1 (Bait)
-7.00
0.00
7.00
Log2 (Mutant/WT)

FIG. 17C

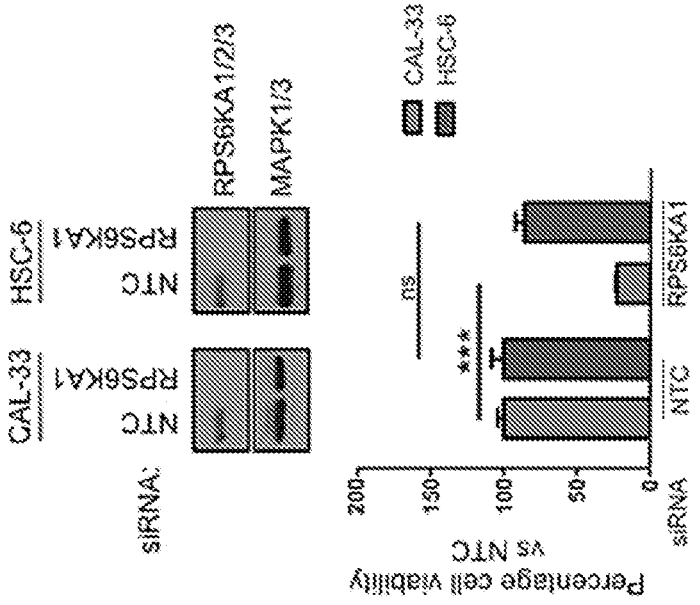
siRNA:
CAL-33
NTC
RPS6KA1
HSC-6
NTC
RPS6KA1
RPS6KA1/2/3
MAPK1/3
CAL-33
HSC-6
ns
***
Percentage cell viability
vs NTC
200
150
100
50
0
siRNA
NTC
RPS6KA1

FIG. 17D

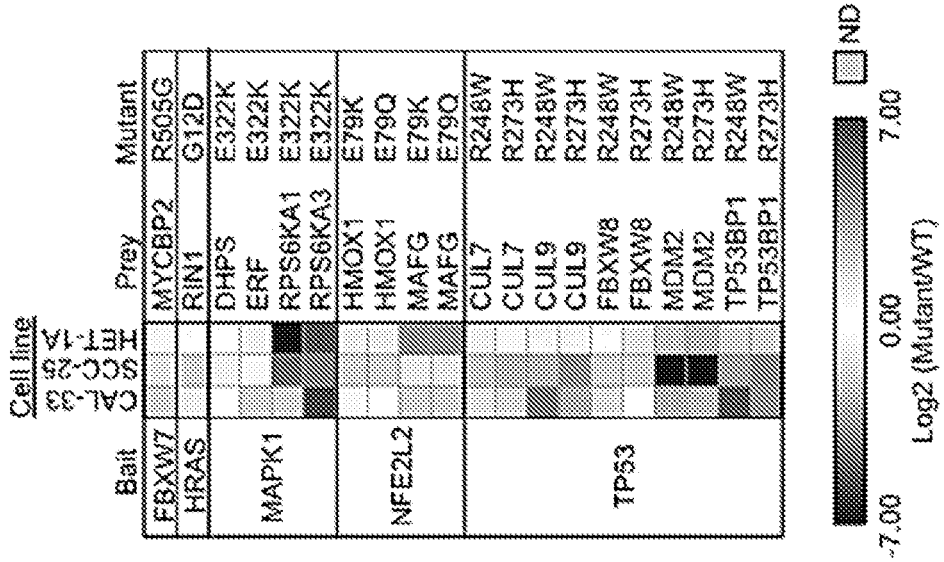
Cell line
CAL-33
SCC-25
HET-1A
Bait
Prey
Mutant
FBXW7
MYCBP2
R505G
HRAS
RIN1
G12D
MAPK1
DHPS
E322K
ERF
E322K
RPS6KA1
E322K
RPS6KA3
E322K
NFE2L2
HMOX1
E79K
HMOX1
E79Q
MAFG
E79K
MAFG
E79Q
TP53
CUL7
R248W
CUL7
R273H
CUL9
R248W
CUL9
R273H
FBXW8
R248W
FBXW8
R273H
MDM2
R248W
MDM2
R273H
TP53BP1
R248W
TP53BP1
R273H
ND
-7.00
0.00
7.00
Log2 (Mutant/WT)

FIG. 18

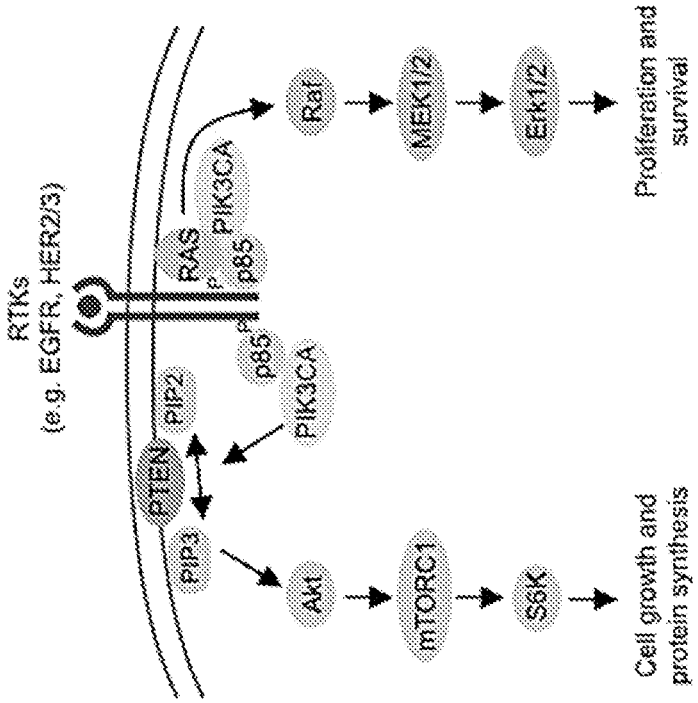
RTKs
(e.g. EGFR, HER2/3)
RAS
PIK3CA
p85
Raf
MEK1/2
Erk1/2
Proliferation and survival
PTEN
PIP2
PIP3
p85
PIK3CA
Akt
mTORC1
S6K
Cell growth and protein synthesis

FIG. 19A

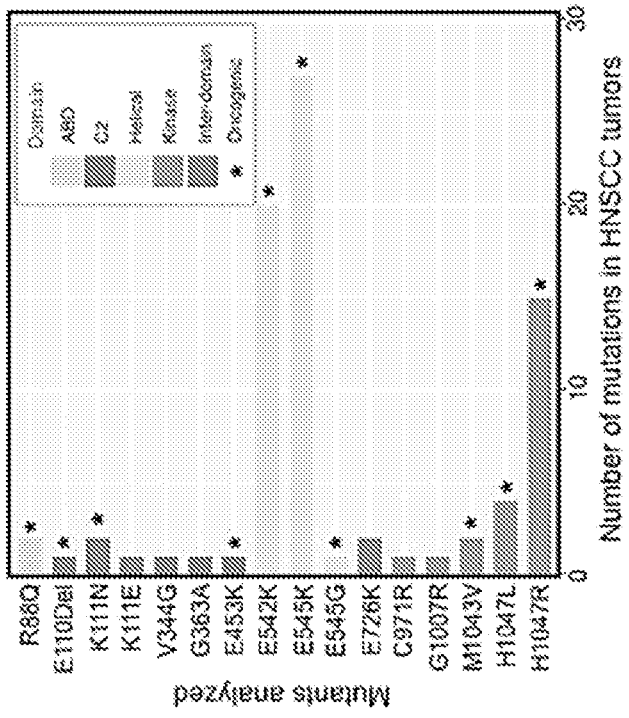
Domain
ABD
C2
Helical
Kinase
Inter-domain
Oncogenic
R88Q
E110Del
K111N
K111E
V344G
G363A
E453K
E542K
E545K
E545G
E726K
C971R
G1007R
M1043V
H1047L
H1047R
Mutants analyzed
0
10
20
30
Number of mutations in HNSCC tumors

FIG. 19B

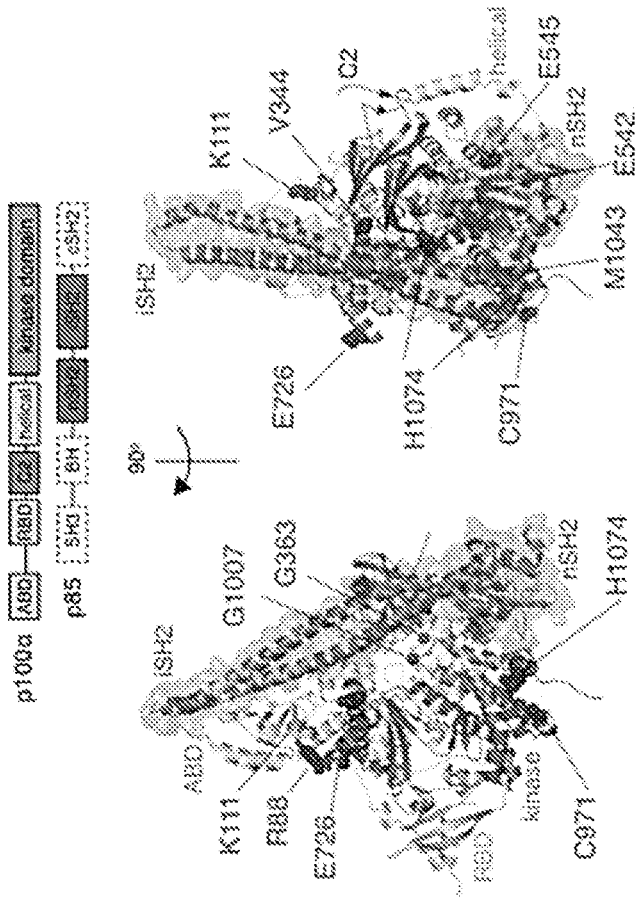
p110α
ABD
RBD
Helical
Kinase domain
p85
SH3
BH
nSH2
iSH2
90°
iSH2
K111
V344
C2
E545
nSH2
E542
M1043
H1074
C971
E726
ABD
K111
R88
E726
G1007
G363
iSH2
nSH2
H1074
C971
kinase

FIG. 19C

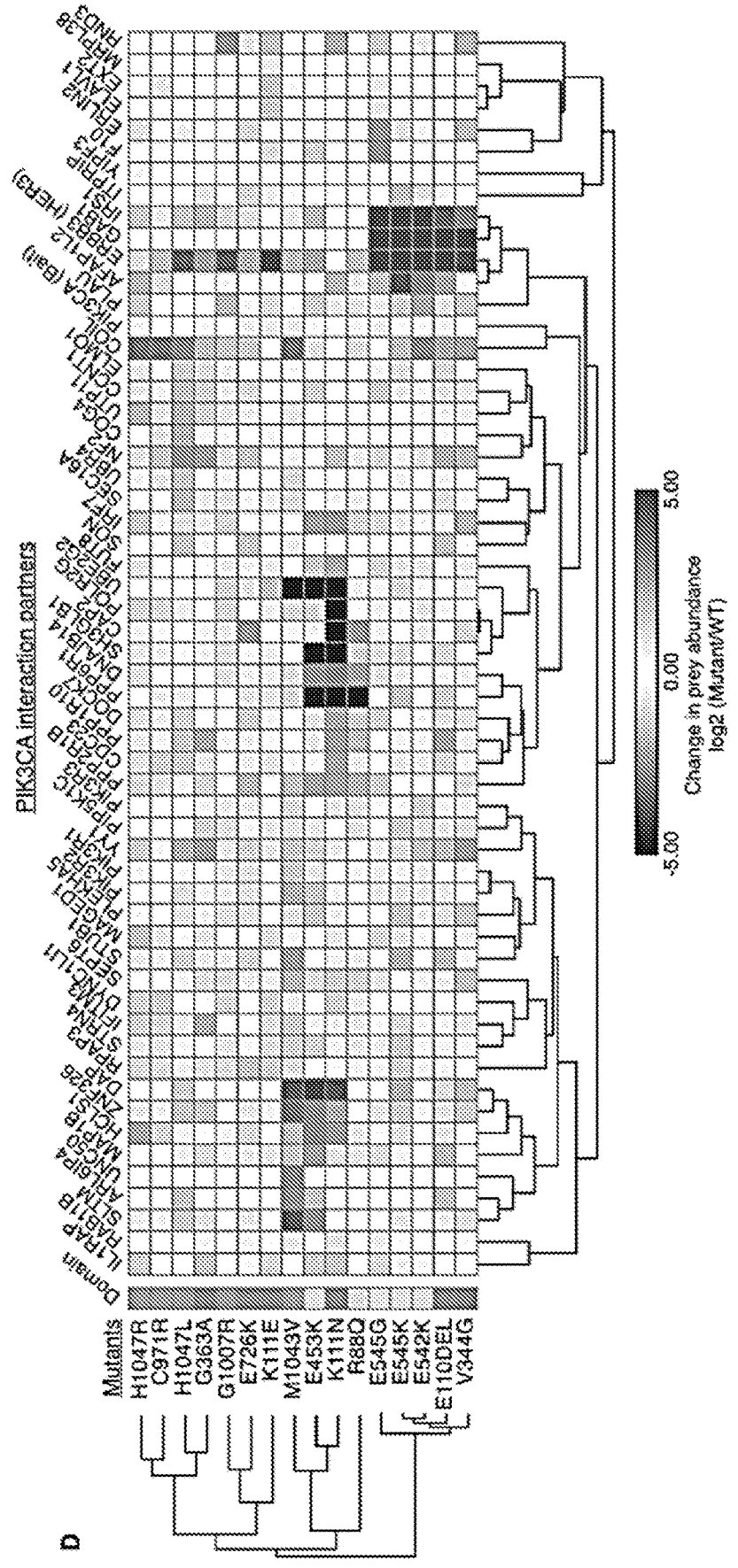
D
Mutants
H1047R
C971R
H1047L
G363A
G1007R
E726K
K111E
M1043V
E453K
K111N
R88Q
E545G
E545K
E542K
E110DELL
V344G
PIK3CA interaction partners
Domain
5.00
0.00
-5.00
Change in prey abundance
log2 (Mutant/WT)

FIG. 19D

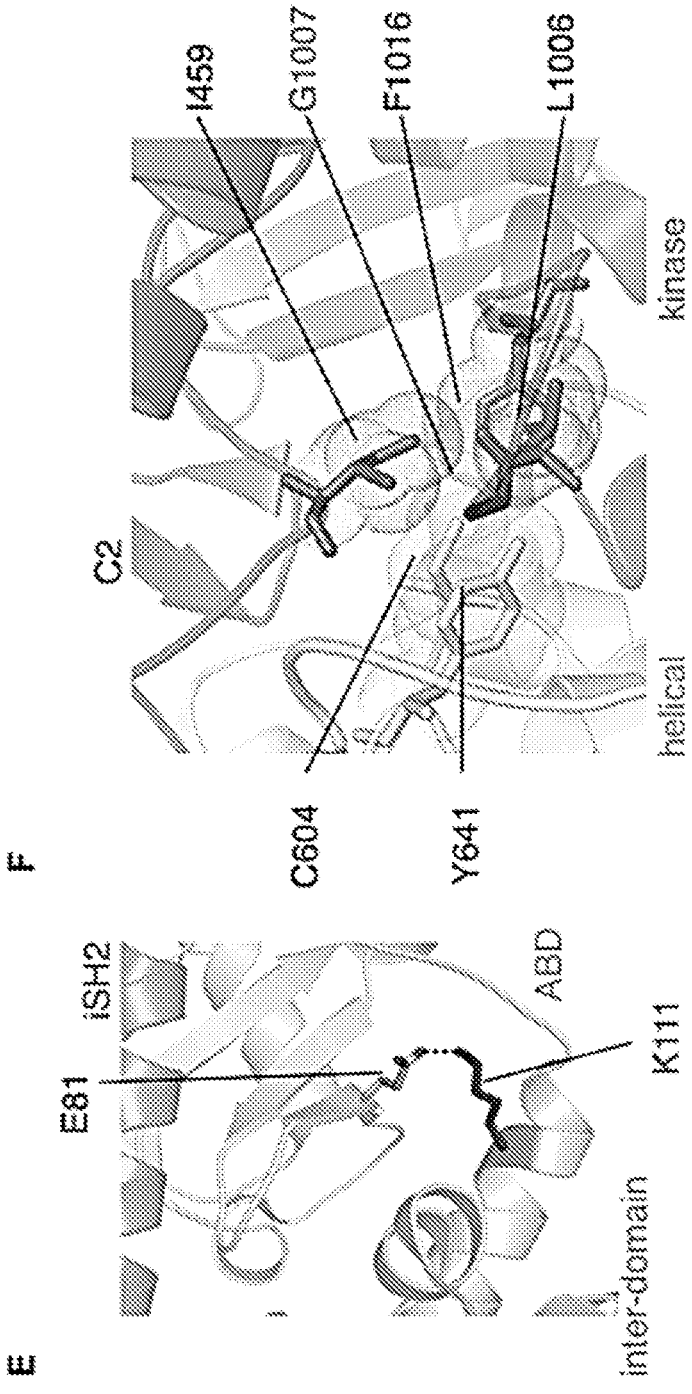

FIG. 19F

FIG. 19E

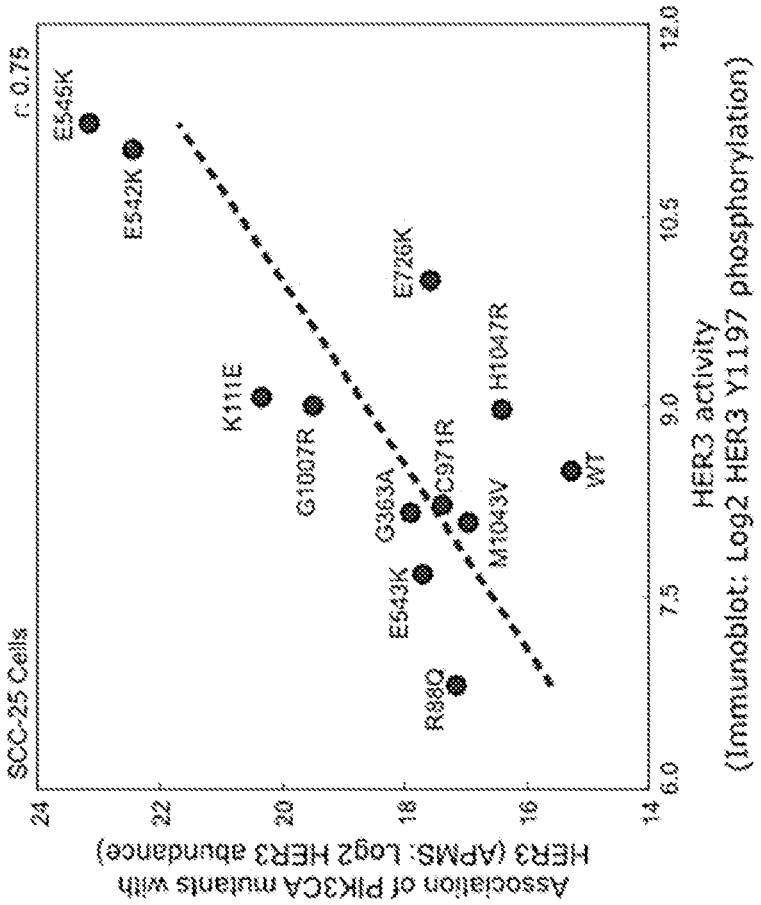
r: 0.75
SCC-25 Cells
E545K
E542K
K111E
G1007R
G363A
E543K
R88Q
C971R
M1043V
E726K
H1047R
WT
24
22
20
18
16
14
6.0
7.5
9.0
10.5
12.0
Association of PIK3CA mutants with HER3 (APMS: Log2 HER3 abundance)
HER3 activity (Immunoblot: Log2 HER3 Y1197 phosphorylation)

FIG. 19G

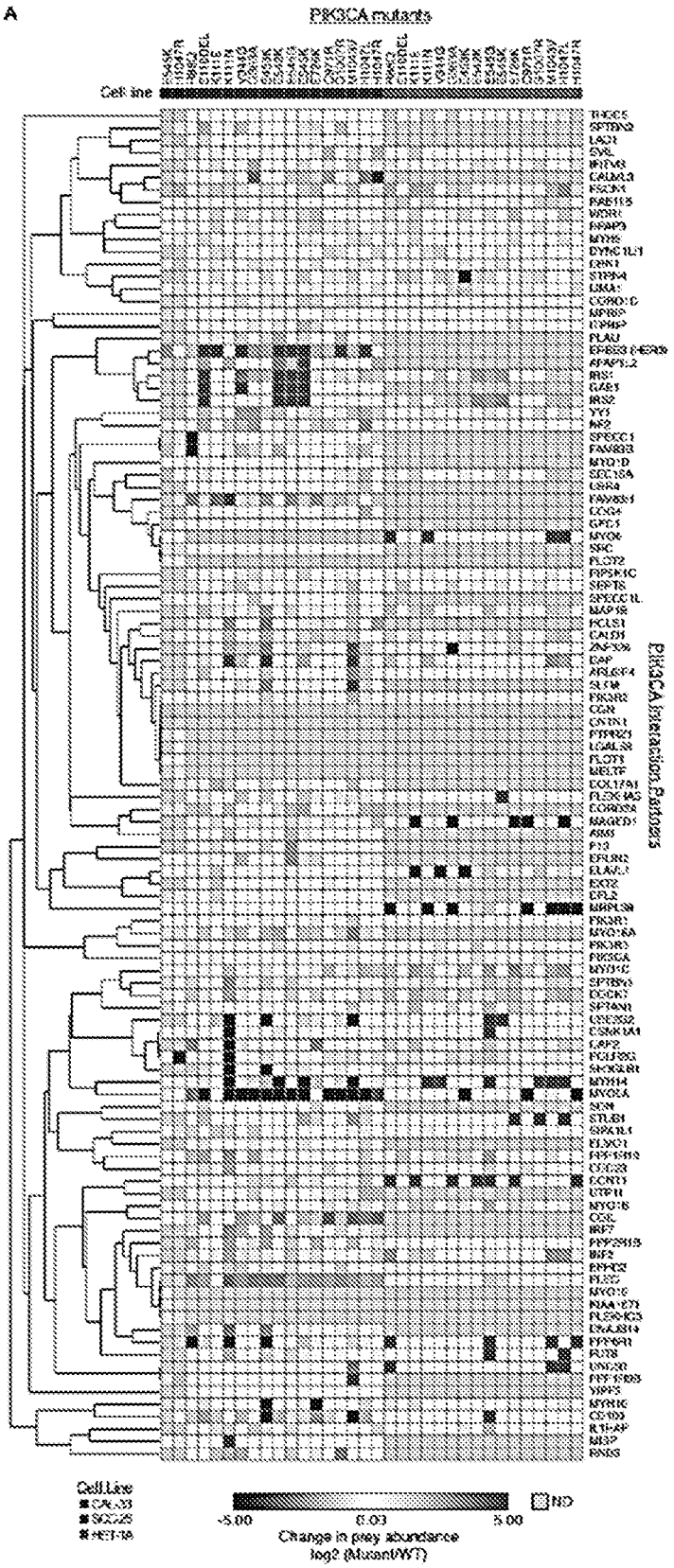
A
PIK3CA mutants
Cell line
PIK3CA interaction Partners
Cell Line
Change in prey abundance
log2 (Mutant/WT)
ND

FIG. 20A

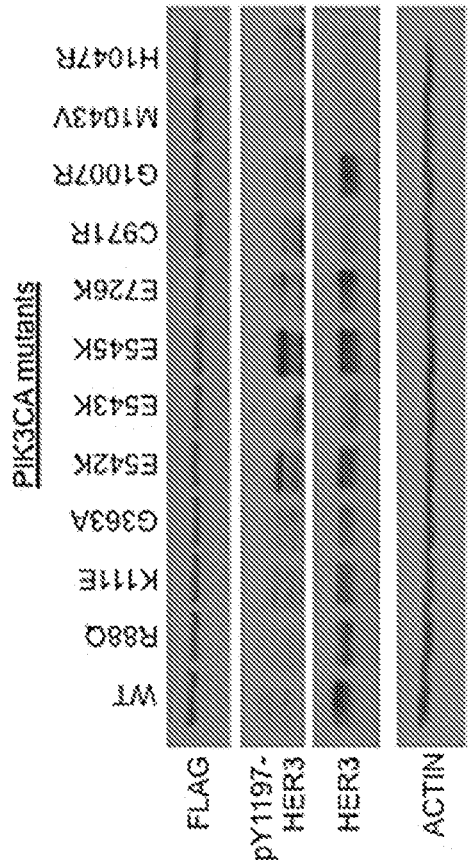
PIK3CA mutants
WT
R88Q
K111E
G363A
E542K
E543K
E545K
E726K
C971R
G1007R
M1043V
H1047R
FLAG
pY1197-HER3
HER3
ACTIN

FIG. 20B

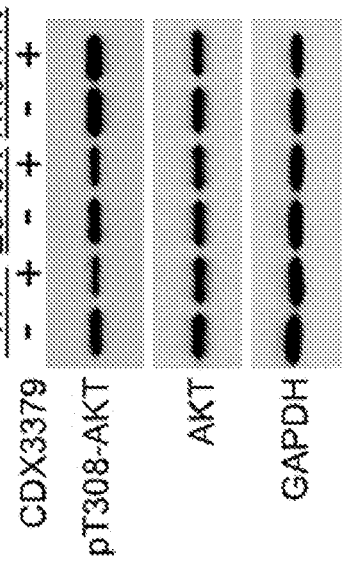

FIG. 20C

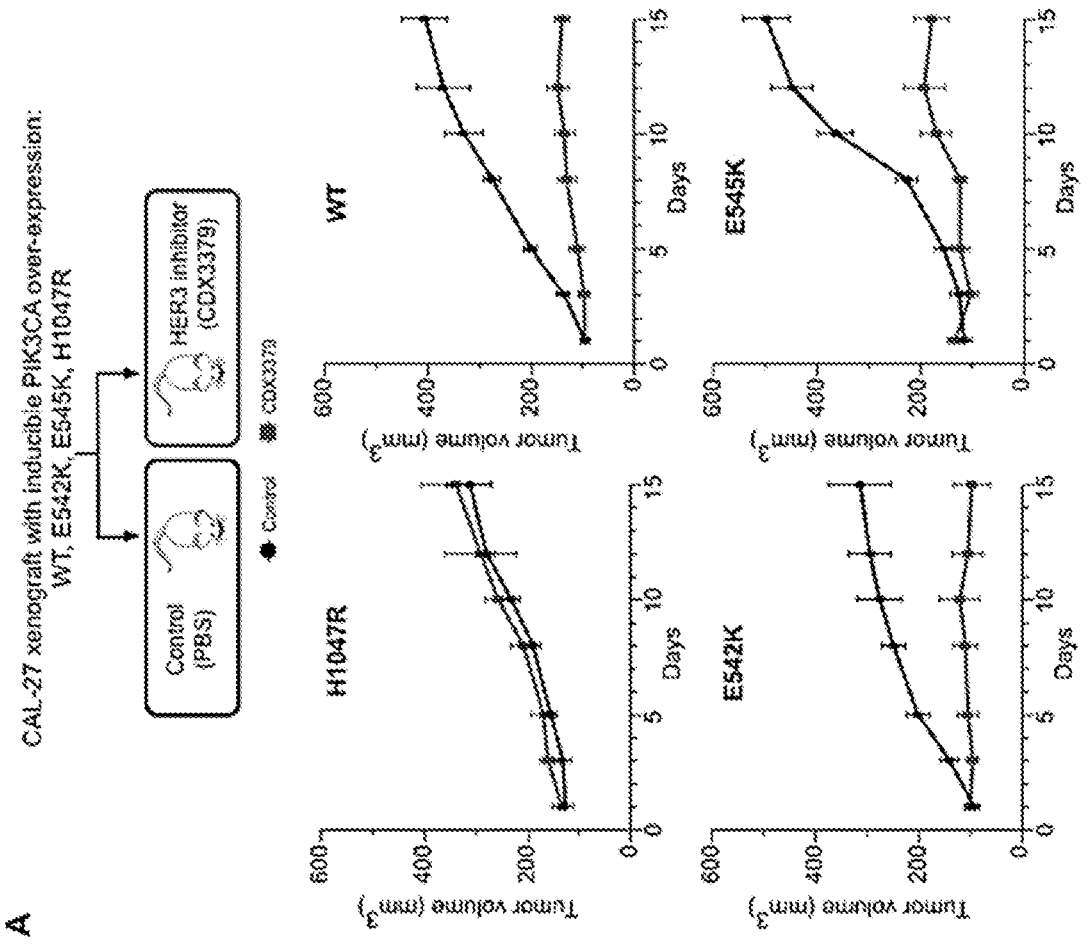
A
CAL-27 xenograft with inducible PIK3CA over-expression:
WT, E542K, E545K, H1047R
Control (PBS)
HER3 inhibitor (COX3379)
Control
coxsara
WT
H1047R
E545K
E542K
Tumor volume (mm3)
Days
0
200
400
600
5
10
15

FIG. 21A

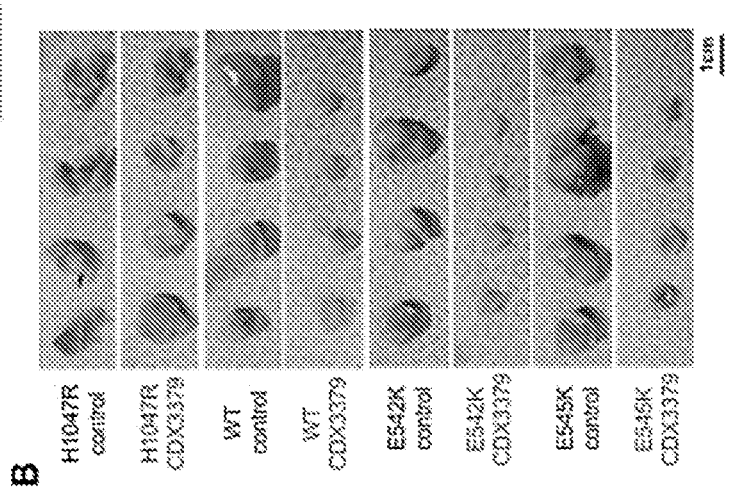
B
H1047R control
H1047R CDX3379
WT control
WT CDX3379
E542K control
E542K CDX3379
E545K control
E545K CDX3379
1cm

FIG. 21B

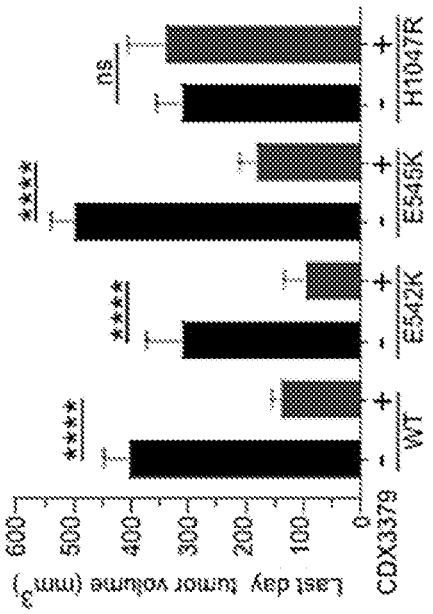
Last day tumor volume (mm³)
600
500
400
300
200
100
0
****
****
****
****
ns
CDX3379
-
+
WT
-
+
E542K
-
+
E545K
-
+
H1047R

FIG. 21C

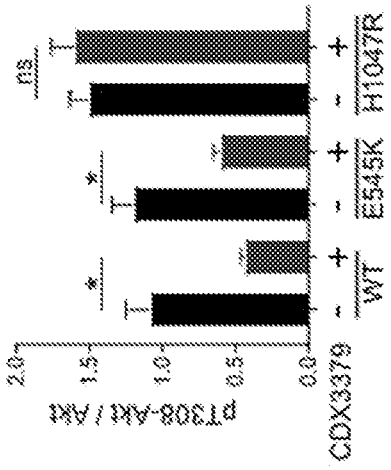

FIG. 21D

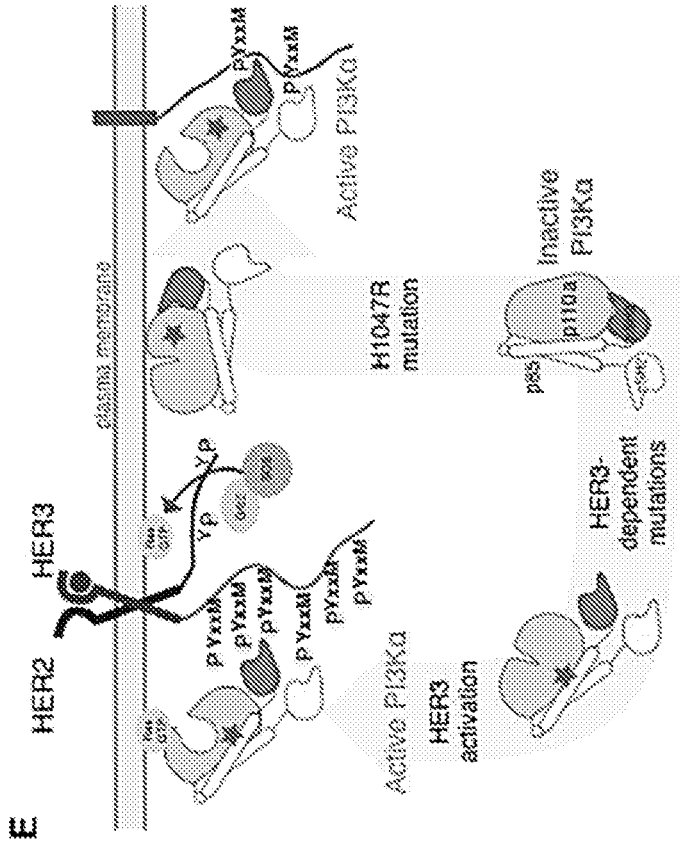
E
HER2
HER3
plasma membrane
pYxxM
Yp
Active PI3Kα
HER3 activation
H1047R mutation
Inactive PI3Kα
p85
p110α
HER3-dependent mutations

FIG. 21E


pLVX-TetOne-puro C-min 3xFLAG DEST (11603 bp)
tggaagggctaattcactcccaaagaagacaagatatccttgatctgtggatctaccacacacaaggctacttccctgattagcagaactacacaccagggccaggg
HIV-1 5 LTR
gtcagatatccactgacctttggatggtgctacaagctagtaccagttgagccagataaggtagaagaggccaataaaggagagaacaccagcttgttacaccctgt
HIV-1 5 LTR
gagcctgcatgggatggatgacccggagagagaagtgttagagtggaggtttgacagccgcctagcatttcatcacgtggcccgagagctgcatccggagtacttca
HIV-1 5 LTR
agaactgctgatatcgagcttgctacaagggactttccgctggggactttccagggaggcgtggcctgggcgggactggggagtggcgagccctcagatcctgcata
HIV-1 5 LTR
taagcagctgctttttgcctgtactgggtctctctggttagaccagatctgagcctgggagctctctggctaactagggaacccactgcttaagcctcaataaagct
HIV-1 5 LTR
tgccttgagtgcttcaagtagtgtgtgcccgtctgttgtgtgactctggtaactagagatccctcagacccttttagtcagtgtggaaaatctctagcagtggcgcc
HIV-1 5 LTR
cgaacagggacttgaaagcgaaagggaaaccagaggagctctctcgacgcaggactcggcttgctgaagcgcgcacggcaagaggcgagggcggcgactggtgagt
HIV-1 psi pack
acgccaaaaattttgactagcggaggctagaaggagagagatgggtgcgagagcgtcagtattaagcgggggagaattagatcgcgatgggaaaaaattcggttaag
HIV-1 psi pack
gccaggggggaaagaaaaaatataaattaaaacatatagtatgggcaagcagggagctagaacgattcgcagttaatcctggcctgttagaaacatcagaaggctgta
gacaaatactgggacagctacaaccatcccttcagacaggatcagaagaacttagatcattatataatacagtagcaaccctctattgtgtgcatcaaaggatagag
ataaaagacaccaaggaagctttagacaagatagaggaagagcaaaacaaaagtaagaccaccgcacagcaagcggccggccgctgatcttcagacctggaggagga
gatatgagggacaattggagaagtgaattatataaatataaagtagtaaaaattgaaccattaggagtagcacccaccaaggcaaagagaagagtggtgcagagaga
aaaaagagcagtgggaataggagctttgttccttgggttcttgggagcagcaggaagcactatgggcgcagcgtcaatgacgctgacggtacaggccagacaattat
RRE
tgtctggtatagtgcagcagcagaacaatttgctgagggctattgaggcgcaacagcatctgttgcaactcacagtctggggcatcaagcagctccaggcaagaatc
RRE
ctggctgtggaaagatacctaaaggatcaacagctcctggggatttggggttgctctggaaaactcatttgcaccactgctgtgccttggaatgctagttggagtaa
RRE
taaatctctggaacagatttggaatcacacgacctggatggagtgggacagagaaattaacaattacacaagcttaatacactccttaattgaagaatcgcaaaacc
agcaagaaaagaatgaacaagaattattggaattagataaatgggcaagtttgtggaattggtttaacataacaaattggctgtggtatataaaattattcataatg
atagtaggaggcttggtaggtttaagaatagtttttgctgtactttctatagtgaatagagttaggcagggatattcaccattatcgtttcagacccacctcccaac

FIG. 22

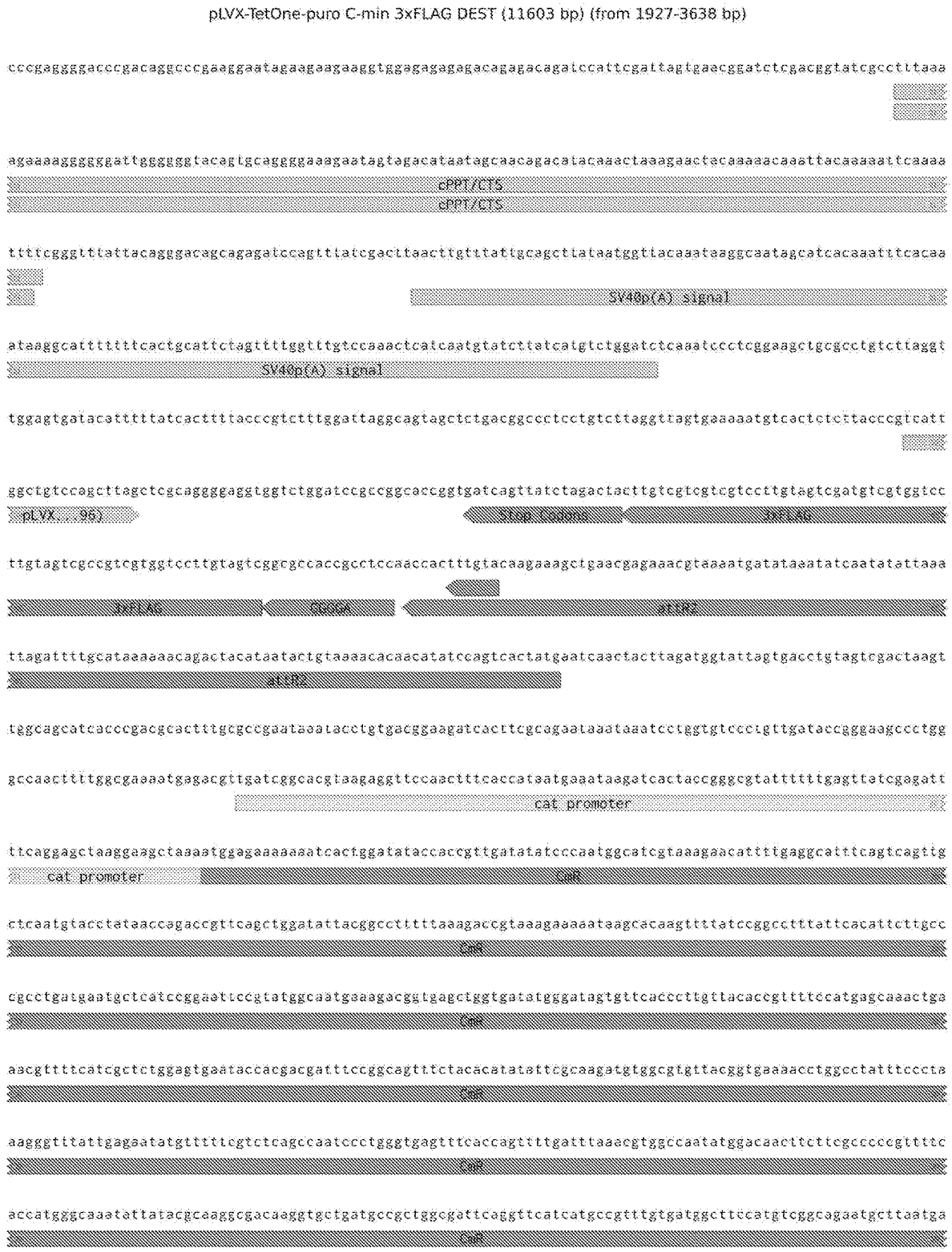

FIG. 22 (continued)

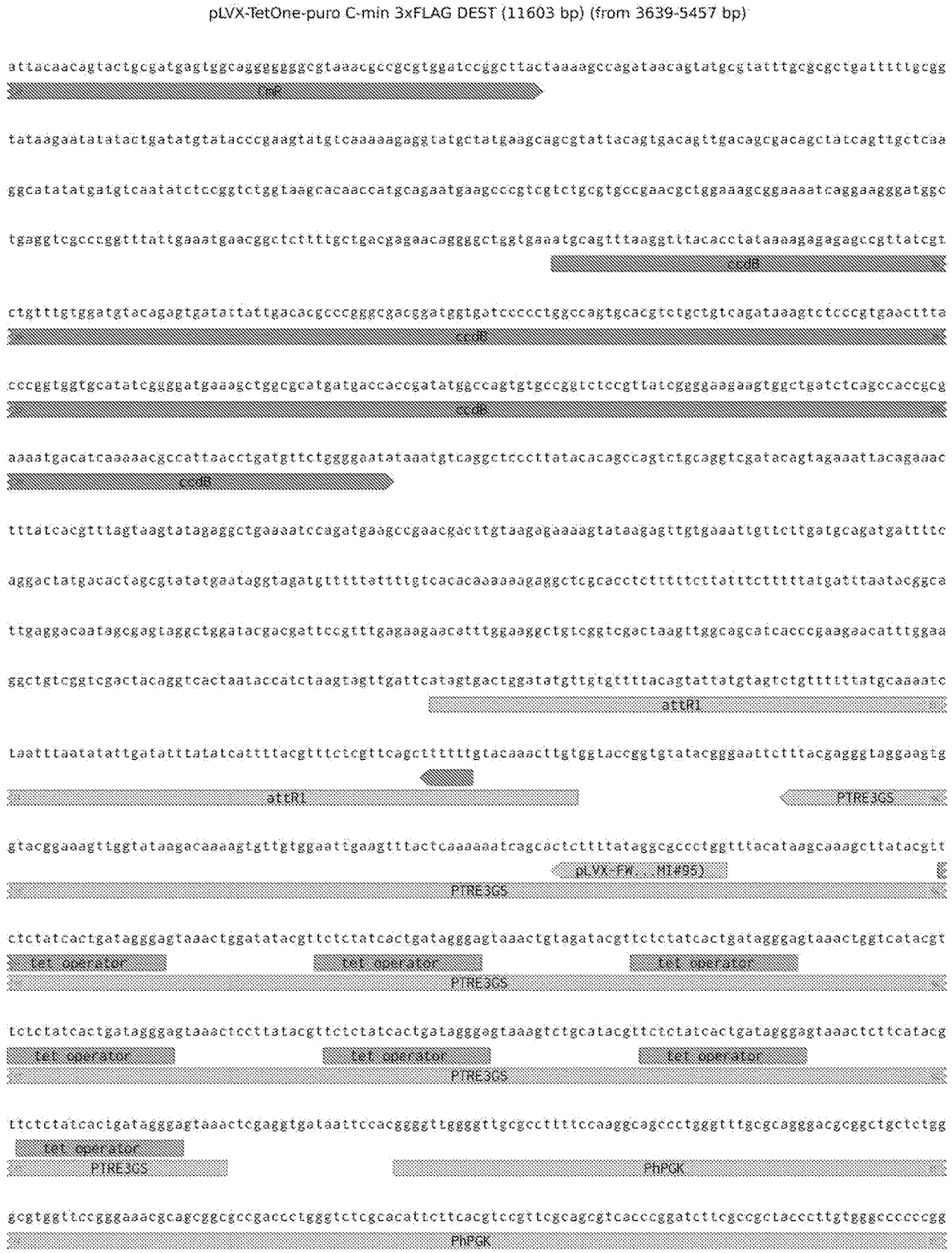

FIG. 22 (continued)

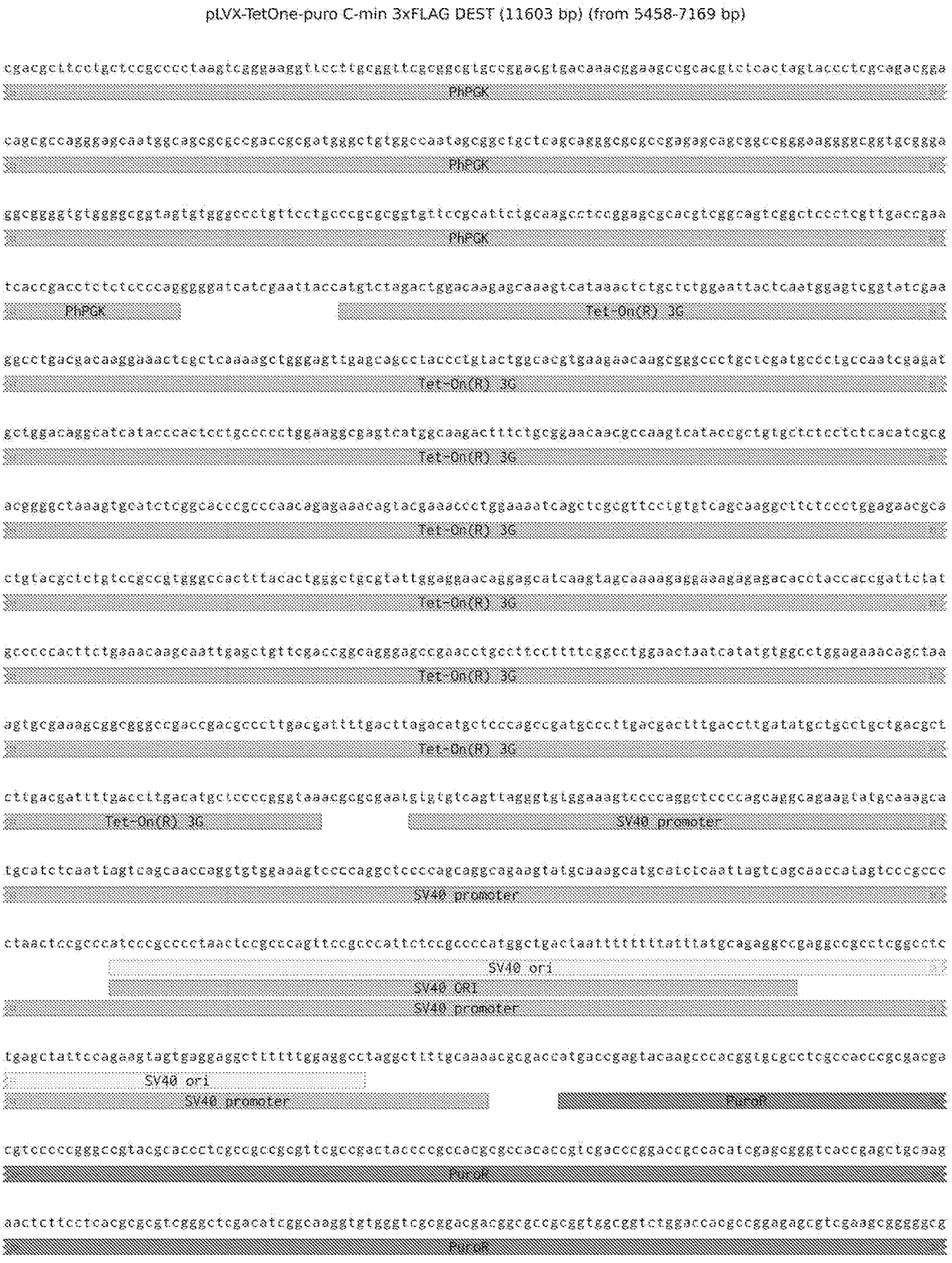

FIG. 22 (continued)

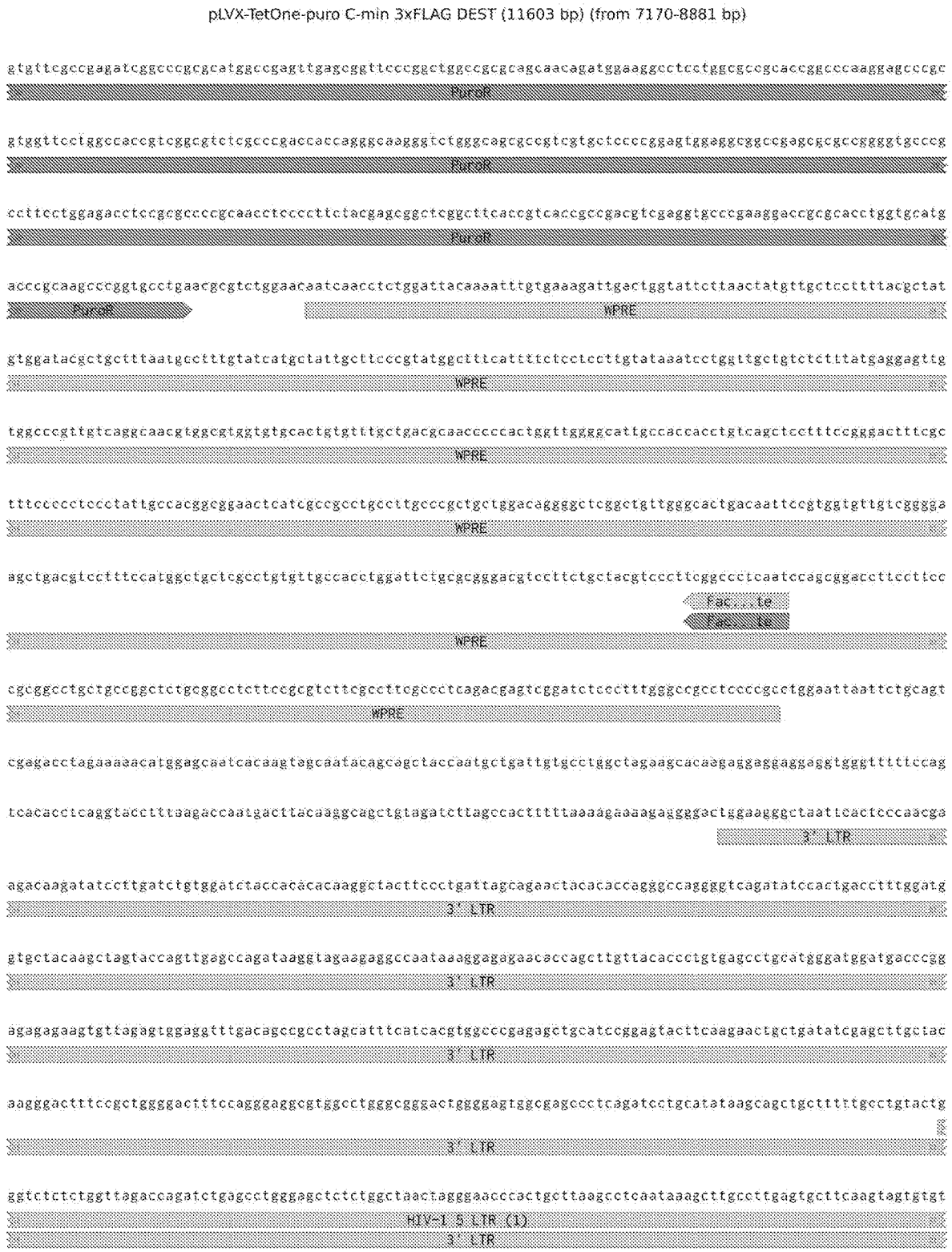

FIG. 22 (continued)

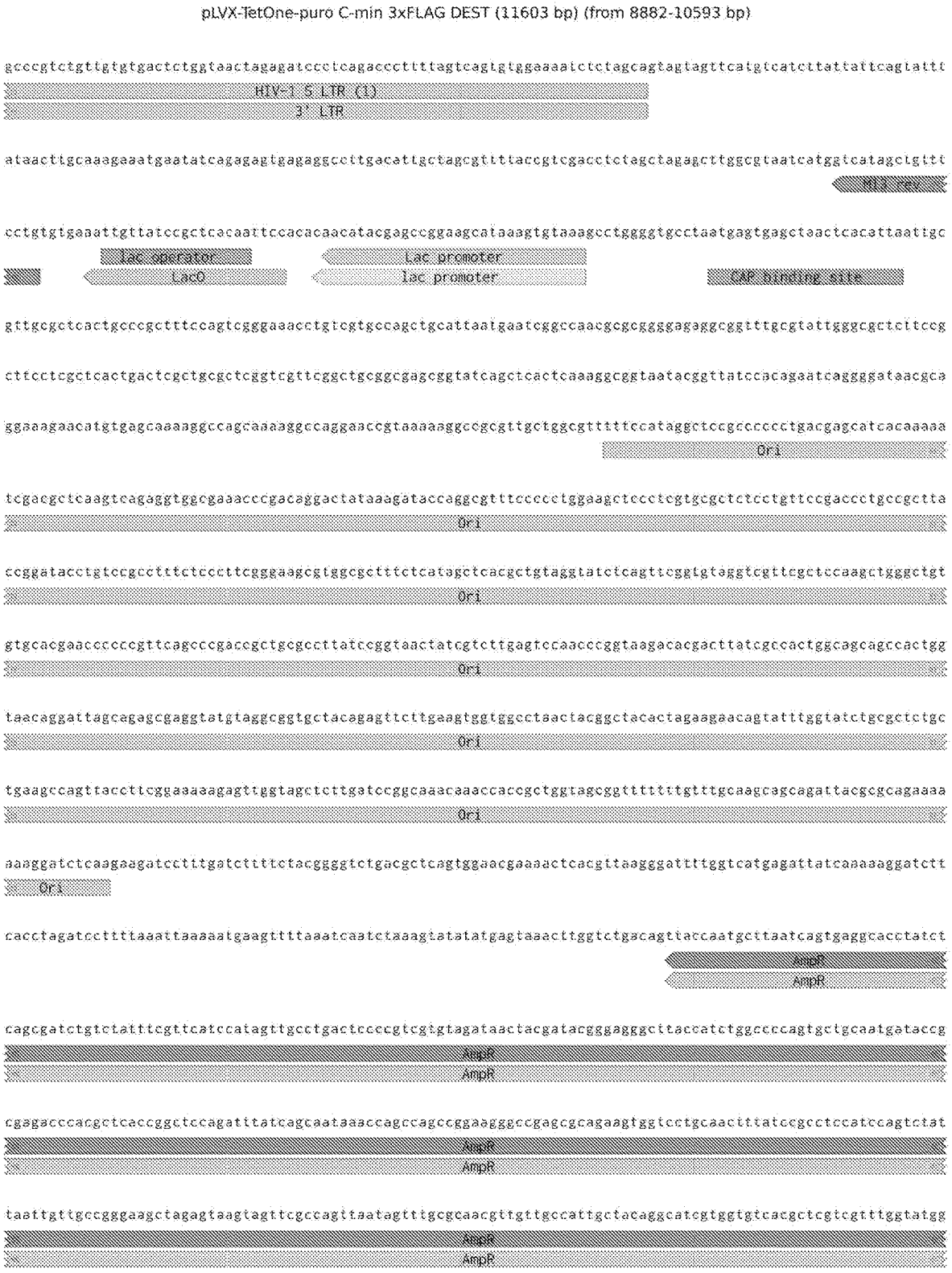

FIG. 22 (continued)

FIG. 22 (continued)


(from 1-1926 bp)
pLVX-TetOne-puro N-min 3xFLAG DEST (11612 bp)
HIV-1 5 LTR
HIV-1 psi pack
RRE

FIG. 23

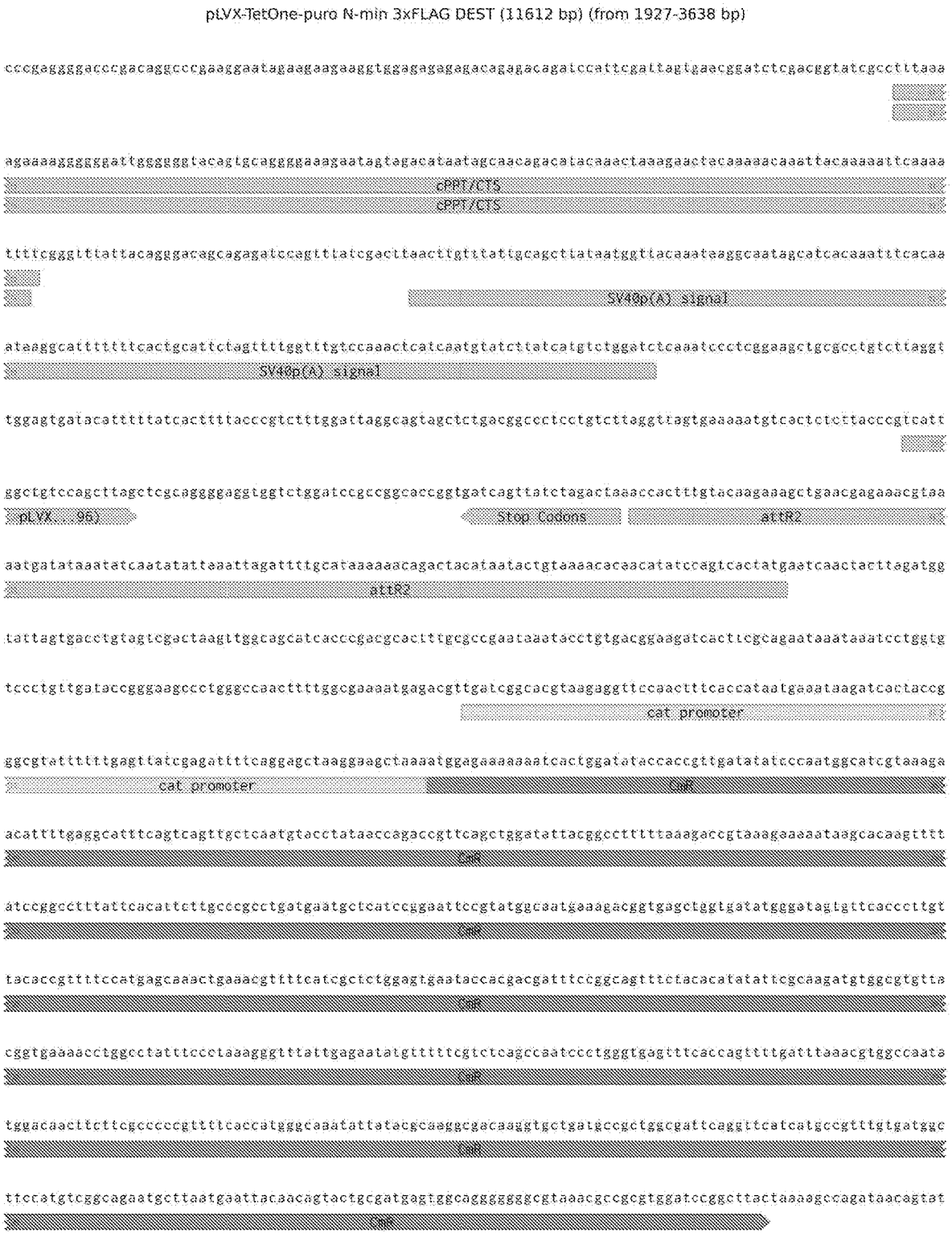

FIG. 23 (continued)

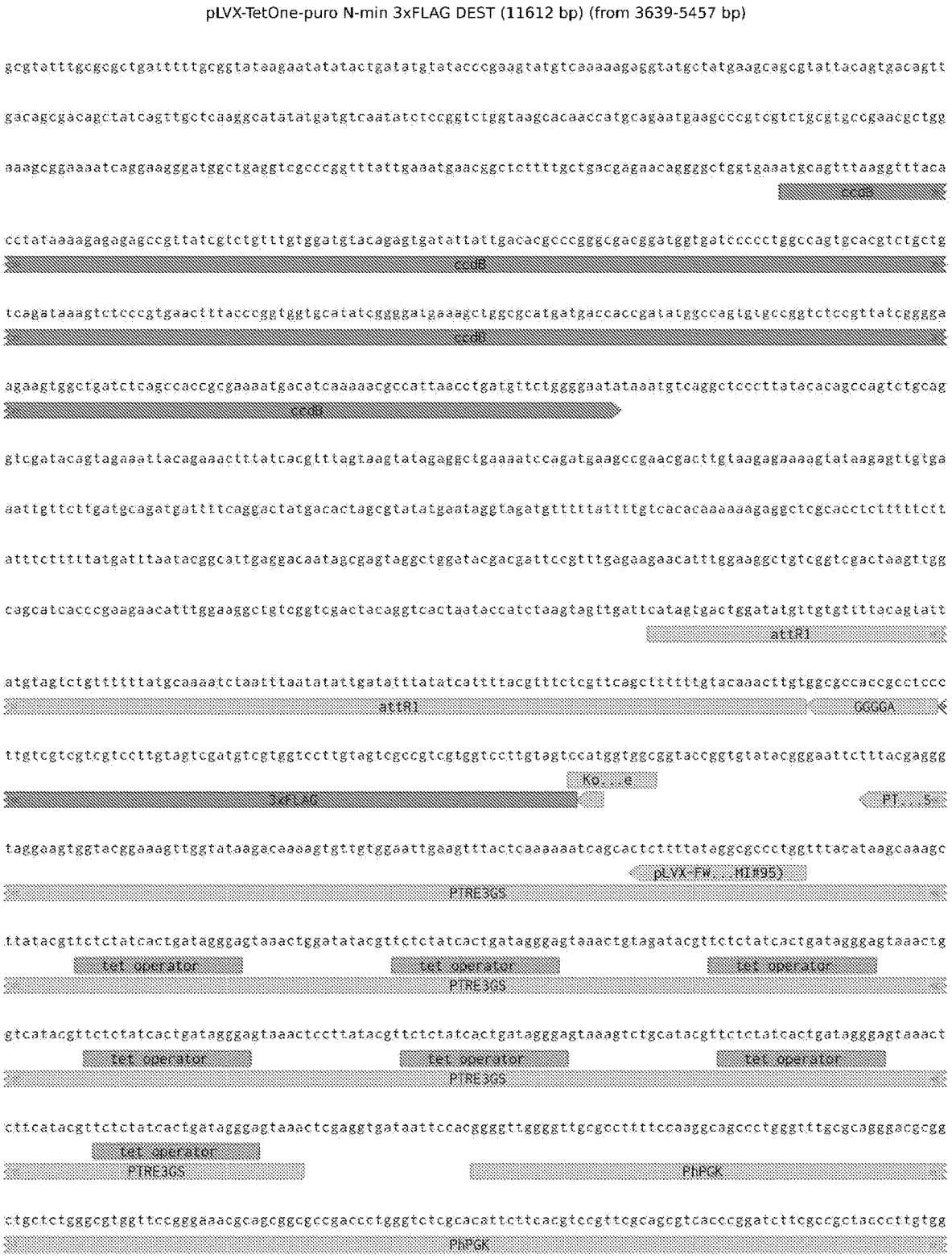

FIG. 23 (continued)

FIG. 23 (continued)

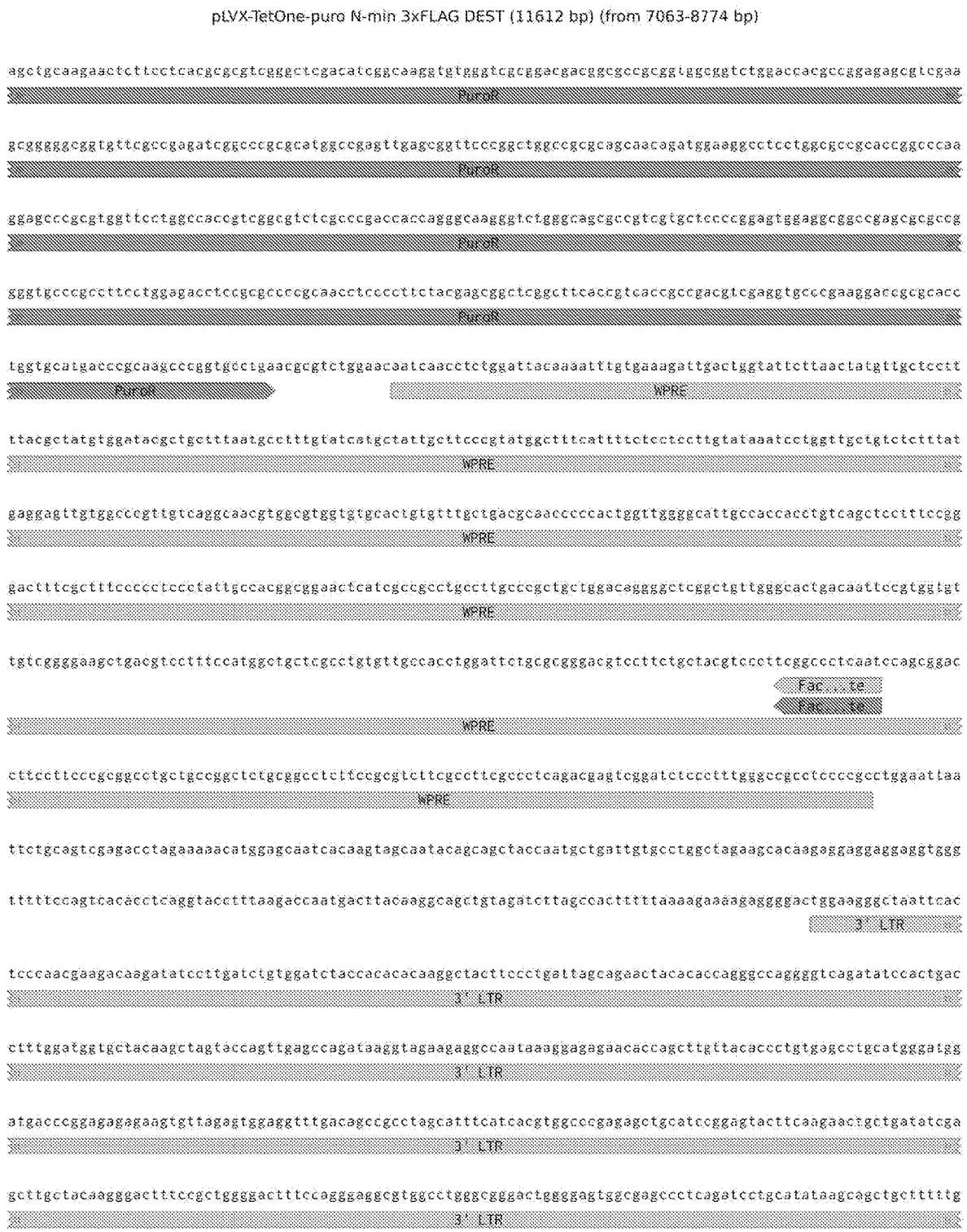

FIG. 23 (continued)

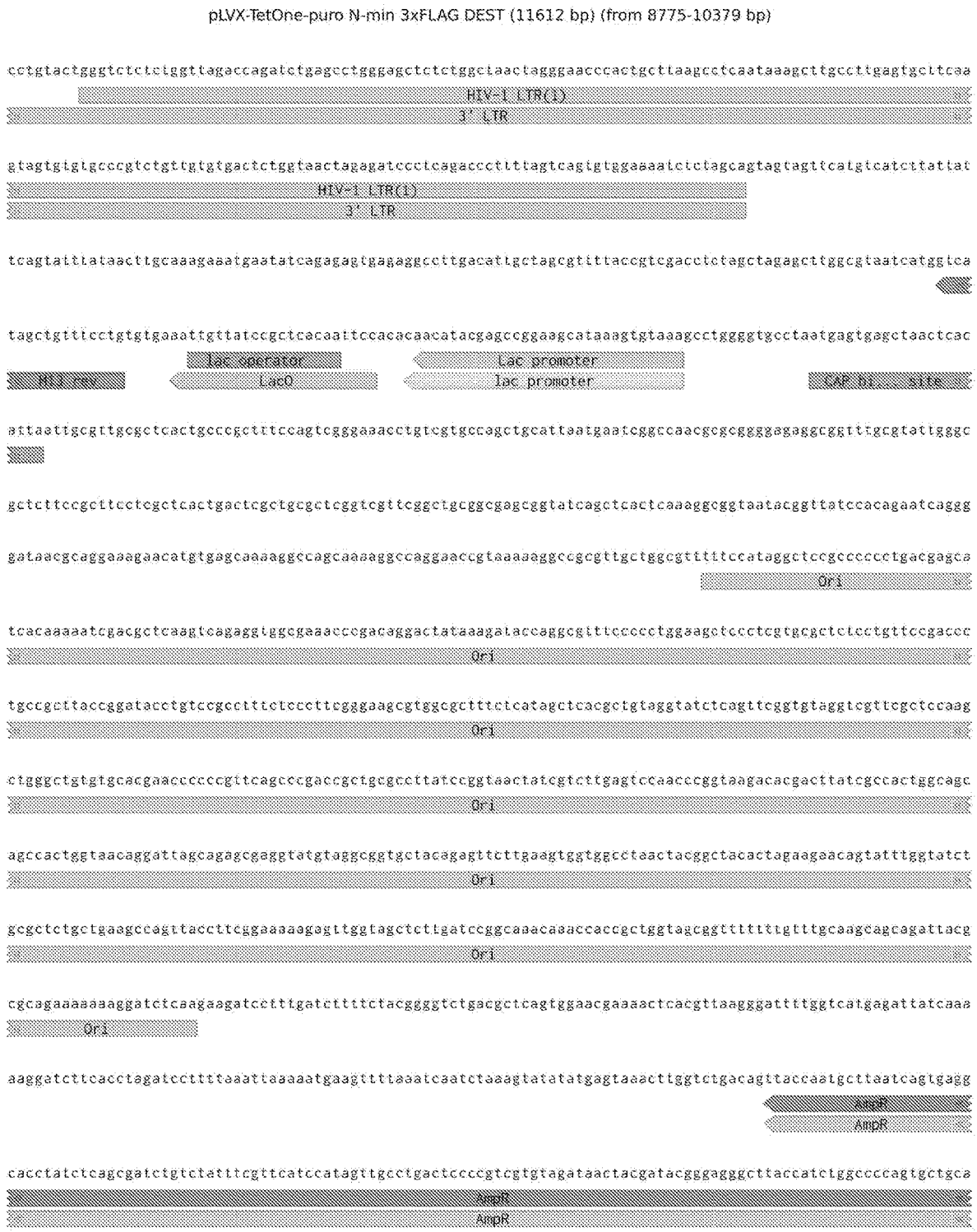

FIG. 23 (continued)

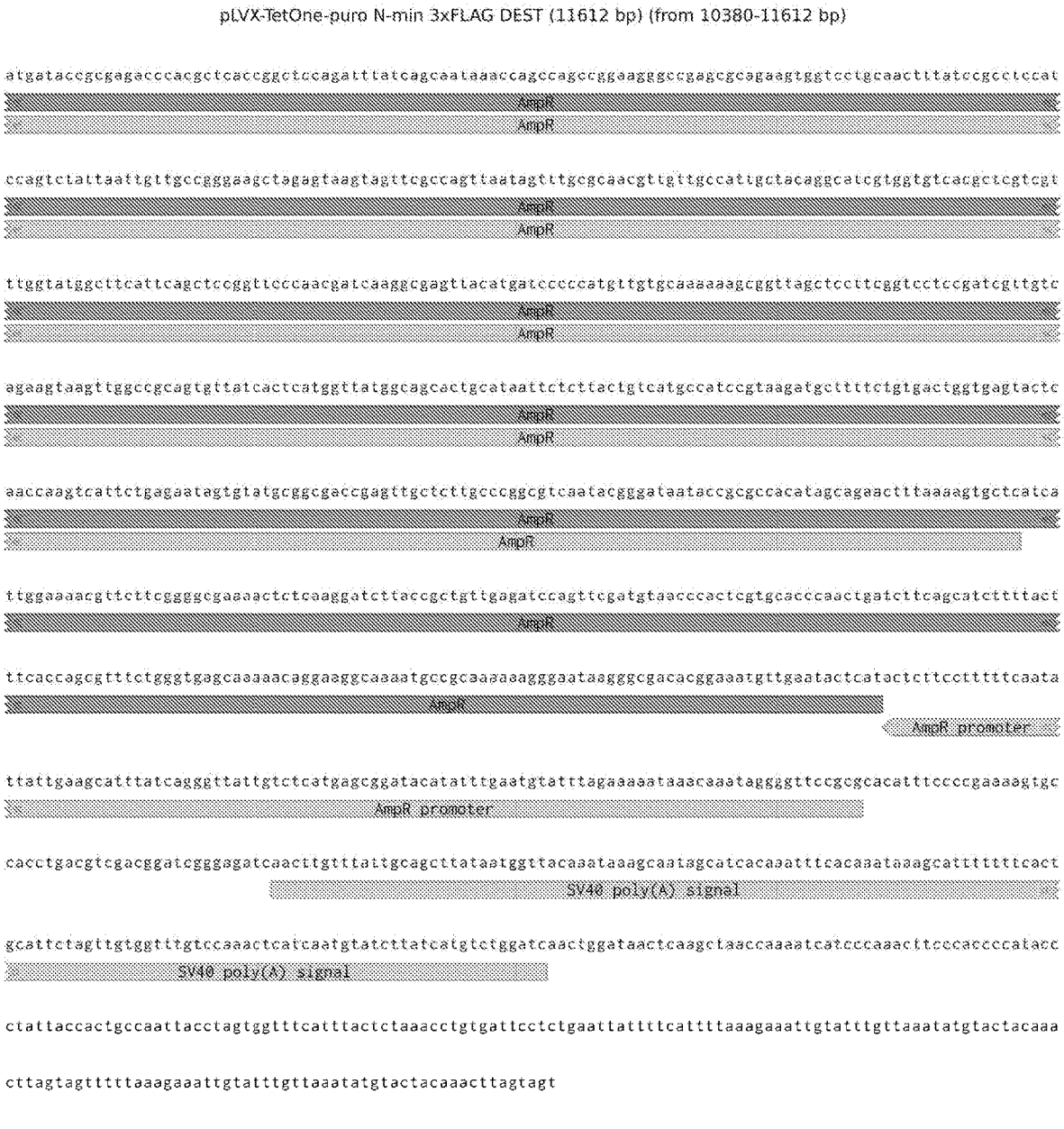

FIG. 23 (continued)

SYSTEMS FOR AND METHODS OF TREATMENT SELECTION

CROSS-REFERENCE TO RELATED APPLICATIONS

[0001] This application claims the benefit of U.S. Application No. 63/091,924, filed on Oct. 14, 2020, the contents of which are hereby incorporated by reference in their entirety.

STATEMENT REGARDING FEDERALLY SPONSORED RESEARCH

[0002] This invention was made with government support under grant number U54 CA209891 awarded by the National Institutes of Health (NIH). The government has certain rights in the invention.

REFERENCE TO AN ELECTRONIC SEQUENCE LISTING

[0003] The contents of the electronic sequence listing (UCAL021US_SeqListing.txt; size: 69,509 bytes; and date of creation: Dec. 15, 2023) is herein incorporated by reference in its entirety.

FIELD OF INVENTION

[0004] The disclosure relates to a system comprising software that identifies drug targets and predicts responsiveness of cancer subjects to certain disease modifying drugs. Embodiments of the disclosure include methods comprising calculating a differential interaction score (DIS), correlating the DIS with the likelihood that a dysfunctional protein-protein interaction is the causal agent of a hyperproliferative disorder, identifying a drug target based on the causal agent, evaluating a therapeutic specific to the drug target, thereby restoring and/or alleviating dysfunction within the protein network, identifying a subject responsive to a hyperproliferative disorder treatment based upon the causal agent, and monitoring the subject's response to the hyperproliferative disorder treatment.

BACKGROUND

[0005] Genome sequencing efforts over the past decade have profiled the genetic landscape of thousands of patient tumors and solidified the concept of cancer as a highly heterogeneous disease (Biankin et al., 2012; Cancer Genome Atlas, Network, 2012, 2015; Cancer Genome Atlas Research, Network, 2008, 2011; Hoadley et al., 2018; Robinson et al., 2015; Stephens et al., 2012). Evidence from these efforts has also revealed that nearly every human gene is altered in cancer, presenting an overwhelming degree of complexity that has limited the power of connecting individual alterations with cancer patient phenotypes. As a consequence, the field has begun to interpret this heterogeneous genetic landscape in the context of hallmark cancer pathways, with the hypothesis that rare individual alterations among a population converge on more commonly altered protein networks and signaling cascades (Hanahan and Weinberg, 2011; Hanahan et al., 2000; Krogan et al., 2015; Vogelstein et al., 2004). As such, a fundamental component of many cancer genome analyses has been the summarization of genetic alterations in the context of well-characterized cancer pathway diagrams (Biankin et al., 2012; Cancer Genome Atlas, Network, 2012, 2015; Cancer Genome Atlas Research, Network, 2008, 2011; Li et al., 2014; Stephens et al., 2012).

[0006] To further facilitate such interpretation, powerful network biology approaches have been developed to bridge the gap between genetic alterations and phenotypes. In such approaches, protein network knowledge is used to aggregate individual tumor mutations and, on the basis of altered networks, predict patient survival and response to therapy (Akavia et al., 2010; Cerami et al., 2010; Consequences and Consortium, Pathway Analysis working group of the International Cancer Genome, 2015; Drier et al., 2013; Hofree et al., 2013; Horn et al., 2018; Leiserson et al., 2015; Li et al., 2016; Paczkowska et al., 2020; Paull et al., 2013; Reyna et al., 2020). However, an important factor in the utility of such network-based approaches is a strong reliance on existing databases of molecular interactions. Publicly available human molecular networks have been populated primarily by systematic efforts to determine protein-protein interactions (PPIs) using large-scale yeast two-hybrid screening (Luck et al., 2020; Rolland et al., 2014) or, more recently, affinity purification-mass spectrometry (AP-MS) (Hein et al., 2015; Huttlin et al., 2015, 2017). The vast majority of PPIs in such databases have been collected either without human cellular context (yeast two-hybrid) or in workhorse cell lines such as HEK293T embryonic kidney cells that lack cancer context. Importantly, there is a growing recognition that such PPIs can vary significantly across cellular contexts (Huttlin et al., 2020). Thus, the generation and incorporation of cancer-specific physical and functional networks may represent a critical component to interpret and predict cancer biology and its clinical outcomes (Krogan et al., 2015).

[0007] Breast cancer (BC) is the most common malignancy in women and the second leading cause of cancer-related death in the United States (American Cancer Society, 2019; Anp et al., 2020; Society, 2019), where an estimated 276,480 women and 2,620 men will be newly diagnosed in 2020 (Anp et al., 2020). The disease has been divided into different subtypes, based largely on the presence or absence of three key proteins: estrogen receptor (ER), progesterone receptor (PR), and human epidermal growth factor receptor 2 (HER2/ERBB2). Despite this and much additional heterogeneity at the molecular level, the majority of BC patients are treated using untailored chemotherapy or hormone therapies. Therefore, an urgent need is to develop targeted therapies matched to the specific molecular alterations in a tumor, with the goal of achieving better efficacy and avoiding unnecessary treatment.

[0008] HNSCC is a cancer affecting squamous mucosal epithelial cells in the oral cavity, pharynx, and larynx, estimated to be the sixth most common malignancy worldwide (Riaz et al., 2014). The primary causes of HNSCC are carcinogen exposure (e.g., alcohol and tobacco) or infection by the human papillomavirus (HPV). Despite a wealth of data detailing the genetic alterations in this tumor type (Cancer Genome Atlas Network, 2015), only two types of targeted therapies are presently available (Riaz et al., 2014). Therefore, HNSCC also presents a unique opportunity to apply emerging, quantitative, systems approaches to identify new diagnostic subtypes and therapeutic targets.

[0009] Network approaches can also be used to further our understanding of existing chemotherapeutic targets, such as PIK3CA, the most commonly mutated oncogene in HNSCC. PIK3CA encodes p110alpha (p110α), the catalytic

subunit of phosphatidylinositol 3-kinase (P1I3K), and is a potent mediator of cellular signaling. It interacts with both intracellular small GTPases (e.g., RAS proteins) as well as receptor kinases (e.g., EGFR) to regulate downstream signaling via both the MAPK/ERK pathway and the Akt/mTOR pathway. Hyperactivation of this pathway is a hallmark of numerous tumor types and can be directly attributed to either amplification or mutation of the PIK3CA gene (Bailey et al., 2018). The majority of PIK3CA mutations reside in the helical (E542K and E545K) and kinase domains (H1047R) and have been studied extensively. For example, the H1047R mutation enhances the association of PI3K with the cell membrane, allowing it to bypass the requirement of association with RAS (Zhao and Vogt, 2008). Meanwhile, helical domain mutants (E545K, E542K) disrupt the interaction of p110α with its auto-inhibitory p85 subunits (PIK3R1/2/3), leading to increased kinase activation (Carson et al., 2008; Miled et al., 2007; Shekar et al., 2005). The functions of the remaining non-canonical mutations are less clear. While some have previously been profiled for oncogenic activity (Dogruluk et al., 2015; Lui et al., 2013; Rudd et al., 2011), much remains to be learned about how these mutants regulate PIK3CA function.

[0010] Accordingly, there remains a need for methods and systems for facilitating interpretation of cancer biology, predicting clinical outcomes, and developing treatment strategies.

SUMMARY OF EMBODIMENTS

[0011] Advances in DNA sequencing technology have enabled the widespread analysis of breast tumor genomes, creating a catalog of genetic mutations that may initiate or drive tumor progression (Cancer Genome Atlas, Network, 2012; Stephens et al., 2012). In addition to common mutations in well-known cancer genes, such as TP53 and PIK3CA, breast cancers harbor many additional mutations, each of which are seen rarely across the patient population (Cancer Genome Atlas, Network, 2012; Stephens et al., 2012). A key question is how these less common alterations, dispersed across a multitude of genes, elicit pathologic consequences, and patient outcomes. An important answer may lie in understanding how individual gene mutations converge on multi-gene functional modules, including the signaling pathways orchestrating cell proliferation and apoptosis and DNA repair complexes (Cho et al., 2016; Creixell et al., 2015; Hofree et al., 2013; Knijnenburg et al., 2018; Leiserson et al., 2015; Paczkowska et al., 2020; Reyna et al., 2020; Sanchez-Vega et al., 2018; Wood et al., 2007).

[0012] PIK3CA and AKT activating mutations and copy-number amplifications are frequently found in many cancer types including BC (Brugge et al., 2007; Carpten et al., 2007; Fruman et al., 2017; Vivanco and Sawyers, 2002; Yuan and Cantley, 2008), indicating that the PI3K/AKT pathway is a key signaling module for cancer cell proliferation, and thus an attractive target for therapeutic intervention (McCubrey et al., 2012; Pal et al., 2010; Yap et al., 2011). Given its substantial role in tumorigenesis, however, how this signaling pathway is regulated by other proteins rather than mutations and/or alterations in the PIK3CA and AKT genes still remains largely unknown.

[0013] BRCA1 is a major hereditary cancer susceptibility gene (Futreal et al., 1994; Miki et al., 1994) that plays critical roles in DNA repair by homologous recombination (HR) (Prakash et al.; Venkitaraman, 2014) in addition to other processes, such as regulation of transcription, RNA splicing and cell cycle (Hatchi et al., 2015; Hill et al., 2014; Mullan et al., 2006; Savage et al., 2014). BRCA1 carries out its functions in concert with other proteins (Li and Greenberg, 2012; Moynahan and Jasin, 2010; Prakash et al.; Yun and Hiom, 2009), leading to many studies of BRCA1-containing complexes and their roles in DNA repair (Escribano-Diaz et al., 2013; Hill et al., 2014; Kim et al., 2007a; Liu et al., 2007; Wang et al., 2009, 2000; Wu et al., 1996; Yu et al., 2003). To date, many of these findings have been based on either immunoprecipitation with antibodies against the WT BRCA1 protein or interrogation of pairwise protein interactions with the yeast two-hybrid system. Moreover, these analyses were done exclusively using WT BRCA1 protein and did not capture how different mutations in BRCA1 might affect its protein interactions.

[0014] To broadly enable a pathway understanding of cancer, a prerequisite is to generate general and comprehensive maps of cancer molecular networks in relevant malignant and premalignant cell contexts. Here, affinity purification combined with mass spectrometry (AP-MS) is used to catalog protein-protein interactions (PPIs) for 40 proteins significantly altered in BC, including multi-dimensional measurements across mutant and normal protein isoforms and across cancerous and non-cancerous cellular contexts. The resulting interaction landscape reveals many PPIs that are private to a specific cell type or distinct between wild-type (WT) and mutant proteins, thereby providing a framework to understand how PPI networks are re-wired by tumor cell states. Finally, analysis of these multi-dimensional interaction maps in the context of the I-SPY 2 clinical trial (Barker et al., 2009) identifies key proteins and protein complexes with promise as biomarkers of therapeutic response.

[0015] Systematic affinity purification and tandem mass spectrometry (AP-MS) experiments were also conducted to map protein networks in the context of head and neck squamous cell carcinoma (HNSCC). Specifically, a comparative AP-MS analysis across 3 cell lines is presented for 31 genes frequently altered in HNSCC, including 16 PIK3CA mutations.

[0016] Without wishing to be bound by theory, these results demonstrate that mapping of protein networks in cancer cells reveals novel mechanisms of cancer pathogenesis, instructs the selection of therapeutic targets, and informs which point mutations in the tumor are most likely to respond to treatment.

[0017] The present disclosure therefore relates to methods of identifying a therapeutic target for a hyperproliferative disorder treatment, the method comprising: (a) compiling genetic data about a population of subjects that has a mutation candidate that causes a hyperproliferative disorder; (b) performing a mass spectrometry analysis on a sample associated with the hyperproliferative disorder to identify dysfunctional protein-protein interactions associated with the hyperproliferative disorder; (c) calculating a differential interaction score (DIS); (d) correlating the DIS with the likelihood that the dysfunctional protein-protein interaction is a causal agent of the hyperproliferative disorder, wherein if the DIS score is above a first threshold, then the causal agent is selected as a therapeutic target for the hyperproliferative disorder treatment, and wherein if the DIS score is

below the first threshold, then the causal agent is not selected as a therapeutic target for the hyperproliferative disorder treatment.

[0018] The disclosure further relates to methods of identifying a therapeutic target for a hyperproliferative disorder treatment, the method comprising: (a) calculating a differential interaction score (DIS); and (b) correlating the DIS with a likelihood that a dysfunctional protein-protein interaction is a causal agent of the hyperproliferative disorder, wherein if the DIS score is above a first threshold, then the causal agent is selected as a therapeutic target for the hyperproliferative disorder treatment, and wherein if the DIS score is below the first threshold, then the causal agent is not selected as a therapeutic target for the hyperproliferative disorder treatment.

[0019] The disclosure further relates to methods of identifying a therapeutic for treating a hyperproliferative disorder, the method comprising screening a candidate compound for binding with, or activity against a therapeutic target, wherein the therapeutic target was identified via a disclosed method.

[0020] The disclosure further relates to methods of predicting a likelihood that a hyperproliferative disorder is responsive to a therapeutic, the method comprising: (a) compiling genetic data about a population of subjects that has a mutation candidate that causes a hyperproliferative disorder; (b) performing a mass spectrometry analysis on a sample associated with the hyperproliferative disorder to identify dysfunctional protein-protein interactions associated with the hyperproliferative disorder; (c) calculating a differential interaction score (DIS); (d) correlating the DIS with the likelihood that the dysfunctional protein-protein interaction is the causal agent of the hyperproliferative disorder; and (e) selecting a therapeutic for treating the hyperproliferative disorder based upon the causal agent.

[0021] The disclosure further relates to methods of identifying a subject likely to respond to a hyperproliferative disorder treatment, the method comprising: (a) compiling genetic data about a population of subjects that has a mutation candidate that causes a hyperproliferative disorder, wherein the population of subjects includes the subject; (b) performing a mass spectrometry analysis on a sample associated with the hyperproliferative disorder to identify dysfunctional protein-protein interactions associated with the hyperproliferative disorder; (c) calculating a differential interaction score (DIS); and (d) correlating the DIS with the likelihood that the dysfunctional protein-protein interaction is a causal agent of the hyperproliferative disorder.

[0022] The disclosure further relates to methods of identifying a subject likely to respond to a hyperproliferative disorder treatment, the method comprising: (a) calculating a differential interaction score (DIS); and (b) correlating the DIS with a likelihood that a dysfunctional protein-protein interaction is a causal agent of the hyperproliferative disorder, wherein if the DIS score is above a first threshold, then the subject is likely to respond to a hyperproliferative disorder treatment based upon the causal agent, and wherein if the DIS score is below the first threshold, then the subject is not likely to respond to the hyperproliferative disorder treatment based upon the causal agent.

[0023] The disclosure further relates to methods of predicting a likelihood that a subject does or does not respond to a hyperproliferative disorder treatment, the method comprising: (a) compiling genetic data about a population of subjects that has a mutation candidate that causes a hyperproliferative disorder, wherein the population of subjects includes the subject; (b) performing a mass spectrometry analysis on a sample associated with the hyperproliferative disorder to identify dysfunctional protein-protein interactions associated with the hyperproliferative disorder; (c) calculating a differential interaction score (DIS); (d) correlating the DIS with the likelihood that the dysfunctional protein-protein interaction is the causal agent of the hyperproliferative disorder; and (e) selecting a cancer treatment for the subject based upon the causal agent.

[0024] The disclosure further relates to computer program products encoded on a computer-readable storage medium, wherein the computer program product comprises instructions for: (a) performing a mass spectrometry analysis on a sample from a subject that has a mutation candidate that causes a hyperproliferative disorder; (b) identifying dysfunctional protein-protein interactions associated with the hyperproliferative disorder; and (c) calculating a differential interaction score (DIS).

[0025] The disclosure further relates to systems for identifying a protein interaction network in a subject, the system comprising: (a) a processor operable to execute programs; (b) a memory associated with the processor; (c) a database associated with said processor and said memory; and (d) a program stored in the memory and executable by the processor, the program being operable for: (i) performing a mass spectrometry analysis on a sample from a subject that has a mutation candidate that causes a hyperproliferative disorder; (ii) identifying dysfunctional protein-protein interactions associated with the hyperproliferative disorder; and (iii) calculating a differential interaction score (DIS).

[0026] The disclosure further relates to methods of treating a cancer in a subject having a genetic alteration in Akt signaling, the method comprising administering to the subject a pharmaceutically effective amount of an Akt inhibitor, wherein the subject was previously identified as being in need of treatment by: (a) performing a mass spectrometry analysis on a sample from the subject; (b) identifying dysfunctional protein-protein interactions associated with the hyperproliferative disorder; and (c) calculating a differential interaction score (DIS).

[0027] The disclosure further relates to methods of treating a cancer in a subject having a genetic alteration in HER3 expression, the method comprising administering to the subject a pharmaceutically effective amount of a HER3 inhibitor, wherein the subject was previously identified as being in need of treatment by: (a) performing a mass spectrometry analysis on a sample from the subject; (b) identifying dysfunctional protein-protein interactions associated with the hyperproliferative disorder; and (c) calculating a differential interaction score (DIS).

[0028] The disclosure further relates to methods of selecting a hyperproliferative disorder treatment for a subject in need thereof, the method comprising: (a) identifying genetic data from the subject in need of treatment; (b) comparing the genetic data from the subject to a compilation of genetic data from population of subjects that has a mutation candidate that causes a hyperproliferative disorder, wherein the population of subjects includes the subject in need thereof; (c) performing a mass spectrometry analysis on a sample from the subject associated with the hyperproliferative disorder to identify dysfunctional protein-protein interactions associated with the hyperproliferative disorder; (d) calculating a

differential interaction score (DIS); (e) correlating the DIS with the likelihood that the dysfunctional protein-protein interaction is a causal agent of the hyperproliferative disorder; and (f) selecting a hyperproliferative disorder treatment for the subject based upon the causal agent.

[0029] Still other objects and advantages of the present disclosure will become readily apparent by those skilled in the art from the following detailed description, wherein it is shown and described only the preferred embodiments, simply by way of illustration of the best mode. As will be realized, the disclosure is capable of other and different embodiments, and its several details are capable of modifications in various obvious respects, without departing from the disclosure. Accordingly, the description is to be regarded as illustrative in nature and not as restrictive.

BRIEF DESCRIPTION OF THE DRAWINGS

[0030] The accompanying figures, which are incorporated in and constitute a part of this specification, illustrate several embodiments and together with the description serve to explain the principles of the invention.

[0031] FIG. **1**A and FIG. **1**B show representative data illustrating protein-protein interaction filtering using compass and SAINTexpress algorithms.

[0032] FIG. **2**A-D show representative data illustrating an overview of high-confidence PPIs from three breast cell lines.

[0033] FIG. **3**A-E show representative data illustrating an overview of protein-protein interaction mapping in breast epithelial cells.

[0034] FIG. **4**A-I show representative data illustrating a differential interaction analysis of the BC-specific interactome.

[0035] FIG. **5** shows representative data illustrating that knockdown of AKT reduces its phosphorylation on S473.

[0036] FIG. **6**A-I show representative data illustrating a comparative interactome analysis of WT and mutant proteins.

[0037] FIG. **7**A-E show representative data illustrating a quantitative analysis of the effect of mutations on the BRCA1 interactome.

[0038] FIG. **8**A-C show representative data illustrating that pathogenic mutations in the BRCT domain of BRCA1 disrupt the interaction with HR proteins.

[0039] FIG. **9**A-G show representative data illustrating that Spinophilin interacts with BRCA1 and regulates DNA damage response via dephosphorylation.

[0040] FIG. **10**A-E show representative data illustrating that knockout of PPP1R9B (encoding Spinophilin) upregulates phosphorylation on many DNA repair proteins.

[0041] FIG. **11**A-H show representative data illustrating an experimental design and workflow for mapping of the head and neck cancer interactions.

[0042] FIG. **12**A-C show representative data illustrating an overview of HC-PPI detection.

[0043] FIG. **13**A-E show representative data illustrating a differential interaction analysis of the HNSCC specific interactome.

[0044] FIG. **14** shows representative data illustrating the properties of differentially interacting proteins.

[0045] FIG. **15**A-I show representative data illustrating that an HNSCC-specific FGFR3:Daple interaction mediates activation of cell migratory proteins.

[0046] FIG. **16**A-C show representative data illustrating that HNSCC-specific FGFR3:Daple interaction mediates activation of Gαi.

[0047] FIG. **17**A-D show representative data illustrating a quantitative interactome analysis of common missense mutations in HNSCC.

[0048] FIG. **18** shows representative heatmap displaying the PPI regulation between WT and mutant baits for all PPIs found commonly in 2 or more cell lines.

[0049] FIG. **19**A-G show representative data illustrating that PIK3CA mutant interactome.

[0050] FIG. **20**A-C show representative data illustrating the PIK3CA mutant interactome and cellular response to CDX3379 treatment.

[0051] FIG. **21**A-E show representative data illustrating in vivo targeting of HER3 in the context of different PIK3CA mutants.

[0052] FIG. **22** and FIG. **23** show representative plasmid maps, SEQ ID NO: 15 and SEQ ID NO:16 respectively, including the nucleic acid sequence with annotations. See also paragraph [0175].

[0053] Additional advantages of the invention will be set forth in part in the description which follows, and in part will be obvious from the description, or can be learned by practice of the invention. The advantages of the invention will be realized and attained by means of the elements and combinations particularly pointed out in the appended claims. It is to be understood that both the foregoing general description and the following detailed description are exemplary and explanatory only and are not restrictive of the invention, as claimed.

DETAILED DESCRIPTION OF EMBODIMENTS

[0054] Before the present systems and methods are described, it is to be understood that the present disclosure is not limited to the particular processes, compositions, or methodologies described, as these may vary. It is also to be understood that the terminology used in the description is for the purposes of describing the particular versions or embodiments only, and is not intended to limit the scope of the present disclosure. Unless defined otherwise, all technical and scientific terms used herein have the same meanings as commonly understood by one of ordinary skill in the art. Although any methods and materials similar or equivalent to those described herein can be used in the practice or testing of embodiments of the present disclosure, the methods, devices, and materials in some embodiments are now described. All publications mentioned herein are incorporated by reference in their entirety. Nothing herein is to be construed as an admission that the present disclosure is not entitled to antedate such disclosure by virtue of prior invention.

Definitions

[0055] Unless otherwise defined herein, scientific and technical terms used in connection with the present disclosure shall have the meanings that are commonly understood by those of ordinary skill in the art. The meaning and scope of the terms should be clear, however, in the event of any latent ambiguity, definitions provided herein take precedent over any dictionary or extrinsic definition. Further, unless otherwise required by context, singular terms shall include pluralities and plural terms shall include the singular.

[0056] The indefinite articles "a" and "an," as used herein in the specification and in the claims, unless clearly indicated to the contrary, should be understood to mean "at least one." The phrase "and/or," as used herein in the specification and in the claims, should be understood to mean "either or both" of the elements so conjoined, i.e., elements that are conjunctively present in some cases and disjunctively present in other cases. Other elements may optionally be present other than the elements specifically identified by the "and/or" clause, whether related or unrelated to those elements specifically identified unless clearly indicated to the contrary. Thus, as a non-limiting example, a reference to "A and/or B," when used in conjunction with open-ended language such as "comprising" can refer, in one embodiment, to A without B (optionally including elements other than B); in another embodiment, to B without A (optionally including elements other than A); in yet another embodiment, to both A and B (optionally including other elements); etc.

[0057] As used herein in the specification and in the claims, "or" should be understood to have the same meaning as "and/or" as defined above. For example, when separating items in a list, "or" or "and/or" shall be interpreted as being inclusive, i.e., the inclusion of at least one, but also including more than one, of a number or list of elements, and, optionally, additional unlisted items. Only terms clearly indicated to the contrary, such as "only one of" or "exactly one of," or, when used in the claims, "consisting of," will refer to the inclusion of exactly one element of a number or list of elements. In general, the term "or" as used herein shall only be interpreted as indicating exclusive alternatives (i.e. "one or the other but not both") when preceded by terms of exclusivity, "either," "one of," "only one of," or "exactly one of." "Consisting essentially of," when used in the claims, shall have its ordinary meaning as used in the field of patent law.

[0058] The term "about" is used herein to mean within the typical ranges of tolerances in the art. For example, "about" can be understood as about 2 standard deviations from the mean.

[0059] According to certain embodiments, when referring to a measurable value such as an amount and the like, "about" is meant to encompass variations of ±20%, ±10%, ±5%, ±1%, ±0.9%, ±0.8%, ±0.7%, ±0.6%, ±0.5%, ±0.4%, ±0.3%, ±0.2% or ±0.1% from the specified value as such variations are appropriate to perform the disclosed methods. When "about" is present before a series of numbers or a range, it is understood that "about" can modify each of the numbers in the series or range.

[0060] The term "at least" prior to a number or series of numbers (e.g. "at least two") is understood to include the number adjacent to the term "at least," and all subsequent numbers or integers that could logically be included, as clear from context. When "at least" is present before a series of numbers or a range, it is understood that "at least" can modify each of the numbers in the series or range.

[0061] Ranges provided herein are understood to include all individual integer values and all subranges within the ranges.

[0062] As used herein, the terms "cancer patient," "individual diagnosed with cancer," and "individual suspected of having cancer" all refer to an individual who has been diagnosed with cancer, has been given a probable diagnosis of cancer, or an individual who has positive PET scans but otherwise lacks major symptoms of cancer and is without a clinical diagnosis of cancer.

[0063] As used herein, the term "animal" includes, but is not limited to, humans and non-human vertebrates such as wild animals, rodents, such as rats, ferrets, and domesticated animals, and farm animals, such as dogs, cats, horses, pigs, cows, sheep, and goats. In some embodiments, the animal is a mammal. In some embodiments, the animal is a human. In some embodiments, the animal is a non-human mammal.

[0064] As used herein, the terms "comprising" (and any form of comprising, such as "comprise," "comprises," and "comprised"), "having" (and any form of having, such as "have" and "has"), "including" (and any form of including, such as "includes" and "include"), or "containing" (and any form of containing, such as "contains" and "contain"), are inclusive or open-ended and do not exclude additional, unrecited elements or method steps.

[0065] The term "diagnosis" or "prognosis" as used herein refers to the use of information (e.g., genetic information or data from other molecular tests on biological samples, signs and symptoms, physical exam findings, cognitive performance results, etc.) to anticipate the most likely outcomes, timeframes, and/or response to a particular treatment for a given disease, disorder, or condition, based on comparisons with a plurality of individuals sharing common nucleotide sequences, symptoms, signs, family histories, or other data relevant to consideration of a patient's health status.

[0066] As used herein, the phrase "in need thereof" means that the animal or mammal has been identified or suspected as having a need for the particular method or treatment. In some embodiments, the identification can be by any means of diagnosis or observation. In any of the methods and treatments described herein, the animal or mammal can be in need thereof. In some embodiments, the subject in need thereof is a human seeking prevention of cancer. In some embodiments, the subject in need thereof is a human diagnosed with cancer. In some embodiments, the subject in need thereof is a human seeking treatment for cancer. In some embodiments, the subject in need thereof is a human undergoing treatment for cancer.

[0067] As used herein, the term "mammal" means any animal in the class Mammalia such as rodent (i.e., mouse, rat, or guinea pig), monkey, cat, dog, cow, horse, pig, or human. In some embodiments, the mammal is a human. In some embodiments, the mammal refers to any non-human mammal. The present disclosure relates to any of the methods or compositions of matter wherein the sample is taken from a mammal or non-human mammal. The present disclosure relates to any of the methods or compositions of matter wherein the sample is taken from a human or non-human primate.

[0068] As used herein, the term "predicting" refers to making a finding that an individual has a significantly enhanced probability or likelihood of benefiting from and/or responding to a chemotherapeutic treatment. In some embodiments, the chemotherapeutic treatment is administration of an Akt modulator. In some embodiments, the chemotherapeutic treatment is administration of a HER3 inhibitor.

[0069] A "score" is a numerical value that may be assigned or generated after normalization of the value based upon the presence, absence, or quantity of dysfunctional protein-protein interactions associated with a hyperprolif-

erative disorder. In some embodiments, the score is normalized in respect to a control data value.

[0070] As used herein, the term "stratifying" refers to sorting individuals into different classes or strata based on the features of cancer. For example, stratifying a population of individuals with breast cancer involves assigning the individuals on the basis of the severity of the disease (e.g., stage 0, stage 1, stage, 2, stage 3, etc.).

[0071] As used herein, the term "subject," "individual," or "patient," used interchangeably, means any animal, including mammals, such as mice, rats, other rodents, rabbits, dogs, cats, swine, cattle, sheep, horses, or primates, such as humans. In some embodiments, the subject is a human seeking treatment for cancer. In some embodiments, the subject is a human diagnosed with cancer. In some embodiments, the subject is a human suspected of having cancer. In some embodiments, the subject is a healthy human being.

[0072] As used herein, the term "threshold" refers to a defined value by which a normalized score can be categorized. By comparing to a preset threshold, a normalized score can be classified based upon whether it is above or below the preset threshold.

[0073] As used herein, the terms "treat," "treated," or "treating" can refer to therapeutic treatment and/or prophylactic or preventative measures wherein the object is to prevent or slow down (lessen) an undesired physiological condition, disorder or disease, or obtain beneficial or desired clinical results. For purposes of the embodiments described herein, beneficial or desired clinical results include, but are not limited to, alleviation of symptoms; diminishment of extent of condition, disorder or disease; stabilized (i.e., not worsening) state of condition, disorder or disease; delay in onset or slowing of condition, disorder or disease progression; amelioration of the condition, disorder or disease state or remission (whether partial or total), whether detectable or undetectable; an amelioration of at least one measurable physical parameter, not necessarily discernible by the patient; or enhancement or improvement of condition, disorder or disease. Treatment can also include eliciting a clinically significant response without excessive levels of side effects. Treatment also includes prolonging survival as compared to expected survival if not receiving treatment.

[0074] As used herein, the term "therapeutic" means an agent utilized to treat, combat, ameliorate, prevent, or improve an unwanted condition or disease of a patient.

[0075] A "therapeutically effective amount" or "effective amount" of a composition is a predetermined amount calculated to achieve the desired effect, i.e., to treat, combat, ameliorate, prevent, or improve one or more symptoms of a viral infection. The activity contemplated by the present methods includes both medical therapeutic and/or prophylactic treatment, as appropriate. The specific dose of a compound administered according to the present disclosure to obtain therapeutic and/or prophylactic effects will, of course, be determined by the particular circumstances surrounding the case, including, for example, the compound administered, the route of administration, and the condition being treated. It will be understood that the effective amount administered will be determined by the physician in the light of the relevant circumstances including the condition to be treated, the choice of compound to be administered, and the chosen route of administration, and therefore the above dosage ranges are not intended to limit the scope of the present disclosure in any way.

[0076] A therapeutically effective amount of compounds of embodiments of the present disclosure is typically an amount such that when it is administered in a physiologically tolerable excipient composition, it is sufficient to achieve an effective systemic concentration or local concentration in the tissue.

[0077] The term "hyperproliferative disorder" refers to a disease or disorder characterized by abnormal proliferation, abnormal growth, abnormal senescence, abnormal quiescence, or abnormal removal of cells in an organism, and includes all forms ofhyperplasias, neoplasias, and cancer. In some embodiments, the hyperproliferative disease is a cancer derived from the gastrointestinal tract or urinary system. In some embodiments, a hyperproliferative disease is a cancer of the adrenal gland, bladder, bone, bone marrow, brain, spine, breast, cervix, gall bladder, ganglia, gastrointestinal tract, stomach, colon, heart, kidney, liver, lung, muscle, ovary, pancreas, parathyroid, penis, prostate, salivary glands, skin, spleen, testis, thymus, thyroid, or uterus. In some embodiments, the term hyperproliferative disease is a cancer chosen from: lung cancer, bone cancer, CMML, pancreatic cancer, skin cancer, cancer of the head and neck, cutaneous or intraocular melanoma, uterine cancer, ovarian cancer, rectal cancer, cancer of the anal region, stomach cancer, colon cancer, breast cancer, testicular, gynecologic tumors (e.g., uterine sarcomas, carcinoma of the fallopian tubes, carcinoma of the endometrium, carcinoma of the cervix, carcinoma of the vagina or carcinoma of the vulva), Hodgkin's disease, cancer of the esophagus, cancer of the small intestine, cancer of the endocrine system (e.g., cancer of the thyroid, parathyroid or adrenal glands), sarcomas of soft tissues, cancer of the urethra, cancer of the penis, prostate cancer, chronic or acute leukemia, solid tumors of childhood, lymphocytic lymphomas, cancer of the bladder, cancer of the kidney or ureter (e.g., renal cell carcinoma, carcinoma of the renal pelvis), or neoplasms of the central nervous system (e.g., primary CNS lymphoma, spinal axis tumors, brain stem gliomas or pituitary adenomas).

[0078] The terms "identical" or "percent identity" or "homology" in the context of two or more nucleic acids, as used herein, refer to two or more sequences or subsequences that are the same or have a specified percentage of nucleotides or amino acid residues that are the same, when compared and aligned (introducing gaps, if necessary) for maximum correspondence, not considering any conservative amino acid substitutions as part of the sequence identity. The percent identity may be measured using sequence comparison software or algorithms or by visual inspection. Various algorithms and software that may be used to obtain alignments of amino acid or nucleotide sequences are well-known in the art.

[0079] These include, but are not limited to, BLAST, ALIGN, Megalign, BestFit, GCG Wisconsin Package, and variations thereof. In some embodiments, two nucleic acids of the invention are substantially identical, meaning they have at least about 70%, at least about 75%, at least about 80%, at least about 85%, at least about 90%, and in some embodiments at least about 95%, 96%, 97%, 98%, 99% nucleotide or amino acid residue sequence identity, when compared and aligned for maximum correspondence, as measured using a sequence comparison algorithm or by visual inspection. In some embodiments, identity exists over a region of the sequences that is at least about 10, at least about 20, at least about 40-60 nucleotides, at least about

60-80 nucleotides or any integral value therebetween. In some embodiments, identity exists over a longer region than 60-80 nucleotides, such as at least about 80-100 nucleotides, and in some embodiments the sequences are substantially identical over the full length of the sequences being compared.

Methods of Developing Protein-Protein Interaction Maps and Identifying Dysfunctional Protein-Protein Interactions

[0080] In some embodiments, the disclosure relates to methods of developing a protein-protein interaction map, the method comprising compiling genetic data about a population of subjects that has a mutation candidate that causes a hyperproliferative disorder. In some embodiments, the method further comprises performing a mass spectrometry analysis on a sample associated with the hyperproliferative disorder, thereby identifying dysfunctional protein-protein interactions associated with the hyperproliferative disorder.

[0081] In some embodiments, disclosed are methods of identifying a dysfunctional protein-protein interaction, the method comprising: (a) identifying genetic data from a subject in need of hyperproliferative disorder treatment; (b) comparing the genetic data from the subject to a compilation of genetic data from a population of subjects that has a mutation candidate that causes a hyperproliferative disorder; and (c) performing a mass spectrometry analysis on a sample from the subject in need of hyperproliferative disorder treatment, thereby identifying dysfunctional protein-protein interactions associated with the hyperproliferative disorder. In some embodiments, the method further comprises: (d) calculating a differential interaction score (DIS). In some embodiments, the method further comprises: (e) correlating the DIS with the likelihood that the dysfunctional protein-protein interaction is a causal agent of the hyperproliferative disorder. In some embodiments, the method further comprises: (f) selecting a hyperproliferative disorder treatment for the subject based upon the causal agent. In some embodiments, the step of identifying the genetic information from a subject comprises sequencing the genetic information from a biopsy or a sample obtained from the subject.

[0082] In some embodiments, the sample is a population of cells. For example, in some embodiments, the population of cells are cancer cells.

[0083] In some embodiments, the mass spectrometry analysis is performed on a plurality of samples. In further embodiments, each sample is a different population of cells. Thus, for example, the cells can be cancer cells or non-cancerous cells. In still further embodiments, each sample is the same population of cells (e.g., cancer cells, non-cancerous cells).

[0084] In some embodiments, the mass spectrometry analysis is performed on a plurality of samples, wherein calculating comprises calculating a SAINTexpress algorithm score for each sample, and averaging the SAINTexpress algorithm scores.

[0085] In some embodiments, the hyperproliferative disorder is a cancer. Examples of cancers include, but are not limited to, a sarcoma, a carcinoma, a hematological cancer, a solid tumor, breast cancer, cervical cancer, gastrointestinal cancer, colorectal cancer, brain cancer, skin cancer, head and neck cancer, prostate cancer, ovarian cancer, thyroid cancer, testicular cancer, pancreatic cancer, liver cancer, endometrial cancer, melanoma, a glioma, leukemia, lymphoma, chronic myeloproliferative disorder, myelodysplastic syndrome, myeloproliferative neoplasm, non-small cell lung carcinoma, and plasma cell neoplasm (myeloma). In further embodiments, the cancer is breast cancer of head and neck cancer. In still further embodiments, the cancer is breast cancer. In yet further embodiments, the cancer is head and neck cancer.

[0086] In some embodiments, the method further comprises harvesting samples with a functional bioassay. In a further embodiment, the functional bioassay is an animal model comprising growth of transformed cell lines.

[0087] In some embodiments, the dysfunctional protein-protein interaction is one or more of a D1:PI3K interaction or a FGFR3: Daple interaction. In some embodiments, the dysfunctional protein-protein interaction is one or more of a BPIFA1: PIK3CA interaction, a S100A3: Akt interaction, a SCGB2A1: PIK3CA interaction, or a Spinophilin: BRCA1 interaction.

Methods of Identifying Therapeutic Targets and of Screening for and Evaluating Therapeutics

[0088] In some embodiments, the disclosure relates to methods of identifying a therapeutic target for a hyperproliferative disorder treatment, the method comprising: (a) compiling genetic data about a population of subjects that has a mutation candidate that causes a hyperproliferative disorder; (b) performing a mass spectrometry analysis on a sample associated with the hyperproliferative disorder to identify dysfunctional protein-protein interactions associated with the hyperproliferative disorder; (c) calculating a differential interaction score (DIS); (d) correlating the DIS with the likelihood that the dysfunctional protein-protein interaction is a causal agent of the hyperproliferative disorder, wherein if the DIS score is above a first threshold, then the causal agent is selected as a therapeutic target for the hyperproliferative disorder treatment, and wherein if the DIS score is below the first threshold, then the causal agent is not selected as a therapeutic target for the hyperproliferative disorder treatment. In some embodiments, the methods further comprise selecting the treatment of a subject.

[0089] In some embodiments, the disclosure relates to methods of identifying a therapeutic target for a hyperproliferative disorder treatment, the method comprising: (a) calculating a differential interaction score (DIS); and (b) correlating the DIS with a likelihood that a dysfunctional protein-protein interaction is a causal agent of the hyperproliferative disorder, wherein if the DIS score is above a first threshold, then the causal agent is selected as a therapeutic target for the hyperproliferative disorder treatment, and wherein if the DIS score is below the first threshold, then the causal agent is not selected as a therapeutic target for the hyperproliferative disorder treatment.

[0090] In some embodiments, the disclosure relates to methods of identifying a therapeutic for treating a hyperproliferative disorder, the method comprising screening a candidate compound for binding with, or activity against a therapeutic target, wherein the therapeutic target was identified via a disclosed method.

[0091] In some embodiments, the disclosure relates to methods of predicting a likelihood that a hyperproliferative disorder is responsive to a therapeutic, the method comprising: (a) compiling genetic data about a population of subjects that has a mutation candidate that causes a hyperproliferative disorder; (b) performing a mass spectrometry

analysis on a sample associated with the hyperproliferative disorder to identify dysfunctional protein-protein interactions associated with the hyperproliferative disorder; (c) calculating a differential interaction score (DIS); (d) correlating the DIS with the likelihood that the dysfunctional protein-protein interaction is the causal agent of the hyperproliferative disorder; and (e) selecting a therapeutic for treating the hyperproliferative disorder based upon the causal agent.

[0092] In some embodiments, the sample is a population of cells. For example, in some embodiments, the population of cells are cancer cells.

[0093] In some embodiments, the mass spectrometry analysis is performed on a plurality of samples. In further embodiments, each sample is a different population of cells. Thus, for example, the cells can be cancer cells or non-cancerous cells. In still further embodiments, each sample is the same population of cells (e.g., cancer cells, non-cancerous cells).

[0094] In some embodiments, the calculating comprises calculating one or more of a SAINTexpress algorithm score and a CompPASS algorithm score. In a further embodiment, the calculating comprises calculating the SAINTexpress algorithm score. In a still further embodiment, the calculating comprises calculating the CompPASS algorithm score. In yet further embodiments, the calculating comprises calculating the SAINTexpress algorithm score and the CompPASS algorithm score.

[0095] Methods of using SAINTexpress algorithms are known by those of skill in the art. See, e.g., Teo, et al. (2014) *J Proteomics* 100: 37-43. As further described herein, a SAINTexpress algorithm can be used for PPI confidence scoring. In various aspects, PPI scoring can be performed separately for each cell line.

[0096] In some embodiments, the SAINTexpress algorithm score is calculated by a formula:

$$P(X_{ij}|*) = \pi_T P(X_{ij}|\lambda_{ij}) + (1-\pi_T)P(X_{ij}|\kappa_{ij}) \quad (1)$$

[0097] wherein X_{ij} is the spectral count for a prey protein i identified in a purification of bait j;

[0098] wherein λ_{ij} is the mean count from a Poisson distribution representing true interaction;

[0099] wherein κ_{ij} is the mean count from a Poisson distribution representing false interaction;

[0100] wherein π_T is the proportion of true interactions in the data; and wherein dot notation represents all relevant model parameters estimated from the data for the pair of prey i and bait j.

[0101] Methods of using CompPASS algorithms are known by those of skill in the art. See, e.g., Huttlin, et al. (2015) *Cell* 162: 425-440; and Sowa, et al. (2009) *Cell* 138: 389-403. As further described herein, a CompPASS algorithm can be used for PPI confidence scoring. In various aspects, PPI scoring can be performed separately for each cell line.

[0102] In some embodiments, the CompPASS algorithm score is calculated by calculating the Z-score, the S-score, the D-score, and the WD-score, as further described herein.

[0103] In some embodiments, the DIS is calculated for a cancer cell line or a plurality of cancer cell lines and also calculated for a normal cell line. The DIS for the cancer cell line or the plurality of cancer cell lines is then compared to the DIS for the normal cell line. If the DIS for the cancer cell line or the plurality of cancer cell lines is greater than the DIS for the normal cell line, the DIS is assigned a positive (+) sign. If the DIS for the cancer cell line or the plurality of cancer cell lines is less than the DIS for the normal cell line, the DIS is assigned a negative (−) sign. Thus, a positive DIS represents a PPI that is enriched in a cancer cell line or a plurality of cancer cell lines, and a negative DIS represents a PPI that is depleted in a cancer cell line or a plurality of cancer cell lines.

[0104] In some embodiments, the DIS is calculated by a first formula:

$$DIS_A(b,p) = S_{C1}(b,p) \times S_{C2}(b,p) \times [1 - S_{C3}(b,p)]$$

wherein DIS_A(b,p) is the DIS for each PPI (b, p) that is conserved in a first cell line and a second cell line, but not shared by a third cell line; wherein S_{C1}(b,p) is the probability of a PPI being present in the first cell line; wherein S_{C2}(b,p) is the probability of a PPI being present in the second cell line; and wherein S_{c3}(b,p) is the probability of a PPI being present in the third cell line; and a second formula:

$$DIS_B(b,p) = [1 - S_{C1}(b,p)] \times [1 - S_{C2}(b,p)] \times S_{C3}(b,p$$

wherein DIS_B(b,p) is the DIS score for each PPI (b, p) that is conserved in the third cell line, but not shared by the first cell line and the second cell line; wherein a (+) sign is assigned if DIS_A(b,p)>DIS_B(b,p); and wherein a (−) sign is assigned if DIS_A(b,p)<DIS_B(b,p).

[0105] In some embodiments, the DIS is calculated by a first formula:

$$DIS_{cancer}(b,p) = S_{C1}(b,p) \times S_{C2}(b,p) \times [1 - S_N(b,p)]$$

wherein DIS_{cancer}(b,p) is the DIS for each PPI (b, p) that is conserved across a cancer cell line, but not shared by a normal cell line; wherein S_{C1}(b,p) is the probability of a PPI being present in a first cancer cell line; wherein S_{C2}(b,p) is the probability of a PPI being present in a second cancer cell line; and wherein S_N(b,p) is the probability of a PPI being present in a normal cell line; and a second formula:

$$DIS_{normal}(b,p) = [1 - S_{C1}(b,p)] \times [1 - S_{C2}(b,p)] \times S_N(b,p)$$

wherein DIS_{normal}(b,p) is the DIS score for each PPI (b, p) that is present in a normal cell line, but depleted in a cancer cell line; and assigning a (+) sign if DIS_{cancer}(b,p)>DIS_{normal}(b,p) and assigning a (−) sign if DIS_{cancer}(b,p)<DIS_{normal}(b,p).

[0106] In some embodiments, the DIS is an average of a SAINTexpress algorithm score and a CompPASS algorithm score. In some further embodiments, the DIS is a SAINTexpress algorithm score.

[0107] In some embodiments, the DIS ranges from 0.0 to 1.0. Thus, in various embodiments, the DIS ranges from 0.0

to 0.9, from 0.0 to 0.8, from 0.0 to 0.7, from 0.0 to 0.6, from 0.0 to 0.5, from 0.0 to 0.4, from 0.0 to 0.3, from 0.0 to 0.2, from 0.0 to 0.1, from 0.1 to 1.0, from 0.2 to 1.0, from 0.3 to 1.0, from 0.4 to 1.0, from 0.5 to 1.0, from 0.6 to 1.0, from 0.7 to 1.0, from 0.8 to 1.0, from 0.9 to 1.0, from 0.1 to 0.9, from 0.2 to 0.8, from 0.3 to 0.7, or from 0.4 to 0.6.

[0108] In some embodiments, a DIS of 0.5 or greater than 0.5 indicates that the dysfunctional protein-protein interaction is likely a causal agent of the hyperproliferative disorder. Thus, in various embodiments, a DIS of greater than 0.5, greater than 0.6, greater than 0.7, greater than 0.8, or greater than 0.9 indicates that the dysfunctional protein-protein interaction is likely a causal agent of the hyperproliferative disorder. In some embodiments, a DIS of 0.5 or greater than 0.5 indicates that the dysfunctional protein-protein interaction is likely a causal agent of the hyperproliferative disorder, and, therefore, indicates that the causal agent should be selected as a therapeutic target for a hyperproliferative disorder treatment.

[0109] In some embodiments, a DIS of 0.5 or less than 0.5 indicates that the dysfunctional protein-protein interaction is not likely a causal agent of the hyperproliferative disorder. Thus, in various embodiments, a DIS of less than 0.5, less than 0.4, less than 0.3, less than 0.2, or less than 0.1 indicates that the dysfunctional protein-protein interaction is not likely a causal agent of the hyperproliferative disorder. In some embodiments, a DIS of 0.5 or less than 0.5 indicates that the dysfunctional protein-protein interaction is not likely a causal agent of the hyperproliferative disorder, and, therefore, indicates that the causal agent should not be selected as a therapeutic target for a hyperproliferative disorder treatment.

[0110] In some embodiments, the mass spectrometry analysis is performed on a plurality of samples, wherein calculating comprises calculating a SAINTexpress algorithm score for each sample, and averaging the SAINTexpress algorithm scores.

[0111] In some embodiments, the hyperproliferative disorder is a cancer. Examples of cancers include, but are not limited to, a sarcoma, a carcinoma, a hematological cancer, a solid tumor, breast cancer, cervical cancer, gastrointestinal cancer, colorectal cancer, brain cancer, skin cancer, head and neck cancer, prostate cancer, ovarian cancer, thyroid cancer, testicular cancer, pancreatic cancer, liver cancer, endometrial cancer, melanoma, a glioma, leukemia, lymphoma, chronic myeloproliferative disorder, myelodysplastic syndrome, myeloproliferative neoplasm, non-small cell lung carcinoma, and plasma cell neoplasm (myeloma). In further embodiments, the cancer is breast cancer of head and neck cancer. In still further embodiments, the cancer is breast cancer. In yet further embodiments, the cancer is head and neck cancer.

[0112] In some embodiments, the method further comprises harvesting samples with a functional bioassay. In a further embodiment, the functional bioassay is an animal model comprising growth of transformed cell lines.

[0113] In some embodiments, the subject is a mammal. In some embodiments, the mammal is a human.

[0114] In some embodiments, the subject has been diagnosed with a need for treatment of the hyperproliferative disorder prior to the administering step.

[0115] In some embodiments, the method further comprises identifying a therapeutic target for a hyperproliferative disorder treatment. In a further embodiment, the therapeutic target is identified as a hyperproliferative disorder treatment if the DIS score is 0.5 or greater than 0.5.

[0116] Thus, in various embodiments, the subject is identified as being likely to respond to a cancer treatment if the DIS score is greater than 0.5, greater than 0.6, greater than 0.7, greater than 0.8, or greater than 0.9.

[0117] In some embodiments, the target is identified as being unlikely to offer a therapeutic benefit as a hyperproliferative disorder treatment if the DIS score is 0.5 or less than 0.5.

[0118] Thus, in various embodiments, the target is identified as being unlikely to offer a therapeutic benefit as a hyperproliferative disorder treatment if the DIS score is less than 0.5, less than 0.4, less than 0.3, less than 0.2, or less than 0.1.

[0119] In some embodiments, the mutation candidate is one or more genes having a mutant protein sequence, wherein the gene is selected from TP53, CDKN2A, PIK3CA, TP63, FADD, SOX2, RHOA, CCND1, EGFR, CASP8, NFE2L2, MAPK1, MYC, PTEN, KEAP1, CUL3, E2F1, FBXW7, PTPRT, GFGR1, RB1, IGF1R, HRAS, TRAF3, TGFBR2, ERBB2, FGFR3, HLA-A, NRAS, STAT3, and XPC. In some embodiments, the mutation candidate is one or more genes having a mutant protein sequence, wherein the gene is selected from PIK3CA, TP53, MTDG, AKT3, CDH1, ERBB2, GATA3, TSPYL5, PTEN, RB1, BRIP1, CBFB, RAF51C, FOXA1, PALB2, ARID1A, ESR1, STK11, CDKN1B, MSH2, AKT1, AKT2, BRCA1, CHEK2, RPA2, EGFR, RAD51D, CASP8, CCND3, CTCF, MLH1, SMARCB1, XPC, SCUBE2, TBX3, XRN2, EZH2, FANCC, HRAS, or SMARCD1.

[0120] In some embodiments, the gene is TP53, PIK3CA, NFE212, MAPK1, FBXW7, or HRAS. In some embodiments, the gene is AKT1, AKT3, BRCA1, BRIP1, CDH1, CHEK2, HRAS, MTDH, PALB2, PIK3CA, or TP53.

[0121] In some embodiments, the gene is NFE2L2 and the mutant protein sequence is E79K or E79Q, wherein the gene is HRAS and the mutant protein sequence is G12D, wherein the gene is TP53 and the mutant protein sequence is R248W or R273H, wherein the gene is MAPK1 and the mutant protein sequence is E322K, or wherein the gene is FBXW7 and the mutant protein sequence is R505G.

[0122] In some embodiments, the gene is AKT1 and the mutant protein sequence is E17K, wherein the gene is AKT3 and the mutant protein sequence is E17K, wherein the gene is BRIP1 and the mutant protein sequence is A745T, wherein the gene is CDH1 and the mutant protein sequence is E243K, wherein the gene is CHEK2 and the mutant protein sequence is 1100delC or K373E, wherein the gene is HRAS and the mutant protein sequence is G12D, wherein the gene is MTDH and the mutant protein sequence is A78S, wherein the gene is PALB2 and the mutant protein sequence is E837K, or wherein the gene is TP53 and the mutant protein sequence is R175H, R248W, or R273H.

[0123] In some embodiments, the gene is PIK3CA and the mutant protein sequence is R88Q, E110Del, K111N, K111E, V344G, G363A, E453K, E542K, E545K, E545G, E726K, C971R, G1007R, M1043V, H1047L, or H1047R. In some embodiments, the gene is PIK3CA and the mutant protein sequence is E545K, M1043V, or H1047R. In some embodiments, the gene is BRCA1 and the mutant protein sequence is I16A, C61G, R71G, Δexon11, S1655F, 5832insC, or M1775R.

[0124] In some embodiments, the dysfunctional protein-protein interaction is one or more of a D1:PI3K interaction or a FGFR3: Daple interaction. In some embodiments, the dysfunctional protein-protein interaction is one or more of a BPIFA1: PIK3CA interaction, a S100A3: Akt interaction, a SCGB2A1: PIK3CA interaction, or a Spinophilin: BRCA1 interaction.

[0125] In some embodiments, the causal agent is HER3. In some embodiments, the causal agent is Akt.

[0126] In some embodiments, the method further comprises selecting a therapeutic target for treating a hyperproliferative disorder in a subject based upon the causal agent. In some embodiments, the method further comprises screening a candidate compound for binding with, or activity against, the therapeutic target. In some embodiments, the method further comprises selecting a candidate compound as a therapeutic for treating a hyperproliferative disorder. In some embodiments, the candidate compound is selected from a database of known treatments for the dysfunctional protein-protein interaction.

[0127] In some embodiments, the hyperproliferative disorder treatment comprises administration of a HER3 inhibitor. Examplers of HER3 inhibitors include, but are not limited to, lapatinib, erlotinib, gefitinib, afatinib, neratinib, CDX-3379, U-31402, HMBD-001, MCLA-128, KBP-5209, Poziotinib, Varlitinib, FCN-411, Elgemtumab, Sirotinib, vaccines to target Her3 for solid tumors, AV2103, AV2103, ETBX-031, MP-EV-20, MP-EV-20/1959, and oligonucleotides to inhibit EGFR, ERBB2, and ERBB3. Additional exemplary HER3 inhibitors are described in US 2018/0362443 A1, U.S. Pat. No. 10,383,878 B2, US 2019/0300624 A1, WO 2018/182420 A1, WO 2015/007219 A1, U.S. Pat. No. 8,735,551 B2, U.S. Pat. No. 10,507,209 B2, U.S. Pat. No. 9,956,222 B2, U.S. Pat. No. 10,487,143 B2, WO 2018/233511 A1, CN106692969A, US 2020/0147193 A1, U.S. Pat. No. 9,346,889 B2, WO 2020/099235 A1, US 2019/0201552 A1, US 2018/0105815 A1, and US 2020/0157542 A1. In some embodiments, the HER3 inhibitor is CDX3379.

[0128] In some embodiments, the hyperproliferative disorder is head and neck cancer, wherein the mutation candidate is a mutant PIK3CA, wherein the causal agent is HER3, and wherein the hyperproliferative disorder treatment comprises administration of a HER3 inhibitor.

[0129] In some embodiments, the hyperproliferative disorder treatment comprises administration of an Akt inhibitor. Examples of Akt inhibitors include, but are not limited to, MK-2206, AZD5363, GSK690693, GDC-0068, GSK2141795, GSK2110183, AT7867, CCT128930, BAY1125976, perifosine, and AKT inhibitor III.

[0130] In some embodiments, the Akt modulator is a PIK3CA modulator. Examples of PIK3CA modulators include, but are not limited to, Alpelisib, Copanlisib hydrochloride, GDC-0077, Bimiralisib, Fimepinostat, Serabelisib, HHCYH-33, omipalisib, and PQR-514.

[0131] In some embodiments, the hyperproliferative disorder is breast cancer, wherein the mutation candidate is a mutant PIK3CA or a mutant BRCA1, wherein the causal agent is Akt, and wherein the hyperproliferative disorder treatment comprises administration of an Akt inhibitor.

Methods of Identifying and Monitoring a Subject's Responsiveness to a Hyperproliferative Disorder Treatment

[0132] In some embodiments, the disclosure relates to methods of identifying a subject likely to respond to a hyperproliferative disorder treatment, the method comprising: (a) compiling genetic data about a population of subjects that has a mutation candidate that causes a hyperproliferative disorder, wherein the population of subjects includes the subject; (b) performing a mass spectrometry analysis on a sample associated with the hyperproliferative disorder to identify dysfunctional protein-protein interactions associated with the hyperproliferative disorder; (c) calculating a differential interaction score (DIS); and (d) correlating the DIS with the likelihood that the dysfunctional protein-protein interaction is a causal agent of the hyperproliferative disorder.

[0133] In some embodiments, the disclosure relates to methods of identifying a subject likely to respond to a hyperproliferative disorder treatment, the method comprising: (a) calculating a differential interaction score (DIS); and (b) correlating the DIS with a likelihood that a dysfunctional protein-protein interaction is a causal agent of the hyperproliferative disorder, wherein if the DIS score is above a first threshold, then the subject is likely to respond to a hyperproliferative disorder treatment based upon the causal agent, and wherein if the DIS score is below the first threshold, then the subject is not likely to respond to the hyperproliferative disorder treatment based upon the causal agent. In some embodiments, the method further comprises: (a) compiling genetic data about a population of subjects comprising the subject, wherein the population of subjects has a mutation candidate that causes the hyperproliferative disorder; and (b) performing a mass spectrometry analysis on a sample associated with the hyperproliferative disorder to identify dysfunctional protein-protein interactions associated with the hyperproliferative disorder.

[0134] In some embodiments, disclosed are methods of predicting a likelihood that a subject does or does not respond to a hyperproliferative disorder treatment, the method comprising: (a) compiling genetic data about a population of subjects that has a mutation candidate that causes a hyperproliferative disorder, wherein the population of subjects includes the subject; (b) performing a mass spectrometry analysis on a sample associated with the hyperproliferative disorder to identify dysfunctional protein-protein interactions associated with the hyperproliferative disorder; (c) calculating a differential interaction score (DIS); (d) correlating the DIS with the likelihood that the dysfunctional protein-protein interaction is the causal agent of the hyperproliferative disorder; and (e) selecting a cancer treatment for the subject based upon the causal agent. In some embodiments, the method further comprises: (f) comparing the DIS score to a first threshold; and (g) classifying the subject as being likely to respond to a hyperproliferative disorder treatment, wherein each of steps (f) and (g) are performed after step (c), and wherein the first threshold is calculated relative to a first control dataset.

[0135] In some embodiments, disclosed are methods of treating a cancer in a subject having a genetic alteration in Akt signaling, the method comprising administering to the subject a pharmaceutically effective amount of an Akt inhibitor, wherein the subject was previously identified as being in need of treatment by: (a) performing a mass spectrometry analysis on a sample from the subject; (b)

identifying dysfunctional protein-protein interactions associated with the cancer; and (c) calculating a differential interaction score (DIS). In some embodiments, the cancer is head and neck cancer.

[0136] In some embodiments, disclosed are methods of treating a cancer in a subject having a genetic alteration in HER3 expression, the method comprising administering to the subject a pharmaceutically effective amount of a HER3 inhibitor, wherein the subject was previously identified as being in need of treatment by: (a) performing a mass spectrometry analysis on a sample from the subject; (b) identifying dysfunctional protein-protein interactions associated with the cancer; and (c) calculating a differential interaction score (DIS). In some embodiments, the cancer is breast cancer.

[0137] In some embodiments, disclosed are methods of selecting a hyperproliferative disorder treatment for a subject in need thereof, the method comprising: (a) identifying genetic data from the subject in need of treatment; (b) comparing the genetic data from the subject to a compilation of genetic data from population of subjects that has a mutation candidate that causes a hyperproliferative disorder, wherein the population of subjects includes the subject in need thereof; (c) performing a mass spectrometry analysis on a sample from the subject associated with the hyperproliferative disorder to identify dysfunctional protein-protein interactions associated with the hyperproliferative disorder; (d) calculating a differential interaction score (DIS); (e) correlating the DIS with the likelihood that the dysfunctional protein-protein interaction is a causal agent of the hyperproliferative disorder; and (f) selecting a hyperproliferative disorder treatment for the subject based upon the causal agent. In some embodiments, the step of identifying the genetic information from a subject comprises sequencing the genetic information from a biopsy or sample obtained from the subject.

[0138] In some embodiments, the sample is a population of cells. For example, in some embodiments, the population of cells are cancer cells.

[0139] In some embodiments, the mass spectrometry analysis is performed on a plurality of samples. In further embodiments, each sample is a different population of cells. Thus, for example, the cells can be cancer cells or non-cancerous cells. In still further embodiments, each sample is the same population of cells (e.g., cancer cells, non-cancerous cells).

[0140] In some embodiments, the calculating comprises calculating one or more of a SAINTexpress algorithm score and a CompPASS algorithm score. In a further embodiment, the calculating comprises calculating the SAINTexpress algorithm score. In a still further embodiment, the calculating comprises calculating the CompPASS algorithm score. In yet further embodiments, the calculating comprises calculating the SAINTexpress algorithm score and the CompPASS algorithm score.

[0141] Methods of using SAINTexpress algorithms are known by those of skill in the art.

[0142] See, e.g., Teo, et al. (2014) *J Proteomics* 100: 37-43. As further described herein, a SAINTexpress algorithm can be used for PPI confidence scoring. In various aspects, PPI scoring can be performed separately for each cell line.

[0143] In some embodiments, the SAINTexpress algorithm score is calculated by a formula:

$$P(X_{ij}|*) = \pi_T P(X_{ij}|\lambda_{ij}) + (1-\pi_T)P(X_{ij}|\kappa_{ij}) \quad (1)$$

wherein X_{ij} is the spectral count for a prey protein i identified in a purification of bait j; wherein λ_{ij} is the mean count from a Poisson distribution representing true interaction; wherein κ_{ij} is the mean count from a Poisson distribution representing false interaction; wherein π_T is the proportion of true interactions in the data; and wherein dot notation represents all relevant model parameters estimated from the data for the pair of prey i and bait j.

[0144] Methods of using CompPASS algorithms are known by those of skill in the art. See, e.g., Huttlin, et al. (2015) *Cell* 162: 425-440; and Sowa, et al. (2009) *Cell* 138: 389-403. As further described herein, a CompPASS algorithm can be used for PPI confidence scoring. In various aspects, PPI scoring can be performed separately for each cell line.

[0145] In some embodiments, the CompPASS algorithm score is calculated by calculating the Z-score, the S-score, the D-score, and the WD-score, as further described herein.

[0146] In some embodiments, the DIS is calculated for a cancer cell line or a plurality of cancer cell lines and also calculated for a normal cell line. The DIS for the cancer cell line or the plurality of cancer cell lines is then compared to the DIS for the normal cell line. If the DIS for the cancer cell line or the plurality of cancer cell lines is greater than the DIS for the normal cell line, the DIS is assigned a positive (+) sign. If the DIS for the cancer cell line or the plurality of cancer cell lines is less than the DIS for the normal cell line, the DIS is assigned a negative (−) sign. Thus, a positive DIS represents a PPI that is enriched in a cancer cell line or a plurality of cancer cell lines, and a negative DIS represents a PPI that is depleted in a cancer cell line or a plurality of cancer cell lines.

[0147] In some embodiments, the DIS is calculated by a first formula:

$$DIS_A(b,p) = S_{C1}(b,p) \times S_{C2}(b,p) \times [1 - S_{C3}(b,p)]$$

wherein DIS_A(b,p) is the DIS for each PPI (b, p) that is conserved in a first cell line and a second cell line, but not shared by a third cell line; wherein S_{C1}(b,p) is the probability of a PPI being present in the first cell line; wherein S_{C2}(b,p) is the probability of a PPI being present in the second cell line; and wherein S_{c3}(b,p) is the probability of a PPI being present in the third cell line; and a second formula:

$$DIS_B(b,p) = [1 - S_{C1}(b,p)] \times [1 - S_{C2}(b,p)] \times S_{C3}(b,p$$

wherein DIS_B(b,p) is the DIS score for each PPI (b, p) that is conserved in the third cell line, but not shared by the first cell line and the second cell line; wherein a (+) sign is assigned if DIS_A(b,p)>DIS_B(b,p); and wherein a (−) sign is assigned if DIS_A(b,p)<DIS_B(b,p).

[0148] In some embodiments, the DIS is calculated by a first formula:

$$DIS_{cancer}(b, p) = S_{C1}(b, p) \times S_{C2}(b, p) \times [1 - S_N(b, p)]$$

wherein DIS_{cancer}(b,p) is the DIS for each PPI (b, p) that is conserved across a cancer cell line, but not shared by a normal cell line; wherein S_{C1}(b,p) is the probability of a PPI being present in a first cancer cell line; wherein S_{C2}(b,p) is the probability of a PPI being present in a second cancer cell line; and wherein S_N(b,p) is the probability of a PPI being present in a normal cell line; and a second formula:

$$DIS_{normal}(b, p) = [1 - S_{C1}(b, p)] \times [1 - S_{C2}(b, p)] \times S_N(b, p)$$

wherein DIS_{normal}(b,p) is the DIS score for each PPI (b, p) that is present in a normal cell line, but depleted in a cancer cell line; and assigning a (+) sign if DIS_{cancer}(b,p)>DIS_{normal}(b,p) and assigning a (−) sign if DIS_{cancer}(b,p)<DIS_{normal}(b,p).

[0149] In some embodiments, the DIS is an average of a SAINTexpress algorithm score and a CompPASS algorithm score. In some further embodiments, the DIS is a SAINTexpress algorithm score.

[0150] In some embodiments, the DIS ranges from about 0.0 to about 1.0. Thus, in various embodiments, the DIS ranges from about 0.0 to about 0.9, from about 0.0 to about 0.8, from about 0.0 to about 0.7, from about 0.0 to about 0.6, from about 0.0 to about 0.5, from about 0.0 to about 0.4, from 0.0 to 0.3, from 0.0 to 0.2, from 0.0 to 0.1, from 0.1 to 1.0, from 0.2 to 1.0, from 0.3 to 1.0, from 0.4 to 1.0, from 0.5 to 1.0, from 0.6 to 1.0, from 0.7 to 1.0, from 0.8 to 1.0, from about 0.9 to about 1.0, from about 0.1 to about 0.9, from about 0.2 to about 0.8, from about 0.3 to about 0.7, or from about 0.4 to about 0.6.

[0151] In some embodiments, a DIS of about 0.5 or greater than about 0.5 indicates that the dysfunctional protein-protein interaction is likely a causal agent of the hyperproliferative disorder. Thus, in various embodiments, a DIS of greater than about 0.5, greater than about 0.6, greater than about 0.7, greater than about 0.8, or greater than about 0.9 indicates that the dysfunctional protein-protein interaction is likely a causal agent of the hyperproliferative disorder.

[0152] In some embodiments, a DIS of 0.5 or less than 0.5 indicates that the dysfunctional protein-protein interaction is not likely a causal agent of the hyperproliferative disorder. Thus, in various embodiments, a DIS of less than 0.5, less than 0.4, less than 0.3, less than 0.2, or less than 0.1 indicates that the dysfunctional protein-protein interaction is likely a causal agent of the hyperproliferative disorder.

[0153] In some embodiments, the mass spectrometry analysis is performed on a plurality of samples, wherein calculating comprises calculating a SAINTexpress algorithm score for each sample, and averaging the SAINTexpress algorithm scores.

[0154] In some embodiments, the hyperproliferative disorder is a cancer. Examples of cancers include, but are not limited to, a sarcoma, a carcinoma, a hematological cancer, a solid tumor, breast cancer, cervical cancer, gastrointestinal cancer, colorectal cancer, brain cancer, skin cancer, head and neck cancer, prostate cancer, ovarian cancer, thyroid cancer, testicular cancer, pancreatic cancer, liver cancer, endometrial cancer, melanoma, a glioma, leukemia, lymphoma, chronic myeloproliferative disorder, myelodysplastic syndrome, myeloproliferative neoplasm, non-small cell lung carcinoma, and plasma cell neoplasm (myeloma). In further embodiments, the cancer is breast cancer of head and neck cancer. In still further embodiments, the cancer is breast cancer. In yet further embodiments, the cancer is head and neck cancer.

[0155] In some embodiments, the method further comprises harvesting samples with a functional bioassay. In a further embodiment, the functional bioassay is an animal model comprising growth of transformed cell lines.

[0156] In some embodiments, the subject is a mammal. In some embodiments, the mammal is a human.

[0157] In some embodiments, the subject has been diagnosed with a need for treatment of the hyperproliferative disorder prior to the administering step.

[0158] In some embodiments, the method further comprises identifying a subject in need of treatment of the hyperproliferative disorder. In a further embodiment, the subject is identified as being likely to respond to a cancer treatment if the DIS score is 0.5 or greater than 0.5. Thus, in various embodiments, the subject is identified as being likely to respond to a cancer treatment if the DIS score is greater than 0.5, greater than 0.6, greater than 0.7, greater than 0.8, or greater than 0.9.

[0159] In some embodiments, the subject is identified as being unlikely to respond to a cancer treatment if the DIS score is 0.5 or less than 0.5. Thus, in various embodiments, the subject is identified as being unlikely to respond to a cancer treatment if the DIS score is less than about 0.5, less than about 0.4, less than about 0.3, less than about 0.2, or less than about 0.1.

[0160] In some embodiments, the mutation candidate is one or more genes having a mutant protein sequence, wherein the gene is selected from TP53, CDKN2A, PIK3CA, TP63, FADD, SOX2, RHOA, CCND1, EGFR, CASP8, NFE2L2, MAPK1, MYC, PTEN, KEAP1, CUL3, E2F1, FBXW7, PTPRT, GFGR1, RB1, IGF1R, HRAS, TRAF3, TGFBR2, ERBB2, FGFR3, HLA-A, NRAS, STAT3, and XPC. In some embodiments, the mutation candidate is one or more genes having a mutant protein sequence, wherein the gene is selected from PIK3CA, TP53, MTDG, AKT3, CDH1, ERBB2, GATA3, TSPYL5, PTEN, RB1, BRIP1, CBFB, RAF51C, FOXA1, PALB2, ARID1A, ESR1, STK11, CDKN1B, MSH2, AKT1, AKT2, BRCA1, CHEK2, RPA2, EGFR, RAD51D, CASP8, CCND3, CTCF, MLH1, SMARCB1, XPC, SCUBE2, TBX3, XRN2, EZH2, FANCC, HRAS, or SMARCD1.

[0161] In some embodiments, the gene is TP53, PIK3CA, NFE212, MAPK1, FBXW7, or HRAS. In some embodiments, the gene is AKT1, AKT3, BRCA1, BRIP1, CDH1, CHEK2, HRAS, MTDH, PALB2, PIK3CA, or TP53.

[0162] In some embodiments, the gene is NFE2L2 and the mutant protein sequence is E79K or E79Q, wherein the gene is HRAS and the mutant protein sequence is G12D, wherein the gene is TP53 and the mutant protein sequence is R248W or R273H, wherein the gene is MAPK1 and the mutant protein sequence is E322K, or wherein the gene is FBXW7 and the mutant protein sequence is R505G.

[0163] In some embodiments, the gene is AKT1 and the mutant protein sequence is E17K, wherein the gene is AKT3 and the mutant protein sequence is E17K, wherein the gene is BRIP1 and the mutant protein sequence is A745T, wherein

the gene is CDH1 and the mutant protein sequence is E243K, wherein the gene is CHEK2 and the mutant protein sequence is 1100delC or K373E, wherein the gene is HRAS and the mutant protein sequence is G12D, wherein the gene is MTDH and the mutant protein sequence is A78S, wherein the gene is PALB2 and the mutant protein sequence is E837K, or wherein the gene is TP53 and the mutant protein sequence is R175H, R248W, or R273H.

[0164] In some embodiments, the gene is PIK3CA and the mutant protein sequence is R88Q, E110Del, K111N, K111E, V344G, G363A, E453K, E542K, E545K, E545G, E726K, C971R, G1007R, M1043V, H1047L, or H1047R. In some embodiments, the gene is PIK3CA and the mutant protein sequence is E545K, M1043V, or H1047R. In some embodiments, the gene is BRCA1 and the mutant protein sequence is I16A, C61G, R71G, Δexon11, S1655F, 5832insC, or M1775R. The nucleic acid sequence of TP53 is found

TP53	NC_000017.11	NM_000546.5

The amino acid sequence of PT53 is:

(SEQ ID NO: 1)

MEEPQSDPSVEPPLSQETFSDLWKLLPENNVLSPLPSQAMDDLM

LSPDDIEQWFTEDPGPDEAPRMPEAAPPVAPAPAAPTPAAPAPA

PSWPLSSSVPSQKTYQGSYGFRLGFLHSGTAKSVTCTYSPALNK

MFCQLAKTCPVQLWVDSTPPPGTRVRAMAIYKQSQHMTEVVRRC

PHHERCSDSDGLAPPQHLIRVEGNLRVEYLDDRNTFRHSVVVPY

EPPEVGSDCTTIHYNYMCNSSCMGGMNRRPILTIITLEDSSGNL

LGRNSFEVRVCACPGRDRRTEEENLRKKGEPHHELPPGSTKRAL

PNNTSSSPQPKKKPLDGEYFTLQIRGRERFEMFRELNEALELKD

AQAGKEPGGSRAHSSHLKSKKGQSTSRHKKLMFKTEGPDSD

The amino acid sequence of PIK3CA is:

(SEQ ID NO: 2)

MQPFSIPVQITLQGSRRRQGRTAFPASGKKRETDYSDGDPLDVH

KRLPSSAGEDRAVMLGFAMMGFSVLMFFLLGTTILKPFMLSIQR

EESTCTAIHTDIMDDWLDCAFTCGVHCHGQGKYPCLQVFVNLSH

PGQKALLHYNEEAVQINPKRDVTDCRVKEKQTLTVSDEHKQ

[0165] In some embodiments, the amino acid sequence of PIK3CA (contiguous) is:

(SEQ ID NO: 3)

MPPRPSSGELWGIHLMPPRILVECLLPNGMIVTLECLREATLIT

IKHELFKEARKYPLHQLLQDESSYIFVSVTQEAEREEFFDETRR

LCDLRLFQPFLKVIEPVGNREEKILNREIGFAIGMPVCEFDMVK

DPEVQDFRRNILNVCKEAVDLRDLNSPHSRAMYVYPPNVESSPE

LPKHIYNKLDKGQIIVVIWVIVSPNNDKQKYTLKINHDCVPEQV

IAEAIRKKTRSMLLSSEQLKLCVLEYQGKYILKVCGCDEYFLEK

YPLSQYKYIRSCIMLGRMPNLMLMAKESLYSQLPMDCFTMPSYS

RRISTATPYMNGETSTKSLWVINSALRIKILCATYVNVNIRDID

KIYVRTGIYHGGEPLCDNVNTQRVPCSNPRWNEWLNYDIYIPDL

PRAARLCLSICSVKGRKGAKEEHCPLAWGNINLFDYTDTLVSGK

MALNLWPVPHGLEDLLNPIGVTGSNPNKETPCLELEFDWFSSVV

KFPDMSVIEEHANWSVSREAGFSYSHAGLSNRLARDNELRENDK

EQLKAISTRDPLSEITEQEKDFLWSHRHYCVTIPEILPKLLLSV

KWNSRDEVAQMYCLVKDWPPIKPEQAMELLDCNYPDPMVRGFAV

RCLEKYLTDDKLSQYLIQLVQVLKYEQYLDNLLVRFLLKKALTN

QRIGHFFFWHLKSEMHNKTVSQRFGLLLESYCRACGMYLKHLNR

QVEAMEKLINLTDILKQEKKDETQKVQMKFLVEQMRRPDFMDAL

QGFLSPLNPAHQLGNLRLEECRIMSSAKRPLWLNWENPDIMSEL

LFQNNEIIFKNGDDLRQDMLTLQIIRIMENIWQNQGLDLRMLPY

GCLSIGDCVGLIEVVRNSHTIMQIQCKGGLKGALQFNSHTLHQW

LKDKNKGEIYDAAIDLFTRSCAGYCVATFILGIGDRHNSNIMVK

DDGQLFHIDFGHFLDHKKKKFGYKRERVPFVLTQDFLIVISKGA

QECTKTREFERFQEMCYKAYLAIRQHANLFINLFSMMLGSGMPE

LQSFDDIAYIRKTLALDKTEQEALEYFMKQMNDAHHGGWTTKMD

WIFHTIKQHALN

The nucleic acid sequence of Akt11 is:

(SEQ ID NO: 4)

```
   1    taattatggg tctgtaacca ccctggactg ggtgctcctc actgacggac ttgtctgaac
  61    ctctctttgt ctccagcgcc cagcactggg cctggcaaaa cctgagacgc ccggtacatg
 121    ttggccaaat gaatgaacca gattcagacc ggcaggggcg ctgtggttta ggaggggcct
 181    ggggtttctc ccaggaggtt tttgggcttg cgctggaggg ctctggactc ccgtttgcgc
 241    cagtggcctg catcctggtc ctgtcttcct catgtttgaa tttctttgct ttcctagtct
 301    ggggagcagg gaggagccct gtgccctgtc ccaggatcca tgggtaggaa caccatggac
 361    agggagagca aacggggcca tctgtcacca ggggcttagg gaaggccgag ccagcctggg
 421    tcaaagaagt caaaggggct gcctggagga ggcagcctgt cagctggtgc atcagaggct
 481    gtggccaggc cagctgggct cggggagcgc cagcctgaga ggagcgcgtg agcgtcgcgg
```

-continued

```
 541    gagcctcggg caccatgagc gacgtggcta ttgtgaagga gggttggctg cacaaacgag
 601    gggagtacat caagacctgg cggccacgct acttcctcct caagaatgat ggcaccttca
 661    ttggctacaa ggagcggccg caggatgtgg accaacgtga ggctcccctc aacaacttct
 721    ctgtggcgca gtgccagctg atgaagacgg agcggccccg gcccaacacc ttcatcatcc
 781    gctgcctgca gtggaccact gtcatcgaac gcaccttcca tgtggagact cctgaggagc
 841    gggaggagtg gacaaccgcc atccagactg tggctgacgg cctcaagaag caggaggagg
 901    aggagatgga cttccggtcg ggctcaccca gtgacaactc aggggctgaa gagatggagg
 961    tgtccctggc caagcccaag caccgcgtga ccatgaacga gtttgagtac ctgaagctgc
1021    tgggcaaggg cactttcggc aaggtgatcc tggtgaagga gaaggccaca ggccgctact
1081    acgccatgaa gatcctcaag aaggaagtca tcgtggccaa ggacgaggtg gcccacacac
1141    tcaccgagaa ccgcgtcctg cagaactcca ggcacccctt cctcacagcc ctgaagtact
1201    ctttccagac ccacgaccgc ctctgctttg tcatggagta cgccaacggg ggcgagctgt
1261    tcttccacct gtcccgggag cgtgtgttct ccgaggaccg ggcccgcttc tatggcgctg
1321    agattgtgtc agccctggac tacctgcact cggagaagaa cgtggtgtac cgggacctca
1381    agctggagaa cctcatgctg gacaaggacg ggcacattaa gatcacagac ttcgggctgt
1441    gcaaggaggg gatcaaggac ggtgccacca tgaagacctt ttgcggcaca cctgagtacc
1501    tggcccccga ggtgctggag gacaatgact acggccgtgc agtggactgg tgggggctgg
1561    gcgtggtcat gtacgagatg atgtgcggtc gcctgccctt ctacaaccag gaccatgaga
1621    agcttttga gctcatcctc atggaggaga tccgcttccc gcgcacgctt ggtcccgagg
1681    ccaagtcctt gctttcaggg ctgctcaaga aggaccccaa gcagaggctt ggcgggggct
1741    ccgaggacgc caaggagatc atgcagcatc gcttctttgc cggtatcgtg tggcagcacg
1801    tgtacgagaa gaagctcagc ccacccttca agccccaggt cacgtcggag actgacacca
1861    ggtattttga tgaggagttc acggcccaga tgatcaccat cacaccacct gaccaagatg
1921    acagcatgga gtgtgtggac agcgagcgca ggccccactt cccccagttc tcctactcgg
1981    ccagcggcac ggcctgaggc ggcggtggac tgcgctggac gatagcttgg agggatggag
2041    aggcggcctc gtgccatgat ctgtatttaa tggtttttat ttctcgggtg catttgagag
2101    aagccacgct gtcctctcga gcccagatgg aaagacgttt ttgtgctgtg ggcagcaccc
2161    tcccccgcag cggggtaggg aagaaaacta tcctgcgggt tttaatttat ttcatccagt
2221    ttgttctccg ggtgtggcct cagccctcag aacaatccga ttcacgtagg gaaatgttaa
2281    ggacttctgc agctatgcgc aatgtggcat tgggggggccg ggcaggtcct gcccatgtgt
2341    cccctcactc tgtcagccag ccgccctggg ctgtctgtca ccagctatct gtcatctctc
2401    tggggccctg ggcctcagtt caacctggtg gcaccagatg caacctcact atggtatgct
2461    ggccagcacc ctctcctggg ggtggcaggc acacagcagc cccccagcac taaggccgtg
2521    tctctgagga cgtcatcgga ggctgggccc ctgggatggg accagggatg ggggatgggc
2581    cagggtttac ccagtgggac agaggagcaa ggtttaaatt tgttattgtg tattatgttg
2641    ttcaaatgca ttttgggggt ttttaatctt tgtgacagga aagccctccc ccttcccctt
2701    ctgtgtcaca gttcttggtg actgtcccac cgggagcctc cccctcagat gatctctcca
2761    cggtagcact tgacctttc gacgcttaac ctttccgctg tcgccccagg ccctccctga
2821    ctccctgtgg gggtggccat ccctgggccc ctccacgcct cctggccaga cgctgccgct
```

-continued

```
2881    gccgctgcac cacggcgttt ttttacaaca ttcaacttta gtatttttac tattataata

2941    taatatggaa ccttccctcc aaattcttca ataaaagttg cttttcaaaa aaaaaaaaaa

3001    aaaaaaaa
```

The HER3 amino acid sequence is

(SEQ ID NO: 5)

```
   1   mrandalqvl gllfslargs evgnsqavcp gtlnglsvtg daenqyqtly klyercevvm

  61   gnleivltgh nadlsflqwi revtgyvlva mnefstlplp nlrvvrgtqv ydgkfaifvm

 121   lnyntnssha lrqlrltqlt eilsggvyie kndklchmdt idwrdivrdr daeivvkdng

 181   rscppchevc kgrcwgpgse dcqtltktic apqcnghcfg pnpnqcchde caggcsgpqd

 241   tdcfacrhfn dsgacvprcp qplvynkltf qlepnphtky qyggvcvasc phnfvvdqts

 301   cvracppdkm evdknglkmc epcgglcpka cegtgsgsrf qtvdssnidg fvnctkilgn

 361   ldflitglng dpwhkipald peklnvfrtv reitgylniq swpphmhnfs vfsnlttigg

 421   rslynrgfsl limknlnvts lgfrslkeis agriyisanr qlcyhhslnw tkvlrgptee

 481   rldikhnrpr rdcvaegkvc dplcssggcw gpgpgqclsc rnysrggvcv thcnflngep

 541   refaheaecf schpecqpme gtatcngsgs dtcaqcahfr dgphcvsscp hgvlgakgpi

 601   ykypdvqnec rpchenctqg ckgpelqdcl gqtlvligkt hltmaltvia glvvifmmlg

 661   gtflywrgrr iqnkramrry lergesiepl dpsekankvl arifketelr klkvlgsgvf

 721   gtvhkgvwip egesikipvc ikviedksgr qsfqavtdhm laigsldhah ivrllglcpg

 781   sslqlvtqyl plgslldhvr qhrgalgpql llnwgvqiak gmyyleehgm vhrnlaarnv

 841   llkspsqvqv adfgvadllp pddkqllyse aktpikwmal esihfgkyth qsdvwsygvt

 901   vwelmtfgae pyaglrlaev pdllekgerl aqpqictidv ymvmvkcwmi denirptfke

 961   laneftrmar dpprylvikr esgpgiapgp ephgltnkkl eevelepeld ldldleaeed

1021   nlatttlgsa lslpvgtlnr prgsqslsp ssgympmnqg nlgescqesa vsgssercpr

1081   pvslhpmprg clasessegh vtgseaelqe kvsmcrsrsr srsprprgds ayhsqrhsll

1141   tpvtplsppg leeedvngyv mpdthlkgtp ssregtlssv glssvlgtee ededeeyeym

1201   nrrrrhspph pprpssleel gyeymdvgsd lsaslgstqs cplhpvpimp tagttpdedy

1261   eymnrqrdgg gpggdyaamg acpaseqgye emrafqgpgh qaphvhyarl ktlrsleatd

1321   safdnpdywh srlfpkanaq rt
```

The nucleotide sequence of HER3 is:

(SEQ ID NO: 6)

```
                    ctccga ggtgggcaac tctcaggcag tgtgtcctgg gactctgaat

       ggcctgagtg tgaccggcga tgctgagaac caataccaga cactgtacaa gctctacgag

       aggtgtgagg tggtgatggg gaaccttgag attgtgctca cgggacacaa tgccgacctc

       tccttcctgc agtggattcg agaagtgaca ggctatgtcc tcgtggccat gaatgaattc

       tctactctac cattgcccaa cctccgcgtg gtgcgaggga cccaggtcta cgatgggaag

       tttgccatct tcgtcatgtt gaactataac accaactcca gccacgctct gcgccagctc

       cgcttgactc agctcaccga gattctgtca gggggtgttt atattgagaa gaacgataag

       ctttgtcaca tggacacaat tgactggagg gacatcgtga gggaccgaga tgctgagata

       gtggtgaagg acaatggcag aagctgtccc ccctgtcatg aggtttgcaa ggggcgatgc
```

-continued

781 tggggtcctg gatcagaaga ctgccagaca ttgaccaaga ccatctgtgc tcctcagtgt

841 aatggtcact gctttgggcc caaccccaac cagtgctgcc atgatgagtg tgccgggggc

901 tgctcaggcc ctcaggacac agactgcttt gcctgccggc acttcaatga cagtggagcc

961 tgtgtacctc gctgtccaca gcctcttgtc tacaacaagc taactttcca gctggaaccc

1021 aatccccaca ccaagtatca gtatggagga gtttgtgtag ccagctgtcc ccataacttt

1081 gtggtggatc aaacatcctg tgtcagggcc tgtcctcctg acaagatgga agtagataaa

1141 aatgggctca agatgtgtga gccttgtggg ggactatgtc ccaaagcctg tgagggaaca

1201 ggctctggga gccgcttcca gactgtggac tcgagcaaca ttgatggatt tgtgaactgc

1261 accaagatcc tgggcaacct ggactttctg atcaccggcc tcaatggaga cccctggcac

1321 aagatccctg ccctggaccc agagaagctc aatgtcttcc ggacagtacg ggagatcaca

1381 ggttacctga acatccagtc ctggccgccc cacatgcaca acttcagtgt tttttccaat

1441 ttgacaacca ttggaggcag aagcctctac aaccggggct tctcattgtt gatcatgaag

1501 aacttgaatg tcacatctct gggcttccga tccctgaagg aaattagtgc tgggcgtatc

1561 tatataagtg ccaataggca gctctgctac caccactctt tgaactggac caaggtgctt

1621 cgggggccta cggaagagcg actagacatc aagcataatc ggccgcgcag agactgcgtg

1681 gcagagggca aagtgtgtga cccactgtgc tcctctgggg gatgctgggg cccaggccct

1741 ggtcagtgct tgtcctgtcg aaattatagc cgaggaggtg tctgtgtgac ccactgcaac

1801 tttctgaatg gggagcctcg agaatttgcc catgaggccg aatgcttctc ctgccacccg

1861 gaatgccaac ccatgggggg cactgccaca tgcaatggct cgggctctga tacttgtgct

1921 caatgtgccc attttcgaga tgggccccac tgtgtgagca gctgccccca tggagtccta

1981 ggtgccaagg gcccaatcta caagtaccca gatgttcaga atgaatgtcg gccctgccat

2041 gagaactgca cccaggggtg taaaggacca gagcttcaag actgtttagg acaaacactg

2101 gtgctgatcg gcaaaaccca tctgacaatg gctttgacag tgatagcagg attggtagtg

2161 attttcatga tgctgggcgg cacttttctc tactggcgtg ggcgccggat tcagaataaa

2221 agggctatga ggcgatactt ggaacggggt gagagcatag agcctctgga ccccagtgag

2281 aaggctaaca aagtcttggc cagaatcttc aaagagacag agctaaggaa gcttaaagtg

2341 cttggctcgg gtgtctttgg aactgtgcac aaaggagtgt ggatccctga gggtgaatca

2401 atcaagattc cagtctgcat taaagtcatt gaggacaaga gtggacggca gagttttcaa

2461 gctgtgacag atcatatgct ggccattggc agcctggacc atgcccacat tgtaaggctg

2521 ctgggactat gcccagggtc atctctgcag cttgtcactc aatatttgcc tctgggttct

2581 ctgctggatc atgtgagaca acaccggggg gcactggggc cacagctgct gctcaactgg

2641 ggagtacaaa ttgccaaggg aatgtactac cttgaggaac atggtatggt gcatagaaac

2701 ctggctgccc gaaacgtgct actcaagtca cccagtcagg ttcaggtggc agattttggt

2761 gtggctgacc tgctgcctcc tgatgataag cagctgctat acagtgaggc caagactcca

2821 attaagtgga tggcccttga gagtatccac tttgggaaat acacacacca gagtgatgtc

2881 tggagctatg gtgtgacagt ttgggagttg atgaccttcg gggcagagcc ctatgcaggg

2941 ctacgattgg ctgaagtacc agacctgcta gagaaggggg agcggttggc acagccccag

3001 atctgcacaa ttgatgtcta catggtgatg gtcaagtgtt ggatgattga tgagaacatt

3061 cgcccaacct ttaaagaact agccaatgag ttcaccagga tggcccgaga cccaccacgg

-continued

```
3121   tatctggtca taaagagaga gagtgggcct ggaatagccc ctgggccaga gccccatggt

3181   ctgacaaaca agaagctaga ggaagtagag ctggagccag aactagacct agacctagac

3241   ttggaagcag aggaggacaa cctggcaacc accacactgg gctccgccct cagcctacca

3301   gttggaacac ttaatcggcc acgtgggagc cagagccttt taagtccatc atctggatac

3361   atgcccatga accagggtaa tcttgggggg tcttgccagg agtctgcagt ttctgggagc

3421   agtgaacggt gcccccgtcc agtctctcta cacccaatgc cacggggatg cctggcatca

3481   gagtcatcag aggggcatgt aacaggctct gaggctgagc tccaggagaa agtgtcaatg

3541   tgtagaagcc ggagcaggag ccggagccca cggccacgcg gagatagcgc ctaccattcc

3601   cagcgccaca gtctgctgac tcctgttacc ccactctccc cacccgggtt agaggaagag

3661   gatgtcaacg gttatgtcat gccagataca cacctcaaag gtactccctc ctcccgggaa

3721   ggcacccttt cttcagtggg tctcagttct gtcctgggta ctgaagaaga agatgaagat

3781   gaggagtatg aatacatgaa ccggaggaga aggcacagtc cacctcatcc ccctaggcca

3841   agttcccttg aggagctggg ttatgagtac atggatgtgg ggtcagacct cagtgcctct

3901   ctgggcagca cacagagttg cccactccac cctgtaccca tcatgcccac tgcaggcaca

3961   actccagatg aagactatga atatatgaat cggcaacgag atggaggtgg tcctgggggt

4021   gattatgcag ccatgggggc ctgcccagca tctgagcaag ggtatgaaga gatgagagct

4081   tttcaggggc ctggacatca ggccccccat gtccattatg cccgcctaaa aactctacgt

4141   agcttagagg ctacagactc tgcctttgat aaccctgatt actggcatag caggcttttc

4201   cccaaggcta atgcccagag aacgtaactc ctgctccctg tggcactcag ggagcattta

4261   atggcagcta gtgcctttag agggtaccgt cttctcccta ttccctctct ctcccaggtc

4321   ccagcccctt ttccccagtc ccagacaatt ccattcaatc tttggaggct tttaaacatt

4381   ttgacacaaa attcttatgg tatgtagcca gctgtgcact ttcttctctt tcccaacccc

       aggaaaggtt ttccttattt tgtgtgcttt cccagtccca ttcctcagct tcttcacagg

       cactcctgga gatatgaagg attactctcc atatcccttc ctctcaggct cttgactact

       tggaactagg ctcttatgtg tgcctttgtt tcccatcaga ctgtcaagaa gaggaaaggg

       aggaaaccta gcagaggaaa gtgtaatttt ggtttatgac tcttaacccc ctagaaagac

       agaagcttaa aatctgtgaa gaaagaggtt aggagtagat attgattact atcataattc

       agcacttaac tatgagccag gcatcatact aaacttcacc tacattatct cacttagtcc

       tttatcatcc ttaaaacaat tctgtgacat acatattatc tcattttaca caaagggaag

       tcgggcatgg tggctcatgc ctgtaatctc agcactttgg gaggctgagg cagaaggatt

       acctgaggca aggagtttga gaccagctta gccaacatag taagaccccc atctc
```

[0166] In some embodiments, the dysfunctional protein-protein interaction is one or more of a D1:PI3K interaction or a FGFR3: Daple interaction. In some embodiments, the dysfunctional protein-protein interaction is one or more of a BPIFA1: PIK3CA interaction, a S100A3: Akt interaction, a SCGB2A1: PIK3CA interaction, or a Spinophilin: BRCA1 interaction.

[0167] In some embodiments, the causal agent is HER3 or a dysfunction in HER3 due to a mutation. In some embodiments, the causal agent is Akt or a dysfunction of Akt due to a mutation

[0168] In some embodiments, the method further comprises selecting a hyperproliferative disorder treatment for the subject based upon the causal agent. In some embodiments, the step of selecting a hyperproliferative disorder treatment comprises selecting a treatment from a database of known treatments for the dysfunctional protein-protein interaction.

[0169] In some embodiments, the hyperproliferative disorder treatment comprises administration of a HER3 inhibitor. Examplers of HER3 inhibitors include, but are not limited to, lapatinib, erlotinib, gefitinib, afatinib, neratinib, CDX-3379, U-31402, HMBD-001, MCLA-128, KBP-5209, Poziotinib, Varlitinib, FCN-411, Elgemtumab, Sirotinib, vaccines to target Her3 for solid tumors, AV2103, AV2103, ETBX-031, MP-EV-20, MP-EV-20/1959, and oligonucle-

otides to inhibit EGFR, ERBB2, and ERBB3. Additional exemplary HER3 inhibitors are described in US 2018/0362443 A1, U.S. Pat. No. 10,383,878 B2, US 2019/0300624 A1, WO 2018/182420 A1, WO 2015/007219 A1, U.S. Pat. No. 8,735,551 B2, U.S. Pat. No. 10,507,209 B2, U.S. Pat. No. 9,956,222 B2, U.S. Pat. No. 10,487,143 B2, WO 2018/233511 A1, CN106692969A, US 2020/0147193 A1, U.S. Pat. No. 9,346,889 B2, WO 2020/099235 A1, US 2019/0201552 A1, US 2018/0105815 A1, and US 2020/0157542 A1. In some embodiments, the HER3 inhibitor is CDX3379.

[0170] In some embodiments, the hyperproliferative disorder is head and neck cancer, wherein the mutation candidate is a mutant PIK3CA, wherein the causal agent is HER3, and wherein the hyperproliferative disorder treatment comprises administration of a HER3 inhibitor.

[0171] In some embodiments, the hyperproliferative disorder treatment comprises administration of an Akt inhibitor. Examples of Akt inhibitors include, but are not limited to, MK-2206, AZD5363, GSK690693, GDC-0068, GSK2141795, GSK2110183, AT7867, CCT128930, BAY1125976, perifosine, and AKT inhibitor III.

[0172] In some embodiments, the Akt modulator is a PIK3CA modulator. Examples of PIK3CA modulators include, but are not limited to, Alpelisib, Copanlisib hydrochloride, GDC-0077, Bimiralisib, Fimepinostat, Serabelisib, HHCYH-33, omipalisib, and PQR-514.

[0173] In some embodiments, the hyperproliferative disorder is breast cancer, wherein the mutation candidate is a mutant PIK3CA or a mutant BRCA1, wherein the causal agent is Akt, and wherein the hyperproliferative disorder treatment comprises administration of an Akt inhibitor.

Systems

[0174] The above-described methods can be implemented in any of numerous ways. For example, the embodiments may be implemented using a computer program product (i.e., software), hardware, software, or a combination thereof. When implemented in software, the software code can be executed on any suitable processor or collection of processors, whether provided in a single computer or distributed among multiple computers.

[0175] Thus, in some embodiments, the disclosure relates to computer program products encoded on a computer-readable storage medium, wherein the computer program product comprises instructions for: (a) performing a mass spectrometry analysis on a sample from a subject that has a mutation candidate that causes a hyperproliferative disorder; (b) identifying dysfunctional protein-protein interactions associated with the hyperproliferative disorder; and (c) calculating a differential interaction score (DIS). In some embodiments, the computer program product further comprises instructions for correlating the DIS with the likelihood that the dysfunctional protein-protein interaction is a causal agent of the hyperproliferative disorder. In some embodiments, the computer program product further comprises instructions for: (d) comparing the DIS score to a first threshold; and (e) classifying the subject as being likely to respond to a hyperproliferative disorder treatment, wherein each of steps (d) and (e) are performed after step (c), and wherein the first threshold is calculated relative to a first control dataset.

[0176] In some embodiments, the disclosure relates to systems comprising a disclosed computer program product, and one or more of: (a) a processor operable to execute programs; and (b) a memory associated with the processor.

[0177] In some embodiments, the disclosure relates to systems for identifying a protein interaction network in a subject, the system comprising: (a) a processor operable to execute programs; (b) a memory associated with the processor; (c) a database associated with said processor and said memory; and (d) a program stored in the memory and executable by the processor, the program being operable for: (i) performing a mass spectrometry analysis on a sample from a subject that has a mutation candidate that causes a hyperproliferative disorder; (ii) identifying dysfunctional protein-protein interactions associated with the hyperproliferative disorder; and (iii) calculating a differential interaction score (DIS).

[0178] Without wishing to be bound by theory, it should be appreciated that a computer may be embodied in any of a number of forms, such as a rack-mounted computer, a desktop computer, a laptop computer, or a tablet computer. Additionally, a computer may be embedded in a device not generally regarded as a computer but with suitable processing capabilities, including a Personal Digital Assistant (PDA), a smart phone, or any other suitable portable or fixed electronic device.

[0179] Also, a computer may have one or more input and output devices. These devices can be used, among other things, to present a user interface. Examples of output devices that can be used to provide a user interface include printers or display screens for visual presentation of output and speakers or other sound generating devices for audible presentation of output.

[0180] Examples of input devices that can be used for a user interface include keyboards, and pointing devices, such as mice, touch pads, and digitizing tablets. As another example, a computer may receive input information through speech recognition or in other audible format.

[0181] Such computers may be interconnected by one or more networks in any suitable form, including a local area network or a wide area network, such as an enterprise network, and intelligent network (IN) or the Internet. Such networks may be based on any suitable technology and may operate according to any suitable protocol and may include wireless networks, wired networks, or fiber optic networks.

[0182] A computer employed to implement at least a portion of the functionality described herein may include a memory, coupled to one or more processing units (also referred to herein simply as "processors"), one or more communication interfaces, one or more display units, and one or more user input devices. The memory may include any computer-readable media, and may store computer instructions (also referred to herein as "processor-executable instructions") for implementing the various functionalities described herein. The processing unit(s) may be used to execute the instructions. The communication interface(s) may be coupled to a wired or wireless network, bus, or other communication means and may therefore allow the computer to transmit communications to and/or receive communications from other devices. The display unit(s) may be provided, for example, to allow a user to view various information in connection with execution of the instructions. The user input device(s) may be provided, for example, to allow the user to make manual adjustments, make selections,

enter data or various other information, and/or interact in any of a variety of manners with the processor during execution of the instructions.

[0183] The various methods or processes outlined herein may be coded as software that is executable on one or more processors that employ any one of a variety of operating systems or platforms. The disclosure also relates to a computer readable storage medium comprising executable instructions. Additionally, such software may be written using any of a number of suitable programming languages and/or programming or scripting tools, and also may be compiled as executable machine language code or intermediate code that is executed on a framework or virtual machine.

[0184] In this respect, various inventive concepts may be embodied as a computer readable storage medium (or multiple computer readable storage media) (e.g., a computer memory, one or more floppy discs, compact discs, optical discs, magnetic tapes, flash memories, circuit configurations in Field Programmable Gate Arrays or other semiconductor devices, or other non-transitory medium or tangible computer storage medium) encoded with one or more programs that, when executed on one or more computers or other processors, perform methods that implement the various embodiments of the invention disclosed herein. The computer readable medium or media can be transportable, such that the program or programs stored thereon can be loaded onto one or more different computers or other processors to implement various aspects of the present invention as discussed above. In some embodiments, the system comprises cloud-based software that executes one or all of the steps of each disclosed method instruction.

[0185] The terms "program" or "software" are used herein in a generic sense to refer to any type of computer code or set of computer-executable instructions that can be employed to program a computer or other processor to implement various aspects of embodiments as discussed above. Additionally, it should be appreciated that according to one aspect, one or more computer programs that when executed perform methods of the present disclosure need not reside on a single computer or processor, but may be distributed in a modular fashion amongst a number of different computers or processors to implement various aspects of the present invention.

[0186] Computer-executable instructions may be in many forms, such as program modules, executed by one or more computers or other devices. Generally, program modules include routines, programs, objects, components, data structures, etc. that perform particular tasks or implement particular abstract data types. Typically, the functionality of the program modules may be combined or distributed as desired in various embodiments.

[0187] Also, data structures may be stored in computer-readable media in any suitable form. For simplicity of illustration, data structures may be shown to have fields that are related through location in the data structure. Such relationships may likewise be achieved by assigning storage for the fields with locations in a computer-readable medium that convey relationship between the fields. However, any suitable mechanism may be used to establish a relationship between information in fields of a data structure, including through the use of pointers, tags or other mechanisms that establish relationship between data elements.

[0188] Also, the disclosure relates to various embodiments in which one or more methods. The acts performed as part of the method may be ordered in any suitable way. Accordingly, embodiments may be constructed in which acts are performed in an order different than illustrated, which may include performing some acts simultaneously, even though shown as sequential acts in illustrative embodiments.

[0189] Computer-implemented embodiments of the disclosure relate to methods of determining a subject likely to respond to cancer disease-modifying agents comprising steps of: (e) comparing the first normalized score to a first threshold relative to a first control dataset of a sample and comparing a second normalized score to a second threshold relative to a control dataset of the sample; and (f) classifying the subject as being likely to respond to a chemotherapeutic treatment based upon results of comparing of step (e) relative to the first and/or second threshold; wherein each of steps (e) and (f) are performed after step (d).

[0190] In some embodiments, the disclosure relates to a system that comprises at least one processor, a program storage, such as memory, for storing program code executable on the processor, and one or more input/output devices and/or interfaces, such as data communication and/or peripheral devices and/or interfaces. In some embodiments, the user device and computer system or systems are communicably connected by a data communication network, such as a Local Area Network (LAN), the Internet, or the like, which may also be connected to a number of other client and/or server computer systems. The user device and client and/or server computer systems may further include appropriate operating system software.

[0191] In some embodiments, components and/or units of the devices described herein may be able to interact through one or more communication channels or mediums or links, for example, a shared access medium, a global communication network, the Internet, the World Wide Web, a wired network, a wireless network, a combination of one or more wired networks and/or one or more wireless networks, one or more communication networks, an a-synchronic or asynchronous wireless network, a synchronic wireless network, a managed wireless network, a non-managed wireless network, a burstable wireless network, a non-burstable wireless network, a scheduled wireless network, a non-scheduled wireless network, or the like.

[0192] Discussions herein utilizing terms such as, for example, "processing," "computing," "calculating," "determining," or the like, may refer to operation(s) and/or process(es) of a computer, a computing platform, a computing system, or other electronic computing device, that manipulate and/or transform data represented as physical (e.g., electronic) quantities within the computer's registers and/or memories into other data similarly represented as physical quantities within the computer's registers and/or memories or other information storage medium that may store instructions to perform operations and/or processes.

[0193] Some embodiments may take the form of an entirely hardware embodiment, an entirely software embodiment, or an embodiment including both hardware and software elements. Some embodiments may be implemented in software, which includes but is not limited to firmware, resident software, microcode, or the like.

[0194] Furthermore, some embodiments may take the form of a computer program product accessible from a computer-usable or computer-readable medium providing

program code for use by or in connection with a computer or any instruction execution system. For example, a computer-usable or computer-readable medium may be or may include any apparatus that can contain, store, communicate, propagate, or transport the program for use by or in connection with the instruction execution system, apparatus, or device.

[0195] In some embodiments, the medium may be or may include an electronic, magnetic, optical, electromagnetic, InfraRed (IR), or semiconductor system (or apparatus or device) or a propagation medium. Some demonstrative examples of a computer-readable medium may include a semiconductor or solid state memory, magnetic tape, a removable computer diskette, a Random Access Memory (RAM), a Read-Only Memory (ROM), a rigid magnetic disk, an optical disk, or the like. Some demonstrative examples of optical disks include Compact Disk-Read-Only Memory (CD-ROM), Compact Disk-Read/Write (CD-R/W), DVD, or the like.

[0196] In some embodiments, a data processing system suitable for storing and/or executing program code may include at least one processor coupled directly or indirectly to memory elements, for example, through a system bus. The memory elements may include, for example, local memory employed during actual execution of the program code, bulk storage, and cache memories which may provide temporary storage of at least some program code in order to reduce the number of times code must be retrieved from bulk storage during execution.

[0197] In some embodiments, input/output or I/O devices (including but not limited to keyboards, displays, pointing devices, etc.) may be coupled to the system either directly or through intervening I/O controllers. In some embodiments, network adapters may be coupled to the system to enable the data processing system to become coupled to other data processing systems or remote printers or storage devices, for example, through intervening private or public networks. In some embodiments, modems, cable modems and Ethernet cards are demonstrative examples of types of network adapters. Other suitable components may be used.

[0198] Some embodiments may be implemented by software, by hardware, or by any combination of software and/or hardware as may be suitable for specific applications or in accordance with specific design requirements. Some embodiments may include units and/or sub-units, which may be separate of each other or combined together, in whole or in part, and may be implemented using specific, multi-purpose or general processors or controllers. Some embodiments may include buffers, registers, stacks, storage units and/or memory units, for temporary or long-term storage of data or in order to facilitate the operation of particular implementations.

[0199] Some embodiments may be implemented, for example, using a machine-readable medium or article which may store an instruction or a set of instructions that, if executed by a machine, cause the machine to perform a method steps and/or operations described herein. Such machine may include, for example, any suitable processing platform, computing platform, computing device, processing device, electronic device, electronic system, computing system, processing system, computer, processor, or the like, and may be implemented using any suitable combination of hardware and/or software. The machine-readable medium or article may include, for example, any suitable type of memory unit, memory device, memory article, memory medium, storage device, storage article, storage medium and/or storage unit; for example, memory, removable or non-removable media, erasable or non-erasable media, writeable or re-writeable media, digital or analog media, hard disk drive, floppy disk, Compact Disk Read Only Memory (CD-ROM), Compact Disk Recordable (CD-R), Compact Disk Re-Writeable (CD-RW), optical disk, magnetic media, various types of Digital Versatile Disks (DVDs), a tape, a cassette, or the like. The instructions may include any suitable type of code, for example, source code, compiled code, interpreted code, executable code, static code, dynamic code, or the like, and may be implemented using any suitable high-level, low-level, object-oriented, visual, compiled and/or interpreted programming language, e.g., C, C++, Java™, BASIC, Pascal, Fortran, Cobol, assembly language, machine code, or the like.

[0200] Many of the functional units described in this specification have been labeled as circuits, in order to more particularly emphasize their implementation independence. For example, a circuit may be implemented as a hardware circuit comprising custom very-large-scale integration (VLSI) circuits or gate arrays, off-the-shelf semiconductors such as logic chips, transistors, or other discrete components. A circuit may also be implemented in programmable hardware devices such as field programmable gate arrays, programmable array logic, programmable logic devices or the like.

[0201] In some embodiment, the circuits may also be implemented in machine-readable medium for execution by various types of processors. An identified circuit of executable code may, for instance, comprise one or more physical or logical blocks of computer instructions, which may, for instance, be organized as an object, procedure, or function. Nevertheless, the executables of an identified circuit need not be physically located together, but may comprise disparate instructions stored in different locations which, when joined logically together, comprise the circuit and achieve the stated purpose for the circuit. Indeed, a circuit of computer readable program code may be a single instruction, or many instructions, and may even be distributed over several different code segments, among different programs, and across several memory devices. Similarly, operational data may be identified and illustrated herein within circuits, and may be embodied in any suitable form and organized within any suitable type of data structure. The operational data may be collected as a single data set, or may be distributed over different locations including over different storage devices, and may exist, at least partially, merely as electronic signals on a system or network.

[0202] The computer readable medium (also referred to herein as machine-readable media or machine-readable content) may be a tangible computer readable storage medium storing the computer readable program code. The computer readable storage medium may be, for example, but not limited to, an electronic, magnetic, optical, electromagnetic, infrared, holographic, micromechanical, or semiconductor system, apparatus, or device, or any suitable combination of the foregoing. As alluded to above, examples of the computer readable storage medium may include but are not limited to a portable computer diskette, a hard disk, a random access memory (RAM), a read-only memory (ROM), an erasable programmable read-only memory (EPROM or Flash memory), a portable compact disc read-

only memory (CD-ROM), a digital versatile disc (DVD), an optical storage device, a magnetic storage device, a holographic storage medium, a micromechanical storage device, or any suitable combination of the foregoing. In the context of this document, a computer readable storage medium may be any tangible medium that can contain, and/or store computer readable program code for use by and/or in connection with an instruction execution system, apparatus, or device.

[0203] The computer readable medium may also be a computer readable signal medium. A computer readable signal medium may include a propagated data signal with computer readable program code embodied therein, for example, in baseband or as part of a carrier wave. Such a propagated signal may take any of a variety of forms, including, but not limited to, electrical, electro-magnetic, magnetic, optical, or any suitable combination thereof. A computer readable signal medium may be any computer readable medium that is not a computer readable storage medium and that can communicate, propagate, or transport computer readable program code for use by or in connection with an instruction execution system, apparatus, or device. As also alluded to above, computer readable program code embodied on a computer readable signal medium may be transmitted using any appropriate medium, including but not limited to wireless, wireline, optical fiber cable, Radio Frequency (RF), or the like, or any suitable combination of the foregoing. In one embodiment, the computer readable medium may comprise a combination of one or more computer readable storage mediums and one or more computer readable signal mediums. For example, computer readable program code may be both propagated as an electro-magnetic signal through a fiber optic cable for execution by a processor and stored on RAM storage device for execution by the processor.

[0204] Computer readable program code for carrying out operations for aspects of the present invention may be written in any combination of one or more programming languages, including an object oriented programming language such as Java, Smalltalk, C++ or the like and conventional procedural programming languages, such as the "C" programming language or similar programming languages. The computer readable program code may execute entirely on a user's computer, partly on the user's computer, as a stand-alone computer-readable package, partly on the user's computer and partly on a remote computer or entirely on the remote computer or server. In the latter scenario, the remote computer may be connected to the user's computer through any type of network, including a local area network (LAN) or a wide area network (WAN), or the connection may be made to an external computer (for example, through the Internet using an Internet Service Provider).

[0205] The program code may also be stored in a computer readable medium that can direct a computer, other programmable data processing apparatus, or other devices to function in a particular manner, such that the instructions stored in the computer readable medium produce an article of manufacture including instructions which implement the function/act specified in the schematic flowchart diagrams and/or schematic block diagrams block or blocks.

[0206] Functions, operations, components and/or features described herein with reference to one or more embodiments, may be combined with, or may be utilized in combination with, one or more other functions, operations, components and/or features described herein with reference to one or more other embodiments, or vice versa.

[0207] The disclosure relates to a computer program product comprising instructions to calculate DIS in connection with a structure of an oncoprotein. In some embodiments, the computer program product comprises instructions for any of the steps identified in the disclosure. In some embodiments, the disclosure relates to a method of imaging a structure of a protein associated with a hyperproliferative disorder, the method comprising: (a) identifying a nucleic acid sequence or protein sequence associated with a hyperproliferative disorder (b) calculating a DIS score associated with the nucleic acid sequence or protein sequence; and (c) creating an image of the structure of the protein based upon the DIS using a system disclosed herein, the image being displayed on a display operably connected to a controller comprising a computer program product disclosed herein.

[0208] In some embodiments, the disclosure relates to methods of imaging a protein, the method comprising: (a) identifying a first protein that co-localizes with a first host protein in one or a plurality of bioassays; (b) calculating a differential interaction score (DIS) corresponding to the first protein in a sample; and (c) predicting the three-dimensional structure of the first protein by integrating the DIS score into a fit. In some embodiments, the first protein is isolated in vitro from a sample. In some embodiments, the sample is from a cell extract or subject. In some embodiments, the first protein is mutated as compared to a wild-type or endogenous, unmutated sequence. In some embodiments, the method is a computer-implemented method performed on a system disclosed herein, comprising instructions for execution of the DIS calculation.

[0209] Although the disclosure has been described with reference to exemplary embodiments, it is not limited thereto. Those skilled in the art will appreciate that numerous changes and modifications may be made to the preferred embodiments of the disclosure and that such changes and modifications may be made without departing from the true spirit of the disclosure. It is therefore intended that the appended claims be construed to cover all such equivalent variations as fall within the true spirit and scope of the disclosure.

[0210] All referenced journal articles, patents, and other publications are incorporated by reference herein in their entireties.

EXAMPLES

[0211] Representative examples of the disclosed methods and systems are illustrated in the following non-limiting methods and examples.

Example 1. The Protein Interaction Landscape of Breast Cancer

Experimental Model and Subject Details

Cloning and Cell Line Generation

[0212] Complementary DNAs (cDNA) of each bait were obtained from human ORFeome collection (v8.1) or Addgene [pcDNA6-ARID1A (#39311), pcDNA3-Casp8 (#11817), hEcadherin-pcDNA3 (#45769), pDONR223_EGFR_WT (#81926), pDONR221-Spinophilin (#87123)]. In case that cDNAs of canonical isoforms were not available, they were synthesized using gBlock fragments (IDT,

Genewiz). These cDNAs were cloned using the Gateway Cloning System (Life Technologies) into a doxycycline-inducible N-term or C-term 3×FLAG-tagged vector modified to be Gateway compatible from the pLVX-Puro vector (Clontech). Point mutant baits were generated via site-directed mutagenesis. All expression vectors were full-sequence verified.

Cell Culture, Lentivirus Production, and Stable Cell Line Generation

[0213] A MDA-MB-231 (ATTC, HTB-26) were maintained in DMEM and Ham's F-12 50/50 (Corning) supplemented with 10% fetal bovine serum (Gibco) and 1% Penicillin/Streptomycin (Corning). MCF10A (ATCC CRL-10317) cells were maintained in DMEM and Ham's F-12 50/50 supplemented with 20% horse serum (Gibco), EGF (PeproTech), Hydrocortisone (Sigma-Aldrich), Cholera toxin (Sigma-Aldrich), Insulin (Sigma-Aldrich) and 1% Penicillin/Streptomycin. HEK293T (ATCC, CRL-3216), MCF7 (ATCC, HTB-22) and U2OS-GFP reporter cell lines (gifts from Dr. Stark at City of Hope National Medical Center) were maintained in DMEM supplemented with 10% fetal bovine serum (Gibco) and 1% Penicillin-Streptomycin. All cells were cultured at 37° C. in a humidified atmosphere with 5% CO_2.

[0214] One day prior to transfection, 5.0 million HEK293T cells were plated in a 15 cm dish. Lentivirus was produced for each protein by using 5 μg of expression vector, 3.33 μg of Gag-Pol-Tat-Rev packaging vector (pJH045 from Judd Hultquist) and VSV-G (pJH046 from Judd Hultquist) mixed with 30 μL of PolyJet DNA Transfection Reagent (SignaGen) in serum free DMEM. DNA complexes were incubated at RT for 25 min and added dropwise to HEK293T cells. After 72 hrs, the lentivirus containing supernatant from infected HEK293T cells was centrifuged at 400×g for 5 min to pellet any debris. The supernatant was filtered through a 0.45 μm PVDF filter. Virions were let to aggregate and precipitate in PEG-6000 (8.5% final) and NaCl (0.3 M final) at 4° C. for 4-8 h. Virions were pelleted by spinning at 3500 rpm for 20 min at 4° C. The pellet was then resuspended in DPBS for a final volume between 800 to 1000 μL and stored at −80° C. until use.

[0215] Stable cell lines were generated by transducing a 10 cm plate at 80% confluency with 200 μL of precipitated lentivirus for 24 hrs. Transduced cells were selected with 2.5 μg/mL of puromycin.

Cell Lysis and Affinity Purification

[0216] Three independent biological replicates of cells were plated in 10 cm dishes. For doxycycline-inducible gene expression, cells were induced at 40-50% confluence with 1 μg/mL doxycycline for 40 hrs. To prepare cell extracts, a 10 cm dish was washed with 1 mL of ice-cold PBS and lysed in 300 μL of S150 lysis buffer (50 mM Tris, pH 7.5, 150 mM NaCl, 1 mM EDTA, 0.5% NP-40, 1 mM DTT, 1× Protease and Phosphatase Inhibitor Cocktail and 125 U Benzonase/mL) using freeze thaw method—5 min on dry ice, followed by 30-45 see thaw in 37° C. water bath with agitation. Cell lysates were clarified by spinning at 13,000×g for 15 min at 4° C. A 20 μL aliquot was saved for western blot.

[0217] For FLAG purification, 25 μL of bead slurry was washed twice with 1 mL of S150 buffer. Supernatants were incubated with Anti-FLAG M2 magnetic beads (M8823, Sigma-Aldrich) or Anti-V5 magnetic beads (M167-11, MBL International) overnight at 4° C. with rotation. The beads were washed one time with 1 mL of S150 buffer containing 0.1% NP40 followed by two washes in detergent free S150 buffer.

[0218] To perform on bead digestion, magnetic beads were resuspended in 15 μL of freshly prepared 8 M urea with 50 mM Tris, pH 9.0, 1 mM DTT and 1 μg LysC and incubated for 1 hr at 37° C. Supernatant was incubated with 3 mM iodoacetamide (IAA) in the dark at room temperature (RT) for 45 min. Quenching IAA with 3 mM DTT for 15 min at RT was followed by another incubation for 1 hr at RT with shaking. Samples were diluted 4-fold by 50 mM

[0219] Tris, pH 8.0 to bring final concentration of urea to 2 M and digested with 1 μg trypsin at 37° C. overnight. Samples were acidified with 10% trifluoroacetic acid (TFA) to final 0.5% (pH<2) and desalted using Nest Tips C18. Tips were conditioned with 80% acetonitrile, 0.1% TFA and sequentially equilibrated three times with 0.1% TFA before applying samples. Bound peptides were sequentially rinsed three times with 0.1% TFA and eluted with 50% acetonitrile and 0.25% formic acid (FA). Eluted peptides were dried under vacuum centrifugation and resuspended in 3% ACN and 0.1% FA prior to mass spectrometry.

Global Endogenous Protein Abundance Analysis

[0220] Following cell lysis, protein concentration was determined using Bradford assay. IAA was added to each sample to a final concentration of 10 mM, and samples were incubated in the dark at room temperature for 30 min.

[0221] Excess IAA was quenched by the addition of dithiothreitol to 10 mM, followed by incubation in the dark at room temperature for 30 min. Samples were then diluted with 0.1 M ammonium bicarbonate, pH 8.0 to a final urea concentration of 2 M. Trypsin (Promega) was added at a 1:100 (enzyme: protein) ratio and digested overnight at 37° C. with rotation. Following digestion, 10% TFA was added to each sample to a final pH~2. Samples were desalted under vacuum using Sep Pak C18 cartridges (Waters). Each cartridge was activated with 1 mL 80% acetonitrile (ACN)/0.1% TFA, then equilibrated three times with 1 mL of 0.1% TFA. Following sample loading, cartridges were washed four times with 1 mL of 0.1% TFA, and samples were eluted four times with 0.5 mL 50% ACN/0.25% FA. 20 μg of each sample was kept for protein abundance measurements, and the remainder was used for phosphopeptide enrichment. Samples were dried by vacuum centrifugation.

Mass Spectrometry Data Acquisition and Analysis

[0222] For AP-MS experiments, samples were resuspended in 15 μL of MS loading buffer (4% formic acid, 2% acetonitrile) and 2 μL were separated by a reversed-phase gradient over a nanoflow 75 μm ID×25 cm long picotip column packed with 1.9 μM C18 particles (Dr. Maisch). Peptides were directly injected over the course of a 75 min acquisition into a Q-Exactive Plus mass spectrometer (Thermo), or over the course of a 90 min acquisition into a Orbitrap Elite mass spectrometer. For analysis of endogenous protein abundances in parental cell lines, ~500 ng of peptides was separated over a 180 min gradient using the same column as for AP-MS experiments, and directly injected into a Q-Exactive Plus mass spectrometer. Raw MS data were searched against the uniprot canonical isoforms of

the human proteome (downloaded Mar. 21, 2018), and using the default settings in MaxQuant (version 1.6.2.10), with a match-between-runs enabled (Cox and Mann, 2008). Peptides and proteins were filtered to 1% false discovery rate in MaxQuant, and identified proteins were then subjected to protein-protein interaction scoring. To quantify changes in interactions between WT and mutant baits, or differences in endogenous protein abundances between parental cell lines, a label free quantification approach was used, in which statistical analysis was performed using MSstats (Choi et al., 2014) from within the artMS R-package. All raw data files and search results are available from the Pride partner ProteomeXchange repository under the PXD019639 identifier (Vizcaino et al. 2014; Perez-Riverol et al. 2019).

Protein-Protein Interaction Scoring

[0223] Protein spectral counts as determined by MaxQuant search results were used for PPI confidence scoring by both SAINTexpress (version 3.6.1) (Teo et al., 2014b) and CompPASS (version 0.0.0.9000) (Huttlin et al., 2015b; Sowa et al., 2009b). All PPI scoring was performed separately for each cell line. For SAINTexpress, control samples in which bait protein was not induced by doxycycline were used. For CompPASS, a stats table representing all no dox-induced samples (at least one per each bait) and WT baits was used. When recovery rates of known PPIs (gold standard) from public databases (CORUM, BioPlex2, and BioGRID low throughput and multivalidated) were monitored by varying thresholds of key metrics of each algorithm (WD per bait percentile for compPASS and BFDR for SAINTexpress, respectively), it is noticeable that CompPASS and SAINTexpress are complementary to each other, in that the best gold standard PPI recovery could be obtained when the PPIs from each algorithm are combined (FIG. **1**A and FIG. **1**B). Therefore, a PPI score was defined on a zero to 1 scale, wherein WD per bait percentile and (1-BFDR) were equally weighted: PPI score=[WD per bait percentile+(1−BFDR)]/2. The PPIs were filtered with PPI score≥0.9.

[0224] Referring to FIG. **1**A, a comparison of PPIs filtered by compPASS and SAINTexpress, respectively, is shown. For each cell line, two sorted lists of PPIs were created based on the WD per bait percentile derived from compPASS score and SAINTexpress BFDR. The numbers of gold standard PPIs among top x PPIs (x=100, 200, . . . , 1,000) in each sorted list were compared. Top shaded portion indicates the gold standard PPIs recovered by SAINTexpress, bottom shaded portion indicates the ones recovered by compPASS, and middle shaded portion indicates the gold standard PPI recovered by both. Combination of compPASS and SAINTexpress best accommodate gold standard PPIs.

[0225] Referring to FIG. **1**B, a comparison of PPI score calculated using compPASS and SAINTexpress scores is shown. Left bars indicate the number of gold standard PPIs recovered using a PPI score calculated using WD per bait percentile (WDpb) and Z per bait percentile (Zpb) from compPASS, and BFDR from SAINTexpress. Right bars indicate the recovery of gold standard PPIs based on a PPI score that only considers WDpb and BFDR. The comparison reveals that WDpb and BFDR are the most deterministic factors in recovering gold standard PPIs from each cell line.

Correspondence Between Interaction Uniqueness and Expression Abundance Analysis

[0226] For each cell line comparison, shared baits were identified. For each bait, unique preys were extracted and their corresponding global abundance log 2FC was annotated. Only preys with a detected measurement in the global abundance analysis were included. Next, the fraction of preys (unique in one cell line or another in binding to a certain bait) with a correlated (gain in interaction=increase in abundance, and vice versa) or anticorrelated (gain in interaction=decrease in abundance, and vice versa) significant change [abs(log 2FC)>1 & adjusted p-value<0.05] in global abundance was calculated (see FIG. **2**D).

[0227] Referring to FIG. **2**D, the percentage of unique interactions (preys) for the same bait between cell lines with a correlated (bottom) or anticorrelated (middle) significant change (≥2-fold change, adjusted p-value<0.05) in abundance. Top indicates unique interactions with no significant change in abundance. Only preys detected by global abundance mass spectrometry analysis are considered.

Differential Interaction Score Calculation

[0228] An important goal of cancer therapy is to identify drug targets that are cancer specific, and are applicable across many patients. As such, comparing PPIs across cell lines to prioritize those that were shared between cancer cell lines, but absent from the MCF10A non-tumorigenic cell line, was of interest. Unfortunately, a simple overlap analysis of BC PPIs identified within each cell line does not faithfully represent whether a given PPI is shared or unique in all cases. The reason for this is that to establish a finite list of BC PPIs, one must establish a threshold for such classification. This threshold strikes a balance between maximizing sensitivity for true interactions, while minimizing the inclusion of erroneous false positive interaction partners, which are often due to non-specific binding to the beads. However, it can also be the case that real PPIs do not meet this threshold (false negatives).

[0229] To compare PPIs across cell lines, a method for calculating a differential interaction score (DIS) and a corresponding false discovery rate (FDR) was developed using AP-MS data across multiple cell lines. This approach uses the SAINTexpress score (Teo et al., 2014b), which is the probability of a PPI being bonafide in a single cell line computed using a mixture of distribution modeling spectral counts of true and false interactions. The probabilities based on the analysis of a single cell line can then be used to calculate a differential interaction score between PPIs present in cancer cells and normal cells. A cancer-specific differential interaction score was defined as the probability of the PPI being present in a cancer cell line but absent in the normal cell line. Let Sc(p1, p2) be the SAINTexpress score of a PPI denoted as (p1, p2) in a cell line c. Given that PPIs are independent events across different cell lines, the differential interaction score is computed for each (p1, p2) as the product of the probability of a bonafide PPI in one cell line and the probability of the PPI being false in the other cell lines, which can be denoted as follows:

$$DIS_{MCF7}(p_1, p_2) =$$

$$S_{MCF7}(p_1, p_2) \times (1 - S_{MDA-MB-231}(p_1, p_2)) \times (1 - S_{MCF10A}(p_1, p_2))$$

$$\text{and } DIS_{MDA-MB-231}(p_1, p_2) = S_{MDA-MB-231}(p_1, p_2) \times$$

$$(1 - S_{MCF7}(p_1, p_2)) \times (1 - S_{MCF10A}(p_1, p_2)) \text{ and } DIS_{MCF10A}(p_1, p_2) =$$

$$S_{MCF10A}(p_1, p_2) \times (1 - S_{MDA-MB-231}(p_1, p_2)) \times (1 - S_{MCF7}(p_1, p_2))$$

[0230] For all differential interaction scores that were calculated, the Bayesian false discovery rate (BFDR) estimates at all possible thresholds (p*) were computed as follows:

$$FDR(p^*) = \frac{\sum_{i,j}(1 - DIS(p_i, p_j)) \times I(DIS(p_i, p_j) > p^*)}{\sum_{i,j} I(DIS(p_i, p_j) > p^*)},$$

where $I\{A\}$ is 1 when A is True and 0 otherwise.

Permutation Test

[0231] A permutation test was performed in which genes were drawn from the list of all genes detected in the global protein abundance analysis of the parental cell lines. The null distribution of the average number of samples with variation was learned from 10,000 random gene lists of equal size to the set of interacting partners. This permutation test was performed individually for non-synonymous mutations, CNVs, and mRNA expression. The information for observed variation of each gene is collected from the TCGA BC cohort (firehose legacy).

IAS Network

[0232] The integrated associated stringency (IAS) network was derived from integration of five major types of protein pairwise relationships recorded in public databases: (1) physical protein-protein interaction; (2) mRNA co-expression; (3) protein co-expression; (4) co-dependence (correlation of cell line growth upon gene knockouts); and (5) sequence-based relationships. A broad survey created a compendium of 127 network features used as inputs to a random forest regression model, trained to best recover the proximity of protein pairs in the Gene Ontology (GO). The final IAS score, ranging from 0 to 1, quantifies all pairwise associations among 19035 human proteins. In this study, stringent protein interactions were displayed with IAS>0.3 when the IAS network was used in figures.

Peptide Phosphorylation Assay

[0233] This assay uses a set of peptide sequences that are derived from computationally curated biological targets of kinases' substrates deposited in PhosphoAtlas (Chen and Coppé, 2012; Olow et al., 2016). Peptides (total 453 peptides from 237 proteins) individually allocated to separate wells in a series of 384-well plates serve as phosphorylatable probes in a large-scale ATP-consumption biochemical assay handled by automated liquid dispensing instruments. For each experimental run, the average value of ATP concentration in sample-containing wells was used for internal normalization to calculate the phosphorylation activity per peptide as the difference in ATP consumption between each peptide-derived read out and the internal mean. For the current study, the analysis of peptide phosphorylation profiles measured in Spinophilin knockout cells was focused on. To prepare protein extracts to run on the assay platform, cells at ~85% confluency were washed three times with cold PBS and lysed with freshly prepared 1× cell lysis buffer (1 ml per 3×106 cells) (10× Cell Lysis Buffer, Cell Signaling; cat #9803) complemented with 1× of Halt Protease & Phosphatase (100×, ThermoScientific; cat #1861281). Cell lysates were collected and spun down at 14,000 rpm for 15 min at 4° C. and supernatants stored at −80° C.

In-Cell Western Blot Assay

[0234] Four independent siRNAs per target gene were purchased from Dharmacon (siGENOME SMARTpool) in Echocompatible 384-well plates (Labcyte #PP-0200) and resuspended in 20 uL nuclease-free water. For the assay, 4 pmol of siRNAs were aliquoted into each well of a black walled clear bottom 96-well plates (Corning #3904) avoiding edges using a Labcyte Echo 525. Plates were then stored at −80° C. On the day of the experiment, plates were thawed for 0.5-1 hour at room temperature, centrifuged at 1000 rpm for 5 minutes, and reconstituted with 20 uL of nuclease free water (Ambion #AM9938) on a rotator for 30 minutes. Transfection reagent was prepared using 0.1% RNAiMax (Invitrogen #13778150) and 20% Optimem (Gibco #31985062) for a seeding density of 4,000 cells per well; reagent was allowed to sit for 10 minutes at room temperature before adding 40 uL to each well and incubated for an additional 20 minutes. Cells grown to a confluency of 80% were lifted using 0.25% Trypsin (BioUltra #V611×), counted, and 4000 cells were seeded per well in a 140 uL volume, resulting in 200 uL total volume for each well. Cells were incubated in a standard incubator at 37° C. and 5% CO_2 for 48 hours. Following the 48-hour incubation, growth media was aspirated and cells were fixed using 50 uL per well of 4% paraformaldehyde solution (Thermo Fisher #PI28908) for 15 minutes. Cells were permeabilized using 50 uL 1:100 dilution of Triton X-100 (Sigma #9002-93-1) in 1×PBS for 30 minutes, then incubated in a 2× blocking solution (2% BSA in 1×PBS) at room temperature for 2 hours. Next, blocking buffer was removed and replaced with 50 uL 1× primary antibody per well, prepared by diluting Total AKT (mouse; Cell Signaling Technologies #2920S) and pAKT S473 (rabbit; Cell Signaling Technologies #4060S) at 1:800 dilution in 1× blocking buffer (1% BSA in 1×PBS). Cells were incubated in 1× primary antibody solution overnight at 4° C. The next morning, cells were washed with 1× wash buffer (250 uL Tween-20 in 50 mL 1×PBS) and incubated for 2 hours in the dark at room temperature with 1× secondary antibody solution containing 1:1000 dilution (in 1% BSA) of anti-mouse (926-32210) and anti-rabbit (926-32211) near-infrared antibodies. Cells were washed using 1× wash buffer and resuspended in 100 uL PBS for fluorescence detection using an LiCOR Odyssey plate scanner (9140). Wavelengths for the antibodies were set to 680 nm for anti-rabbit and 800 nm for anti-mouse. To measure cell viability, PBS was aspirated and cells were stained with 50 uL Janus Green Stain (Abcam #ab111622) for 5 minutes at room temperature. Cells were washed using ultrapure water and lysed with 100 ul 0.5m HCl shaking at 400 rpm for 10 minutes. A standard microplate spectrophotometer was used to measure OD 595 nm.

Co-Immunoprecipitation and Western Blot Analysis

[0235] Cell extracts were prepared using the same protocol as described in the Cell lysis and affinity purification. To ensure the same amount of proteins for each sample, supernatant was quantified by Bradford protein assay prior incubation with the beads. After overnight incubation with beads at 4° C., as previously described, proteins were eluted from the beads by boiling in 2×SDS Sample Buffer (Alfa Aesar) diluted in S150 buffer and stored at −20° C.

[0236] For immunoblots, samples were loaded onto 7.5% Mini-PROTEAN® TGX™ Precast Protein Gel (Bio-Rad). After gel electrophoresis, the samples were transferred to a membrane with Trans-Blot Turbo Transfer System (Bio-Rad). Membranes were blocked with 5% Milk TBST for 1 h at RT and incubated in the blocking solution overnight at 4° C. with the indicated antibodies. The incubation was followed by washing with TBST and 1 hr incubation at RT with secondary antibodies. Bands were detected using an ECL chemiluminescence detection method with KwikQuant Ultra Digital ECL-solution, KwikQuant™ Imager and analyzed with KwikQuant Image Manager Software (all Kindle Biosciences, LLC).

DSB GFP Reporter Assay

[0237] U2OS cells were reverse transfected by plating 2×105 cells in antibiotic-free media in a 12 well plate. Each well already contained preformed transfection complexes with 20 pmol siRNA and 3.6 μL Lipofectamine RNAiMAX Reagent (Invitrogen) in Opti-MEM used according to the manufacturer's protocol. After 20 hrs, 2×105 cells were transferred to 6 well plates and left to recover until the next day. Transient I-SceI transfection was performed 48 hrs post initial reverse transfection. 1.92 μg I-SceI expression vector, prepared by Mini or Midi Kit (Qiagen), was used along with 24 pmol siRNA and 8.64 μL Lipofectamine 2000 Transfection Reagent (Invitrogen) in Opti-MEM according to the manufacturer's protocol. Cells were incubated with transfection complexes for 3 hrs at 37° C. followed by gentle washing and addition of fresh growth media with antibiotics.

Flow Cytometric Analysis

[0238] Approximately 72 hrs after I-SceI transfection, cells were trypsinized, washed with PBS, fixed in 1% formaldehyde and transferred to V-bottom 96-well plates. DNA repair activity was assessed by a quantification of the percentages of GFP+ cells using the Attune NxT Flow Cytometer (ThermoFisher), and analyzed using FlowJo software (FlowJo, LLC). Experiments were performed in triplicates and error bars expressed as standard deviation (SD).

Western Blot Analysis

[0239] Protein extracts were performed as described previously. After Bradford analysis, samples were boiled in 1×SDS Sample Buffer, before proceeding with gel electrophoresis and protein transfer onto a membrane. To detect the protein of interest, the membranes were incubated with indicated antibodies.

I-SPY 2 TRIAL: Patients, Data, and Analysis

[0240] This correlative study involved 375 (MK2206 arm: 94; veliparib/carboplatin (VC) arm: 71; Ctr: 210) women with high-risk stage II and III early breast cancer who were enrolled in the multicenter, multi-arm, neo-adjuvant I-SPY 2 TRIAL (NCT01042379; IND 105139) (Barker et al., 2009). Detailed descriptions of the design, eligibility, and study assessments in the I-SPY 2 trial have been reported previously, including the efficacy of investigational agents VC (Rugo et al., 2016) and MK-2206 (Chien et al., 2020). I-SPY 2 TRIAL patients are randomized either to the control arm [paclitaxel followed by doxorubicin/cyclophosphamide; T→AC; plus trastuzumab (and later pertuzumab) if HER2+] or one of the active experimental arms. The investigational agent MK2206 was active in the trial from September 2012 to May 2014. MK2206 arm patients received MK2206 plus standard chemotherapy (n=94; M+T→AC), with trastuzumab if HER2+. 72 HER2-patients were randomized to the VC arm from May 2010 to July 2012, and treated with veliparib and carboplatin in addition to standard taxane/anthracycline chemotherapy (VC+T→AC) (Rugo et al., 2016). All patients signed informed consent to allow research on and use of their biospecimen samples (Chien et al., 2020; Rugo et al., 2016). Pre-treatment tumor samples were assayed using Agilent 44K (32627) or 32K (15746) expression arrays; and these data were combined into a single gene-level dataset after batch-adjusting using ComBat (Johnson et al., 2007). In the pre-specified analysis plan as previously summarized (Wolf et al., 2017; Wulfkuhle et al., 2018), logistic regression is used to assess association with pCR in the control and experimental-arm treated populations individually. Relative biomarker performance between arms (biomarker×treatment interaction) is assessed using a logistic model (pCR~treatment+biomarker+treatment×biomarker). Analysis is also performed adjusting for HR/HER2 (binary) status (pCR-treatment+biomarker+treatment:biomarker+HR+HER2). Markers were analyzed individually; p-values are descriptive.

Results

Protein-Protein Interaction Mapping of Breast Cancer Drivers

[0241] A panel of genes that are associated with molecular alterations in BC were collected, and the list (Cancer Genome Atlas, Network, 2012; Stephens et al., 2012) was used to guide the selection of 40 proteins for generation of PPI networks. The selected targets included proteins with well-known roles in BC (e.g., TP53, PIK3CA, CDH1, and BRCA1) as well as less-well appreciated proteins with recurrent mutations (e.g., CHEK2) (Beca et al., 2017; Chen et al., 2017; Epping et al., 2011; Fuqua et al., 2014; Goldberg et al., 2017; Harkness et al., 2015; Hoenerhoff et al., 2009; Lin et al., 2014; Mimori et al., 2002; Morales et al., 2016; Thompson et al., 2012; Tokunaga et al., 2014; Zheng et al., 2011). This list was inclusive, as 93% of BC tumors in TCGA harbor an alteration in one or more of these 40 genes (FIG. **3**A).

[0242] Referring to FIG. **3**A, the gene alteration frequencies from the breast invasive carcinoma (TCGA Firehose Legacy) dataset for the 40 genes selected as AP-MS baits in this study are shown. Each patient is represented by a grey box that is colored based on the occurrence and type of alteration(s) observed in that patient. In total, 93% (1028 out of 1108) of BC patients have non-synonymous mutation, chromosomal copy-number alteration (CNA), or mRNA/protein expression alteration in one or more of these 40 genes. Existing gene alterations in MCF7 and MDA-MB-231 are shown in the right.

[0243] Three breast cell lines derived from human mammary epithelium were selected: MCF7 (ER+, luminal A subtype), MDA-MB-231 (ER-, PR-, HER2-triple-negative TN subtype), and MCF10A (non-tumorigenic mammary epithelial cells). These particular cell lines were selected because they have been shown to replicate therapeutically relevant responses found in BC tumors (Iorio et al., 2016), their RNA profiles are highly correlated with those of BC tumors (Yu et al., 2019), and ER+ and TN subtypes together account for approximately 90% of BC patients (Santagata et al., 2014). It was reasoned that comparing protein networks among ER+, TN, and nontumorigenic models would allow study of how PPI networks are altered between normal and tumorigenic backgrounds as well as influenced by different mammary epithelial lineages.

[0244] To generate PPI maps, "bait" proteins were cloned into triple FLAG-tagged lentiviral vectors, individually transduced into each cell line and expressed in biological triplicate via a doxycycline inducible promoter (FIG. **3**B). See also FIG. **22** and FIG. **23**. Cells were harvested after approximately 40 hr doxycycline-induction, and anti-FLAG tag-based affinity purification was performed followed by mass spectrometry to detect interacting "prey" proteins in an unbiased manner. Two PPI scoring algorithms were employed to quantify high-confidence interacting proteins: compPASS (Huttlin et al., 2015a; Sowa et al., 2009a) and SAINTexpress (Teo et al., 2014a). The AP-MS data was independently analyzed using these two algorithms and monitored recovery rates of known PPIs from public databases (serving as gold standards) by varying the thresholds of key metrics in each algorithm (WD per bait percentile for compPASS and BFDR for SAINTexpress, respectively). Without wishing to be bound by theory, it was found that the best gold-standard PPI recovery was obtained when data from both algorithms were combined (FIG. **1**A and FIG. **1**B). Using this approach, a total of 589 high-confidence PPIs involving 493 prey proteins were identified (FIGS. **2**A, **2**B, and **3**C).

[0245] Referring to FIG. **2**A, receiver operating characteristic (ROC) curve illustrating high recovery of gold standards (sensitivity) are shown.

[0246] Referring to FIG. **2**B, the number of high-confidence PPIs per cell line for each bait are shown.

[0247] Referring to FIG. **3**B, the experimental workflow in which each bait was expressed in biological triplicate in 3 cell lines and subjected to AP-MS analysis is shown.

[0248] Referring to FIG. **3**C, the majority (79%) of the high-confidence PPIs identified in this study are not represented in a panel of public PPI databases (CORUM, BioPlex 2.0, or BioGRID low throughput & multivalidated).

[0249] Collectively, 79% of the BC PPIs identified were not previously reported in protein-protein interaction databases (CORUM, BioPlex 2.0, or BioGRID low throughput and multivalidated) (FIG. **3**C). Without wishing to be bound by theory, the high percentage of novel interactions may reflect cell type-specific PPIs as nearly all systematic protein-protein interaction analyses to date have been performed in HEK293T or HeLa cell lines (Hein et al., 2015; Huttlin et al., 2015a, 2017, 2020). This study is the first to collect large-scale human PPI data in cell line contexts physiologically relevant to breast cancer.

[0250] PPIs often suggest functional relationships among proteins that work together to accomplish a specific cellular process. Previously, a significant enrichment of frequently mutated proteins was found in large PPI repositories (Bouhaddou et al., 2019; Creixell et al., 2015; Eckhardt et al., 2018; Hofree et al., 2013; Leiserson et al., 2015; Paczkowska et al., 2020; Reyna et al., 2020). Similarly, it was investigated whether the BC PPI network showed enrichment for three major types of alterations—non-synonymous mutations, chromosomal CNVs, and mRNA expression alterations—documented in the BC TCGA cohort. Accordingly, the average frequency of each alteration was calculated for prey proteins detected in the PPIs, compared to background expectation (STAR Methods and FIG. **2**C). It was observed that BC-associated mutations were significantly enriched in BC PPIs, but that CNVs and mRNA expression alterations were not (FIG. **3**D). Specific enrichment of mutations was found in preys detected in either of the two cancer cell lines (MCF7, MDA-MB-231) but not in the preys of non-cancerous MCF10A cells (FIG. **3**E). Without wishing to be bound by theory, this result supports the notion that the interaction partners of frequently mutated cancer proteins are also under positive pressure for mutations.

[0251] Referring to FIG. **2**C, volcano plots displaying the differential abundance of endogenous proteins between cell lines used in this study are shown. Colored data points (left and right sides) indicate proteins that have ≤5.6-fold difference in protein abundance between cell lines and an adjusted p-value<0.05.

[0252] Referring to FIG. **3**D, the frequency of non-synonymous mutations, chromosomal CNVs, or mRNA expression alterations of 10,000 random size-matched permutations taken from the list of genes detected in the global protein abundance analysis is shown. The white circle indicates the median of the random sampling, and the grey bar represents ±1 standard deviation. The frequency of alterations found in the prey retrieved in our PPI dataset is indicated in the solid colored.

[0253] Referring to FIG. **3**E, a Venn diagram illustrating the overlap of PPIs (PPI score≥0.9) across the 3 cell lines is shown. PPI score is an average of the PPI confidence scores calculated from compPASS and SAINTexpress. The frequency of non-synonymous mutations of the prey genes in each sector of the Venn diagram was compared to those of 10,000 random size-matched permutations as in FIG. **3**D. The p-values for mutation enrichment in each prey set were shown in a shaded scale, where a stronger gray represents more significant mutation enrichment.

Key Resources Table I.

Reagent	Source	Identifier
Antibodies		Cat#
pSTK11	Cell Signaling Techologies	3482
STK11	Cell Signaling Techologies	3050
pAMPK	Cell Signaling Techologies	2535
AMPK	Cell Signaling Techologies	5832
pSIKs	Abcam	Ab199474
SIK1	Thermo Fisher Scientific	PA5-42799
Phospho-AKT (Ser473)(D9E) XP Rabbit mAb	Cell Signaling Techologies	4060S
Akt (pan)(40D4) Mouse mAb	Cell Signaling Techologies	2920S
Goat Anti-Mouse Secondary Antibody 800CW LI-COR	LI-COR	926-32210
Goat Anti-Rabbit Secondary Antbidoy 800CW LI-COR	LI-COR	926-32211
BRCA1 (D-9)	Santa Cruz Biotechnology	sc-6954
BARD1 (E-11)	Santa Cruz Biotechnology	sc-74559
RBBP8	Santa Cruz Biotechnology	sc-271339
Spinophilin/ Neurabin-II (D-7)	Santa Cruz Biotechnology	sc-373974
UIMC1	Abcam	ab-124763
BRIP1	Abcam	ab-180853
MLH1	Abcam	ab-92312
Beta-Tubulin	Sigma-Aldrich	T8328
Actin (13E5)	Cell Signaling Techologies	4970

-continued

Key Resources Table I.

Reagent	Source	Identifier
Anti-Mouse	Cell Signaling Techologies	7076
Anti-Rabbit	Cell Signaling Techologies	7074
Cell Culture Media		**Cat#**
High glucose Dulbecco's modified Eagle's medium (DMEM)	Corning	MT10017CV
DMEM and Ham's F-12 50/50	Corning	MT10092CV
Chemicals, Drugs, Peptides, and Enzymes		**Cat#**
Fetal Bovine Serum	Gibco	A3160502
Penicillin/ Streptomycin	Corning	MT30002C1
Gag-Pol-Tat-Rev		pJH045
VSV-G		pJH046
PolyJet DNA Transfection Reagent	SigmaGen Laboratories	SL100688
8.5% PEG-6000	Sigma-Millipore	528877
Puromycin	Sigma	P8833
Blasticidin S HCI	Gibco	R21001
Doxycycline	Selleckchem	S4163
100X Halt™ Protease and Phosphatase Inhibitor Single-Use Cocktail, EDTA-Free	Thermo Scientific	78443
Benzonase	Sigma	E1014-25KU
LysC	Wako Chemicals	129-02543
Iodacetamide (IAA)	BioUltra	I1149
Trypsin	Promega	V611X
6X SDS Sample Buffer	Alfa Aesar	J61337-AD
Hydrocortisone	Sigma-Aldrich	HO888-1G
Insulin Solution Human 19278	Sigma-Aldrich	501656853

-continued

Key Resources Table I.

Reagent	Source	Identifier
Animal-Free Recombinant Human EGF	PeproTech	10781-696 (EA)
Cholera Toxin	Sigma-Aldrich	C-8052
Janus Green Stan	Abcam	Ab111622
Invitrogen Nuclease-Free Water	Ambion	AM9938
16% Paraformaldehyde	Thermo Fisher	PI28908
Triton X-100	Sigma-Aldrich	9002-93-1
Lipofectamine2000	Invitrogen	11668019
Lipfectamine RNAiMAX	Invitrogen	13778150
Opt-mem Reduced Serum	Gibco	31985070
Laboratory equipment and beads		**Cat#**
0.45 μM PVDF filter	Millipore	MM_NF_SLHV033RS
Nest Tips C18	The Nest Group	SUM SS18V
Anti-FLAG M2 magnetic beads	Sigma-Aldrich	M8823
Anti-V5 magentic beads	MBL International	M167-11
Ni-NTA Magnetic Agarose Beads	Qiagen	36111
Micro Bio-Spin chromatography Columns	Bio-Rad	7326204
7.5% Mini-PROTEAN® TGX™ Precast Protein Gel	Bio-Rad	4561024
Trans-Blot Turbo Transfer System	Bio-Rad	
KiwkQuant Ultra Digital ECL-solution	Kindle Biosciences, LLC	R1002
KwikQuant™ Imager	Kindle Biosciences, LLC	
KwikQuant Image Manager Software	Kindle Biosciences, LLC	

-continued

Key Resources Table I.

Reagent	Source	Identifier
Echo Qualified Labcyte 384-well platesCorning	Dharmacon	cat# PP-0200
Clear-bottom 96 Well Plates	Corning	CLS3904
Li-Cor Odyssey CLx	Li-Cor	9140
Deposited Data		**Cat#**
Raw MS files and MaxQuant search files	Proteome Xchange Pride partner Repository	Identifier: PXD019639 Username: reviewer58609@ebi.ac.uk Password: vymSibLr
Experimental Models: Cell Lines		**Cat#**
HEK293T	ATCC	CRL-3216
U2OS	Gunn and Stark, 2012	Jeremy Stark's laboratory
MDA-MB-231	ATCC	HTB-26
MCF7	ATCC	HTB-22
MCF10A	ATCC	CRL-10317
siRNA		**Cat#**
AKT1-siGENOME SMARTpool	Dharmacon	M-003000-03-0005
AKT2-siGENOME SMARTpool	Dharmacon	M-003001-02-0005
AKT3-siGENOME SMARTpool	Dharmacon	M-003002-02-0005
S100A3-siGENOME SMARTpool	Dharmacon	M-011767-00-0005
KRT32-siGENOME SMARTpool	Dharmacon	M-011310-01-0005
PIK3CA-siGENOME SMARTpool	Dharmacon	M-003018-03-0005
PTEN-siGENOME SMARTpool	Dharmacon	M-003023-02-0005
BPIFA1-siGENOME SMARTpool	Dharmacon	M-008613-00-0005
BPIFB1-siGENOME SMARTpool	Dharmacon	M-010095-01-0005

-continued

Key Resources Table I.

Reagent	Source	Identifier
SCGB2A1-siGENOME SMARTpool	Dharmacon	M-019606-01-0005
PRR4-siGENOME SMARTpool	Dharmacon	M-012367-02-0005
MUC5B-siGENOME SMARTpool	Dharmacon	M-184282-00-0005
ZG16B-siGENOME SMARTpool	Dharmacon	M-015971-01-0005
ANXA1-siGENOME SMARTpool	Dharmacon	M-011161-01-0005
IRS1-siGENOME SMARTpool	Dharmacon	M-003015-01-0005
APOA1-siGENOME SMARTpool	Dharmacon	M-010994-00-0005
LTF-siGENOME SMARTpool	Dharmacon	M-19661-01-0005
PIK3R1-siGENOME SMARTpool	Dharmacon	M-003020-04-0005
PIGR-siGENOME SMARTpool	Dharmacon	M-017729-00-0005
PIP-siGENOME SMARTpool	Dharmacon	M-004904-00-0005
NTC#1-siGENOME	Dharmacon	D-001210-02-05
NTC#2-siGENOME	Dharmacon	D-001210-04-05
Spinophilin #4-siGENOME	Dharmacon	D-014932-02-0010
Spinophilin #5-siGENOME	Dharmacon	D-014932-03-0010
BRCA-296-siGENOME	Dharmacon (Anantha et al., 2017)	CTM-554665 (GGAACCUGUCUCCACAAA GdTdT) (SEQ ID NO: 7)
TP53BP1-siGENOME SMARTpool	Dharmacon	M-003548-01-0005
BRCA2-1949-siGENOME	Dharmacon (Anatha et al., 2017)	CTM-566149 (gaagaaugcagguuuaau adTdT) (SEQ ID NO: 8)

-continued

Key Resources Table I.

Reagent	Source	Identifier
Software and Algorithms		
FlowJo v106.1	FlowJo, LLC	https://www.flowjo.com/
Attune NxT Flow Cytometer	ThermoFisher	
Li-Cor Imaging Studio Software	Li-Cor	https://www.licor.com/bio/image-studio/
atMS	Bioconductor	https://www.bioconductor/org/packages/release/bioc/html/artMS.html
MSstats	Bioconductor	https://www.bioconductor.org/packages/release/bioc/html/MSstats.html
Max Quant (version 1.6.2.10)	Jurgen Cox Lab	https://www.maxquant.org/
CompPASS (version 0.0.0.9000)	Github	https://github.com/dnusinow/cRomppass/blob/master/R/comppass.R
SAINTexpress (version 3.6.1)	Sourceforge	https://sourceforge.net/projects/saint-apms/files/
InstantClue		http://www.instantclue.unikoeln.de/

[0254] Out of 589 PPIs identified, 81% were not shared with other cell lines, reflecting high cell type-specificity of PPIs in different genetic contexts (FIG. **3**E). It was speculated that differential protein abundance across cell lines might provide one explanation for cell type-specific PPIs. However, while some changes in interaction could be explained by changes in protein abundance, many cases were also found with the opposite behavior, in which a gain in interaction was observed with a concomitant decrease in protein abundance (FIG. **2**D).

Cell Type-Specific Interactions Reveal Novel Modulator of AKT

[0255] To compare PPIs across cell lines, a cancer-specific differential interaction score (DIS) was defined as the probability of the PPI being present in a cancer cell line (either MCF7 or MDA-MB-231) but absent in the normal cell line (MCF10A, Key Resources Table I). The results of this differential scoring analysis were used to visualize the entire BC PPI network showing PPIs that are (1) private to a cancer cell line, (2) private to non-cancerous MCF10A cells, or (3) conserved in the two cancer cell lines but absent in the non-cancerous context (FIG. **4**A).

[0256] Referring to FIG. **4**A, an interactome of the union of all high-confidence PPIs detected across all cell lines is shown. Edges are colored based on their differential interaction, with darker edges representing PPIs that are enriched to BC cell lines (unique to either MDA-MB-231 or MCF7) as compared to MCF10A cells (shown in teal edges). Dotted line represents the physical protein-protein association (validated in other studies) with high Integrated Association Stringency score. AKT subnetwork is outlined in a dotted circle.

[0257] Among interactions private to a cancer cell line, it was found that the HRAS proto-oncogene and the tumor suppressor kinase STK11 (also known as LKB1) interact with a set of DNA damage response (DDR) proteins (PDS5A, FANCI, MMS19, GPS1) in MCF7 and MDA-MB-231 cells, respectively (FIG. **4**B). Given the previous observations that silencing of HRAS and STK11 lead to defective DNA repair and genome instability (Grabocka et al., 2014), these interactions may provide insights into direct effectors by which HRAS and STK11 modulate DDR. STK11 also interacted with cell adhesion factors in MCF10A cells (PLEKHA7 and PKP4, FIG. **4**B), consistent with its role in cell autonomous polarization (Baas et al., 2004; Forcet et al., 2005; Zhang et al., 2008) and actin filament assembly at the cellular leading edge (Xu et al., 2010). Interestingly, CDH1 but not STK11 was found to interact with these same proteins in MDA-MB-231 cells. CDH1 plays critical roles as a master regulator of cell-cell adhesion via adherens junctions, cell polarity and cell migration (Brieher and Yap, 2013; van Roy and Berx, 2008), and abrogation of CDH1 expression is a hallmark of the epithelial-to-mesenchymal transition (Canel et al., 2013). The observed interaction patterns suggest that STK11 may contribute to cell polarity and focal adhesion via a physical interaction with PLEKHA7 and PKP4, but that it requires the cellular ability to form adherens junctions. This may explain the lack of interaction of STK11 with PLEKHA7 and PKP4 in MDA-

MB-231, which do not normally express CDH1 due to promoter hypermethylation (Lombaerts et al., 2006; Tate et al., 2012).

[0258] Referring to FIG. **4**B, PPIs connecting HRAS, STK11, and CDH1 are shown. HRAS and STK11 have several interactors including MMS19 in BC cells involved in cellular response to DNA damage stimulus. STK11 and CDH1 interact with PKP4 and PLEKHA7 in a cell type-specific manner, implying differential regulation of cell adhesion and cell-cell junction in non-BC and BC cells.

[0259] The cell-line specific analysis also revealed contextual interactions with AKT, the central signaling kinase frequently deregulated in BC and many other types of human cancers (Guerrero-Zotano et al., 2016; Manning and Cantley, 2007; Manning and Toker, 2017; Vivanco and Sawyers, 2002). In particular, AKT1 and its paralog AKT3 were both found to interact with S100 Calcium Binding Protein A3 (S100A3) and keratin KRT32, specifically in MDA-MB-231 cells (FIG. **4**C). To probe the role of these proteins in regulating AKT kinase activities, small interfering RNA (siRNA)-mediated knockdown of S100A3 and KRT32 was performed, and phosphorylation of AKT at S473, a proxy of AKT activation (Alessi et al., 1996, 1997; Sarbassov et al., 2005; Stokoe et al., 1997), was monitored. Depletion of S100A3 and KRT32 significantly reduced normalized phospho-AKT (pAKT) levels in MDA-MB-231 but not in the other two cell lines (FIG. **4**D). In contrast, knockdown of AKT1, AKT2, or AKT3 led to the expected reduction of pAKT in all three cell lines (FIG. **5**). Without wishing to be bound by theory, these results indicate that S100A3 and KRT32 are functionally relevant, cell-type specific activators of the AKT pathway. One plausible explanation for the cell type-specificity of S100A3 is higher protein expression in MDA-MB-231 cells (>4-fold), a trend also observed in RNA-seq studies (Papatheodorou et al., 2020).

[0260] Referring to FIG. **4**C, AKT (AKT1/2/3) subnetwork has many cell type-specific interactors. AKT1 and AKT3 interact with S100A3 and KRT32 in MDA-MB-231 cells.

[0261] Referring to FIG. **4**D, small interfering RNA-mediated knockdown of S100A3 and KRT32 significantly reduces phospho-AKT (S473) level in MDA-MB-231 cells. pAKT level was normalized to non-targeting control (NTC) and cell numbers as well as total AKT level. * p-value<0.05.

[0262] Referring to FIG. **5**, small interfering RNA-mediated knockdown of AKT1, AKT2, and AKT3 reduces phospho-AKT (S473) level in all three cell lines analyzed. pAKT (S473) intensity was normalized to non-targeting control (NTC) and cell numbers. *** pvalue<0.001, ** p-value<0.01, * p-value<0.05.

[0263] These results were also analyzed in the context of I-SPY 2, a neoadjuvant, adaptive clinical platform trial for high risk early stage breast cancer (Barker et al., 2009). It was found that patients who achieved pathologic complete response (pCR) to the pan-AKT allosteric inhibitor MK2206 (Chien et al., 2020) had pre-treatment tumors with significantly higher S100A3 mRNA expression than those of non-responding patients (p=0.03, FIG. **4**E). In contrast, tumors in the control arm receiving only standard chemotherapy did not show any significant difference in S100A3 expression between responsive and non-responsive groups. Thus, high S100A3 expression may provide a biomarker of AKT pathway activation predictive of response to AKT-targeted therapy (Odds Ratio 2.5, FIG. **4**F). As high S100A3 expression positively regulates AKT activity, such regulation may create a dependence on the AKT pathway akin to oncogene addiction.

[0264] Referring to FIG. **4**E, a box plot shows that the patient group (enrolled in the I-SPY 2 clinical trial) with pathologic complete response (pCR) to MK2206 (pan-AKT inhibitor) had pre-treatment tumors with significantly higher S100A3 mRNA expression (Likelihood ratio (LR) p-value=0.032) than those of non-responding patients. In the control arm, there is no difference in S100A3 expression between pCR and no pCR groups.

[0265] Referring to FIG. **4**F, a mosaic plot shows that BC patients who did pCR to MK2206 had 2.5 times more likely had higher mRNA expression of S100A3 in their pre-treatment tumors (Odds Ratio=2.5). In the control arm, there is no significant difference in pCR between low and high S100A3 expression groups. Numbers in each block represent the patient sample size. Column width indicates the relative proportion of the S100A3 low and high expression group on the patient population.

Interactions Conserved Across BC Contexts

[0266] A number of PPIs were commonly observed in both MCF7 and MDA-MB-231 BC cells but not in a non-cancerous tissue context (FIG. **4**G). Notably, this group of prey proteins was not as frequently mutated in BC as those distinct to one of the two cancer cell lines (FIG. **3**E), although some clearly play central roles in cancer cell proliferation. For instance, protein interactions among cyclins (e.g., CCND3), cyclin-dependent kinases (CDKs 2,4,5,6) and CDK inhibitors (CDKN1B) were seen predominantly in BC but not normal cells. These interactions may reflect dysregulated activation of CDKs and uncontrolled cell cycle progression in BC (Malumbres and Barbacid, 2001; Santo et al., 2015), providing the rationale for CDK4/6-targeted therapy (Hamilton and Infante, 2016; Lim et al., 2016; Niu et al., 2019).

[0267] Referring to FIG. **4**G, high-confidence PPIs that are commonly detected only in two cancer cell lines (MDA-MB-231 and MCF7) but not in non-cancerous MCF10A cells are shown. Node and edge styles and colors as seen in FIG. **4**A.

[0268] It was also found that STK11 interacts with STRADA and CAB39 (also known as M025) preferentially in the two cancer cell lines (FIG. **4**G). STRADA and CAB39 form a heterotrimeric complex with STK11 (Baas et al., 2003, 2004; Zeqiraj et al., 2009a) to properly position the activation loop of STK11 in an active conformation (Zeqiraj et al., 2009b), enabling STK11 to phosphorylate and activate downstream kinases, including AMP-activated protein kinases (AMPKs) and salt-inducible kinases (SIKs) involved in energy homeostasis and cell cycle regulation (FIG. **4**H) (Alessi et al., 2006; Hardie et al., 2013; Hollstein et al., 2019). The increased associations of STK11 with STRADA and CAB39 suggested that STK11 activity is generally increased in cancer. Consistent with this speculation, it was found that both total and activated STK11 (phosphorylated at Ser428) are more abundant in MCF7 and MDA-MB-231 than in MCF10A cells (FIG. **4**I). Furthermore, phosphorylation of STK11 downstream targets, including SIK1, SIK2, SIK3, and AMPK, was higher in the two BC cell lines (FIG. **4**I). Increased STK11 activity may

support cellular fitness by balancing energy production with anabolic metabolism, as previously seen in hepatocellular carcinoma (Lee et al., 2015).

[0269] Referring to FIG. **4**H, STK11 forms a heterotrimeric complex with CAB39 and STRADA to activate its kinase activity and phosphorylate downstream kinases including AMPK and SIK for regulating energy homeostasis and cell cycle.

[0270] Referring to FIG. **4**I, STK11 kinase activity was monitored by measuring total and phosphorylation levels of its known downstream substrates (AMPK and SIKs) as well as itself. The following phospho-epitopes were detected by antibodies: pSTK11 (pS428), pAMPKu (pT172), pSIKs [pSIK1 (pT182), pSIK2 (pT175), pSIK3 (pT163)].

Comparative Network Analysis Between Wild-Type and Mutant Cancer Proteins

[0271] Many BC proteins are recurrently mutated in tumors, but how these mutations affect and re-wire PPIs has not been extensively analyzed. 11 proteins with frequent or known pathogenic mutations in BC were selected, and AP-MS was performed on both the WT and mutant isoforms to quantitatively measure changes in PPIs (FIG. **6**A). The E17K mutation of AKT1 and AKT3 is an activating mutation that causes constitutive membrane association of AKT kinases (Carpten et al., 2007; Davies et al., 2008; Landgraf et al., 2008; Lindhurst et al., 2011; Rudolph et al., 2016). Intriguingly, while WT AKT1 was found to interact with CSTB, CRNN, and SPRR3, the AKT1 E17K mutant was not. Similarly, the aforementioned S100A3 and KRT32 exclusively interacted with WT AKT3 but not the E17K mutant (FIG. **6**B). Without wishing to be bound by theory, these results indicate that a conformational change of AKT may be induced by the E17K mutation in the pleckstrin homology domain. Alternatively, the resulting constitutive membrane localization of AKT may significantly affect its pattern of PPIs. Overexpression of CRNN and SPRR3 has been noted to activate AKT (Cho et al., 2010; Li et al., 2019), similar to the roles of S100A3 and KRT32 (FIG. **4**D). Without wishing to be bound by theory, the results here indicate these proteins activate the AKT pathway through direct interaction with AKT1 in a manner that is disrupted by AKT mutation.

[0272] Referring to FIG. **6**A, proteins analyzed for both WT and mutant forms are listed.

[0273] Referring to FIG. **6**B, changes in abundance of high-confidence preys between each mutant and the corresponding WT protein were quantified. Each dot represents an individual PPI. Highly differential PPIs between WT and mutant are annotated, with the line color representing the cell line from which that PPI was quantified.

[0274] The CHEK2 1100delC and K373E mutations are associated with cancer predisposition (Apostolou and Papasotiriou, 2017; Kumar and Bose, 2017), and both mutations disrupt CHEK2 kinase activity (Higashiguchi et al., 2016; Kumar and Bose, 2017). It was found that CHEK2 proteins with either of these mutations show a marked increase in abundance of their interacting preys (FIG. **6**B), most of which participate in the actin cytoskeleton, including MYO5B, MYO6, MYH10, SIPA1L3 and SPECCI (Gene Ontology Biological Process GO:0015629, FDR=9.09×10-4). These two mutations may abrogate nuclear localization of CHEK2, allowing it to interact with cytoskeleton proteins in the cytoplasm. Interestingly, expression of the CHEK2 1100delC mutant induces cell migration and invasion in gastric cancer cells (Hong et al., 2017), suggesting that association of CHEK2 mutants with actin cytoskeleton proteins may contribute to cellular invasion and metastasis.

[0275] Due to the high prevalence of TP53 mutations in BC patients, three of the most common mutations were selected for quantitative AP-MS analysis (FIG. **6**C). It was found that all three mutations abolished the interaction with CDKN1A and MDM2, as previously reported (Kim et al., 2017; Li et al., 2011; Schulz-Heddergott and Moll, 2018). In addition, it was found that these mutations disrupt the interaction with RRAD (FIG. **6**D), a Ras-related small GTPase (Reynet and Kahn, 1993) associated with poor prognosis in lung and breast cancers when lowly expressed (Suzuki et al., 2007). Cancer cells, often under hypoxic conditions, preferentially utilize glycolysis (Cairns et al., 2011; Warburg, 1956), such that TP53 has been known to repress glycolysis for tumor suppression (Aylon and Oren, 2011; Feng and Levine, 2010; Gottlieb and Vousden, 2010). As one of the mechanisms of this suppression, TP53 transcriptionally activates RRAD, which in turn represses glycolysis through inhibition of GLUT1 translocation to the plasma membrane (Zhang et al., 2014). Without wishing to be bound by theory, these results suggest that TP53 may also regulate RRAD via direct protein interaction, and that the three oncogenic TP53 mutations abolish this regulatory function in BC cells. In addition to RRAD, several other PPIs were differentially affected by these TP53 mutations. For example, interactions with DnaJ/Hsp40 family proteins (DNAJA3, DNAJB1, and DNAJC7) and BAG5 were significantly increased in the R175H conformational mutant but not in the two DNA contact mutants (R248W and R273H) (FIG. **6**D), consistent with the role of these proteins in protecting conformational TP53 mutants from degradation, thus promoting mutant TP53 accumulation (Parrales et al., 2016; Qi et al., 2014; Yue et al., 2016).

[0276] Referring to FIG. **6**C, a lollipop plot representing the location of TP53 mutations and the number of BC patients bearing a given TP53 mutation from TCGA (Firehose Legacy) study is shown. TAD, transactivation domain; Tetramerization, tetramerization domain.

[0277] Referring to FIG. **6**D, relative quantification of the abundance of high-confidence TP53 preys observed in MDA-MB-231 cells is shown. Preys detected only in WT are represented in deep blue while preys detected only in mutants are in deep red. All three TP53 mutants were expressed and detected at a similar level. The interaction of TP53 with CDKN1A and MDM2 are strongly diminished in all three pathogenic TP53 mutants tested as previously known. ND, not detected.

Novel Regulators of PIK3CA Signaling

[0278] Activation of PIK3CA via receptor tyrosine kinase (RTK) or oncogenic mutations leads to membrane recruitment and activation of AKT (FIG. **6**E) (Alessi et al. 1996; Alessi et al. 1997; Stokoe et al. 1997; Sarbassov et al. 2005). In BC, mutations at E545 and H1047 residues are most frequently found (FIG. **6**F). Using AP-MS, 20 prey proteins that interact with PIK3CA were identified, 18 of which were observed only in MCF7 cells. These patterns may reflect activation of PI3K signaling due to PIK3CA E545K mutation, which is present in MCF7. Of the 18 proteins, only 4 (IRS1 and PIK3R1/2/3) were previously known interactors. Of note, it was found that many of these novel PPIs are

significantly decreased, and in some cases completely abolished, by different PIK3CA mutations (FIG. **6**G). To determine whether these PIK3CA interactors modulate the PI3K/AKT pathway, whether depletion of each target by siRNA affects downstream AKT activation was tested by measuring cellular phospho-AKT (pS473) levels in an in-cell western blot assay (Chen et al., 2005). Non-targeting control siRNAs (NTCs) as well as siRNAs targeting PIK3CA (a positive regulator) and PTEN (a negative regulator) were included as controls (Breuleux et al., 2009; Brognard et al., 2007; Cantley and Neel, 1999; He et al., 2008; Sarbassov et al., 2005; Uche and Kane, 2016). As expected, knockdown of PIK3CA in MCF7 cells significantly diminished pAKT signal, while knockdown of PTEN augmented it (FIG. **6**H). Intriguingly, knockdown of the PIK3CA interactors BPIFA1 and SCGB2A1 (also named SPLUNC1 and Mammaglobin-B, respectively) increased pAKT activity to a degree higher than or the same as the PTEN knockdowns, suggesting that these two proteins are negative regulators of the PI3K/AKT pathway (FIG. **6**H). Importantly, proteins for which knockdown increased pAKT (especially BPIFA1, BPIFB1, PRR4, and ZG16B) showed significantly reduced interactions with kinase domain mutants of PIK3CA (M1043V and H1047R) compared to a helical domain mutant (E545K) (FIG. **6**I). Without wishing to be bound by theory, these results imply that mutations in the kinase domain may relieve PIK3CA from negative regulation by multiple factors.

[0279] Referring to FIG. **6**E, an overview of the receptor tyrosine kinase (RTK)-PI3K signaling cascade leading to the phosphorylation (T308 and S473) and activation of AKT pathway is shown.

[0280] Referring to FIG. **6**F, a lollipop plot representing the sites of PIK3CA mutations and the number of BC patients bearing a given PIK3CA mutation from TCGA (Firehose Legacy) study is shown.

[0281] Referring to FIG. **6**G, relative quantification of the abundance of high-confidence preys observed from pull-down of PIK3CA (WT and mutants) in MCF7 cells is shown. Same color scheme as in FIG. **6**D.

[0282] Referring to FIG. **6**H, the level of AKT S463 phosphorylation (as proxy of activation) was measured upon siRNA-mediated knockdown of PIK3CA interacting preys and control genes (PTEN and PIK3CA). The intensity of AKT pS473 was normalized to non-targeting control (NTC), total AKT, and cell counts. Proteins whose knockdown increases pAKT are labeled in multiple colors.

[0283] Referring to FIG. **6**I, changes in the abundance of PIK3CA interacting proteins from each PIK3CA mutant pull-down are represented as box plots, in which the proteins that increase pAKT upon knockdown are labeled as in H. Association of these proteins with M1043V and H1047R mutants is significantly abolished, compared to E545K mutant. * p-value<0.05.

Effect of Pathogenic Mutations on the BRCA1 Interactome

[0284] To comprehensively catalog the BRCA1 interactome and how pathogenic BRCA1 mutations alter these interaction profiles, AP-MS was performed on WT and pathogenic variants reported in cancer patients, including C61G and R71G in the N-terminal RING domain (Drost et al., 2011; Górski et al., 2000; Vega et al., 2001) and 51655F, 5382insC and M1775R in the C-terminal tandem BRCT domain (Anantha et al., 2017; Clapperton et al., 2004; Dever et al., 2011; Levy-Lahad et al., 1997) (FIG. **7**A). Given that alternative splicing in cancer often generates BRCA1 isoforms lacking exon 11, which confers residual HR activity and therapeutic resistance (Wang et al., 2016a), this isoform was also included in the analysis. The I26A separation of function mutation in the RING domain, which abrogates E3 ubiquitin ligase activity but retains BARD1 binding, was also analyzed (Shakya et al., 2011). The expression of these BRCA1 proteins was induced in all three breast cell lines; however, only MDA-MB-231 cells (harboring the TP53 R280K mutation) supported ectopic 3×FLAG-BRCA1 expression. These observations were consistent with previous studies, which have shown that ectopic overexpression of BRCA1 (both WT and mutants) is not stably maintained without a compensatory TP53 mutation (Arizti et al., 2000; Buller et al., 2001; Holstege et al., 2009; McAllister and Wiseman, 2002). AP-MS experiments in MDAMB-231 cells identified 128 high-confidence interactions from 8 BRCA1 constructs (WT and 7 mutants, PPI score≥0.65, FIG. **8**A); of these interacting proteins, 70 showed ≥8-fold change (FIG. **7**B and FIG. **8**B).

[0285] Referring to FIG. **7**A, functional domains in the BRCA1 gene and the location of mutations analyzed by AP-MS are shown.

[0286] Referring to FIG. **7**B, relative quantification of the abundance of prey proteins (PPI score≥0.65, >8-fold change) identified by BRCA1 AP-MS in MDA-MB-231 cells is shown. All prey abundance values were normalized by 3×FLAG-tagged BRCA1 levels in their respective AP-MS experiments. Preys detected only in WT are represented in deep blue while preys detected only in mutants are in deep red. A group of proteins involved in HR repair (boxed in green) are clustered together, wherein RING domain and BRCT domain BRCA1 mutants show distinct PPI abundance profiles. Spinophilin has not previously been known to have a function relevant to HR repair. UBE2N is boxed in sky blue. ND, not detected.

[0287] Referring to FIG. **8**A, relative quantification of the abundance of prey proteins (PPI score≥0.65) identified by BRCA1 AP-MS in MDAMB-231 cells is shown. Preys detected only in WT are represented in deep blue while preys detected only in mutants are in deep red. ND, not detected.

[0288] Referring to FIG. **8**B, PPIs across all BRCA1 proteins analyzed (WT and 7 mutants) are visualized in a network view. A selective set of prey proteins (PPI score≥0.65, ≥8-fold change) is shown. Proteins playing crucial roles in DNA repair by homologous recombination are circled in pink.

[0289] These data revealed a number of previously unidentified BRCA1-interacting proteins, along with known interactors, many of which were differentially affected by mutations in different domains of BRCA1. For example, HR proteins previously known to interact with BRCA1 (including BRIP1, RBBP8, and UIMC1) (Clapperton et al., 2004; Kim et al., 2007b; Sobhian et al., 2007; Yu and Chen, 2004) had a similar pattern of interaction loss (boxed in green in FIG. **7**B) associated with BRCT domain mutants (S1655F, 5382insC, M1775R), whereas RING domain mutants (I26A, C61G, R71G) maintained these interactions. In a separate pattern, it was found that the C61G RING domain mutant abolishes interaction with BARD1 (FIG. **7**B), as previously reported (Nelson and Holt, 2010; Wu et al., 1996). Several interactions could be confirmed by co-IP/western blot analysis (FIG. **7**C). Without wishing to be bound by theory, these

results suggest that RING domain mutants are hypomorphic and may retain some BRCA1 functions, which could explain at least in part why the BRCA1 C61G variant is only moderately sensitive to cisplatin and poly (ADP-ribose) polymerase (PARP) inhibitors and becomes readily resistant to these drugs (Drost et al., 2016; Wang et al., 2016b).

[0290] Referring to FIG. **7**C, PPIs of selected proteins with BRCA1 (WT or C61G mutant) were confirmed by co-immunoprecipitation with antiFLAG antibody followed by western blot analysis.

[0291] A ubiquitin E2-conjugating enzyme, UBE2N (also known as UBC13), was found to interact with WT BRCA1, but to a lesser degree with mutant forms of BRCA1 (PPI score<0.6) (boxed in sky blue in FIG. **7**B). For example, consistent with reports from yeast two-hybrid studies (Christensen et al., 2007), a six-fold reduction in UBE2N associated with the I26A mutant compared to WT was found, suggesting that UBE2N interacts with BRCA1 through the RING domain. Notably, the M1775R BRCT domain mutation also dramatically reduced the interaction with UBE2N (FIG. **7**B), suggesting that M1775 residue in the BRCTs domain may also contribute to the interaction with UBE2N, although the underlying mechanism is currently unclear. Depletion of UBE2N shows HR defects including altered RAD51 filament formation and E3 Ub ligase function of BRCA1 (Zhao et al., 2007), indicating a critical role of UBE2N in HR repair.

[0292] Consistent with the cell line models, it was found that baseline UBE2N mRNA expression was significantly lower in I-SPY 2 BC patients who achieved pCR to the PARP-inhibitor (veliparib)/carboplatin (Rugo et al., 2016) in comparison to non-responsive patients (p=0.034, FIG. **7**D). In contrast, BC tumors in the control arm did not show any significant difference in UBE2N expression between pCR and no pCR groups. Without wishing to be bound by theory, these results indicate that expression of UBE2N may serve as a biomarker of response to PARP inhibitors and other DNA repair targeted therapies (Odds Ratio=2.9, FIG. **7**E).

[0293] Referring to FIG. **7**D, a box plot shows that the patient group (enrolled in the I-SPY 2 clinical trial) with pCR to veliparib (PARP inhibitor) and carboplatin (VC) had pre-treatment tumors with significantly lower UBE2N mRNA expression (LR p-value=0.034) than those of non-responding patients. In contrast, BC patient tumors in the control arm did not show any significant difference in UBE2N expression between pCR and no pCR groups.

[0294] Referring to FIG. **7**E, a mosaic plot shows that BC patients who did pCR to VC in addition to standard chemotherapy had 2.9 times more likely had lower mRNA expression of UBE2N in their pre-treatment tumors (Odds Ratio=2.9). In the control arm, there is no significant difference in pCR between low and high UBE2N expression groups. Numbers in each block represent the patient sample size. Column width indicates the relative proportion of the UBE2N low and high expression group on the patient population

Spinophilin is a Novel BRCA1-Interacting Protein

[0295] Another protein interacting with BRCA1 in a mutation-dependent manner was Spinophilin (encoded by PPP1R9B), a known neuronal scaffolding protein that regulates synaptic transmission through its ability to target protein phosphatase 1 (PP1) to dendritic spines where it inactivates glutamate receptors (Allen et al., 1997; Feng et al., 2000; Sarrouilhe et al., 2006). Binding of Spinophilin to BRCA1 was unanticipated, and it was abolished by BRCT domain mutations similar to the pattern observed earlier for HR proteins (FIG. **7**B). MSstats analysis of differential interactions between BRCA1 wild-type and BRCT domain mutants demonstrated that an intact BRCT domain is required for the BRCA1-Spinophilin interaction (FIG. **8**C). Such recognition of the BRCT domain has been previously reported for BRCA1 interactions with FAM175A, BRIP1, and RBBP8 (Clapperton et al., 2004; Leung and Glover, 2011; Wu et al., 2016; Yu and Chen, 2004). Spinophilin was previously observed but unexplored in a systematic analysis of proteins interacting with the BRCT domain of BRCA1 (Woods et al., 2012).

[0296] Referring to FIG. **8**C, volcano plots show proteins that differentially interact with BRCA1 between WT and mutants. The BRCT domain mutations tested (S1655F, M1775R, 5382insC) completely abolish the interaction of BRCA1 with Spinophilin as well as BRIP1 and RBBP8, while C61G mutation in the RING domain abrogates the interaction with BARD1. Colored data points indicate proteins that have ≤4-fold difference in protein interaction between WT and mutants and an adjusted p-value<0.05.

[0297] Reciprocal AP-MS was performed using 3×FLAG-tagged Spinophilin in MDA-MB-231 cells, which confirmed the interaction of Spinophilin with BRCA1 as well as with PP1 catalytic subunits (PPP1CA, PPP1CB, PPP1CC) (FIG. **9**A). It was also found that Spinophilin interacts with additional proteins involved in DNA repair including WDR48 and MCM10. Without wishing to be bound by theory, these AP-MS results suggest that Spinophilin may participate in and/or regulate DNA repair by interacting with various DNA repair and replication proteins, including BRCA1. To explore this hypothesis, the effect of Spinophilin knockdown on DNA repair was analyzed by HR and single-strand annealing (SSA). In these assays, DNA Double Strand Breaks (DSBs) were induced by I-SceI endonuclease, which cleaves non-functional GFP cassettes engineered in the genome of U2OS reporter cell lines (DR-GFP and SAGFP) (Bhargava et al., 2018; Gunn and Stark, 2012). DSB repair that depends on the HR or SSA mechanism restores a functional GFP gene, yielding a readout tied to fluorescent signal intensity. Upon Spinophilin knockdown, HR activity was significantly reduced compared to NTC siRNA (FIG. **9**B-C and FIG. **10**A). In the same assay, knockdown of BRCA1 greatly decreased HR as expected (Anantha et al., 2017), while depletion of a protein functioning in an alternative DNA repair pathway did not (TP53BP1, nonhomologous end joining). Similarly, knockdown of Spinophilin significantly reduced SSA activity, comparable to BRCA1 depletion, while BRCA2 depletion dramatically increased SSA as seen previously (Anantha et al., 2017) (FIG. **9**D-E), implying that Spinophilin promotes both HR and SSA-mediated DSB repair.

[0298] Referring to FIG. **9**A, AP-MS of 3×FLAG-tagged Spinophilin (SPN, encoded by PPP1R9B) identifies BRCA1 (highlighted in a red edge) and other DDR-related proteins as well as PP1 catalytic subunits (PPP1CA, PPP1CB, and PPP1CC) in MDA-MB231 cells.

[0299] Referring to FIG. **9**B, a schematic of the HR reporter assay is shown. The DR-GFP reporter contains two defective copies of the GFP gene, one disrupted by an I-SceI site and the other lacking a promoter. I-SceI cutting of the first copy generates a DSB, and repair by HR with the

second copy as a template leads to restoration of a functional GFP gene. siRNA-mediated knockdown of HR-related genes leads to reduction of GFP+cells (a proxy of HR activity) compared to NTC experiments.

[0300] Referring to FIG. **9**C, HR activities upon depletion of SPN relative to NTC (set to 100%). Depletion of BRCA1 and TP53BP1 was included and analyzed as controls. Data shown are the means from six independent experiments for each siRNA. Error bars represent standard deviations (SDs). **** p-value<1.0×10^{-5}.

[0301] Referring to FIG. **9**D, a schematic of the SA-GFP reporter assay is shown. The SA-GFP reporter contains a 5'-fragment of GFP (5'-GFP) and a 3'-fragment of GFP (Sce3'-GFP) that contains an I-SceI site. Repair of the DSB in Sce3'-GFP using 266 nt homology by single-strand annealing (SSA) restores a functional GFP gene.

[0302] Referring to FIG. **9**E, SSA activities upon depletion of SPN relative to NTC (set to 100%) are shown. Depletion of BRCA1 and BRCA2 was included and analyzed as controls. Data shown are the means±SDs from six independent experiments for each siRNA. **** p-value<1.0×10^{-4}, *** p-value<1.0×10^{-3}.

[0303] Referring to FIG. **10**A, levels of BRCA1, SPN, I-SceI and β-tubulin proteins in U2OS/DR-GFP cells following knockdown were analyzed by western blot.

[0304] Because Spinophilin is a regulatory subunit of PP1, it was hypothesized that it targets PP1 to specific DNA repair proteins, including BRCA1, for dephosphorylation. To uncover potential dephosphorylation targets under this model, a high-throughput peptide phosphorylation assay platform was used (Coppé et al., 2019a; Coppe et al., 2019; Coppé et al., 2019b). This system utilizes a collection of peptide sequences derived from biological targets of multiple kinases, which serves as phosphorylatable probes in a large-scale ATP-consumption assay (Chen and Coppé, 2012; Olow et al., 2016). In this assay, changes in phosphorylation (i.e., ATPconsumption) of peptide substrates derived from various proteins, including BRCA1 and the DSB-associated histone H2AX as well as proteins unrelated to DNA repair (e.g., INCENP, BCAR1), were measured in Spinophilin-disrupted (FIG. **10**B-D) and parental cells (Key Resources Table I). Without wishing to be bound by theory, it was found that BRCA1 residues at T509, S1387, and S1423, as well as H2AX at S140 (γ-H2AX), were significantly increased in phosphorylation in Spinophilin-disrupted cell lysates compared to lysates from parental cells, and, in fact, were among the top 20 most increased sites (FIG. **9**F and FIG. **10**E). These results were in contrast to phosphorylation of the INCENP and BCAR1 peptides, which were not significantly changed by Spinophilin disruption. BRCA1 pT509 enhances nuclear localization and transcriptional activity of BRCA1 (Hinton et al., 2007), and pS1387 and pS1423 sites in the BRCA1 SQ-cluster region are critical for HR repair and cell-cycle checkpoint functions (Beckta et al., 2015; Cortez et al., 1999; Xu et al., 2002). γ-H2AX is a hallmark of DNA DSB (Rogakou et al., 1998) and initiates a signaling cascade to recruit various DSB repair proteins to properly repair the DNA damage (Lukas et al., 2011). Without wishing to be bound by theory, these results suggest that Spinophilin regulates BRCA1 and DDR signaling via dephosphorylation. Spinophilin knockdown may induce persistent phosphorylation of BRCA1 (and likely other DDR proteins, including H2AX), which could inhibit proper progression to subsequent repair or resetting activated DDR signaling to the initial homeostatic state following repair of damaged DNA (FIG. **9**G). In agreement with these results, persistent γ-H2AX due to depletion of phosphatase PP2A has been reported to result in inefficient DSB repair (Chowdhury et al., 2005).

[0305] Referring to FIG. **9**F, selective peptides derived from BRCA1 and H2AX as well as two non-DNA repair proteins (INCENP and BCAR1) were individually mixed with lysates from either SPN KO or parental cells and subsequently monitored for phosphorylation by measuring ATP consumption. Net peptide phosphorylation (difference between SPN KO and parental cells) was calculated from two independent runs as shown in the y-axis. Error bars represent standard deviations (SDs). * p-value<0.05, ** p-value<0.01.

[0306] Referring to FIG. **9**G, a model for the role of SPN in regulating DDR is shown.

[0307] Referring to FIG. **10**B, functional domains/motifs in the PPP1R9B gene and the location of CRISPR/Cas9-mediated cut site to introduce INDELS to generate knockout (KO) clones are shown.

[0308] Referring to FIG. **10**C, confirmation of knockout by western blot analysis using u-Spinophilin (SPN) antibody is shown.

[0309] Referring to FIG. **10**D, exome sequencing verified disruption of PPP1R9B alleles in two knockout clones (#9 and #22).

[0310] Referring to FIG. **10**E, top 20 most increased phosphosites in SPN KO cell lysates, compared to parental MDA-MB-231 cell lysates are shown. Net phosphorylation of the peptides derived from 237 proteins including BRCA1 and H2AX was calculated based on ATP consumption between SPN KO and parental cell lysates. Peptides from INCENP and BCAR1 are shown as unaffected controls. Kinase(s) known to phosphorylate each phosphosite is also listed.

Discussion

[0311] Here, comprehensive interaction maps were generation for 40 frequently altered breast cancer proteins. These data represent the first large-scale study of biophysical interactions in breast cancer and across multiple cell lines of human breast tissue origin, providing a useful and relevant PPI resource to study breast cancer biology. Prey proteins private to either of the two BC cell lines are more frequently mutated in breast tumors than preys from non-tumorigenic cells (FIG. **3**E), implying that proteins interacting with cancer drivers may also contribute to the onset of cancer.

[0312] Approximately 79% of PPIs identified have not been previously reported (FIG. **3**C), and 81% are not shared across cell lines (FIG. **3**E). These findings illustrate a significant rewiring of PPIs driven by different cellular contexts, as recently seen by another large-scale AP-MS study (Huttlin et al., 2020). Without wishing to be bound by theory, these results suggest that protein abundance in a cell line is not the sole mechanism for PPI specificity (FIG. **2**D). Presumably other features, such as differential posttranslational modifications (PTM), cellular compartmentalization, and/or mutational status of proteins may contribute to cell type-specificity.

[0313] S100A3 activates AKT signaling via protein interaction in MDA-MB-231 cells (FIG. **4**C-D). Consistently, ≤4-fold higher protein abundance of S100A3 was observed

in MDA-MB-231 cells than the other two cell lines, and it is known that chromosome 1q21.3 containing the S100A3 gene is amplified in all BC subtypes but with a higher percentage in TN breast tumors like MDA-MB-231 (31% compared to 10-12% for luminal and HER2+) (Goh et al., 2017). Consistent with these findings, higher S100A3 expression was predictive of a successful clinical response to an AKT inhibitor among BC patients in the I-SPY 2 trial (FIG. **4**E). Without wishing to be bound by theory, these results suggest that S100A3 is an oncogenic driver activating the AKT signaling pathway, preferentially in TN tumors, and holds potential as a biomarker to segregate patients for AKT-directed therapy. Novel interactors of PIK3CA that negatively regulate the PI3K/AKT pathway were also identified (FIG. **6**H). BPIFA1 is a lipid-binding protein with antimicrobial and immunomodulatory functions (Britto and Cohn, 2015; Ning et al., 2014). It is significantly downregulated in nasopharyngeal carcinoma (Bingle and Bingle, 2011; Lemaire et al., 2003; Zhang et al., 2003) and its single-nucleotide polymorphisms are associated with increased susceptibility to this tumor type (He et al., 2005). The BPIFA1-PIK3CA interaction identified suggests that BPIFA1 may directly modulate PI3K-AKT via PPI. BPIFA1 also increases the expression of PTEN via downregulating the miR-141 oncogene (Chen et al., 2013), thus it is also possible that knockdown of BPIFA1 may indirectly activate PI3K/AKT.

[0314] Another PIK3CA interactor, SCGB2A1, is a small secreted protein highly differentially expressed in multiple types of cancer including ovary, endometrium, and breast (Aihara et al., 1999; Bellone et al., 2013; Tassi et al., 2008). Previous studies have shown that SCGB2A1 is expressed at lower levels in luminal breast cancer compared to histologically normal breast epithelium (Zubor et al., 2015), and that overexpression of SCGB2A1 inhibits the viability of luminal BC cell lines with activated PI3K (including MCF7) via induction of apoptosis (Zhang et al., 2020). Provided that SCGB2A1 acts as a negative regulator of the PI3K-AKT pathway, elevated expression of SCGB2A1 may lead to inhibition of PI3K activity on which cell viability relies. Intriguingly, mutations in the PIK3CA kinase domain (M1043V and H1047R) significantly abolished the interaction with most of the other negative regulators identified (including BPIFA1, BPIFB1, PRR4, and ZG16B but not SCGB2A1), while these interactions were not severely affected by a helical domain mutation (E545K) (FIG. **6**I). Considering that one of the steps in PIK3CA activation involves a conformational change in the kinase domain, which promotes PIK3CA membrane localization (Burke et al., 2012; Liu et al., 2014), these negative regulators may bind to the kinase domain and/or prevent the conformational change. Presumably, kinase domain mutants (e.g., H1047R) that become activated by mimicking this step may be refractory to negative regulation by these proteins. Alternatively, given that BPIFA1/B1 binds membrane lipids via the bactericidal/permeability-increasing fold (BPI) (Alva and Lupas, 2016; Beamer, 2003), some of these proteins may block the membrane localization of the PIK3CA kinase domain by interfering with its lipid binding.

[0315] In an effort to comprehensively identify BRCA1-interacting proteins in breast cancer cells, several novel interacting proteins were found, including Spinophilin, which acts as a regulatory subunit of PP1 (FIG. **7**B-C and FIG. **9**A). Knockdown of Spinophilin led to significant impairment in DSB repair by both HR and SSA pathways (FIG. **9**C and FIG. **9**E), establishing that this protein has a defined role in DNA repair. Consistent with its BRCA1 association, Spinophilin knockout revealed a net increase in phosphorylation on several phosphosites (pT509, pS1387, pS1423) (FIG. **9**F), all of which are known to potentiate the DNA repair function of BRCA1 (Beckta et al., 2015; Cortez et al., 1999; Hinton et al., 2007; Xu et al., 2002). These residues are phosphorylated by AKT (T509) (Altiok et al., 1999; Nelson et al., 2010) and ATM/ATR (S1387, S1423) (Cortez et al., 1999; Gatei et al., 2000, 2001; Kim et al., 1999) but the opposing phosphatase(s) has not been identified. These results indicate that Spinophilin may dephosphorylate these residues and thus modulate BRCA1 functions via direct interaction (FIG. **9**G).

[0316] A related intriguing question is how depletion of Spinophilin decreases HR and SSA repair activity. One plausible explanation is that prolonged phosphorylation of BRCA1 (and likely other DDR proteins as well) is inhibitory to multiple steps during DNA repair, including DSB-end resection, which is a prerequisite for HR and SSA. In agreement with this hypothesis, continuous DNA damage signaling and phosphorylation of several DDR proteins (including H2AX, NBN, RPA2, and CHEK2) induced by short double-stranded DNA molecules (mimicking DNA DSB) was shown to disorganize the cellular DNA repair system and inhibit DSB repair (Quanz et al., 2009). Alternatively, but not exclusively, Spinophilin may play a role in initiating the DSB repair process by removing constitutive phosphorylations that inhibit the function of DDR proteins. Supporting this scenario, a phosphoproteomic study revealed that over one-third of the captured phospho-peptides were dephosphorylated within minutes of DNA damage (Bensimon et al., 2010). Additionally, Spinophilin may be involved in counteracting DSB-induced phosphorylation events, thus promoting recycling of DDR proteins as DNA damage is being repaired. Given that somatic alterations to Spinophilin are more frequent in breast cancer than alterations to BRCA1 (approximately 8% versus 2%, respectively) (Cancer Genome Atlas, Network, 2012), this protein may be worthy of further study as a significant cancer-associated gene in DSB repair.

[0317] In summary, this study demonstrates that systematic PPI maps effectively identify new cancer susceptibility genes and recognize new druggable vulnerabilities in breast cancer. These maps provide a useful resource in contextualizing uncharacterized mutations within signaling pathways and protein complexes. Further analysis of genetic and functional interactions (gene-gene, gene-drug) of proteins in the map will help to decode their biological mechanisms and guide the development of cancer treatment strategies.

Example 2. A Protein Network Map of Head and Neck Cancer Reveals PIK3CA Mutant Drug Sensitivity

Experimental Methods

Bait Cloning

[0318] Baits were cloned using the Gateway Cloning System (Life Technologies) into a doxycycline-inducible N-term or C-term 3×FLAG-Tagged vector modified to be Gateway compatible from the pLVX-Puro vector (Clontech) by the Krogan lab. Point mutant baits were cloned via

site-directed mutagenesis. All expression vectors were sequence validated (Genewiz).

Cell-Culture, Lentivirus Production, and Stable Cell Line Generation

[0319] HEK293T (ATCC, CRL-3216) and CAL-33 were maintained in DMEM (Corning) supplemented with 10% FBS (Gibco) and 1% Penicillin-Streptomycin (Corning). HET-1A was maintained in BEGM™ (Lonza), consisting of Broncho Epithelial Basal medium (BEBM) with the additives of the Bullet kit except GA-1000 (gentamycin-amphotericin B mix). SCC-25 was maintained in DMEM/F12 (Corning) with 10% FBS (Gibco), 1% Penicillin-Streptomycin (Corning) and 400 ng/mL hydrocortisone (Sigma). HET-1A was obtained from American Type Culture Collection and SCC-25 was obtained from Thomas Carey (University of Michigan), CAL-33 were provided by Gerard Milano (University of Nice, Nice, France). All cells were maintained in a humidified 37° C. incubator with 5% CO_2. Stably transduced HET-1A, SCC-25, and CAL-33 cell lines were maintained in puromycin (2 μg/mL, 2.5 μg/mL, and 0.7 μg/mL, respectively). Bait expression was induced by 1 vμg/ml doxycycline for 40 hrs. All cell lines were authenticated by the University of California, Berkeley Cell Culture Facility. Lentivirus was produced for each bait by packaging 5ug bait vector, 3.33 μg of Gag-Pol-Tat-Rev packaging vector (pJH045 from Judd Hultquist), 1.66 μg of VSV-G packaging vector (pJH046 from Judd Hultquist) with 30 μL of PolyJet (SignaGen). After incubating at room temperature for 25 min, DNA complexes were added dropwise to HEK293T cells (15 cm plate, ~80% confluency). Lentivirus-containing supernatant was collected after 72 hrs and filtered through a 0.45 μm PVDF filter. Lentivirus particles were precipitated with PEG-6000 (8.5% final) and NaCl (0.3 M final) at 4° C. for 4-8 hrs. Particles were pelleted via centrifugation at 2,851×g for 20 min at 4° C. and resuspended in DPBS for a final volume ~800-1000 μL. Stable cell lines were generated by transducing a 10 cm plate (~80% confluency) with 200 uL of precipitated lentivirus for 24 hrs before selecting with puromycin for a minimum of 2 days.

Affinity Purification

[0320] One 10 cm plate of cells (~80% confluency) was washed with ice-cold DPBS and lysed with 300 μL of ice-cold lysis buffer (50 mM Tris pH 7.4, 150 mM NaCl, 1 mM EDTA, 0.5% NP40, 1 mM DTT, 1× protease inhibitor cocktail (Roche, complete mini EDTA free), 125U Benzonase/mL). Lysates were flash-frozen on dry ice for 5-10 min, followed by a 30-45 s thaw in 37° C. water bath with agitation, and rotation at 4° C. for 15 min. Lysate was clarified by centrifugation at 13000×g for 15 min at 4° C. A 30 μL lysate aliquot was saved for future BCA assay and western blot.

[0321] For FLAG purification, 25 μL of bead slurry (Anti-Flag M2 Magnetic Beads, Sigma) was washed twice with 1 mL of ice-cold wash buffer (50 mM Tris pH 7.4, 150 mM NaCl, 1 mM EDTA) and all of the remaining lysate was incubated with the anti-FLAG beads at 4° C. with rotation for 2 hrs. After incubation, flow-through was removed and beads were washed once with 500 μL of wash buffer with 0.05% NP40 and twice with 1 mL of wash buffer (no NP40). Bound proteins were eluted by incubating beads with 15 μL of 100 ug/ml 3×FLAG peptide in 0.05% RapiGest in wash buffer for 15 min at RT with shaking. Supernatants were removed and elution was repeated. Eluates were combined and 10 μL of 8 M urea, 250 mM Tris, 5 mM DTT (final concentration ~1.7 M urea, 50 mM Tris, and 1 mM DTT) was added to give a final total volume of ~45 μL. Samples were incubated at 60° C. for 15 min and allowed to cool to room temperature. IODO was added to a final concentration of 3 mM and incubated at room temperature for 45 min in the dark. DTT was added to a final concentration of 3 mM before adding 1 μg of sequencing-grade trypsin (Promega) and incubating at 37° C. overnight. Samples were acidified to 0.5% TFA (ph<2) with 10% TFA stock and incubated for 30 min before desalting on C18 stage tip (Rainin).

Mass Spectrometry Data Acquisition and Analysis

[0322] For AP-MS experiments, samples were resuspended in 15 μL of MS loading buffer (4% formic acid, 2% acetonitrile) and 2 μL were separated by a reversed-phase gradient over a nanoflow 75 μm ID×25 cm long picotip column packed with 1.9 μM C18 particles (Dr. Maisch). Peptides were directly injected over the course of a 75 min acquisition into a Q-Exactive Plus mass spectrometer (Thermo), or over the course of a 90 min acquisition into a Orbitrap Elite mass spectrometer. Raw MS data were searched against the uniprot canonical isoforms of the human proteome (downloaded Mar. 21, 2018), and using the default settings in MaxQuant (version 1.6.2.10), with a match-between-runs enabled (Cox and Mann, 2008). Peptides and proteins were filtered to 1% false discovery rate in MaxQuant, and identified proteins were then subjected to protein-protein interaction scoring. To quantify changes in interactions between WT and mutant baits, a label free quantification approach was used, in which statistical analysis was performed using MSstats (Choi et al., 2014) from within the artMS Bioconductor R-package. All raw data files and search results are available from the Pride partner ProteomeXchange repository under the PXD019469 identifier (Perez-Riverol et al., 2019; Vizcaino et al., 2014).

Targeted Proteomic Analysis

[0323] Targeted proteomic analysis of APMS samples was performed on a Thermo Q-Exactive Plus mass spectrometer using the same HPLC conditions as described for original AP-MS experiments. All peptide and fragment ion selection, as well as quantitative data extraction was performed using Skyline (MacLean et al., 2010). Quantitative values were then imported into PRISM 8 software to perform normalization by bait abundance and statistical testing (2-tailed, unpaired t-test).

Protein-Protein Interaction Scoring

[0324] Protein spectral counts as determined by MaxQuant search results were used for PPI confidence scoring by both SAINTexpress (version 3.6.1) (Teo et al., 2014) and CompPASS (version 0.0.0.9000) (Huttlin et al., 2015; Sowa et al., 2009). All PPI scoring was performed separately for each cell line. For SAINTexpress, control samples in which bait protein was not induced by addition of doxycycline were used. For CompPASS, a stats table representing all WT baits was used. After scoring, the CompPASS WD and Z-score were normalized within a given bait for each cell line. The total list of candidate PPIs was filtered to those that

met the following criteria: SAINTexpress BFDR=<0.05, WD percentile by bait>=0.95, and Z-score percentile by bait≤=0.95. PPIs passing all 3 of these criteria were considered to be high-confidence PPIs. To enable visualization and analysis of PPIs by confidence score among these 3 criteria, a PPI score was calculated: [(WD percentile by bait+Z-score percentile by bait)/2)+(1−BFDR)]/2. This score places both the PPI confidence from SAINTexpress and CompPASS on a zero to 1 scale, with 1 being the highest confidence, and then takes the weighted average of these confidence scores.

Permutation Test

[0325] A permutation test was performed in which genes were drawn from the list of all genes detected in the global protein abundance analysis of the parental cell lines. The null distribution of the average number of samples with variation was learned from 10,000 random gene lists of equal size to the set of interacting partners. This permutation test was performed individually for mutations (excluding silent mutations), CNVs, and mRNA expression. The information for observed variation of each gene is collected from the TCGA head and neck cancer cohort (firehose legacy; downloaded from cbioportal.org/datasets).

Protein-Protein Interaction Scoring: CompPASS

[0326] CompPASS is an acronym for Comparative Proteomic Analysis Software Suite. It relies on an unbiased comparative approach for identifying high-confidence candidate interacting proteins (HCIPs for short) from the hundreds of proteins typically identified in IP-MS/MS experiments. There are several scoring metrics calculated as part of comPASS: The Z-score, the S-score, the D-score, and the WD-score. The S-score, D-score, and WD-score were all developed empirically based on their ability to effectively discriminate known interactors from known background proteins. Each score has advantages and disadvantages, and each are used to assess distinct aspects of the dataset. However, the primary score use to determine the high-confidence protein-protein interaction dataset is the WD-score. Typically, the top 5% of the WD-score scores are taken (more information under "Determining Thresholds").

The Z-Score.

[0327] The first score is the conventional Z-score, which determines the number of standard deviations away from the mean (Eq. 1) at which a measurement lies (Eq. 2). In Eq. 1 & 2× is the TSC, i is the bait number, j is the interactor, n denotes which interactor is being considered, k is the total number of baits, and s is the standard deviation of the TSC mean.

$$\bar{x}_j = \frac{\sum_{?} x_{i,j}}{k} : n = 1, 2, \ldots m \quad \text{(Eq. 1)}$$

$$z_{i,j} = \frac{x_{i,j} \cdot \bar{x}_j}{\sigma_j} \quad \text{(Eq. 2)}$$

? indicates text missing or illegible when filed

[0328] Each interactor for each bait has a Z-score calculated and therefore, the same interactor will have a different Z-score depending on the bait (assuming the TSC is different when identified for that bait). Although the Z-score can effectively identify interactors who's TSC is significantly different from the mean, if an interactor is unique (found in association with only 1 bait), then it fails to discriminate between interactors with a single TSC ("one hit wonders") and another that may have 20 TSC or 50 TSC, etc. In this way, the Z-score will tend to upweight unique proteins, no matter their abundance. This can be dangerous since the stochastic nature of data-dependent acquisition mass spectrometry leads to spurious identification of proteins. These would be assigned the maximal Z-score as they would be unique, however they likely do not represent bonafide interactors.

The S-Score.

[0329] The next score is the S-score which incorporates the frequency of the observed interactor and its' abundance (TSC). Both the D- and WD-scores are based on the S-score, sharing the same fundamental formulation, but have additional terms that add increasing resolving power. The S-score (Eq. 3) is essentially a uniqueness and abundance measurement.

$$S_{i,j} = -\sqrt{\left(\frac{k}{\sum_{?} f_{i,j}}\right)} x_{i,j}\,; \quad \text{(Eq. 3)}$$

$$f_{i,j} = \begin{cases} 1 : x_{i,j} > 0 \\ x_{i,j} \end{cases}$$

? indicates text missing or illegible when filed

[0330] In Eq. 3, the variables are the same as for Eq. 1 & 2.f is a term which is 0 or 1 depending on whether or not the interacting protein is found in a given bait. Placed in the summation across all baits, it is a counting term and therefore, k/Sf is the inverse ratio (or frequency) of this interactor across all baits. The smaller f, the larger this value becomes and thus upweights interactors that are rare. The term $X_{i,j}$ is the TSC for interactor j from bait i and therefore multiplying by this value scales the S-score with increasing interactor TSC—this provides a higher score to interactors having high TSC and are therefore more abundant and less likely to be stochastically sampled. Although increasing the resolution above using the Z-score alone (the S-score can discriminate between unique one hit wonders and unique interactors with high TSC), the S-score will give its highest values to interactors that very rare and can lead to one hit wonders being scored among the top proteins. However, with a stringent cut-off value, the S-score reliably identifies HCIPs and bona fide interacting proteins but at this level, is prone to miss lower abundant likely interacting proteins. In order to address this limitation, the S-score was modified to take into account the reproducibility of the interactor for a given bait—a quantity that can be determined as a result of performing duplicate mass spectrometry runs. After adding this modification, the S-score becomes the D-score (Eq. 4).

The D-Score.

[0331] The D-score is fundamentally the same as the S-score except with an added power term to take into account the reproducibility of the interaction. The term p can either be 1 (if the interactor was found in 1 of 2 duplicate runs) or 2 (if the interactor was found in both duplicate runs).

$$D_{i,j} = -\sqrt{\left(\frac{k}{\sum_{?} f_{i,j}}\right)^{p} x_{i,j}}; \quad \text{(Eq. 4)}$$

$$f_{i,j} = \begin{cases} 1 : x_{i,j} > 0 \\ x_{i,j} \end{cases}$$

$p = ?$

? indicates text missing or illegible when filed

[0332] If p is 1 (the interactor was found in 1 of 2 duplicates) then the D-score is the same as the S-score. Adding the reproducibility term now allows for better discrimination between a true one hit wonder (a protein found with 1 peptide in a single run, not in the duplicate) which is likely a false positive versus a true interactor with low (even 1) TSC that is found in both duplicate runs. Although powerful in its ability to delineate HCIPs from background proteins, the D-score still relies heavily on the frequency term, k/Sf, and will thus assign lower scores to more frequently observed proteins. In the vast majority of the cases, this is of course a good thing since these proteins are more than likely background. However, in the event that a canonical background protein is a bonafide interactor for a specific bait, its D-score would likely be too low for passing the D-score threshold (discussed below) and would not be considered a HCIP. Another example pertains to CompPASS analysis of baits from within the same biological network or pathway. In the case of the Dub Project, most of these proteins do not share interactors as this analysis was performed across a protein family—in which case the D-score works very well. However sometimes baits do share interactors as these proteins are part of the same biological pathway and determining these share interactors (and hence the connections among these proteins) is critical for a reliable assessment of the pathway. In these cases, the D-score works fairly well for most interactors, however it can downweigh very commonly found bona fide interactors (especially when these interactors have low TSC). To address this limitation, a weighting factor to be added into the D-score was devised, and the WD-score (or Weighted D-score; Eq. 5) was created.

The WD-Score.

[0333] Upon examination of frequently observed proteins (considered background) that are either known not to be a bona fide interactor for any bait and those that are known to be true interactors for a subset of baits, it is found that the distributions of the TSC for these groups vary in a correlated manner. In the first case, where these "background" proteins are never true interactors, the standard deviation of the TSC (s_{TSC}) is smaller than that of the latter case ("background" proteins that are known to be true interactors for specific baits). This occurs since real background protein abundance is mainly determined by the amount of resin used in the IP whereas in the case of a background protein becoming a true interactor, its TSC then rises far above this consistent level (and thus cause s_{TSC} to increase. In fact, when S_{TSC} is systematically examined across all proteins found in >50% of the IP-MS/MS datasets, the proteins that are known to be real interactors for specific baits are found to have a S_{TSC} that is >100% of the TSC mean for that protein across all IPs. Therefore, a weight factor term is introduced as w_j and is essentially the S_{TSC}/TSC mean for interactor j (shown below).

$$WD_{i,j} = -\sqrt{\left(\frac{k}{\sum_{?} f_{i,j}}\omega_j\right)^{p} x_{i,j}} \quad \text{(Eq. 5)}$$

$$\omega_j = \left(\frac{\sigma_i}{\bar{x}_i}\right), \bar{x}_j = \frac{\sum_{?} x_{i,j}}{k} : n = 1, 2, \ldots m,$$

$$\text{if } \omega_j \times 1\ ? \ \omega_j = 1$$

$$\text{if } \omega_j > 1\ ? \ \omega_j = \omega_j$$

$$f_{i,j} = \begin{cases} 1 : x_{i,j} > 0 \\ x_{i,j} \end{cases}$$

$p = ?$

? indicates text missing or illegible when filed

[0334] The weight factor, w_j, is added as a multiplicative factor to the frequency term in order to offset this low value for interactors that are found frequently across baits but will only be >1 if the conditions in Eq. 5 are met. If these conditions are not met, then o_j is set to 1 and the WD-score is the same as the D-score. In this way, only if a frequent interactor displays the observed characteristics of a true interactor will its score increase due to the weight factor.

[0335] To determine score thresholds for determining high-confidence protein-protein interactions, randomly generated simulated run data are compared against. In order to create simulated random runs, the data from actual experiments is first used to create the proteome observed from the experiments. To do this, each protein is represented by its TSC from each run—in other words, if a protein is found with a total of 450 TSC summed across all real runs, then it is represented 450 times. Simulated runs are then created by randomly drawing from this "experimental proteome" until 300 proteins are selected and the total TSC for the simulated run is ~1500 (these are the average values found across the actual experiments). Next, scores are calculated for the random runs to determine the distributions of the scores for random data. Finally, for each score, the corresponding value above which 5% of the random data lies is found, and that value taken to be that score's threshold. Although 5% of the random data is above this threshold value, an examination of the TSC distribution for these random data is expected to show that ≤99% have TSC<4. Therefore, although there are false positive HCIPs in real datasets, this distribution can now be used to assign a p-value for proteins passing the score thresholds. In this way, an argument can be

made that a protein passing a score threshold and found to have high enough TSC (reflected in the p-value) is very likely to be a real interactor. A suitable approximation for this above described method is to simply take the minimal value of the top 5% of the scores for each metric and set that value to be the threshold for that score.

Protein-Protein Interaction Scoring: SAINT

[0336] The aim of SAINT is to convert the label free quantification (spectral count X_{ij}) for a prey protein i identified in a purification of bait j into the probability of true interaction between the two proteins, P(True|X_{ij}). The spectral counts for each prey-bait pair are modeled with a mixture distribution of two components representing true and false interactions. Note that these distributions are specific to each bait-prey pair. The parameters for true and false distributions, P(X_{ij}|True) and P(X_{ij}|False), and the prior probability π_T of true interactions in the dataset, are inferred from the spectral counts for all interactions involving prey i and bait j. SAINT normalizes spectral counts to the length of the proteins and to the total number of spectra in the purification.

[0337] The spectral counts for prey i in purification with bait j are considered to be either from a Poisson distribution representing true interaction (with mean count λ_{ij}) or from a Poisson distribution representing false interaction (with mean count κ_{ij}). In the form of probability distribution, the following formula is written:

$$P(X_{ij}|*) = \pi_T P(X_{ij}|\lambda_{ij}) + (I - \pi_T)P(X_{ij}|\kappa_{ij}) \quad (1)$$

where π_T is the proportion of true interactions in the data, and dot notation represents all relevant model parameters estimated from the data (here, specifically for the pair of prey i and bait j). The individual bait-prey interaction parameters λ_{ij} and κ_{ij} are estimated from joint modeling of the entire bait-prey association matrix, with the probability distribution (likelihood) of the form $P(X|\bullet)=\Pi_{i,j}P(X_{ij}|\bullet)$. The proportion π_T is also estimated from the model, which relies on latent variables in the sampling algorithm (see below).

[0338] When at least three control purifications are available, and assuming that the control purifications provide a robust representation of nonspecific interactors, the parameter κ_{ij} can be estimated from spectral counts for prey i observed in the negative controls. This is equivalent to assuming

$$P(X_{ij}|*) = \prod_{?} \left(\pi_T P(X_{ij}|\lambda_{ij}) + (I - \pi_T)P(X_{ij}|\kappa_{ij})\right) \times \prod_{?} (P(X_{ij}|\kappa_{ij})) \quad (2)$$

? indicates text missing or illegible when filed

where E and C denote the group of experimental purifications and the group of negative controls, respectively. This leads to a semi-supervised mixture model in the sense that there is a fixed assignment to false interaction distribution for negative controls. As negative controls guarantee sufficient information for inferring model parameters for false interaction distributions, Bayesian nonparametric inference using Dirichlet process mixture priors can be used to derive the posterior distribution of protein-specific abundance parameters in the model. As a result, the mean parameters in the Poisson likelihood functions follow a nonparametric posterior distribution, allowing more flexible modeling at the proteome level. Under this setting, all model parameters are estimated from an efficient Markov chain Monte Carlo algorithm.

[0339] To elaborate on the two distributions, the mean parameter for each distribution is assumed to have the following form. For false interactions, it is assumed that spectral counts follow a Poisson distribution with mean count:

$$\log(\kappa_{ij}) = \log(l_i) + \log(c_j) + \gamma_0 + \mu_i \quad (3)$$

where l_i is the sequence length of prey i, and c_j is the bait coverage, the spectral count of the bait in its own purification experiment, γ_0 is the average abundance of all contaminants and μ_i is prey i specific mean difference from γ_0. For true interactions, it is assumed that spectral counts follow a Poisson distribution with mean count:

$$\log(\lambda_{ij}) = \log(l_i) + \log(c_j) + \beta_0 + \alpha_{bj} + \alpha_{pi} \quad (4)$$

where β_0 is the average abundance of prey proteins in those cases where they are true interactors of the bait, α_{bj} is bait j specific abundance factor and α_{pi} is prey i specific abundance factor. In other words, the mean spectral count for a prey protein in a true interaction is calculated using a multiplicative model combining bait- and prey-specific abundance parameters. This formulation substantially reduces the number of parameters in the model, avoiding the need to estimate every λ_{ij} separately.

[0340] For datasets without negative control purifications, the mixture component distributions for true and false interactions have to be identified solely from experimental (non-control) purifications. In this case, a user-specified threshold is applied to divide preys into high-frequency and low-frequency groups, denoted as Y_i=1 or 0 if prey i belongs to the high- or low-frequency group, respectively. An arbitrary 20% threshold is applied in the case of the DUB dataset; however, the results are not expected to be very sensitive to the choice of the threshold. For preys in the high frequency group, the model considers spectral counts for the observed prey proteins (ignoring zero count data, which represent the absence of protein identification), as there are sufficient data to estimate distribution parameters. In the low-frequency group, non-detection of a prey is included to help the separation of high-count from low-count hits. The entire mixture model can then be expressed as

$$P(X_{ij}|?) = \prod_{ij} (\pi_T P(X_{ij}|\lambda_{ij}) + (1 - \pi_T)P(X_{ij}|\kappa_{ij}))^{Z_{ij}} \quad (5)$$

? indicates text missing or illegible when filed

where Z_{ij}=1(Y_i=0)+1(Y_i=1,X_{ij}>0) and the false and true interaction distributions are modeled by equations (3) and (4), respectively.

[0341] The posterior probability of a true interaction given the data is computed using Bayes rule

$$P(\text{true} \mid X_{ij}) = T_{ij} / (T_{ij} + F_{ij}) \quad (6)$$

where $T_{ij}=\pi_T P(X_{ij}|\lambda_{ij})$ and $F_{ij}=(1-\pi_T) P(X_{ij}|\kappa_{ij})$. If there are replicate purifications for bait j, the final probability is computed as an average of individual probabilities over replicates. Note that one alternative approach is to compute the probability assuming conditional independence over replicates, that is, $\Pi_{k\in j}P(X_{ijk}|\lambda_{ijk})$ and $\Pi_{k\in j}P(X_{ijk}|\kappa_{ijk})$ for true and false interactions, with additional index k denoting replicates for bait j. Unlike average probability, this probability puts less emphasis on the degree of reproducibility, and thus may be more appropriate in datasets where replicate analysis of the same bait is performed using different experimental conditions (for example, purifications using different affinity tags) to increase the coverage of the interactome.

[0342] When probabilities have been calculated for all interaction partners, the Bayesian false discovery rate (FDR) can be estimated from the posterior probabilities as follows. For each probability threshold p*, the Bayesian FDR is approximated by

$$FDR(p^*) = \left(\sum_k 1(p_k \geq p^*)(1-p_k)\right) \Big/ \left(\sum_k 1(p_k \geq p^*)\right) \quad (7)$$

where p_k is the posterior probability of true interaction of protein pair k. The output from SAINT allows the user to select a probability threshold to filter the data to achieve the desired FDR.

Comparing Protein Interactions Using Hierarchical Clustering

[0343] Hierarchical clustering is performed on interactions for distinct but related proteins, including viral proteins, cancer proteins, or proteins from other diseases, which are hereout simply referred to as "conditions." First, protein interactions that pass the master threshold (defined in "High-confidence protein interaction scoring" section above) in at least one condition are assembled. New interaction scores (K) are created by taking the average of several interaction scores. This is done to provide a single score that captures the benefits from each scoring method. Clustering is then done using this new Interaction Score (K). Clustering is performed using the ComplexHeatmap package in R, using the "average" clustering method and "euclidean" distance metric. K-means clustering is applied to capture all possible combinations of interaction patterns between conditions.

Differential Interaction Score (DIS) Analysis

[0344] To compare PPIs across conditions (i.e., cell lines, viruses, diseases), a method for calculating a differential interaction score (DIS) was developed, and a corresponding false discovery rate (FDR) can be calculated using AP-MS data across multiple conditions. This approach uses the SAINTexpress score (G. Teo, et al., SAINTexpress: improvements and additional features in Significance Analysis of INTeractome software. *J. Proteomics.* 100, 37-43 (2014)), which is the probability of a PPI being bonafide in a single condition. Here, Sc(b, p) is the SAINTexpress score of a specific PPI denoted as (b, p) in a condition c. Here, an example is provided using three distinct conditions, C1, C2, and C3. Given that PPIs are independent events across different conditions, the differential interaction score is calculated for each PPI (b, p) as the product of the probability of a PPI being present in two of the conditions but absent in the third for each PPI:

$$DIS_A(b, p) = S_{C1}(b, p) \times S_{C2}(b, p) \times [1 - S_{C3}(b, p)]$$

[0345] This differential interaction score highlights PPIs that are strongly conserved across two of the conditions, but not shared by the third. Additionally, PPIs that are present in the one conditions, but depleted in the other two, can be highlighted as follows:

$$DIS_B(b, p) = [1 - S_{C1}(b, p)] \times [1 - S_{C2}(b, p)] \times S_{C3}(b, p)]$$

[0346] These two DIS scores can be further merged to define a single score for each PPI, where if $DIS_A > DIS_B$, the DIS is assigned a positive (+) sign, while if $DIS_A < DIS_B$, the unified DIS is assigned a negative (−) sign. In this way, the DIS for each PPI is represented by a continuum, in which negative DIS scores represent PPIs depleted in two of the three conditions, while positive DIS scores represent PPIs enriched in two of the three conditions. Additionally, for all differential interaction scores calculated, the Bayesian false discovery rate (BFDR) (G. Teo, G. Liu, J. Zhang, A. I. Nesvizhskii, A.-C. Gingras, H. Choi, SAINTexpress: improvements and additional features in Significance Analysis of INTeractome software. *J. Proteomics.* 100, 37-43 (2014)) estimates are also computed at all possible thresholds (p*) as follows:

$$FDR(p^*) = \frac{\sum_{i,i} (1 - DIS(p_i, p_j)) \times I\{DIS(p_i, p_j) > p^*\}}{\sum_{i,j} I\{DIS(p_i, p_j) > p^*\}},$$

where

$I\{A\}$ is 1

when

A is True

and

0 otherwise.

[0347] Note, while these scores are used here for comparison across 3 conditions, it can also be used more simply to compare between any two conditions. Such a comparison is calculated as follows where DIS_{112} results in PPIs specific to condition 1 have a positive DIS value, while PPIs specific to condition 2 results in a negative DIS value:

$$DIS_{C1/C2}(p_1, p_2) = S_{C1}(p_1, p_2) \times (1 - S_{C2}(p_1, p_2))$$

or

$$DIS_{C3/C2}(p_1, p_2) = S_{C3}(p_1, p_2) \times (1 - S_{C2}(p_1, p_2))$$

or

$$DIS_{C3/C1}(p_1, p_2) = S_{C3}(p_1, p_2) \times (1 - S_{C1}(p_1, p_2))$$

Differential Interaction Scoring

[0348] To compare PPIs across cell lines, a method for calculating a differential interaction score (DIS) and a corresponding false discovery rate (FDR) using AP-MS data across multiple cell lines was developed. This approach uses the SAINTexpress score (Teo et al., 2014), which is the probability of a PPI being bonafide in a single cell line. Here, Sc(b, p) was used as the SAINTexpress score of a specific PPI denoted as (b, p) in a cell line c. Given that PPIs are independent events across different cell lines, the differential interaction score was calculated for each PPI (b, p) as the product of the probability of a PPI being present in both cancer cell lines but absent in the HET-1A normal cell line as follow for each PPI:

$$DI(?)(b, p) = S_{CAL-33}(b, p) \times (?)(b, p) \times [I - S_{HET-1A}(b, p)]$$

(?) indicates text missing or illegible when filed

[0349] This differential interaction score highlights PPIs that are strongly conserved across two cancer cell lines, but not shared by the normal cell line. Additionally, PPIs that are present in the control HET-1A cell line, but depleted in both cancer cell lines can be highlighted as follows:

$$DI(?)(b, p) = [1 - S_{CAL-33}(b, p)] \times [(?) - (?)(b, p)] \times S_{HET-1A}(b, p)$$

(?) indicates text missing or illegible when filed

[0350] These two DIS scores were merged to define a single score for each PPI, where if DIS cancer>DISnormal, the DIS is assigned a positive (+) sign, while if DIScancer<DISnormal, the unified DIS is assigned a negative (−) sign. In this way, the DIS for each PPI is represented by a continuum, in which negative DIS scores represent PPIs depleted in HNSCC, while positive DIS scores represent PPIs enriched in HNSCC. Additionally, for all differential interaction scores that were calculated, the Bayesian false discovery rate (BFDR) (Teo et al., 2014) estimates were also computed at all possible thresholds (p*) as follows:

$$FDR(p^*) = \frac{(?)}{(?)},$$

where

$I\{A\}$ is 1

when

A is True

and

0 otherwise.

(?) indicates text missing or illegible when filed

[0351] Note, while these scores were used for comparison across 3 cell lines, it can also be used more simply to compare between any two cell lines. Such a comparison is calculated as follows where DISLineA/LineB results in PPIs specific to cell line A have a positive DIS value, while PPIs specific to cell line B results in a negative DIS value:

$$DI(?)(p_1, p_2) = S_{CAL-33}(p_1, p_2) \times (1 - (?)(p_1, p_2))$$

or

$$DI(?)(p_1, p_2) = (?)(p_1, p_2) \times (1 - (?)(p_1, p_2))$$

or

$$DI(?)(p_1, p_2) = (?)(p_1, p_2) \times (1 - (?)(p_1, p_2)).$$

(?) indicates text missing or illegible when filed

MAPK1 Validation Experiments

[0352] CAL-33 and HSC-6 cells were transiently transfected with 20 nM non-targeting control siRNA (Dharmacon Cat #D-001810-10) or RPS6KA1 siRNA pool (Origene Cat #SR304161). After 24 hrs, cells were seeded in 96-well plates (for viability assessment) in quadruplicate and 6-well plates (for lysate preparation). After 72 hrs, 96-well plates were stained with crystal violet for 30 min, washed with tap water, and allowed to dry for 24 hrs. Crystal violet stain was dissolved in 5% SDS solution and the resulting solution was quantified using a colorimetric plate reader at 570 nM. Lysates were procured from the 6-well plates using RIPA lysis buffer. Immunoblotting was performed to validate RPS6KA1 knockdown and PVDF membranes were probed using a RSK1/2/3 antibody (CST #9355). Total ERK1/2 (CST #4695) was used as a loading control.

NanoBiT GAi1 Dissociation Assay

[0353] The NanoBiT G-protein dissociation assay, based on a split-luciferase system, was performed as previously described with some modifications (Inoue et al., 2019). All DNA constructs were provided by Dr. Asuka Inoue (Tohoku University, Japan). NanoBiT plasmids (pCAGGS) include Gαi1-LgBiT, Gβ1-native, and SmBiT-Gγ2 (CAAX C68S mutant). Gαi-DREADD (pcDNA3.1) was used as a synthetic Gαi-coupled GPCR. Briefly, CAL-33 and HET-1A cells were seeded on poly-D-lysine coated (Sigma, Cat #P7280), opaque, white 96-well plates (Falcon Cat #353296). The following day cells were transfected with NanoBiT and receptor plasmids using Lipofectamine 3000 (ThermoFisher Scientific, Cat #L3000008) according to manufacturer recommendations for a 12-well scale (10 μL transfection mix to each well). The NanoBiT plasmids were mixed at a ratio of 100 ng Gαi1-LgBiT, 500 ng Gβ1, 500 ng SmBiT-Gγ2, and 200 ng of receptor if needed. For gene knockdown experiments, 10 pmol of pooled siControl (Dharmacon, Cat #D-001810-10-20), siFGFR3 (Mission siRNA, Cat #SIHK0780, SIHK0781, SIHK0782), or siDaple (Dharmacon, Cat #L-033364-01-0005) was included in the plasmid mix. Media was changed the following day. Two days after transfection, media was aspirated from each well and washed once with HBSS. Cells were incubated in HBSS with a final concentration of 5 μM native coelenterazine (Biotium, Cat #10110-1) for 30 minutes at room temperature protected from light. Basal luminescence was read and ligand prepared for final concentrations of 10 ng/mL human bFGF (Roche Cat #11123149001) and 10 μM clozapine-N-oxide (Cayman Chemical, Cat #NC1044836).

After ligand addition, luminescence was read in kinetic loops (each well ~every 30 seconds) for 60 minutes total (Tecan Spark). Raw luminescent values were normalized to the corresponding basal value for each well and subsequently to the mean vehicle ratio (raw/basal) at time 0. Significance was calculated using a one-way ANOVA at the 60 minute time point.

Scratch Migration Assay

[0354] CAL-33 cells were seeded on 12-well plates coated with 10 μg/mL fibronectin in PBS (Sigma Aldrich, Cat #F2006-1MG). Once cells reached confluence, a vertical scratch was made with a pipette tip and washed well with PBS before adding serum-free media. Cells were stimulated with vehicle, 10 ng/mL bFGF, or 1% serum for 24 hours. Images were taken at the 0 and 24 hour time points (2× magnification) and the scratch area was quantified using ImageJ. Percent scratch closure was calculated for each well and significance assessed using a one-way ANOVA.

Phosphorylated PAK, ERK, and siRNA Knockdown Confirmation Immunoblots

[0355] CAL-33 and HET-1A cells were seeded on poly-D-lysine-coated 6-well plates. Cells were transfected with siRNA using Lipofectamine RNAiMAX (Thermo Fisher Scientific, Cat #100014472) according to manufacturer recommendations. After overnight serum starvation, cells were stimulated with vehicle, 10 ng/mL bFGF, or 10 μM CNO. Cells were washed once with PBS and lysed in RIPA buffer (50 mM Tris-HCl pH 6.8, 150 mM NaCl, 1% NP-40, 0.5% sodium deoxycholate, 0.1% SDS) with protease and phosphatase inhibitors (Bimake, Cat #B14001, B15001-A/B). Lysates were briefly sonicated and cleared by centrifugation before boiling in Laemmli sample buffer (Bio-Rad Cat #1610747). After separation on 10% acrylamide gels and transfer to PVDF membranes, membranes were blocked with 2% BSA in TBST before incubating with antibodies. Primary antibodies against phospho-PAK1(S199/204)/PAK2(S192/197) (1:1000, Cell Signaling Technology, Cat #2605), PAK1 (1:2000, Cell Signaling Technology, Cat #2602), PAK2 (1:2000, Cell Signaling Technology, Cat #2608), pERK (1:2000, Cell Signaling Technology, Cat #9106), ERK (1:2000, Cell Signaling Technology, Cat #9102), FGFR3 (1:2000, OriGene, Cat #TA801078), Daple (1:1000, Millipore EMD, Cat #ABS515), and GAPDH (1:10000, Cell Signaling Technology, Cat #2118) were used. After washing with TBST, membranes were incubated in secondary goat anti-rabbit HRP (1:20000, Southern Biotech, Cat #4010-05) and goat anti-mouse HRP (1:20000, Southern Biotech, Cat #1010-05) antibodies for chemiluminescent development.

CDX3379 Treatment In Vivo and In Vitro Experiments

[0356] All the animal studies using HNSCC tumor xenografts were approved by the University of California, San Diego Institutional Animal Care and Use Committee (IACUC), with protocol ASP #S15195. All mice were obtained from Charles River Laboratories (Worcester, MA). To establish tumor xenografts, HNSCC cells were transplanted into both flanks (2 million per tumor) of female athymic mice (nu/nu, 4-6 weeks of age and weighing 16-18 g). Mice were fed with doxycycline food (6 g/kg) from Newco Distributors (Rancho Cucamonga, CA, USA) to induce PIK3CA expression. When average tumor volume reached 100 mm^3, the mice were randomized into groups and treated by intraperitoneal (IP) injection with vehicle (PBS) or CDX3379 (10 mg/kg, twice a week) for approximately 15 days. The mice were sacrificed at the indicated time points (or when mice succumbed to disease, as determined by the ASP guidelines).

Phosphorylated HER3 Immunoblots

[0357] Wild-type (WT) or mutant PIK3CA with FLAG-tag were expressed by lentiviral transduction in SCC-25 cells. Collected cells were washed with ice-cold PBS twice and then lysed with RIPA lysis buffer (150 mM Tris, pH 7.4, 100 mM NaF, 120 mM NaCl, 100 mM sodium orthovanadate, with 1 tablet protease inhibitor cocktail (Roche 31075800) and 1 tablet phosphatase inhibitor cocktail (Roche 04906837001) added. Lysates (30 μg) were resolved by SDS-PAGE, transferred to PVDF membranes (Bio-Rad #1620177), and incubated with primary antibodies (1:1000) at 4° C. overnight. Membranes were then washed and incubated with Goat Anti-Rabbit IgG(H+L)-HRP Conjugated secondary antibodies (1:5000) (Bio-Rad #170-6515) for 1 hr at room temperature, followed by washing four times with TBST. Antibodies against P-HER3-Y1197 (#4561) and HER3 (#12708) were from Cell Signaling Technology, and anti-B-tubulin (ab6276) was from Abcam. Blots were quantified with ImageJ software, and the intensity of P-HER3-Y1197 signal was normalized to FLAG-PIK3CA intensity.

IAS Background Network

[0358] The integrated associated stringency (IAS) network was derived from integration of five major types of protein pairwise relationships recorded in public databases: (1) physical protein-protein interaction; (2) mRNA co-expression; (3) protein co-expression; (4) co-dependence (correlation of cell line growth upon gene knockouts); and (5) sequence-based relationships. A broad survey created a compendium of 127 network features used as inputs to a random forest regression model, trained to best recover the proximity of protein pairs in the Gene Ontology (GO). The final IAS score, ranging from 0 to 1, quantifies all pairwise associations among 19035 human proteins. In this study, stringent protein interactions were displayed with IAS>0.3 when the IAS network was used in figures.

Data Analysis

[0359] Instant Clue software was used for the generation and statistical analysis of some figures (Nolte et al., 2018). Heatmaps were generated with Morpheus (https://software.broadinstitute.org/morpheus).

Results

Mapping of the Head and Neck Cancer Interactome

[0360] To characterize the protein-protein interaction landscape of HNSCC, proteins were selected based on altered molecular pathways identified from the TCGA analysis of HNSCC tumors FIG. **11**A) (Cancer Genome Atlas, Network, 2015). Additional proteins were added based on genes with recurrent point mutations or a previously published association with HNSCC (Li et al., 2014; Martin et al., 2014; Molinolo et al., 2009; Stransky et al., 2011). In total, 33 protein baits were selected, of which 31 were found to be experimentally tractable (Key Resources Table 2).

Importantly, 99% of HNSCC patients harbor an alteration in one or more of these proteins (FIG. HA).

[0361] Referring to FIG. **11**A, the alteration frequencies from the HNSCC TCGA provisional dataset (n=530 patients) for the 31 experimentally tractable genes selected as AP-MS baits in this study are shown. Proteins analyzed in this study are listed, along with the percentage of patients with an alteration in that gene/protein. Each patient is represented by a grey box that is colored based on the occurrence and type of alteration(s) observed in that patient. Both the wild-type and mutant protein sequence(s) were analyzed for genes highlighted in gray. The genetic alteration types in the two cancer cell lines (CAL-33 and SCC-25) are also displayed.

Key Resources Table 2.

Reagent or Resource	Source	Identifier
Cell lines	ATCC	HEK293T, HET-1A
Cell lines	Thomas Carey (University of Michigan)	SCC-25
Cell lines	Gerard Milano (University of Nice, Nice, France)	CAL-33
NanoBiT G-protein dissociation assay	Dr. Asuka Inoue (Tohoku University, Japan)	NanoBiT plasmids (pCAGGS) include Gαi1-LgBiT, Gβ1-native, and SmBiT-Gγ2 (CAAX C68S mutant). Gαi-DREADD (pcDNA3.1)
Antibodies		
RSK1/2/3 antibody	Cell Signaling Technology	9355
ERK1/2	Cell Signaling Technology	4695
Phosphor-PAK1(S199/204)/ PAK2(S192/197)	Cell Signaling Technology	2605
PAK1	Cell Signaling Technology	2602
PAK2	Cell Signaling Technology	2608
pERK	Cell Signaling Technology	9106
FGFR3	OriGene	TA801078
Daple	Millipore EMD	ABS515
GAPDH	Cell Signaling Technology	2118
Secondary goat anti-rabbit HRP	Southern Biotech	4010-05
P-HER3-Y1197	Cell Signaling Technology	4561
HER3	Cell Signaling Technology	12708
Goat anti-mouse HRP	Southern Biotech	1010-05
Anti-B-tubulin	Abcam	ab6276
ERK	Cell Signaling Technology	9102
Deposited data		
Unprocessed peptide files	This paper	PRIDE ProteomeXchange: PXD019469
Raw data	This paper	PRIDE ProteomeXchange: PXD019469
Chemicals, Peptides, and Recombinant Proteins		
Tris	G-Biosciences	RC108
Acetonitrile, HPLC grade (CAN)	Thermo Fisher Scientific	A955-4
cOmplete protease inhibitor cocktail tablets mini, EDTA-free	Roche	11846 170 001
Dithiothreitol (DTT)	Sigma-Aldrich	43819
Formic acid (FA)	Thermo Fisher Scientific	28905
Iodoacetamide (IAA)	Acros Organic	122270250
Sequencing-grade modified trypsin	Promega	V5111
Benzonase	Sigma	E1014-25KU
Trifluoroacetic acid (TFA)	Thermo Fisher Scientific	28904
Urea	Sigma-Aldrich	U5378-1kg
Fetal bovine serum (FBS)	Gibco	A3160502
DMEM	Corning	MT10013CV
DMEM/F12	Corning	MT10092CV
Water, HPLC grade	Sigma-Aldrich	270733-4 L
Igepal (NP-40)	Sigma-Aldrich	I3021
Minimal Essential Media	Corning	10-009-CV
Opti-MEM	Thermo Fisher Scientific	31985062
BEGM ™ (Lonza)	Lonza	CC-3170
1% Penicillin-Streptomycin	Corning	MT30002CI

-continued

Key Resources Table 2.

Reagent or Resource	Source	Identifier
Paraformaldehyde, 4% solution in PBS	Thermo Scientific	MFCD00133991
PolyJet	SignaGen	SL 100688
Lipfectamine 3000	ThermoFisher Scientific	L30000008
Hydrocortisone	Sigma	H6909-10ML
Rapigest	Waters	186001861
3x Flag Peptide	Sigma	FA4799-4MG
Anti-Flag M2 Magnetic Beads	Sigma	M8823-5ML
Lipofectamine RNAiMAX	Thermo Fisher Scientific	100014472
siFGFR3	Sigma Aldrich	SIHK0780, SIHK0781, SIHK0782
Native coelenterazine	Biotium	10110-1
Pooled siControl	Dharmacon	D-001810-10-20
siDaple	Dharmacon	L-033364-01-0005
10 μM clozapine-N-oxide	Cayman Chemical	NC1044836
5 μM native coelenterazine	Biotium	10110-1
RPS6KA1 siRNA pool	OriGene	SR304161
Non-targeting control siRNA	Dharmacon	D-001810-10
Triton X-100	Thermo Scientific	9002-93-1
Software and Algorithms		
artMS	Bioconductor	https://www.bioconductor.org/packages/release/bioc/html/artMS.html
MSstats	Bioconductor	https://bioconductor.org/packages/release/bioc/html/MSstats/html
Skyline	MacCoss Lab	https://skyline.ms/project/home/begin.view?
The R Project for Statistical Computing	R Core Team, 2019. R: A language and environment for statistical computing. R Foundation for Statistical Computing, Vienna, Austria.	http://www.r-project.org/index.html
Morpheus	Broad Institute	https://software.broadinstitute.org/morpheus
MaxQuant (version 1.6.2.10)	Jurgen Cox Lab	https://www.maxquant.org/
InstantClue		http://www.instantclue.uni-koein.de/
CompPASS (version 0.0.0.9000)	Github	https://github.com/dnusinow/cRomppass/blob/master/R/comppass.R
SAINTexpress (version 3.6.1)	Sourceforge	https://sourceforge.net/projects/saint-apms/files/
Other		
1.9 μM C18 particles	Dr. Maisch	R119.aq.0001
Picotip column	New Objective	PF360-75-10-N-5
C18 Stage tips	Rainin	17014047
Orbitrap Elite mass spectrometer	Thermo Fisher Scientific	IQLAAEGAAPFADBMAZQ
Q-Exactive Plus mass spectrometer	Thermo Fisher Scientific	IQLAAEGAAPFALGMBDK

[0362] For those baits with recurrent point mutations, both the wild-type (WT) and mutant forms of the protein were tagged, purified, and analyzed. Each bait was expressed as a 3×FLAG-tagged protein under the control of a doxycycline-inducible promoter in biological triplicate in three separate cell lines (FIG. **11**B). Two HPV-negative HNSCC cell lines were selected (SCC-25 and CAL-33) that harbor many genetic alterations present in the HNSCC patient population (FIG. **11**A) and have previously been shown to have RNA profiles highly correlated with those of HNSCC patients (Spearman correlation=0.66 and 0.69 for CAL-33 and SCC-25, respectively) (Cancer Genome Atlas, Network, 2015; Li et al., 2014; Martin et al., 2014; Yu et al., 2019). Additionally, an immortalized non-tumorigenic cell line, HET-1A, was selected from a similar anatomical location (esophagus) for comparison. Then, a previously described AP-MS workflow was utilized to identify PPIs from these three cell lines (FIG. **11**B) (Jager et al., 2011). Importantly, a conservative and high-confidence protein-protein interaction map was elected for report by requiring PPIs to pass stringent criteria by two complementary PPI scoring algorithms; SAINTexpress and CompPASS (Key Resources Table 2) (Huttlin et al., 2015; Sowa et al., 2009; Teo et al., 2014). Using this workflow, a total of 771 high-confidence

PPIs (HC-PPIs) involving 654 proteins were identified (FIGS. **11**B and **12**A-B), for an average of 25 PPIs per bait gene.

[0363] Referring to FIG. **11**B, the experimental workflow in which each bait was expressed in biological triplicate in 3 cell lines and subjected to AP-MS analysis is shown.

[0364] It has been previously shown that alteration profiles in cancer are organized into molecular networks in which the interaction partners of frequently altered proteins incur a higher rate of alteration than a random selection of genes (Bouhaddou et al., 2019; Eckhardt et al., 2018; Hofree et al., 2013; Leiserson et al., 2015). Thus, whether the HNSCC HC-PPI set was enriched was tested for different types of alterations measured in the HNSCC TCGA cohort (Key Resources Table 2). The dataset was, indeed, highly enriched for preys with point mutations; however, this enrichment was not observed for alterations in mRNA expression or for chromosomal rearrangements (FIG. **11**C-E).

[0365] Referring to FIG. **11**C-E, a permutation test illustrating the frequency of CNVs (FIG. **11**C), mRNA alterations (FIG. **11**D), or mutations (FIG. **11**E) from randomly selected genes in the HNSCC TCGA data is shown. The white circle indicates the median of the random sampling, and the grey bar represents +/−1 standard deviation. The frequency of alterations found in the prey retrieved in this PPI dataset is indicated in the black circle.

[0366] Of the 771 HC-PPIs detected, the majority (85%) had not been previously reported in public PPI databases FIG. **11**F). This high percentage of novel interactions is consistent with other AP-MS publications (Hein et al., 2015; Huttlin et al., 2015, 2017) and likely reflects differences across cellular contexts, as nearly all systematic PPI analyses to date have been performed in HEK293T or HeLa cell lines (Hein et al., 2015; Huttlin et al., 2015, 2017). This proportion of novel interactions is also supported by the observation of a high degree of specificity in PPIs observed even within the cell lines in this study (FIG. **11**G), with only 24 PPIs being conserved as HC-PPIs across all cell lines analyzed (FIG. **11**H and FIG. **12**C). Notably, many well-studied cancer proteins are included in the novel interactions. For example, physical interactions were observed between the proto-oncoprotein MYC and each of two DNA repair proteins, PARP1 and TOP1. MYC has previously been shown to regulate PARP1 activity (Pyndiah et al., 2011), but this is the first evidence of a physical interaction between these two proteins. The MYC:PARP1 interaction is supported by previous studies reporting MYC:TOP1 (Kalkat et al., 2018) and PARPI:TOP1 interactions (Czubaty et al., 2005).

[0367] Referring to FIG. **11**F, the percentage of HC-PPIs identified in a panel of public PPI databases (CORUM, BioPlex 2.0, or BioGRID low throughput and multivalidated) is shown.

[0368] Referring to FIG. **11**G, a clustering analysis of all HC-PPIs (n=771) based on their PPI score, which is an average of the confidence scores reported from SAINTexpress and CompPASS score (see Key Resources Table 2 for details). A PPI score of 1.0 represents the highest confidence in a PPI.

[0369] Referring to FIG. **11**H, a Venn diagram illustrating the overlap in HC-PPIs among the 3 cell lines is shown. For this analysis, only those PPIs passing the HC-PPI filtering criteria by both SAINTexpress and CompPASS were classified as an HC-PPI within an individual cell line.

[0370] Referring to FIG. **12**A, a receiver operating characteristic (ROC) curve illustrating high recovery of gold standards (sensitivity) is shown.

[0371] Referring to FIG. **12**B, the number of HC-PPIs per cell line for each bait is shown.

[0372] Referring to FIG. **12**C, HC-PPIs that were detected across all cell lines (n=24) are shown. PPIs between preys from public databases having a high IAS score (see Key Resources Table 2) are also plotted as dotted lines (Zheng et al.).

[0373] Similarly, purification of tagged KEAP1 revealed an interaction with AJUBA, a scaffolding protein involved in the regulation of numerous cellular processes, including negative regulation of Wnt/β-catenin signaling (Haraguchi et al., 2008). Until recently, AJUBA was not associated with HNSCC; however, tumor genome analysis revealed it is inactivated in 7% of HPV-negative tumors (Cancer Genome Atlas, Network, 2015). The KEAPI:AJUBA interaction was further supported by the identification of a physical connection between KEAP1 and SQSTM1, a known AJUBA interactor (Copple et al., 2010; Fan et al., 2010; Feng and Longmore, 2005; Lau et al., 2010).

A Statistical Approach to Evaluate Cell-Type Specificity of Interactions

[0374] To identify interactions with relevance to cancer biology, PPIs were compared across cell lines and those that are shared among CAL-33 and SCC-25, the two HNSCC cancer cell lines, but absent in the HET-1A non-tumorigenic cell line were prioritized. However, a simple overlap analysis of the sets of HC-PPIs identified by each cell line does not faithfully represent whether a PPI is shared. For example, a PPI might erroneously appear to be specific for a single cell line when it passes the threshold for HC-PPIs in that cell line (i.e., a true positive) while falling slightly below the threshold (i.e., false negative) in a second. Accordingly, a method for calculating differential interaction scores (DIS) for each PPI was developed, with associated Bayesian false discovery rates (BFDR). This method is based on the SAINTexpress score (Teo et al., 2014), which reports on the probability of a PPI in a single cell line given the AP-MS data. Here, quantitative SAINTexpress probabilities were combined across the three cell lines to generate the DIS (Key Resources Table 2), allowing for the identification of PPIs that are enriched in either the two cancer cell lines or the non-cancerous cells.

[0375] Application of the DIS method to the HC-PPIs identified numerous interactions specific to HNSCC cells as well as those specific to the HET-1A non-tumorigenic background (FIG. **13**A-B). For example, the interaction profile for cyclin D1 was dramatically rewired between HNSCC and HET-1A (FIG. **13**C). Cyclin D1, encoded by the CCND1 gene, is one of the most commonly altered oncogenes in HNSCC, being amplified in 31% of HPV-negative HNSCC tumors (Cancer Genome Atlas, Network, 2015). It was observed that cyclin D1 interacts with the cyclin-dependent kinase inhibitors CDKN1A (p21) and CDKN1B (p27) in all three cell lines, but preferentially interacts with multiple cyclin-dependent kinases (CDKs) only in HNSCC cells. This interaction preference was not unexpected, as CCND1:CDK4/6 interactions are known to be essential for cell proliferation and, thus, can contribute to uncontrolled

cell cycle progression in cancer cells (Hamilton and Infante, 2016). A previously uncharacterized interaction of cyclin D1 was also found with components of the PI3K complex (PIK3CA, PIK3R1/2) exclusively in HET-1A cells. The specificity of this interaction, along with several others, was further supported by targeted proteomic analysis (FIG. **13**C and FIG. **14**). While cyclin D1 is canonically associated with the nucleus, it is also known to localize to the plasma membrane (Fusté et al., 2016). Conversely, while PI3K is often associated with cytoplasmic and membrane localization, it can also have nuclear localization (Davis et al., 2015). Without wishing to be bound by theory, the finding of a cyclin D1:PI3K kinase complex suggests that in HET-1A cells, either cyclin D1 or PI3K are present in a non-canonical subcellular location.

[0376] Referring to FIG. **13**A, an interactome of the union of all HC-PPIs detected across all cell lines is shown. Edges are colored based on their differential interaction score (DIS), with pink edges representing PPIs that are enriched in HNSCC (both SCC-25 and CAL-33) as compared to HET-1A cells, and teal lines representing PPIs that are depleted from HNSCC cell lines. IAS connections represent physical protein-protein association derived from in prior studies (Zheng et al.) (see Key Resources Table 2).

[0377] Referring to FIG. **13**B, for baits with |DIS|>0.5, the fraction of PPIs for that bait having HNSCC-enriched PPIs with DIS>0.5, or HNSCC-depleted DIS<−0.5 is shown.

[0378] Referring to FIG. **13**C, a CCND1 interactome is shown. Here the SAINTexpress score, used for calculation of the DIS, is displayed for each cell line within the prey node, ND indicates not detected.

[0379] Referring to FIG. **14**, an overview of PPI specificity as determined by DIS values for a selection of PPIs and targeted proteomic analysis for these PPIs measuring bait and prey protein abundances is shown. All prey quantification is normalized to the bait level level expression in the respective cell line. All p-values are the result of a 2-tailed unpaired t-test.

Identification of a Novel FGFR3:Daple Interaction that Regulates Gαi-Mediated Migratory Signaling

[0380] To uncover cancer-specific interactions, PPIs were ranked by their DIS (FIG. **13**D), focusing on those PPIs with greatest enrichment (DIS>0.5) or depletion (DIS<−0.5) in the HNSCC cell lines (FIG. **13**E). This analysis prioritized a novel interaction between FGFR3 and CCDC88C, which was strongly observed in both CAL-33 and SCC-25 cells but not in HET-1A (FIG. **15**A). FGFR3 is a receptor tyrosine kinase (RTK) that recognizes fibroblast growth factor (FGF) and mediates cellular proliferation, survival and differentiation. Meanwhile, CCDC88C, also known as Daple, is a 228-kDa scaffolding protein with roles in mediating both canonical and non-canonical Wnt signaling (Aznar et al., 2017, 2018; Ishida-Takagishi et al., 2012; Oshita et al., 2003). Daple regulates Wnt through its interaction with the protein Disheveled (Dvl) (Oshita et al., 2003), and it can also interact with RTKs, including EGFR and ERBB2 (HER2) (Aznar et al., 2018), leading to its phosphorylation and dissociation from Disheveled (Aznar et al., 2018). Upon this dissociation, Daple translocates from the cytoplasm to the plasma membrane where it functions as a guanine nucleotide exchange factor (GEF) to activate G proteins (Gαi) and promote Akt signaling, cell migration, and invasion (FIG. **15**B) (Aznar et al., 2015). The previously-described ERBB2:Daple interaction (Aznar et al., 2018) was detected in CAL-33 cells, as well as a novel FGFR3:Daple interaction, which was hypothesized to function to promote Gαi activation in an FGFR3-dependent manner.

[0381] Referring to FIG. **13**D, DIS for the entire interactome represented in panel A ranked by DIS is shown.

[0382] Referring to FIG. **13**E, a subnetwork of the interactome of the HNSCC-enriched and -depleted interactions is shown.

[0383] Referring to FIG. **15**A, a differential scoring analysis of the FGFR3 interactome highlights CCDC88C (Daple) as an HNSCC-specific interaction partner to both FGFR3 and ERBB2 (HER2).

[0384] Referring to FIG. **15**B, activation of RTKs can disrupt the interaction between Disheveled (Dvl) and Daple, allowing Daple to function as a GEF for Gαi. GTP binding causes dissociation of the G protein, leaving Gβγ subunits free to activate migratory signaling through Rac and PAK.

[0385] To test this idea, a split luciferase assay (Gαi NanoBiT) was used, in which signal is lost upon activation of Gαi and dissociation from Gβγ (FIG. **15**C and FIG. **16**A). As a control, an engineered Designer Receptor Exclusively Activated by Designer Drugs (DREADD) receptor was first transfected, and the resulting cell population stimulated with the DREADD ligand, clozapine-N-oxide (CNO). Robust Gαi activation and corresponding loss of luciferase signal was observed in both CAL-33 and HET-1A cell lines (FIG. **15**D).

[0386] Next, it was observed that in the CAL-33 cells, where the interaction between FGFR3 and Daple was detected, FGF stimulation can also induce Gαi activation; however, no such activation occurred in HET-1A cells (FIG. **15**E). Using siRNA knockdowns, it was found that Gαi activation in CAL-33 cells was dependent on both FGFR3 and Daple (FIG. **15**E-F and FIG. **16**B). Of note, FGF also rapidly induced ERK phosphorylation in both CAL-33 and HET-1A cells, in line with canonical RTK signaling (FIG. **16**C). It was also observed that FGF-mediated Gαi activation in CAL-33 cells results in downstream phosphorylation of PAK1/2, an event not observed in HET-1A (FIG. **15**G). PAK1/2 activity is known to promote cell migration and invasion and is associated with aggressive tumor behavior and poor patient prognosis in HNSCC (Park et al., 2015). Thus, whether FGF stimulation promoted cell migration was also evaluated. Indeed, a statistically significant increase equivalent to that of stimulation with serum was observed (FIG. **15**H and FIG. **15**I). Without wishing to be bound by theory, these results support a novel mechanism for regulating Gαi activity via FGFR3 and Daple, resulting in increased PAK1/2 activation and cell migration.

[0387] Referring to FIG. **15**C, NanoBiT biosensor measures Gαi activation through dissociation of the luciferase split between Gα and Gβγ. CNO mediates canonical GPCR signaling through the synthetic Gαi-coupled DREADD receptor. FGF mediates HNSCC-specific signaling through FGFR3 and Daple.

[0388] Referring to FIG. **15**D, CAL-33 (HNSCC) and HET-1A (normal) cells expressing the Gαi NanoBiT and DREADD receptor were stimulated with CNO (10 μM) and Gαi activity was measured by a drop in luminescence over 60 minutes (***P<0.001 when compared with the vehicle-treated group).

[0389] Referring to FIG. **15**E, similarly, luminescence was measured in CAL-33 and HET-1A cells transfected with Gαi NanoBiT and siRNA (control, FGFR3, or Daple) and stimu-

lated with FGF (1Ong/mL) (***P<0.001 when compared with the vehicle-treated group).

[0390] Referring to FIG. **15**F, immunoblot analysis of CAL-33 subject to siRNA knockdown is shown.

[0391] Referring to FIG. **15**G, PAK1/2 autophosphorylation was measured by immunoblot analysis over a time course of FGF stimulation (0, 5, 10, 30, 60 minutes) in CAL-33 and HET-1A cells.

[0392] Referring to FIG. **15**H, a vertical scratch was introduced to fibronectin-plated CAL-33 cells. Images were taken at 0 and 24 hours after FGF stimulation (scale bar=200 μm). (I) Quantification of replicate scratch closure assays from panel H (*P<0.05 when compared with the vehicle-treated group).

[0393] Referring to FIG. **16**A, luminescence was measured over 60 minutes in mock transfected CAL-33 cells stimulated with FGF (10 ng/mL).

[0394] Referring to FIG. **16**B, as shown in FIG. **15**E, luminescence was measured in CAL-33 cells transfected with Gαi NanoBiT, and siRNA (control, FGFR3, or Daple) and stimulated with FGF (10 ng/mL). Additionally, luminescence was measured in CAL-33 cells transfected with Gαi NanoBiT, Gαi-DREADD, and siRNA (control, FGFR3, or Daple) and stimulated with CNO (10 μM). HET-1A cells were transfected with Gαi NanoBiT alone or with the additional Gαi-DREADD and stimulated with FGF or CNO, respectively (FIG. **15**D and FIG. **15**E). Luminescence was measured over 60 minutes with a decrease in luminescent signal demonstrating Gαi activation (***P<0.001 when compared with the vehicle-treated group).

[0395] Referring to FIG. **16**C, ERK phosphorylation over a time course was measured by immunoblotting in CAL-33 and HET-1A cells stimulated with FGF (10 ng/mL).

Quantitative Analysis of the Effect of Mutations on the PPI Landscape

[0396] In addition to comparing the specificity of interactions across tumor and non-tumor cell lines, AP-MS data for both WT and mutant proteins was compared to identify mutant-regulated interactions. Mutations selected for this analysis were those found to be highly recurrent in HNSCC tumor genomes, considering recurrent point mutations and single amino acid deletions (Key Resources Table 2). A label-free quantitative proteomics approach was used to quantify the differential prey abundances between WT and mutant baits analyzed within the same cell line. As a negative control experiment, the correlation of prey abundances for two very similar mutations on NFE2L2, E79K, and E79Q were first examined. Very high correlation in prey abundance (r=0.96) was observed for these similar mutant isoforms (FIG. **17**A). Good correlation was also seen for a second control experiment comparing R248W and R273H mutations in TP53 (r=0.83, FIG. **17**A). Without wishing to be bound by theory, these results suggest not only a high degree of biological similarity between these individual point mutations on the same protein, but also a high degree of technical accuracy in our quantification of PPIs.

[0397] Referring to FIG. **17**A, quantification of PPI regulation of two distinct mutations on NFE2L2 (left) or TP53 (right), respectively, is shown.

[0398] PPIs were quantitatively analyzed for missense mutations on six different proteins in total (FIG. **17**B; note PIK3CA is displayed in FIG. **18**). This analysis identified several previously described mutation-dependent PPIs including those involving NFE2L2, a transcriptional activator that regulates genes involved in the oxidative stress response. Under normal conditions, protein levels of NRF2, which is encoded by NFE2L2, are maintained at low levels by its association with the KEAP1 protein, which promotes its proteasome-mediated degradation. Previous work has shown that the interaction between NRF2 and KEAP1 is lost in the context of NFE2L2 E79K/Q mutations (Shibata et al., 2008), leading to increased NRF2 and promotion of carcinogenesis (Taguchi and Yamamoto, 2017). Consistent with this work, it was observed the interaction between NRF2 and KEAP1 is the most dependent on NFE2L2 mutations (FIG. **17**B).

[0399] Referring to FIG. **17**B, quantification of HC-PPIs for all mutants analyzed, with the exception of PIK3CA mutants, is shown. Each dot represents an individual PPI. A selection of interactions that are highly differential between WT and mutant are annotated, with the line color representing the cell line from which that PPI was quantified.

[0400] An unexpected finding was that the HRAS G12D mutant caused a general increase in the abundance of its interaction partners. Mutant HRAS is known to have increased plasma membrane localization, and, accordingly, it was found that the gained interactions included several proteins related to hemidesmosome assembly, including PLEC, LAMA3, LAMB3, and LAMC2. In particular, LAMA3 (laminin u3), LAMB3 (laminin 03), and LAMC2 (laminin γ2) are extracellular matrix proteins that function in epidermal adhesion and together form the laminin 332 heterotrimeric complex. The laminin 332 complex is highly expressed in many squamous cell carcinomas, including HNSCC where it is associated with increased tumor invasion and metastasis, and, consequently, worse prognosis (Marinkovich, 2007). Analysis of HRAS mutation and genetic alterations (mutation and CNVs) in the laminin 332 complex in HNSCC tumors revealed a statistically significant mutual exclusivity (q=0.042), suggesting functional redundancy. While this interaction between intracellular HRAS and an extracellular complex is unexpected, laminin 332 expression is known to cause clustering of RTKs and subsequent activation of Ras pathways (Tsuruta et al., 2008). It may be that the observed HRAS:laminin 332 interaction is tethered by MET, an RTK which is also find to be 2.9-fold increase in interaction with mutant HRAS.

[0401] Some of the most consistently regulated PPIs in the entire dataset were interactions of MAPK1 with RPS6KA1 and RPS6KA3, which were lost in the context of E322K mutation across all six cell lines examined (FIG. **17**D). MAPK1 encodes ERK2, a protein kinase functioning directly upstream of RPS6KA1/3 (RSK1/2) in the Ras/Raf/MEK/ERK pathway that is activated in many types of cancer. The MAPK1 E322K mutation results in constitutive activation of this kinase (Arvind et al., 2005), which is associated with anchorage-independent growth (Mahalingam et al., 2008) and resistance to Raf/MEK inhibitors (Goetz et al., 2014). Structural analysis indicates that E322 coordinates a network of electrostatic interactions important for protein binding, and that mutation of this residue to a positively charged lysine destabilizes binding with RPS6KA1/3 (Alexa et al., 2015; Brenan et al., 2016; Mahalingam et al., 2008; Taylor et al., 2019). The functional consequences of the MAPK1:RPS6KA1 PPI were further tested by performing siRNA knockdown of RPS6KA1 in a cellular background of either MAPK1 WT/WT (CAL-33

cells) or MAPK1 WT/E322K (HSC-6) alleles (FIG. **17**D). It was observed that in the WT/WT background, but not WT/E322K, knockdown of RPSK6A1 caused a dramatic loss in cell viability, indicating a reliance on this signaling pathway for cell survival in MAPK1 WT/WT cells. While the exact mechanism for this difference in cell viability is unclear, it may be that in the context of a WT/E322K heterozygosity, the presence of E322K can function in a dominant-negative manner, rewiring cellular signaling to maintain survival independent of RPS6KA1.

[0402] Referring to FIG. **17**C, regulation of the MAPK1-interacting protein RPS6KA1 (RSK1) across a panel of six cell lines is shown.

[0403] Referring to FIG. **17**D, immunoblot validation and cell viability upon siRNA knockdown of RPS6KA1 in CAL-33 cells, which endogenously harbor homozygous WT MAPK1, or the HSC-6 cell line, which is MAPK1 heterozygous (WT/E322K), are shown. MAPK1/3 (ERK1/2) total protein immunoblot is shown as a control (***P<0.001 when compared with the non-targeting control (NTC) siRNA).

Quantitative Analysis of the Mutant PIK3CA Interactome

[0404] PIK3CA encodes p110alpha (p110α), the catalytic subunit of phosphatidylinositol 3-kinase (PI3K). PI3K is a potent mediator of cellular signaling, interacting with both intracellular small GTPases (e.g., RAS proteins) as well as receptor kinases (e.g., EGFR) to regulate downstream signaling via both the MAPK/ERK pathway and the Akt/mTOR pathway (FIG. **19**A). Here, 16 different PIK3CA mutations observed in HNSCC patients were selected, and the effects of these mutations were quantitatively assessed on p110α interaction partners (FIG. **19**B). These mutations were not limited to a particular region of the p110α structure but resided over many different surfaces (FIG. **19**C). Examining the protein-protein interaction profiles of WT PIK3CA and the corresponding mutants in SCC-25 cells revealed a cluster of mutants (M1043V, E453K, and K111N) for which the same set of preys had increased interaction, particularly for DAP, death-associated protein 1 (FIG. **19**D). Interestingly, a downstream component of PI3K signaling, mTOR, has been shown to phosphorylate DAP, leading to autophagy suppression (Koren et al., 2010a, 2010b). The strengthening of the DAP interaction may result in increased DAP phosphorylation and promotion of cell survival in the context of these oncogenic mutations. This same set of PIK3CA mutants exhibited a reduction of interactions with a second group of preys (FIG. **19**D), including SH3GLB1 (Endophilin B1), which is known to interact with other lipid kinases, such as Class-III PIK3C3, to promote autophagy (Takahashi et al., 2007). The loss of SH3GLB1 interaction with these PIK3CA mutants may serve to reduce autophagy-promoting signals.

[0405] Referring to FIG. **19**A, an overview of the PIK3CA signaling pathway, which is often stimulated by RTKs that interact with PIK3CA to stimulate RAS/Raf-mediated or Akt/mTORC1-mediated downstream signaling is shown.

[0406] Referring to FIG. **19**B, analyzed PIK3CA mutants and their frequency in HNSCC tumors from TCGA is shown. Asterisk (*) denotes mutations annotated as oncogenic in OncoKB (Chakravarty et al., 2017). Graph bars corresponding to each mutation were color-coded to indicate their localization within the p110α domain (as indicated in the legend in top right corner).

[0407] Referring to FIG. **19**C, selected PIK3CA mutations were mapped on the structure of PI3K (PDB: 4L23) (Zhao et al., 2014) by highlighting the mutated residues as red spheres.

[0408] Referring to FIG. **19**D, quantification of PPIs for all HC-PPIs detected in the SCC-25 cell lines is shown (all cell lines displayed in FIG. **18**).

[0409] Perhaps the most striking observation from the mutant PIK3CA interactome was the very high similarity in interaction patterns of five of the PIK3CA mutants (E110DEL, V344G, E542K, E545G, and E545K) (FIG. **19**D), driven by a strong increase in interaction of these mutants with three proteins, ERBB3 (HER3), GAB1, and IRS1. These prey proteins all share the property of multiple YxxM motifs, representing consensus binding sites for the two SH2 domains (nSH2 and cSH2) located in the PI3K p85 regulatory subunit connected by the iSH2 coiled coil domain (Songyang et al., 1994). Engagement of phosphorylated YxxM motifs with the SH2 domains of p85 is essential for PI3K signaling by releasing p110α autoinhibition and mediating recruitment of PI3K to the plasma membrane (Dornan and Burke, 2018). The helical domain mutants (E545K, E545G, E542K) disrupt the interaction of p110α with its auto-inhibitory p85 subunits, making the p85 nSH2 domain more readily available for interaction with phosphorylated YxxM motifs. Outside of this primary cluster of mutations, other mutation sites (e.g., K111E and G1007R) were also observed with a strong increase in HER3 binding. In these cases also, mutations are expected to compromise the p85-imposed inhibition of the p110α catalytic module, either by disruption of the ABD domain relative to the inhibitory iSH2 module of p85 (K111E, FIG. **19**E), or by disruption of a hydrophobic cluster coordinating amino acids from multiple p110α domains (G1007R, FIG. **19**F).

[0410] Referring to FIG. **19**E, a cartoon representation of a zoomed-in view of PI3K illustrating a salt bridge formed between K11 and E81 (PDB: 4L23) is shown.

[0411] Referring to FIG. **19**E, a zoomed-in view depicting interactions made by G1007 in PI3K (PDB: 4L23) is shown.

[0412] These results led to the hypothesis that the differential binding observed across PIK3CA mutants may correlate with HER3 activation. Indeed, a strong correlation between the association of individual PIK3CA mutants with HER3 was observed, as measured by AP-MS, and HER3 activation, as measured by immunoblotting of Y1197 phosphorylation (r=0.75, FIG. **19**G and FIG. **20**B). Activation of HER3 has previously been recognized as important in HNSCC, and clinical trials of inhibitors of HER3 signaling have been completed or are underway using a variety of agents, including the monoclonal antibody CDX3379 (Duvvuri et al., 2019). It was thus hypothesized that an HER3 inhibitor might prove particularly effective in the context of PIK3CA helical domain mutants, which show increased binding to HER3 and correlate with increased phosphorylation of HER3, in comparison to other mutants (FIG. **19**D-G). To test this hypothesis, isogenic CAL-27 cell lines overexpressing either WT, E542K, E545K, or H1047R mutant isoforms of PIK3CA were generated, and injected into the flanks of athymic nude mice (Key Resources Table 2). Importantly, CAL-27 cells were used, as they are diploid for WT PIK3CA. Mice were then treated with either saline (control) or the HER3 inhibitor CDX3379 over the course of 15 days, and tumor size was monitored (FIG. **21**A-C). Tumors harboring the H1047R mutant, which did not bind

highly to or increase phosphorylation of HER3, were resistant to CDX3379. In contrast, CDX3379 treatment of xenograft models harboring the helical domain mutants, E542K and E545K, resulted in almost complete inhibition of tumor growth. This finding was unanticipated as all PIK3CA mutations have been thought to confer resistance to HER3 inhibition.

[0413] Referring to FIG. **19**G, a correlation of Log 2 HER3 interaction levels from AP-MS experiments and Log 2 HER3 Y1197 phosphorylation levels from immunoblot analysis is shown. All values are normalized by FLAG-PIK3CA levels in their respective experiments.

[0414] Referring to FIG. **20**A, quantification of PPIs for all HC-PPIs detected in all cell lines is shown.

[0415] Referring to FIG. **20**B, an immunoblot of total and phosphorylated HER3 (Y1197), total HER3, Actin (loading control), and FLAG peptide in SCC-25 cells expressing a panel of FLAG-tagged PIK3CA mutants is shown.

[0416] Referring to FIG. **20**C, a representative immunoblot of phosphorylated Akt (T308), total Akt, and GAPDH (loading control), in CAL-27 cells expressing WT, E545K, or H1047R PIK3CA is shown. Cells were treated in vitro with either DMSO or the CDX3379 (1 μg/ml, 1 hr).

[0417] Referring to FIG. **21**A-C, CAL-27 cells expressing inducible PIK3CA variants were transplanted into athymic nude mice. Mice were fed with doxycycline to induce PIK3CA expression. When tumor volumes reached approximately 100 mm^3, mice were treated with vehicle (PBS) or CDX3379 (10 mg/kg, twice a week) for approximately 15 days, as indicated. Shown are (FIG. **21**A) tumor growth curves, (FIG. **21**B) representative tumor images, and (FIG. **21**C) last day tumor volume (****P<0.0001 when compared with the control-treated group).

[0418] To further investigate the mechanisms regulating these in vivo phenotypes, the levels of phosphorylated Akt (pAkt), a downstream mediator of PI3K signaling, were assessed in CAL-27 cells. For mutants in which CDX3379 treatment inhibited tumor growth in vivo (E542K and E545K), in vitro treatment resulted in significant downregulation of pAkt levels, whereas no such decrease was observed for the CDX3379-resistant H1047R-expressing cells (FIG. **21**D and FIG. **20**C).

[0419] Referring to FIG. **21**D, quantification of immunoblot analysis of signaling events in the same CAL-27 cells in vitro is shown. PIK3CA variant expression was induced by doxycycline (1 μg/ml in culture medium), cells were treated with CDX3379 (1 μg/ml, 1 hr), and lysates were analyzed by immunoblotting as indicated. Densitometry analysis of western blots was performed using ImageJ. Data are represented as mean±SEM, n=3 in each group. (*P<0.05 when compared with the control-treated group).

Discussion

[0420] In this study, the physical landscape of protein-protein interactions targeting genes genetically linked to HNSCC were examined, revealing hundreds of novel PPIs. It was observed that these interactions are highly specific to the cell line of study, with PPIs shared between cancer cell lines being no more similar than those shared between these cancer cell lines and the non-tumorigenic HET-1A cells. In support of previous observations (Huttlin et al., 2020), these results suggest the exciting premise that there remains a vast network of PPIs left to discover beyond the thousands annotated from HEK293T and HeLa cells (Hein et al., 2015; Huttlin et al., 2015, 2017). It is anticipated that developments in high-throughput protein complex determination, such as co-elution (Salas et al., 2020), proximity-labeling (Lobingier et al., 2017; Samavarchi-Tehrani et al., 2020), and cross-linking MS (Klykov et al., 2018), will enable the rapid advancement of systematic PPI mapping in a diverse array of cancer cell contexts.

[0421] An important goal of cancer therapy is to identify drug targets that are applicable across many patients and that achieve high specificity for cancer cells among a heterogeneous tumor cell population. In the context of PPIs, this goal requires moving beyond simply cataloging protein-protein interactions towards robust comparative analysis of PPIs across cellular contexts. For this purpose, a differential interaction score (DIS) was created, and the value of this DIS to statistically compare PPIs across contexts was demonstrated, which will aid in not only understanding the underlying biology behind HNSCC, but other cancers and disease in general.

A Novel FGFR3:Daple Interaction Promotes Cell Motility

[0422] It is becoming increasingly evident that Daple has a greater diversity of cellular roles than initially appreciated. Early work established its role in mediating both canonical and non-canonical Wnt signaling via the Frizzled receptor (Ara et al., 2016; Aznar et al., 2017; Ishida-Takagishi et al., 2012; Oshita et al., 2003). Further studies have shown Daple is activated by RTK (Aznar et al., 2018) and can function as a non-receptor GEF capable of activating Gαi and Rac1 (Aznar et al., 2015). The findings disclosed herein build upon these findings by demonstrating that FGF stimulation can activate Gαi in a Daple- and FGFR3-dependent manner, which results in activation of PAK1/2 kinases and cell motility. This work also suggests that the previously undescribed connection between FGFR3 and Daple mediates Gαi and PAK1/2 activation; no such activation was observed in HET-1A cells which lack this interaction.

[0423] Importantly, PAK1 expression is highly correlated with aggressive tumor behavior and poor patient prognosis in HNSCC (Park et al., 2015; Parvathy et al., 2016). The finding that FGFR3 can mediate HNSCC-specific activation of PAK1/2 becomes increasingly important as FGFR inhibitors progress towards the clinic. Phase II clinical trials with rogaratinib, an FGFR inhibitor, are underway for HNSCC patients with FGFR1/2/3 mRNA overexpression (NCT03088059), after phase I trials demonstrated a 67% objective response rate for solid tumors with FGFR mRNA overexpression (Schuler et al., 2019). Additionally, a complete response was observed in a metastatic HNSCC tumor with multiple FGFR amplifications, including FGFR3, when treated with a pan-FGFR inhibitor (Dumbrava et al., 2018). Further work may determine if the FGFR3:Daple interaction results in frequent coupling of FGFR and PAK1/2 activity in HNSCC patients and if other cancer types exploit this novel signaling mechanism. More direct studies are necessary to determine the extent to which FGFR and PAK1/2 activity contribute to clinical outcomes, as PAK1/2 activity could serve as an additional biomarker of patients benefiting from FGFR targeted therapy.

Tumor Response to HER3 Inhibition is Dependent Upon PIK3CA Mutation Status

[0424] These results also highlight that the oncogenic mechanisms of individual PIK3CA mutations can be influ-

enced by differences in PPI, and these differences can be exploited for therapeutic benefit. For example, helical domain mutations activate PI3K primarily by compromising the interactions between the p85 regulatory module and the p110α catalytic module. It was found that these mutants show increased binding to HER3, increased HER3 phosphorylation, and dependence on HER3 signaling to drive tumorigenesis (FIG. **21**E). In contrast, the H1047R mutant is oncogenic independently of HER3 signaling. These features of PI3K mutants seemingly contradict previous studies showing that addition of the phosphorylated YXXM motif-containing peptides increases in vitro catalytic activity of the H1047H mutant but not the helical domain mutants (Carson et al., 2008). It is postulated that phosphorylated RTK tails are necessary not for activation of the helical domain PI3K mutants, but for their recruitment to the plasma membrane where they need to interact with RasGTP for full activation (Zhao and Vogt, 2008). This strong dependence renders cells with such mutations sensitive to HER3 inhibition. These data also show that proteins with high density of YxxM motifs, such as HER3 and IRS1/2, are particularly efficient in synergizing with the PI3K helical domain mutants in which the two SH2 domains contained within the p85 regulatory module are more available. A number of other PI3K mutants that share HER3 binding features with the helical domain mutants were also identified, and it was predicted that their oncogenic potential is also HER3-dependent (FIG. **21**E). In contrast, H1047R mutation increases PI3K membrane a localization (Burke et al., 2012; Carson et al., 2008; Gkeka et al., 2014; Liu et al., 2014) and confers RasGTP independence (Zhao and Vogt, 2008). While full activation of the H1047R PIK3CA mutation still requires binding of phosphorylated RTKs, the Ras independence and innate membrane localization of this mutation enables HER3-independent tumor growth and the observed resistance of this mutant to HER3-targeted therapy.

[0425] Referring to FIG. **21**E, the PI3K complex is maintained in an inactive state via auto-inhibition of the p110α (PIK3CA) catalytic subunit by the p85 regulatory subunits. Mutations in p110α can promote activation of this complex by different mechanisms. Helical domain mutants relieve auto-inhibition by the p85 subunits, which in turn seek interactions with YxxM motifs, showing preference for proteins with high YxxM density, such as HER3 and IRS1/2. In contrast, the localization of the H1047R mutation blocks auto-inhibition of the kinase domain by one p85 regulatory subunit; thus, interaction with only a single YxxM motif by the remaining p85 subunit is required for PI3K activation.

[0426] Clinical inhibition of HER3 in HNSCC patients is currently being pursued in phase II clinical trials with the monoclonal antibody CDX3379 (NCT03254927). This drug locks the HER3 extracellular domain in an inactive configuration (Lee et al., 2015) and prevents not only dimerization with co-activating RTKs (e.g., HER2) but also activation of HER3 by neuregulins (e.g., NRG1). These properties make HER3 a particularly promising target, as NRG1 is expressed at higher levels in HNSCC than in any other tumor type (Alvarado et al., 2017). The results presented here further suggest that HER3 inhibitors present an opportunity to potently target specific PIK3CA mutant tumors, a utility that had not been evaluated previously. This is important, as PIK3CA is one of the most commonly mutated oncogenes in HNSCC (Cancer Genome Atlas, Network, 2015), yet targeting of PIK3CA in the clinic has been limited by toxicity (Janku et al., 2018), likely due to its pleiotropic roles in cancer and maintenance of normal cell states. In light of these findings, patient pre-selection, such as exclusion of PIK3CA H1047R mutation carriers and inclusion of those harboring helical domain mutants, may be a valuable consideration as future phases of clinical trials proceed.

[0427] In summary, this study outlines a framework for elucidating genetic complexity through multidimensional maps of cancer cell biology and demonstrates that such maps can reveal novel mechanisms of cancer pathogenesis, instructs the selection of therapeutic targets, and informs which point mutations in the tumor are most likely to respond to treatment. As such, it is anticipated that the generation and incorporation of cancer-specific physical and functional networks may represent a critical component to interpret and predict cancer biology and its clinical outcomes.

REFERENCES

[0428] Aihara, T., Fujiwara, Y., Ooka, M., Sakita, I., Tamaki, Y., and Monden, M. (1999). Mammaglobin B as a novel marker for detection of breast cancer micrometastases in axillary lymph nodes by reverse transcription-polymerase chain reaction. Breast Cancer Res. Treat. 58, 137-140.

[0429] Alessi, D. R., Andjelkovic, M., Caudwell, B., Cron, P., Morrice, N., Cohen, P., and Hemmings, B. A. (1996). Mechanism of activation of protein kinase B by insulin and IGF-1. The EMBO Journal 15, 6541-6551.

[0430] Alessi, D. R., James, S. R., Downes, C. P., Holmes, A. B., Gaffney, P. R., Reese, C. B., and Cohen, P. (1997). Characterization of a 3-phosphoinositide-dependent protein kinase which phosphorylates and activates protein kinase Balpha. Curr. Biol. 7, 261-269.

[0431] Alessi, D. R., Sakamoto, K., and Bayascas, J. R. (2006). LKB1-dependent signaling pathways. Annu. Rev. Biochem. 75, 137-163.

[0432] Allen, P. B., Ouimet, C. C., and Greengard, P. (1997). Spinophilin, a novel protein phosphatase 1 binding protein localized to dendritic spines. Proc. Natl. Acad. Sci. U.S.A 94, 9956-9961.

[0433] Altiok, S., Batt, D., Altiok, N., Papautsky, A., Downward, J., Roberts, T. M., and Avraham, H. (1999). Heregulin induces phosphorylation of BRCA1 through phosphatidylinositol 3-Kinase/AKT in breast cancer cells. J. Biol. Chem. 274, 32274-32278.

[0434] Alva, V., and Lupas, A. N. (2016). The TULIP superfamily of eukaryotic lipid-binding proteins as a mediator of lipid sensing and transport. Biochim. Biophys. Acta 1861, 913-923.

[0435] American Cancer Society (2019). Cancer Facts & FIGS. **2019**. American Cancer Society.

[0436] Anantha, R. W., Simhadri, S., Foo, T. K., Miao, S., Liu, J., Shen, Z., Ganesan, S., and Xia, B. (2017). Functional and mutational landscapes of BRCA1 for homology-directed repair and therapy resistance. Elife 6.

[0437] Anp, P. H. V. R. M. C., Viale, P. H., R N, M S, CNS, and ANP (2020). The American Cancer Society's Facts & Figures: 2020 Edition. Journal of the Advanced Practitioner in Oncology 11.

[0438] Apostolou, P., and Papasotiriou, I. (2017). Current perspectives on CHEK2 mutations in breast cancer. Breast Cancer 9, 331-335.

[0439] Arizti, P., Fang, L., Park, I., Yin, Y., Solomon, E., Ouchi, T., Aaronson, S. A., and Lee, S. W. (2000). Tumor suppressor p53 is required to modulate BRCA1 expression. Mol. Cell. Biol. 20, 7450-7459.

[0440] Aylon, Y., and Oren, M. (2011). New plays in the p53 theater. Curr. Opin. Genet. Dev. 21, 86-92.

[0441] Baas, A. F., Boudeau, J., Sapkota, G. P., Smit, L., Medema, R., Morrice, N. A., Alessi, D. R., and Clevers, H. C. (2003). Activation of the tumour suppressor kinase LKB1 by the STE20-like pseudokinase STRAD. EMBO J. 22, 3062-3072.

[0442] Baas, A. F., Kuipers, J., van der Wel, N. N., Batlle, E., Koerten, H. K., Peters, P. J., and Clevers, H. C. (2004). Complete polarization of single intestinal epithelial cells upon activation of LKB1 by STRAD. Cell 116, 457-466.

[0443] Barker, A. D., Sigman, C. C., Kelloff, G. J., Hylton, N. M., Berry, D. A., and Esserman, L. J. (2009). I-SPY 2: An Adaptive Breast Cancer Trial Design in the Setting of Neoadjuvant Chemotherapy. Clinical Pharmacology & Therapeutics 86, 97-100.

[0444] Beamer, L. J. (2003). Structure of human BPI (bactericidal/permeability-increasing protein) and implications for related proteins. Biochem. Soc. Trans. 31, 791-794.

[0445] Beca, F., Kensler, K., Glass, B., Schnitt, S. J., Tamimi, R. M., and Beck, A. H. (2017). EZH2 protein expression in normal breast epithelium and risk of breast cancer: results from the Nurses' Health Studies. Breast Cancer Research 19.

[0446] Beckta, J. M., Dever, S. M., Gnawali, N., Khalil, A., Sule, A., Golding, S. E., Rosenberg, E., Narayanan, A., KehnHall, K., Xu, B., et al. (2015). Mutation of the BRCA1 S Q-cluster results in aberrant mitosis, reduced homologous recombination, and a compensatory increase in non-homologous end joining. Oncotarget 6.

[0447] Bellone, S., Tassi, R., Betti, M., English, D., Cocco, E., Gasparrini, S., Bortolomai, I., Black, J. D., Todeschini, P., Romani, C., et al. (2013). Mammaglobin B (SCGB2A1) is a novel tumour antigen highly differentially expressed in all major histological types of ovarian cancer: implications for ovarian cancer immunotherapy. British Journal of Cancer 109, 462-471.

[0448] Bensimon, A., Schmidt, A., Ziv, Y., Elkon, R., Wang, S.-Y., Chen, D. J., Aebersold, R., and Shiloh, Y. (2010). ATM-Dependent and -Independent Dynamics of the Nuclear Phosphoproteome After DNA Damage. Science Signaling 3, rs3-rs3.

[0449] Bhargava, R., Sandhu, M., Muk, S., Lee, G., Vaidehi, N., and Stark, J. M. (2018). C-NHEJ without indels is robust and requires synergistic function of distinct XLF domains. Nat. Commun. 9, 2484.

[0450] Bingle, L., and Bingle, C. D. (2011). Distribution of human PLUNC/BPI fold-containing (BPIF) proteins. Biochem. Soc. Trans. 39, 1023-1027.

[0451] Bouhaddou, M., Eckhardt, M., Chi Naing, Z. Z., Kim, M., Ideker, T., and Krogan, N. J. (2019). Mapping the protein-protein and genetic interactions of cancer to guide precision medicine. Curr. Opin. Genet. Dev. 54, 110-117.

[0452] Breuleux, M., Klopfenstein, M., Stephan, C., Doughty, C. A., Barys, L., Maira, S.-M., Kwiatkowski, D., and Lane, H. A. (2009). Increased AKT S473 phosphorylation after mTORC1 inhibition is rictor dependent and does not predict tumor cell response to PI3K/mTOR inhibition. Mol. Cancer Ther. 8, 742-753.

[0453] Brieher, W. M., and Yap, A. S. (2013). Cadherin junctions and their cytoskeleton(s). Current Opinion in Cell Biology 25, 39-46.

[0454] Britto, C. J., and Cohn, L. (2015). Bactericidal/Permeability-Increasing Protein Fold-Containing Family Member A1 in Airway Host Protection and Respiratory Disease. Am. J. Respir. Cell Mol. Biol. 52, 525-534.

[0455] Brognard, J., Sierecki, E., Gao, T., and Newton, A. C. (2007). PHLPP and a second isoform, PHLPP2, differentially attenuate the amplitude of Akt signaling by regulating distinct Akt isoforms. Mol. Cell 25, 917-931.

[0456] Brugge, J., Hung, M.-C., and Mills, G. B. (2007). A new mutational AKTivation in the PI3K pathway. Cancer Cell 12, 104-107.

[0457] Buller, R. E., Lallas, T. A., Shahin, M. S., Sood, A. K., Hatterman-Zogg, M., Anderson, B., Sorosky, J. I., and Kirby, P. A. (2001). The p53 mutational spectrum associated with BRCA1 mutant ovarian cancer. Clin. Cancer Res. 7, 831-838.

[0458] Burke, J. E., Perisic, O., Masson, G. R., Vadas, O., and Williams, R. L. (2012). Oncogenic mutations mimic and enhance dynamic events in the natural activation of phosphoinositide 3-kinase p110α (PIK3CA). Proc. Natl. Acad. Sci. U.S.A 109, 15259-15264.

[0459] Cairns, R. A., Harris, I. S., and Mak, T. W. (2011). Regulation of cancer cell metabolism. Nat. Rev. Cancer 11, 85-95.

[0460] Cancer Genome Atlas, Network (2012). Comprehensive molecular portraits of human breast tumours. Nature A 490, 61-70.

[0461] Canel, M., Serrels, A., Frame, M. C., and Brunton, V. G. (2013). E-cadherin-integrin crosstalk in cancer invasion and metastasis. Journal of Cell Science 126, 393-401.

[0462] Cantley, L. C., and Neel, B. G. (1999). New insights into tumor suppression: PTEN suppresses tumor formation by restraining the phosphoinositide 3-kinase/AKT pathway. Proc. Natl. Acad. Sci. U.S.A 96, 4240-4245.

[0463] Carpten, J. D., Faber, A. L., Horn, C., Donoho, G. P., Briggs, S. L., Robbins, C. M., Hostetter, G., Boguslawski, S., Moses, T. Y., Savage, S., et al. (2007). A transforming mutation in the pleckstrin homology domain of AKT1 in cancer. Nature 448, 439-444.

[0464] Chen, Z., and Coppé, J.-P. (2012). Method and System for Building and Using a Centralized and Harmonized Relational Database.

[0465] Chen, C.-C., Juan, C.-W., Chen, K.-Y., Chang, Y.-C., Lee, J.-C., and Chang, M.-C. (2017). Upregulation of RPA2 promotes NF-κB activation in breast cancer by relieving the antagonistic function of menin on NF-κB-regulated transcription. Carcinogenesis 38, 196-206.

[0466] Chen, H., Kovar, J., Sissons, S., Cox, K., Matter, W., Chadwell, F., Luan, P., Vlahos, C. J., Schutz-Geschwender, A., and Olive, D. M. (2005). A cell-based immunocytochemical assay for monitoring kinase signaling pathways and drug efficacy. Anal. Biochem. 338, 136-142.

[0467] Chen, P., Guo, X., Zhou, H., Zhang, W., Zeng, Z., Liao, Q., Li, X., Xiang, B., Yang, J., Ma, J., et al. (2013). SPLUNC1 regulates cell progression and apoptosis

through the miR-141-PTEN/p27 pathway, but is hindered by LMP1. PLoS One 8, e56929.

[0468] Chien, A. J., Tripathy, D., Albain, K. S., Symmans, W. F., Rugo, H. S., Melisko, M. E., Wallace, A. M., Schwab, R., Helsten, T., Forero-Torres, A., et al. (2020). MK-2206 and Standard Neoadjuvant Chemotherapy Improves Response in Patients With Human Epidermal Growth Factor Receptor 2-Positive and/or Hormone Receptor Negative Breast Cancers in the I-SPY 2 Trial. J. Clin. Oncol. 38, 1059-1069.

[0469] Cho, A., Shim, J. E., Kim, E., Supek, F., Lehner, B., and Lee, I. (2016). MUFFINN: cancer gene discovery via network analysis of somatic mutation data. Genome Biology 17.

[0470] Cho, D.-H., Jo, Y. K., Roh, S. A., Na, Y.-S., Kim, T. W., Jang, S. J., Kim, Y. S., and Kim, J. C. (2010). Upregulation of SPRR3 promotes colorectal tumorigenesis. Mol. Med. 16, 271-277.

[0471] Choi, M., Chang, C.-Y., Clough, T., Broudy, D., Killeen, T., MacLean, B., and Vitek, O. (2014). MSstats: an R package for statistical analysis of quantitative mass spectrometry-based proteomic experiments. Bioinformatics 30, 2524-2526.

[0472] Chowdhury, D., Keogh, M.-C., Ishii, H., Peterson, C. L., Buratowski, S., and Lieberman, J. (2005). gamma-H2AX dephosphorylation by protein phosphatase 2A facilitates DNA double-strand break repair. Mol. Cell 20, 801-809.

[0473] Christensen, D. E., Brzovic, P. S., and Klevit, R. E. (2007). E2-BRCA1 RING interactions dictate synthesis of mono- or specific polyubiquitin chain linkages. Nat. Struct. Mol. Biol. 14, 941-948.

[0474] Clapperton, J. A., Manke, I. A., Lowery, D. M., Ho, T., Haire, L. F., Yaffe, M. B., and Smerdon, S. J. (2004). Structure and mechanism of BRCA1 BRCT domain recognition of phosphorylated BACH1 with implications for cancer. Nat. Struct. Mol. Biol. 11, 512-518.

[0475] Coppe, J. P., Mori, M., Pan, B., Yau, C., Wolf, D. M., Ruiz-Saenz, A., Brunen, D., Prahallad, A., CornelissenSteijger, P., Kemper, K., et al. (2019). Mapping phospho-catalytic dependencies of therapy-resistant tumours reveals actionable vulnerabilities. Nat. Cell Biol. 21, 778-790.

[0476] Coppé, J.-P., Mapping, K. A., Mori, M., and Pan, B. (2019a). High-Throughput Kinase Activity Mapping (HT-KAM) system: biochemical assay. Protocol Exchange.

[0477] Coppé, J.-P., Yau, C., and Wolf, D. M. (2019b). High-Throughput Kinase Activity Mapping (HT-KAM) system: analysis of phospho-catalytic profiles. Protocol Exchange.

[0478] Cortez, D., Wang, Y., Qin, J., and Elledge, S. J. (1999). Requirement of ATM-dependent phosphorylation of brca1 in the DNA damage response to double-strand breaks. Science 286, 1162-1166.

[0479] Cox, J., and Mann, M. (2008). MaxQuant enables high peptide identification rates, individualized p.p.b.-range mass accuracies and proteome-wide protein quantification. Nat. Biotechnol. 26, 1367-1372.

[0480] Creixell, P., Reimand, J., Haider, S., Wu, G., Shibata, T., Vazquez, M., Mustonen, V., Gonzalez-Perez, A., Pearson, J., Sander, C., et al. (2015). Pathway and network analysis of cancer genomes. Nat. Methods 12, 615-621.

[0481] Davies, M. A., Stemke-Hale, K., Tellez, C., Calderone, T. L., Deng, W., Prieto, V. G., Lazar, A. J. F., Gershenwald, J. E., and Mills, G. B. (2008). A novel AKT3 mutation in melanoma tumours and cell lines. Br. J. Cancer 99, 1265-1268.

[0482] Dever, S. M., Golding, S. E., Rosenberg, E., Adams, B. R., Idowu, M. O., Quillin, J. M., Valerie, N., Xu, B., Povirk, L. F., and Valerie, K. (2011). Mutations in the BRCT binding site of BRCA1 result in hyper-recombination. Aging 3, 515-532.

[0483] Drost, R., Bouwman, P., Rottenberg, S., Boon, U., Schut, E., Klarenbeek, S., Klijn, C., van der Heijden, I., van der Gulden, H., Wientjens, E., et al. (2011). BRCA1 RING function is essential for tumor suppression but dispensable for therapy resistance. Cancer Cell 20, 797-809.

[0484] Drost, R., Dhillon, K. K., van der Gulden, H., van der Heijden, I., Brandsma, I., Cruz, C., Chondronasiou, D., Castroviejo-Bermejo, M., Boon, U., Schut, E., et al. (2016). BRCA1185delAG tumors may acquire therapy resistance through expression of RING-less BRCA1. J. Clin. Invest. 126, 2903-2918.

[0485] Eckhardt, M., Zhang, W., Gross, A. M., Von Dollen, J., Johnson, J. R., Franks-Skiba, K. E., Swaney, D. L., Johnson, T. L., Jang, G. M., Shah, P. S., et al. (2018). Multiple Routes to Oncogenesis Are Promoted by the Human Papillomavirus-Host Protein Network. Cancer Discovery 8, 1474-1489.

[0486] Epping, M. T., Meijer, L. A. T., Krijgsman, O., Bos, J. L., Pandolfi, P. P., and Bernards, R. (2011). TSPYL5 suppresses p53 levels and function by physical interaction with USP7. Nat. Cell Biol. 13, 102-108.

[0487] Escribano-Diaz, C., Orthwein, A., Fradet-Turcotte, A., Xing, M., Young, J. T., Tkac, J., Cook, M. A., Rosebrock, A. P., Munro, M., Canny, M. D., et al. (2013). A cell cycle-dependent regulatory circuit composed of 53BP1-RIF1 and BRCA1-CtIP controls DNA repair pathway choice. Mol. Cell 49, 872-883.

[0488] Feng, Z., and Levine, A. J. (2010). The regulation of energy metabolism and the IGF-1/mTOR pathways by the p53 protein. Trends Cell Biol. 20, 427-434.

[0489] Feng, J., Yan, Z., Ferreira, A., Tomizawa, K., Liauw, J. A., Zhuo, M., Allen, P. B., Ouimet, C. C., and Greengard, P. (2000). Spinophilin regulates the formation and function of dendritic spines. Proc. Natl. Acad. Sci. U.S.A 97, 9287-9292.

[0490] Forcet, C., Etienne-Manneville, S., Gaude, H., Fournier, L., Debilly, S., Salmi, M., Baas, A., Olschwang, S., Clevers, H., and Billaud, M. (2005). Functional analysis of Peutz-Jeghers mutations reveals that the LKB1 Cterminal region exerts a crucial role in regulating both the AMPK pathway and the cell polarity. Hum. Mol. Genet. 14, 1283-1292.

[0491] Fruman, D. A., Chiu, H., Hopkins, B. D., Bagrodia, S., Cantley, L. C., and Abraham, R. T. (2017). The PI3K Pathway in Human Disease. Cell 170, 605-635.

[0492] Fuqua, S. A. W., Gu, G., and Rechoum, Y. (2014). Estrogen receptor (ER) α mutations in breast cancer: hidden in plain sight. Breast Cancer Res. Treat. 144, 11-19.

[0493] Futreal, P. A., Liu, Q., Shattuck-Eidens, D., Cochran, C., Harshman, K., Tavtigian, S., Bennett, L. M., HaugenStrano, A., Swensen, J., and Miki, Y. (1994).

BRCA1 mutations in primary breast and ovarian carcinomas. Science 266, 120-122.

[0494] Gatei, M., Scott, S. P., Filippovitch, I., Soronika, N., Lavin, M. F., Weber, B., and Khanna, K. K. (2000). Role for ATM in DNA damage-induced phosphorylation of BRCA1. Cancer Res. 60, 3299-3304.

[0495] Gatei, M., Zhou, B.-B., Hobson, K., Scott, S., Young, D., and Khanna, K. K. (2001). Ataxia Telangiectasia Mutated (ATM) Kinase and ATM and Rad3 Related Kinase Mediate Phosphorylation of Brca1 at Distinct and Overlapping Sites IN VIVO ASSESSMENT USING PHOSPHO-SPECIFIC ANTIBODIES. J. Biol. Chem. 276, 17276-17280.

[0496] Goh, J. Y., Feng, M., Wang, W., Oguz, G., Yatim, S. M. J. M., Lee, P. L., Bao, Y., Lim, T. H., Wang, P., Tam, W. L., et al. (2017). Chromosome 1921.3 amplification is a trackable biomarker and actionable target for breast cancer recurrence. Nat. Med. 23, 1319-1330.

[0497] Goldberg, M., Bell, K., Aronson, M., Semotiuk, K., Pond, G., Gallinger, S., and Zbuk, K. (2017). Association between the Lynch syndrome gene MSH2 and breast cancer susceptibility in a Canadian familial cancer registry. J. Med. Genet. 54, 742-746.

[0498] Górski, B., Byrski, T., Huzarski, T., Jakubowska, A., Menkiszak, J., Gronwald, J., Plużańska, A., Bçbenek, M., Fischer-Maliszewska, L., Grzybowska, E., et al. (2000). Founder Mutations in the BRCA1 Gene in Polish Families with Breast-Ovarian Cancer. Am. J. Hum. Genet. 66, 1963-1968.

[0499] Gottlieb, E., and Vousden, K. H. (2010). p^{53} regulation of metabolic pathways. Cold Spring Harb. Perspect. Biol. 2, a001040.

[0500] Grabocka, E., Pylayeva-Gupta, Y., Jones, M. J. K., Lubkov, V., Yemanaberhan, E., Taylor, L., Jeng, H. H., and Bar-Sagi, D. (2014). Wild-type H- and N-Ras promote mutant K-Ras-driven tumorigenesis by modulating the DNA damage response. Cancer Cell 25, 243-256.

[0501] Guerrero-Zotano, A., Mayer, I. A., and Arteaga, C. L. (2016). PI3K/AKT/mTOR: role in breast cancer progression, drug resistance, and treatment. Cancer Metastasis Rev. 35, 515-524.

[0502] Gunn, A., and Stark, J. M. (2012). I-SceI-based assays to examine distinct repair outcomes of mammalian chromosomal double strand breaks. Methods Mol. Biol. 920, 379-391.

[0503] Hamilton, E., and Infante, J. R. (2016). Targeting CDK4/6 in patients with cancer. Cancer Treat. Rev. 45, 129-138.

[0504] Hardie, D. G., Grahame Hardie, D., and Alessi, D. R. (2013). LKB1 and AMPK and the cancer-metabolism link-ten years after. BMC Biology 11.

[0505] Harkness, E. F., Barrow, E., Newton, K., Green, K., Clancy, T., Lalloo, F., Hill, J., and Evans, D. G. (2015). Lynch syndrome caused by MLH1 mutations is associated with an increased risk of breast cancer: a cohort study. J. Med. Genet. 52, 553-556.

[0506] Hatchi, E., Skourti-Stathaki, K., Ventz, S., Pinello, L., Yen, A., Kamieniarz-Gdula, K., Dimitrov, S., Pathania, S., McKinney, K. M., Eaton, M. L., et al. (2015). BRCA1 recruitment to transcriptional pause sites is required for Rloop-driven DNA damage repair. Mol. Cell 57, 636-647.

[0507] He, X., Zhu, Z., Johnson, C., Stoops, J., Eaker, A. E., Bowen, W., and DeFrances, M. C. (2008). PIK3IP1, a negative regulator of PI3K, suppresses the development of hepatocellular carcinoma. Cancer Res. 68, 5591-5598.

[0508] A He, Y., Zhou, G., Zhai, Y., Dong, X., Lv, L., He, F., and Yao, K. (2005). Association of PLUNC gene polymorphisms with susceptibility to nasopharyngeal carcinoma in a Chinese population. J. Med. Genet. 42, 172-176.

[0509] Hein, M. Y., Hubner, N. C., Poser, I., Cox, J., Nagaraj, N., Toyoda, Y., Gak, I. A., Weisswange, I., Mansfeld, J., Buchholz, F., et al. (2015). A human interactome in three quantitative dimensions organized by stoichiometries and abundances. Cell 163, 712-723.

[0510] Higashiguchi, M., Nagatomo, I., Kijima, T., Morimura, O., Miyake, K., Minami, T., Koyama, S., Hirata, H., Iwahori, K., Takimoto, T., et al. (2016). Clarifying the biological significance of the CHK 2 K373E somatic mutationdiscovered in The Cancer Genome Atlas database. FEBS Lett. 590, 4275-4286.

[0511] Hill, S. J., Rolland, T., Adelmant, G., Xia, X., Owen, M. S., Dricot, A., Zack, T. I., Sahni, N., Jacob, Y., Hao, T., et al. (2014). Systematic screening reveals a role for BRCA1 in the response to transcription-associated DNA damage. Genes Dev. 28, 1957-1975.

[0512] Hinton, C. V., Fitzgerald, L. D., and Thompson, M. E. (2007). Phosphatidylinositol 3-kinase/Akt signaling enhances nuclear localization and transcriptional activity of BRCA1. Exp. Cell Res. 313, 1735-1744.

[0513] Hoenerhoff, M. J., Chu, I., Barkan, D., Liu, Z.-Y., Datta, S., Dimri, G. P., and Green, J. E. (2009). BMI1 cooperates with H-RAS to induce an aggressive breast cancer phenotype with brain metastases. Oncogene 28, 3022-3032.

[0514] Hofree, M., Shen, J. P., Carter, H., Gross, A., and Ideker, T. (2013). Network-based stratification of tumor mutations. Nat. Methods 10, 1108-1115.

[0515] Hollstein, P. E., Eichner, L. J., Brun, S. N., Kamireddy, A., Svensson, R. U., Vera, L. I., Ross, D. S., Rymoff, T. J., Hutchins, A., Galvez, H. M., et al. (2019). The AMPK-Related Kinases SIK1 and SIK3 Mediate Key TumorSuppressive Effects of LKB1 in NSCLC. Cancer Discov. 9, 1606-1627.

[0516] Holstege, H., Joosse, S. A., van Oostrom, C. T. M., Nederlof, P. M., de Vries, A., and Jonkers, J. (2009). High incidence of protein-truncating TP53 mutations in BRCA1-related breast cancer. Cancer Res. 69, 3625-3633.

[0517] Hong, Y., Shi, J., Ge, Z., and Wu, H. (2017). Associations between mutations of the cell cycle checkpoint kinase 2 gene and gastric carcinogenesis. Mol. Med. Rep. 16, 4287-4292.

[0518] Huttlin, E. L., Ting, L., Bruckner, R. J., Gebreab, F., Gygi, M. P., Szpyt, J., Tam, S., Zarraga, G., Colby, G., Baltier, K., et al. (2015a). The BioPlex Network: A Systematic Exploration of the Human Interactome. Cell 162, 425-440.

[0519] Huttlin, E. L., Ting, L., Bruckner, R. J., Gebreab, F., Gygi, M. P., Szpyt, J., Tam, S., Zarraga, G., Colby, G., Baltier, K., et al. (2015b). The BioPlex Network: A Systematic Exploration of the Human Interactome. Cell 162, 425-440.

[0520] Huttlin, E. L., Bruckner, R. J., Paulo, J. A., Cannon, J. R., Ting, L., Baltier, K., Colby, G., Gebreab, F., Gygi, M. P., Parzen, H., et al. (2017). Architecture of the human

interactome defines protein communities and disease networks. Nature 545, 505-509.

[0521] Huttlin, E. L., Bruckner, R. J., Navarrete-Perea, J., Cannon, J. R., Baltier, K., Gebreab, F., Gygi, M. P., Thornock, A., Zarraga, G., Tam, S., et al. (2020). Dual Proteome-scale Networks Reveal Cell-specific Remodeling of the Human Interactome.

[0522] Iorio, F., Knijnenburg, T. A., Vis, D. J., Bignell, G. R., Menden, M. P., Schubert, M., Aben, N., Gonçalves, E., Barthorpe, S., Lightfoot, H., et al. (2016). A Landscape of Pharmacogenomic Interactions in Cancer. Cell 166, 740-754.

[0523] Johnson, W. E., Li, C., and Rabinovic, A. (2007). Adjusting batch effects in microarray expression data using empirical Bayes methods. Biostatistics 8, 118-127.

[0524] Kim, E. M., Jung, C.-H., Kim, J., Hwang, S.-G., Park, J. K., and Um, H.-D. (2017). The p53/p21 Complex Regulates Cancer Cell Invasion and Apoptosis by Targeting Bcl-2 Family Proteins. Cancer Res. 77, 3092-3100.

[0525] Kim, H., Huang, J., and Chen, J. (2007a). CCDC98 is a BRCA1-BRCT domain-binding protein involved in the DNA damage response. Nature Structural & Molecular Biology 14, 710-715.

[0526] Kim, H., Chen, J., and Yu, X. (2007b). Ubiquitin-binding protein RAP80 mediates BRCA1-dependent DNA damage response. Science 316, 1202-1205.

[0527] Kim, S. T., Lim, D. S., Canman, C. E., and Kastan, M. B. (1999). Substrate specificities and identification of putative substrates of ATM kinase family members. J. Biol. Chem. 274, 37538-37543.

[0528] Knijnenburg, T. A., Wang, L., Zimmermann, M. T., Chambwe, N., Gao, G. F., Cherniack, A. D., Fan, H., Shen, H., Way, G. P., Greene, C. S., et al. (2018). Genomic and Molecular Landscape of DNA Damage Repair Deficiency across The Cancer Genome Atlas. Cell Rep. 23, 239-254 e6.

[0529] Kumar, R. D., and Bose, R. (2017). Analysis of somatic mutations across the kinome reveals loss-of-function mutations in multiple cancer types. Sci. Rep. 7, 6418.

[0530] Landgraf, K. E., Pilling, C., and Falke, J. J. (2008). Molecular Mechanism of an Oncogenic Mutation That Alters Membrane Targeting: Glu17Lys Modifies the PIP Lipid Specificity of the AKT1 P H Domaint. Biochemistry 47, 12260-12269.

[0531] Lee, S.-W., Li, C.-F., Jin, G., Cai, Z., Han, F., Chan, C.-H., Yang, W.-L., Li, B.-K., Rezaeian, A. H., Li, H.-Y., et al. (2015). Skp2-dependent ubiquitination and activation of LKB1 is essential for cancer cell survival under energy stress. Mol. Cell 57, 1022-1033.

[0532] Leiserson, M. D. M., Vandin, F., Wu, H.-T., Dobson, J. R., Eldridge, J. V., Thomas, J. L., Papoutsaki, A., Kim, Y., Niu, B., McLellan, M., et al. (2015). Pan-cancer network analysis identifies combinations of rare somatic mutations across pathways and protein complexes. Nat. Genet. 47, 106-114.

[0533] Lemaire, F., Millon, R., Young, J., Cromer, A., Wasylyk, C., Schultz, I., Muller, D., Marchal, P., Zhao, C., Melle, D., et al. (2003). Differential expression profiling of head and neck squamous cell carcinoma (HNSCC). Br. J. Cancer 89, 1940-1949.

[0534] Leung, C. C. Y., and Glover, J. N. M. (2011). BRCT domains: easy as one, two, three. Cell Cycle 10, 2461-2470.

[0535] Levy-Lahad, E., Catane, R., Eisenberg, S., Kaufman, B., Hornreich, G., Lishinsky, E., Shohat, M., Weber, B. L., Beller, U., Lahad, A., et al. (1997). Founder BRCA1 and BRCA2 mutations in Ashkenazi Jews in Israel: frequency and differential penetrance in ovarian cancer and in breast-ovarian cancer families. Am. J. Hum. Genet. 60, 1059-1067.

[0536] Li, M. L., and Greenberg, R. A. (2012). Links between genome integrity and BRCA1 tumor suppression. Trends Biochem. Sci. 37, 418-424.

[0537] Li, C., Xiao, L., Jia, J., Li, F., Wang, X., Duan, Q., Jing, H., Yang, P., Chen, C., Wang, Q., et al. (2019). Cornulin Is Induced in Psoriasis Lesions and Promotes Keratinocyte Proliferation via Phosphoinositide 3-Kinase/Akt Pathways. J. Invest. Dermatol. 139, 71-80.

[0538] Li, D., Marchenko, N. D., Schulz, R., Fischer, V., Velasco-Hernandez, T., Talos, F., and Moll, U. M. (2011). Functional inactivation of endogenous MDM2 and CHIP by HSP90 causes aberrant stabilization of mutant p53 in human cancer cells. Mol. Cancer Res. 9, 577-588.

[0539] Lim, J. S. J., Turner, N. C., and Yap, T. A. (2016). CDK4/6 Inhibitors: Promising Opportunities beyond Breast Cancer. Cancer Discovery 6, 697-699.

[0540] Lin, Y.-C., Lee, Y.-C., Li, L.-H., Cheng, C.-J., and Yang, R.-B. (2014). Tumor suppressor SCUBE2 inhibits breast cancer cell migration and invasion through the reversal of epithelial-mesenchymal transition. J. Cell Sci. 127, 85-100.

[0541] Lindhurst, M. J., Sapp, J. C., Teer, J. K., Johnston, J. J., Finn, E. M., Peters, K., Turner, J., Cannons, J. L., Bick, D., Blakemore, L., et al. (2011). A mosaic activating mutation in AKT1 associated with the *Proteus* syndrome. N. Engl. J. Med. 365, 611-619.

[0542] Liu, S., Knapp, S., and Ahmed, A. A. (2014). The structural basis of PI3K cancer mutations: from mechanism to therapy. Cancer Res. 74, 641-646.

[0543] Liu, Z., Wu, J., and Yu, X. (2007). CCDC98 targets BRCA1 to DNA damage sites. Nat. Struct. Mol. Biol. 14, 716-720.

[0544] Lombaerts, M., van Wezel, T., Philippo, K., Dierssen, J. W. F., Zimmerman, R. M. E., Oosting, J., van Eijk, R., Eilers, P. H., van de Water, B., Cornelisse, C. J., et al. (2006). E-cadherin transcriptional downregulation by promoter methylation but not mutation is related to epithelial-to-mesenchymal transition in breast cancer cell lines. Br. J. Cancer 94, 661-671.

[0545] Lukas, J., Lukas, C., and Bartek, J. (2011). More than just a focus: The chromatin response to DNA damage and its role in genome integrity maintenance. Nat. Cell Biol. 13, 1161-1169.

[0546] Malumbres, M., and Barbacid, M. (2001). To cycle or not to cycle: a critical decision in cancer. Nat. Rev. Cancer 1, 222-231.

[0547] Manning, B. D., and Cantley, L. C. (2007). AKT/PKB signaling: navigating downstream. Cell 129, 1261-1274.

[0548] Manning, B. D., and Toker, A. (2017). AKT/PKB Signaling: Navigating the Network. Cell 169, 381-405.

[0549] McAllister, K. A., and Wiseman, R. W. (2002). Are Trp53 rescue of Brcal embryonic lethality and Trp53/Brcal breast cancer association related? Breast Cancer Res. 4, 54-57.

[0550] McCubrey, J. A., Steelman, L. S., Chappell, W. H., Abrams, S. L., Franklin, R. A., Montalto, G., Cervello, M., Libra, M., Candido, S., Malaponte, G., et al. (2012).

[0551] Ras/Raf/MEK/ERK and PI3K/PTEN/Akt/mTOR cascade inhibitors: how mutations can result in therapy resistance and how to overcome resistance. Oncotarget 3, 1068-1111.

[0552] Miki, Y., Swensen, J., Shattuck-Eidens, D., Futreal, P. A., Harshman, K., Tavtigian, S., Liu, Q., Cochran, C., Bennett, L. M., and Ding, W. (1994). A strong candidate for the breast and ovarian cancer susceptibility gene BRCA1. Science 266, 66-71.

[0553] Mimori, K., Inoue, H., Shiraishi, T., Ueo, H., Mafune, K.-I., Tanaka, Y., and Mori, M. (2002). A single-nucleotide polymorphism of SMARCB1 in human breast cancers. Genomics 80, 254-258.

[0554] Morales, J. C., Richard, P., Patidar, P. L., Motea, E. A., Dang, T. T., Manley, J. L., and Boothman, D. A. (2016). XRN2 Links Transcription Termination to DNA Damage and Replication Stress. PLoS Genet. 12, e1006107.

[0555] Moynahan, M. E., and Jasin, M. (2010). Mitotic homologous recombination maintains genomic stability and suppresses tumorigenesis. Nat. Rev. Mol. Cell Biol. 11, 196-207.

[0556] Mullan, P. B., Quinn, J. E., and Harkin, D. P. (2006). The role of BRCA1 in transcriptional regulation and cell cycle control. Oncogene 25, 5854-5863.

[0557] Nelson, A. C., and Holt, J. T. (2010). Impact of RING and BRCT domain mutations on BRCA1 protein stability, localization and recruitment to DNA damage. Radiat. Res. 174, 1-13.

[0558] Nelson, A. C., Lyons, T. R., Young, C. D., Hansen, K. C., Anderson, S. M., and Holt, J. T. (2010). AKT regulates BRCA1 stability in response to hormone signaling. Mol. Cell. Endocrinol. 319, 129-142.

[0559] Ning, F., Wang, C., Berry, K. Z., Kandasamy, P., Liu, H., Murphy, R. C., Voelker, D. R., Nho, C. W., Pan, C.-H., A Dai, S., et al. (2014). Structural characterization of the pulmonary innate immune protein SPLUNC1 and identification of lipid ligands. FASEB J. 28, 5349-5360.

[0560] Niu, Y., Xu, J., and Sun, T. (2019). Cyclin-Dependent Kinases 4/6 Inhibitors in Breast Cancer: Current Status, Resistance, and Combination Strategies. J. Cancer 10, 5504-5517.

[0561] Olow, A., Chen, Z., Niedner, R. H., Wolf, D. M., Yau, C., Pankov, A., Lee, E. P., Brown-Swigart, L., van't Veer, L. J., and Coppe, J. P. (2016). An Atlas of the Human Kinome Reveals the Mutational Landscape Underlying Dysregulated Phosphorylation Cascades in Cancer. Cancer Res. 76, 1733-1745.

[0562] Paczkowska, M., Barenboim, J., Sintupisut, N., Fox, N. S., Zhu, H., Abd-Rabbo, D., Mee, M. W., Boutros, P. C., PCAWG Drivers and Functional Interpretation Working Group, Reimand, J., et al. (2020). Integrative pathway enrichment analysis of multivariate omics data. Nat. Commun. 11, 735.

[0563] Pal, S. K., Reckamp, K., Yu, H., and Figlin, R. A. (2010). Akt inhibitors in clinical development for the treatment of cancer. Expert Opin. Investig. Drugs 19, 1355-1366.

[0564] Papatheodorou, I., Moreno, P., Manning, J., Fuentes, A. M.-P., George, N., Fexova, S., Fonseca, N. A., Ftillgrabe, A., Green, M., Huang, N., et al. (2020). Expression Atlas update: from tissues to single cells. Nucleic Acids Res. 48, D77-D83.

[0565] Parrales, A., Ranjan, A., Iyer, S. V., Padhye, S., Weir, S. J., Roy, A., and Iwakuma, T. (2016). DNAJA1 controls the fate of misfolded mutant p53 through the mevalonate pathway. Nat. Cell Biol. 18, 1233-1243.

[0566] Prakash, R., Zhang, Y., Feng, W., and Jasin, M. Homologous recombination and human health: the roles of BRCA1, BRCA2, and associated proteins. Cold Spring Harb Perspect Biol. 2015; 7: a016600.

[0567] Qi, M., Zhang, J., Zeng, W., and Chen, X. (2014). DNAJB1 stabilizes MDM2 and contributes to cancer cell proliferation in a p53-dependent manner. Biochim. Biophys. Acta 1839, 62-69.

[0568] Quanz, M., Chassoux, D., Berthault, N., Agrario, C., Sun, J.-S., and Dutreix, M. (2009). Hyperactivation of DNAPK by double-strand break mimicking molecules disorganizes DNA damage response. PLoS One 4, e6298.

[0569] Reyna, M. A., Haan, D., Paczkowska, M., Verbeke, L. P. C., Vazquez, M., Kahraman, A., Pulido-Tamayo, S., Barenboim, J., Wadi, L., Dhingra, P., et al. (2020). Pathway and network analysis of more than 2500 whole cancer genomes. Nat. Commun. 11, 729.

[0570] Reynet, C., and Kahn, C. R. (1993). Rad: a member of the Ras family overexpressed in muscle of type II diabetic humans. Science 262, 1441-1444.

[0571] Rogakou, E. P., Pilch, D. R., Orr, A. H., Ivanova, V. S., and Bonner, W. M. (1998). DNA double-stranded breaks induce histone H2AX phosphorylation on serine 139. J. Biol. Chem. 273, 5858-5868.

[0572] van Roy, F., and Berx, G. (2008). The cell-cell adhesion molecule E-cadherin. Cell. Mol. Life Sci. 65, 3756-3788. Rudolph, M., Anzeneder, T., Schulz, A., Beckmann, G., Byrne, A. T., Jeffers, M., Pena, C., Politz, O., Köchert, K., Vonk, R., et al. (2016). AKT1 E17K mutation profiling in breast cancer: prevalence, concurrent oncogenic alterations, and blood-based detection. BMC Cancer 16, 622.

[0573] Rugo, H. S., Olopade, O. I., DeMichele, A., Yau, C., van't Veer, L. J., Buxton, M. B., Hogarth, M., Hylton, N. M., Paoloni, M., Perlmutter, J., et al. (2016). Adaptive Randomization of Veliparib-Carboplatin Treatment in Breast Cancer. N. Engl. J. Med. 375, 23-34.

[0574] Sanchez-Vega, F., Mina, M., Armenia, J., Chatila, W. K., Luna, A., La, K. C., Dimitriadoy, S., Liu, D. L., Kantheti, H. S., Saghafinia, S., et al. (2018). Oncogenic Signaling Pathways in The Cancer Genome Atlas. Cell 173, 321-337.e10.

[0575] Santagata, S., Thakkar, A., Ergonul, A., Wang, B., Woo, T., Hu, R., Harrell, J. C., McNamara, G., Schwede, M., Culhane, A. C., et al. (2014). Taxonomy of breast cancer based on normal cell phenotype predicts outcome.

[0576] Santo, L., Siu, K. T., and Raje, N. (2015). Targeting Cyclin-Dependent Kinases and Cell Cycle Progression in Human Cancers. Semin. Oncol. 42, 788-800.

[0577] Sarbassov, D. D., Guertin, D. A., Ali, S. M., and Sabatini, D. M. (2005). Phosphorylation and regulation of Akt/PKB by the rictor-mTOR complex. Science 307, 1098-1101.

[0578] Sarrouilhe, D., di Tommaso, A., M6tay6, T., and Ladeveze, V. (2006). Spinophilin: from partners to functions. Biochimie 88, 1099-1113.

[0579] Savage, K. I., Gorski, J. J., Barros, E. M., Irwin, G. W., Manti, L., Powell, A. J., Pellagatti, A., Lukashchuk,

N., McCance, D. J., McCluggage, W. G., et al. (2014). Identification of a BRCA1-mRNA splicing complex required for efficient DNA repair and maintenance of genomic stability. Mol. Cell 54, 445-459.

[0580] Schulz-Heddergott, R., and Moll, U. M. (2018). Gain-of-Function (GOF) Mutant p53 as Actionable Therapeutic Target. Cancers 10.

[0581] Shakya, R., Reid, L. J., Reczek, C. R., Cole, F., Egli, D., Lin, C.-S., deRooij, D. G., Hirsch, S., Ravi, K., Hicks, J. B., et al. (2011). BRCA1 tumor suppression depends on BRCT phosphoprotein binding, but not its E3 ligase activity. Science 334, 525-528.

[0582] Sobhian, B., Shao, G., Lilli, D. R., Culhane, A. C., Moreau, L. A., Xia, B., Livingston, D. M., and Greenberg, R. A. (2007). RAP80 targets BRCA1 to specific ubiquitin structures at DNA damage sites. Science 316, 1198-1202.

[0583] Society, A. C. (2019). Breast Cancer Facts and Figures 2019-2020. Am. Cancer Soc 1-44.

[0584] Sowa, M. E., Bennett, E. J., Gygi, S. P., and Harper, J. W. (2009a). Defining the human deubiquitinating enzyme interaction landscape. Cell 138, 389-403.

[0585] Sowa, M. E., Bennett, E. J., Gygi, S. P., and Harper, J. W. (2009b). Defining the Human Deubiquitinating Enzyme Interaction Landscape. Cell 138, 389-403.

[0586] Stephens, P. J., Tarpey, P. S., Davies, H., Van Loo, P., Greenman, C., Wedge, D. C., Nik-Zainal, S., Martin, S., Varela, I., Bignell, G. R., et al. (2012). The landscape of cancer genes and mutational processes in breast cancer. Nature 486, 400-404.

[0587] Stokoe, D., Stephens, L. R., Copeland, T., Gaffney, P. R. J., Reese, C. B., Painter, G. F., Holmes, A. B., McCormick, F., and Hawkins, P. T. (1997). Dual Role of Phosphatidylinositol-3,4,5-trisphosphate in the Activation of Protein Kinase B. Science 277, 567-570.

[0588] Suzuki, M., Shigematsu, H., Shames, D. S., Sunaga, N., Takahashi, T., Shivapurkar, N., Iizasa, T., Minna, J. D., Fujisawa, T., and Gazdar, A. F. (2007). Methylation and gene silencing of the Ras-related GTPase gene in lung and breast cancers. Ann. Surg. Oncol. 14, 1397-1404.

[0589] Tassi, R. A., Bignotti, E., Falchetti, M., Calza, S., Ravaggi, A., Rossi, E., Martinelli, F., Bandiera, E., Pecorelli, S., and Santin, A. D. (2008). Mammaglobin B expression in human endometrial cancer. Int. J. Gynecol. Cancer 18, 1090-1096.

[0590] Tate, C. R., Rhodes, L. V., Segar, H. C., Driver, J. L., Pounder, F. N., Burow, M. E., and Collins-Burow, B. M. (2012). Targeting triple-negative breast cancer cells with the histone deacetylase inhibitor panobinostat. Breast Cancer Res. 14, R79.

[0591] Teo, G., Liu, G., Zhang, J., Nesvizhskii, A. I., Gingras, A. C., and Choi, H. (2014a). SAINTexpress: improvements and additional features in Significance Analysis of INTeractome software. J. Proteomics 100, 37-43.

[0592] Teo, G., Liu, G., Zhang, J., Nesvizhskii, A. I., Gingras, A.-C., and Choi, H. (2014b). SAINTexpress: improvements and additional features in Significance Analysis of INTeractome software. J. Proteomics 100, 37-43.

[0593] Thompson, E. R., Doyle, M. A., Ryland, G. L., Rowley, S. M., Choong, D. Y. H., Tothill, R. W., Thorne, H., kConFab, Barnes, D. R., Li, J., et al. (2012). Exome sequencing identifies rare deleterious mutations in DNA repair genes FANCC and BLM as potential breast cancer susceptibility alleles. PLoS Genet. 8, e1002894.

[0594] Tokunaga, E., Nakashima, Y., Yamashita, N., Hisamatsu, Y., Okada, S., Akiyoshi, S., Aishima, S., Kitao, H., Morita, M., and Maehara, Y. (2014). Overexpression of metadherin/MTDH is associated with an aggressive phenotype and a poor prognosis in invasive breast cancer. Breast Cancer 21, 341-349.

[0595] Uche, U. N., and Kane, L. P. (2016). PIK3IP1—A novel negative regulator of PI3K. The Journal of Immunology 196, 57.9-57.9.

[0596] Vega, A., Campos, B., Bressac-de-Paillerets, B., Bond, P. M., Janin, N., Douglas, F. S., Domenech, M., Baena, M., Pericay, C., Alonso, C., et al. (2001). The R71GBRCAlis a founder Spanish mutation and leads to aberrant splicing of the transcript. Human Mutation 17, 520-521.

[0597] Venkitaraman, A. R. (2014). Cancer suppression by the chromosome custodians, BRCA1 and BRCA2. Science 343, 1470-1475.

[0598] Vivanco, I., and Sawyers, C. L. (2002). The phosphatidylinositol 3-Kinase AKT pathway in human cancer. Nat. Rev. Cancer 2, 489-501.

[0599] Vizcaíno, J. A., Deutsch, E. W., Wang, R., Csordas, A., Reisinger, F., Rios, D., Dianes, J. A., Sun, Z., Farrah, T., Bandeira, N., et al. (2014). ProteomeXchange provides globally coordinated proteomics data submission and dissemination. Nat. Biotechnol. 32, 223-226.

[0600] Wang, B., Hurov, K., Hofmann, K., and Elledge, S. J. (2009). NBA1, a new player in the Brcal A complex, is required for DNA damage resistance and checkpoint control. Genes Dev. 23, 729-739.

[0601] Wang, Y., Cortez, D., Yazdi, P., Neff, N., Elledge, S. J., and Qin, J. (2000). BASC, a super complex of BRCA1-associated proteins involved in the recognition and repair of aberrant DNA structures. Genes Dev. 14, 927-939.

[0602] Wang, Y., Bernhardy, A. J., Cruz, C., Krais, J. J., Nacson, J., Nicolas, E., Peri, S., van der Gulden, H., van der Heijden, I., O'Brien, S. W., et al. (2016a). The BRCA1-Δ11q Alternative Splice Isoform Bypasses Germline Mutations and Promotes Therapeutic Resistance to PARP Inhibition and Cisplatin. Cancer Res. 76, 2778-2790.

[0603] Wang, Y., Krais, J. J., Bernhardy, A. J., Nicolas, E., Cai, K. Q., Harrell, M. I., Kim, H. H., George, E., Swisher, E. M., Simpkins, F., et al. (2016b). RING domain-deficient BRCA1 promotes PARP inhibitor and platinum resistance. J. Clin. Invest. 126, 3145-3157.

[0604] Warburg, O. (1956). On the origin of cancer cells. Science 123, 309-314.

[0605] Wolf, D. M., Yau, C., Sanil, A., Glas, A., Petricoin, E., Wulfkuhle, J., Severson, T. M., Linn, S., Brown-Swigart, L., Hirst, G., et al. (2017). DNA repair deficiency biomarkers and the 70-gene ultra-high risk signature as predictors of veliparib/carboplatin response in the I-SPY 2 breast cancer trial. NPJ Breast Cancer 3, 31.

[0606] Wood, L. D., Parsons, D. W., Jones, S., Lin, J., Sjöblom, T., Leary, R. J., Shen, D., Boca, S. M., Barber, T., Ptak, J., et al. (2007). The genomic landscapes of human breast and colorectal cancers. Science 318, 1108-1113.

[0607] Woods, N. T., Mesquita, R. D., Sweet, M., Carvalho, M. A., Li, X., Liu, Y., Nguyen, H., Thomas, C. E.,

Iversen, E. S., Marsillac, S., et al. (2012). Charting the Landscape of Tandem BRCT Domain-Mediated Protein Interactions. Science Signaling 5, rs6-rs6.

[0608] Wu, L. C., Wang, Z. W., Tsan, J. T., Spillman, M. A., Phung, A., Xu, X. L., Yang, M. C., Hwang, L. Y., Bowcock, A. M., and Baer, R. (1996). Identification of a RING protein that can interact in vivo with the BRCA1 gene product. Nat. a Genet. 14, 430-440.

[0609] Wu, Q., Paul, A., Su, D., Mehmood, S., Foo, T. K., Ochi, T., Bunting, E. L., Xia, B., Robinson, C. V., Wang, B., et al. (2016). Structure of BRCA1-BRCT/Abraxas Complex Reveals Phosphorylation-Dependent BRCT Dimerization at DNA Damage Sites. Mol. Cell 61, 434-448.

[0610] Wulfkuhle, J. D., Yau, C., Wolf, D. M., Vis, D. J., Gallagher, R. I., Brown-Swigart, L., Hirst, G., Voest, E. E., DeMichele, A., Hylton, N., et al. (2018). Evaluation of the HER/PI3K/AKT Family Signaling Network as a Predictive Biomarker of Pathologic Complete Response for Patients With Breast Cancer Treated With Neratinib in the I-SPY 2 TRIAL. JCO Precision Oncology 1-20.

[0611] Xu, B., O'Donnell, A. H., Kim, S.-T., and Kastan, M. B. (2002). Phosphorylation of serine 1387 in Brcal is specifically required for the Atm-mediated S-phase checkpoint after ionizing irradiation. Cancer Res. 62, 4588-4591.

[0612] Xu, X., Omelchenko, T., and Hall, A. (2010). LKB1 tumor suppressor protein regulates actin filament assembly through Rho and its exchange factor Dbl independently of kinase activity. BMC Cell Biol. 11, 77.

[0613] Yap, T. A., Yan, L., Patnaik, A., Fearen, I., Olmos, D., Papadopoulos, K., Baird, R. D., Delgado, L., Taylor, A., Lupinacci, L., et al. (2011). First-in-man clinical trial of the oral pan-AKT inhibitor MK-2206 in patients with advanced solid tumors. J. Clin. Oncol. 29, 4688-4695.

[0614] Yu, X., and Chen, J. (2004). DNA damage-induced cell cycle checkpoint control requires CtIP, a phosphorylationdependent binding partner of BRCA1 C-terminal domains. Mol. Cell. Biol. 24, 9478-9486.

[0615] Yu, K., Chen, B., Aran, D., Charalel, J., Yau, C., Wolf, D. M., van't Veer, L. J., Butte, A. J., Goldstein, T., and Sirota, M. (2019). Comprehensive transcriptomic analysis of cell lines as models of primary tumors across 22 tumor types. Nature Communications 10.

[0616] Yu, X., Chini, C. C., He, M., Mer, G., and Chen, J. (2003). The BRCT domain is a phospho-protein binding domain. Science 302, 639-642.

[0617] Yuan, T. L., and Cantley, L. C. (2008). PI3K pathway alterations in cancer: variations on a theme. Oncogene 27, 5497-5510.

[0618] Yue, X., Zhao, Y., Huang, G., Li, J., Zhu, J., Feng, Z., and Hu, W. (2016). A novel mutant p53 binding partner BAG5 stabilizes mutant p53 and promotes mutant p53 GOFs in tumorigenesis. Cell Discov 2, 16039.

[0619] Yun, M. H., and Hiom, K. (2009). CtIP-BRCA1 modulates the choice of DNA double-strand-break repair pathway throughout the cell cycle. Nature 459, 460-463.

[0620] Zeqiraj, E., Filippi, B. M., Goldie, S., Navratilova, I., Boudeau, J., Deak, M., Alessi, D. R., and van Aalten, D. M. F. (2009a). ATP and MO25alpha regulate the conformational state of the STRADalpha pseudokinase and activation of the LKB1 tumour suppressor. PLoS Biol. 7, e1000126.

[0621] Zeqiraj, E., Filippi, B. M., Deak, M., Alessi, D. R., and van Aalten, D. M. F. (2009b). Structure of the LKB1-STRADMO25 complex reveals an allosteric mechanism of kinase activation. Science 326, 1707-1711.

[0622] Zhang, B., Nie, X., Xiao, B., Xiang, J., Shen, S., Gong, J., Zhou, M., Zhu, S., Zhou, J., Qian, J., et al. (2003). Identification of tissue-specific genes in nasopharyngeal epithelial tissue and differentially expressed genes in nasopharyngeal carcinoma by suppression subtractive hybridization and cDNA microarray. Genes Chromosomes Cancer 38, 80-90.

[0623] Zhang, C., Liu, J., Wu, R., Liang, Y., Lin, M., Liu, J., Chan, C. S., Hu, W., and Feng, Z. (2014). Tumor suppressor p53 negatively regulates glycolysis stimulated by hypoxia through its target RRAD. Oncotarget 5, 5535-5546.

[0624] Zhang, L., Yan, X., Yu, S., Zhong, X., Tian, R., Xu, L., Bian, X., and Su, J. (2020). LINC00365-SCGB2A1 axis A inhibits the viability of breast cancer through targeting NF-cB signaling. Oncol. Lett. 19, 753-762.

[0625] Zhang, S., Schafer-Hales, K., Khuri, F. R., Zhou, W., Vertino, P. M., and Marcus, A. I. (2008). The tumor suppressor LKB1 regulates lung cancer cell polarity by mediating cdc42 recruitment and activity. Cancer Res. 68, 740-748.

[0626] Zhao, G. Y., Sonoda, E., Barber, L. J., Oka, H., Murakawa, Y., Yamada, K., Ikura, T., Wang, X., Kobayashi, M., Yamamoto, K., et al. (2007). A critical role for the ubiquitin-conjugating enzyme Ubcl3 in initiating homologous recombination. Mol. Cell 25, 663-675.

[0627] Zheng, W., Cong, X.-F., Cai, W.-H., Yang, S., Mao, C., and Zou, H.-W. (2011). Current evidences on XPC polymorphisms and breast cancer susceptibility: a meta-analysis. Breast Cancer Res. Treat. 128, 811-815.

[0628] Zubor, P., Hatok, J., Moricova, P., Kajo, K., Kapustova, I., Mendelova, A., Racay, P., and Danko, J. (2015). Gene expression abnormalities in histologically normal breast epithelium from patients with luminal type of breast cancer. Mol. Biol. Rep. 42, 977-988.

[0629] Akavia, U. D., Litvin, O., Kim, J., Sanchez-Garcia, F., Kotliar, D., Causton, H. C., Pochanard, P., Mozes, E., Garraway, L. A., and Pe'er, D. (2010). An integrated approach to uncover drivers of cancer. Cell 143, 1005-1017.

[0630] Alexa, A., Gógl, G., Glatz, G., Garai, A., Zeke, A., Varga, J., Dudás, E., Jeszenöi, N., Bodor, A., Hetényi, C., et al. (2015). Structural assembly of the signaling competent ERK2-RSK1 heterodimeric protein kinase complex. Proc. Natl. Acad. Sci. U.S.A 112, 2711-2716.

[0631] Alvarado, D., Ligon, G. F., Lillquist, J. S., Seibel, S. B., Wallweber, G., Neumeister, V. M., Rimm, D. L., McMahon, G., and LaVallee, T. M. (2017). ErbB activation signatures as potential biomarkers for anti-ErbB3 treatment in HNSCC. PLoS One 12, e0181356.

[0632] Ara, H., Takagishi, M., Enomoto, A., Asai, M., Ushida, K., Asai, N., Shimoyama, Y., Kaibuchi, K., Kodera, Y., A and Takahashi, M. (2016). Role for Daple in non-canonical Wnt signaling during gastric cancer invasion and metastasis. Cancer Sci. 107, 133-139.

[0633] Arvind, R., Shimamoto, H., Momose, F., Amagasa, T., Omura, K., and Tsuchida, N. (2005). A mutation in the common docking domain of ERK2 in a human cancer cell line, which was associated with its constitutive phosphorylation. Int. J. Oncol. 27, 1499-1504.

[0634] Aznar, N., Midde, K. K., Dunkel, Y., Lopez-Sanchez, I., Pavlova, Y., Marivin, A., Barbazán, J., Murray, F., Nitsche, U., Janssen, K.-P., et al. (2015). Daple is a novel non-receptor GEF required for trimeric G protein activation in Wnt signaling. Elife 4, e07091.

[0635] Aznar, N., Sun, N., Dunkel, Y., Ear, J., Buschman, M. D., and Ghosh, P. (2017). A Daple-Akt feed-forward loop enhances noncanonical Wnt signals by compartmentalizing (3-catenin. Mol. Biol. Cell 28, 3709-3723.

[0636] Aznar, N., Ear, J., Dunkel, Y., Sun, N., Satterfield, K., He, F., Kalogriopoulos, N. A., Lopez-Sanchez, I., Ghassemian, M., Sahoo, D., et al. (2018). Convergence of Wnt, growth factor, and heterotrimeric G protein signals on the guanine nucleotide exchange factor Daple. Sci. Signal. 11.

[0637] Bailey, M. H., Tokheim, C., Porta-Pardo, E., Sengupta, S., Bertrand, D., Weerasinghe, A., Colaprico, A., Wendl, M. C., Kim, J., Reardon, B., et al. (2018). Comprehensive Characterization of Cancer Driver Genes and Mutations. Cell 174, 1034-1035.

[0638] Biankin, A. V., Waddell, N., Kassahn, K. S., Gingras, M. C., Muthuswamy, L. B., Johns, A. L., Miller, D. K., Wilson, P. J., Patch, A. M., Wu, J., et al. (2012). Pancreatic cancer genomes reveal aberrations in axon guidance pathway genes. Nature 491, 399-405.

[0639] Bouhaddou, M., Eckhardt, M., Chi Naing, Z. Z., Kim, M., Ideker, T., and Krogan, N. J. (2019). Mapping the protein-protein and genetic interactions of cancer to guide precision medicine. Curr. Opin. Genet. Dev. 54, 110-117.

[0640] Brenan, L., Andreev, A., Cohen, O., Pantel, S., Kamburov, A., Cacchiarelli, D., Persky, N. S., Zhu, C., Bagul, M., Goetz, E. M., et al. (2016). Phenotypic Characterization of a Comprehensive Set of MAPK1/ERK2 Missense Mutants. Cell Rep. 17, 1171-1183.

[0641] Burke, J. E., Perisic, O., Masson, G. R., Vadas, O., and Williams, R. L. (2012). Oncogenic mutations mimic and enhance dynamic events in the natural activation of phosphoinositide 3-kinase p110α (PIK3CA). Proc. Natl. Acad. Sci. U.S.A 109, 15259-15264.

[0642] Cancer Genome Atlas, Network (2012). Comprehensive molecular portraits of human breast tumours. Nature 490, 61-70.

[0643] Cancer Genome Atlas, Network (2015). Comprehensive genomic characterization of head and neck squamous cell carcinomas. Nature 517, 576-582.

[0644] Cancer Genome Atlas Network (2015). Comprehensive genomic characterization of head and neck squamous cell carcinomas. Nature 517, 576-582.

[0645] Cancer Genome Atlas Research, Network (2008). Comprehensive genomic characterization defines human glioblastoma genes and core pathways. Nature 455, 1061-1068.

[0646] Cancer Genome Atlas Research, Network (2011). Integrated genomic analyses of ovarian carcinoma. Nature 474, 609-615.

[0647] Carson, J. D., Van Aller, G., Lehr, R., Sinnamon, R. H., Kirkpatrick, R. B., Auger, K. R., Dhanak, D., Copeland, R. A., Gontarek, R. R., Tummino, P. J., et al. (2008). Effects of oncogenic p1Oalpha subunit mutations on the A lipid kinase activity of phosphoinositide 3-kinase. Biochem. J 409, 519-524.

[0648] Cerami, E., Demir, E., Schultz, N., Taylor, B. S., and Sander, C. (2010). Automated network analysis identifies core pathways in glioblastoma. PLoS One 5, e8918.

[0649] Chakravarty, D., Gao, J., Phillips, S. M., Kundra, R., Zhang, H., Wang, J., Rudolph, J. E., Yaeger, R., Soumerai, T., Nissan, M. H., et al. (2017). OncoKB: A Precision Oncology Knowledge Base. JCO Precis Oncol 2017.

[0650] Choi, M., Chang, C.-Y., Clough, T., Broudy, D., Killeen, T., MacLean, B., and Vitek, O. (2014). MSstats: an R package for statistical analysis of quantitative mass spectrometry-based proteomic experiments. Bioinformatics 30, 2524-2526.

[0651] Consequences, T. M., and Consortium, Pathway Analysis working group of the International Cancer Genome (2015). Pathway and network analysis of cancer genomes. Nat. Methods 12, 615-621.

[0652] Copple, I. M., Lister, A., Obeng, A. D., Kitteringham, N. R., Jenkins, R. E., Layfield, R., Foster, B. J., Goldring, C. E., and Park, B. K. (2010). Physical and functional interaction of sequestosome 1 with KeapI regulates the Keap1-Nrf2 cell defense pathway. J. Biol. Chem. 285, 16782-16788.

[0653] Cox, J., and Mann, M. (2008). MaxQuant enables high peptide identification rates, individualized p.p.b.-range mass accuracies and proteome-wide protein quantification. Nat. Biotechnol. 26, 1367-1372.

[0654] Czubaty, A., Girstun, A., Kowalska-Loth, B., Trzcinska, A. M., Purta, E., Winczura, A., Grajkowski, W., and Staron, K. (2005). Proteomic analysis of complexes formed by human topoisomerase I. Biochim. Biophys. Acta 1749, 133-141.

[0655] Davis, W. J., Lehmann, P. Z., and Li, W. (2015). Nuclear PI3K signaling in cell growth and tumorigenesis. Front Cell Dev Biol 3, 24.

[0656] Dogruluk, T., Tsang, Y. H., Espitia, M., Chen, F., Chen, T., Chong, Z., Appadurai, V., Dogruluk, A., Eterovic, A. K., Bonnen, P. E., et al. (2015). Identification of Variant-Specific Functions of PIK3CA by Rapid Phenotyping of Rare Mutations. Cancer Res. 75, 5341-5354.

[0657] Dornan, G. L., and Burke, J. E. (2018). Molecular Mechanisms of Human Disease Mediated by Oncogenic and Primary Immunodeficiency Mutations in Class IA Phosphoinositide 3-Kinases. Front. Immunol. 9, 575.

[0658] Drier, Y., Sheffer, M., and Domany, E. (2013). Pathway-based personalized analysis of cancer. Proc. Natl. Acad. Sci. U.S.A 110, 6388-6393.

[0659] Dumbrava, E. I., Alfattal, R., Miller, V. A., and Tsimberidou, A. M. (2018). Complete Response to a Fibroblast Growth Factor Receptor Inhibitor in a Patient With Head and Neck Squamous Cell Carcinoma Harboring FGF Amplifications. JCO Precis Oncol 2.

[0660] Duvvuri, U., George, J., Kim, S., Alvarado, D., Neumeister, V. M., Chenna, A., Gedrich, R., Hawthorne, T., LaVallee, T., Grandis, J. R., et al. (2019). Molecular and Clinical Activity of CDX-3379, an Anti-ErbB3 Monoclonal Antibody, in Head and Neck Squamous Cell Carcinoma Patients. Clin. Cancer Res. 25, 5752-5758.

[0661] Eckhardt, M., Zhang, W., Gross, A. M., Von Dollen, J., Johnson, J. R., Franks-Skiba, K. E., Swaney, D. L., Johnson, T. L., Jang, G. M., Shah, P. S., et al. (2018). Multiple Routes to Oncogenesis Are Promoted by the Human Papillomavirus-Host Protein Network. Cancer Discov. 8, 1474-1489.

[0662] Fan, W., Tang, Z., Chen, D., Moughon, D., Ding, X., Chen, S., Zhu, M., and Zhong, Q. (2010). Keapl facilitates p62-mediated ubiquitin aggregate clearance via autophagy. Autophagy 6, 614-621.

[0663] Feng, Y., and Longmore, G. D. (2005). The LIM protein Ajuba influences interleukin-1-induced NF-kappaB A activation by affecting the assembly and activity of the protein kinase Czeta/p62/TRAF6 signaling complex. Mol. Cell. Biol. 25, 4010-4022.

[0664] Fusté, N. P., Castelblanco, E., Felip, I., Santacana, M., Fernández-Hernández, R., Gatius, S., Pedraza, N., Pallards, J., Cemeli, T., Valls, J., et al. (2016). Characterization of cytoplasmic cyclin D1 as a marker of invasiveness in cancer. Oncotarget 7, 26979-26991.

[0665] Gkeka, P., Evangelidis, T., Pavlaki, M., Lazani, V., Christoforidis, S., Agianian, B., and Cournia, Z. (2014). Investigating the structure and dynamics of the PIK3C A wild-type and H1047R oncogenic mutant. PloS Comput. Biol. 10, e1003895.

[0666] Goetz, E. M., Ghandi, M., Treacy, D. J., Wagle, N., and Garraway, L. A. (2014). ERK mutations confer resistance to mitogen-activated protein kinase pathway inhibitors. Cancer Res. 74, 7079-7089.

[0667] Hamilton, E., and Infante, J. R. (2016). Targeting CDK4/6 in patients with cancer. Cancer Treat. Rev. 45, 129-138.

[0668] Hanahan, D., and Weinberg, R. A. (2011). Hallmarks of cancer: the next generation. Cell 144, 646-674.

[0669] Hanahan, D., Douglas, H., and Weinberg, R. A. (2000). The Hallmarks of Cancer. Cell 100, 57-70.

[0670] Haraguchi, K., Ohsugi, M., Abe, Y., Semba, K., Akiyama, T., and Yamamoto, T. (2008). Ajuba negatively regulates the Wnt signaling pathway by promoting GSK-3beta-mediated phosphorylation of beta-catenin. Oncogene 27, 274-284.

[0671] Hein, M. Y., Hubner, N. C., Poser, I., Cox, J., Nagaraj, N., Toyoda, Y., Gak, I. A., Weisswange, I., Mansfeld, J., Buchholz, F., et al. (2015). A Human Interactome in Three Quantitative Dimensions Organized by Stoichiometries and Abundances. Cell 163, 712-723.

[0672] Hoadley, K. A., Yau, C., Hinoue, T., Wolf, D. M., Lazar, A. J., Drill, E., Shen, R., Taylor, A. M., Cherniack, A. D., Thorsson, V., et al. (2018). Cell-of-Origin Patterns Dominate the Molecular Classification of 10,000 Tumors from 33 Types of Cancer. Cell 173, 291-304.e6.

[0673] Hofree, M., Shen, J. P., Carter, H., Gross, A., and Ideker, T. (2013). Network-based stratification of tumor mutations. Nat. Methods 10, 1108-1115.

[0674] Horn, H., Lawrence, M. S., Chouinard, C. R., Shrestha, Y., Hu, J. X., Worstell, E., Shea, E., Ilic, N., Kim, E., Kamburov, A., et al. (2018). NetSig: network-based discovery from cancer genomes. Nat. Methods 15, 61-66.

[0675] Huttlin, E. L., Ting, L., Bruckner, R. J., Gebreab, F., Gygi, M. P., Szpyt, J., Tam, S., Zarraga, G., Colby, G., Baltier, K., et al. (2015). The BioPlex Network: A Systematic Exploration of the Human Interactome. Cell 162, 425-440.

[0676] Huttlin, E. L., Bruckner, R. J., Paulo, J. A., Cannon, J. R., Ting, L., Baltier, K., Colby, G., Gebreab, F., Gygi, M. P., Parzen, H., et al. (2017). Architecture of the human interactome defines protein communities and disease networks. Nature 545, 505-509.

[0677] Huttlin, E. L., Bruckner, R. J., Navarrete-Perea, J., Cannon, J. R., Baltier, K., Gebreab, F., Gygi, M. P., Thornock, A., Zarraga, G., Tam, S., et al. (2020). Dual Proteome-scale Networks Reveal Cell-specific Remodeling of the Human Interactome.

[0678] Inoue, A., Raimondi, F., Kadji, F. M. N., Singh, G., Kishi, T., Uwamizu, A., Ono, Y., Shinjo, Y., Ishida, S., Arang, N., et al. (2019). Illuminating G-Protein-Coupling Selectivity of GPCRs. Cell 177, 1933-1947.e25.

[0679] Ishida-Takagishi, M., Enomoto, A., Asai, N., Ushida, K., Watanabe, T., Hashimoto, T., Kato, T., Weng, L., Matsumoto, S., Asai, M., et al. (2012). The Dishevelled-associating protein Daple controls the non-canonical A Wnt/Rac pathway and cell motility. Nat. Commun. 3, 859.

[0680] Jäger, S., Cimermancic, P., Gulbahce, N., Johnson, J. R., McGovern, K. E., Clarke, S. C., Shales, M., Mercenne, G., Pache, L., Li, K., et al. (2011). Global landscape of HIV-human protein complexes. Nature 481, 365-370.

[0681] Janku, F., Yap, T. A., and Meric-Bernstam, F. (2018). Targeting the PI3K pathway in cancer: are we making headway? Nat. Rev. Clin. Oncol. 15, 273-291.

[0682] Kalkat, M., Resetca, D., Lourenco, C., Chan, P.-K., Wei, Y., Shiah, Y.-J., Vitkin, N., Tong, Y., Sunnerhagen, M., Done, S. J., et al. (2018). MYC Protein Interactome Profiling Reveals Functionally Distinct Regions that Cooperate to Drive Tumorigenesis. Mol. Cell 72, 836-848.e7.

[0683] Klykov, O., Steigenberger, B., Pekta, S., Fasci, D., Heck, A. J. R., and Scheltema, R. A. (2018). Efficient and robust proteome-wide approaches for cross-linking mass spectrometry. Nat. Protoc.

[0684] Koren, I., Reem, E., and Kimchi, A. (2010a). Autophagy gets a brake: DAPi, a novel mTOR substrate, is activated to suppress the autophagic process. Autophagy 6, 1179-1180.

[0685] Koren, I., Reem, E., and Kimchi, A. (2010b). DAP1, a novel substrate of mTOR, negatively regulates autophagy. Curr. Biol. 20, 1093-1098.

[0686] Krogan, N. J., Lippman, S., Agard, D. A., Ashworth, A., and Ideker, T. (2015). The cancer cell map initiative: defining the hallmark networks of cancer. Mol. Cell 58, 690-698.

[0687] Lau, A., Wang, X.-J., Zhao, F., Villeneuve, N. F., Wu, T., Jiang, T., Sun, Z., White, E., and Zhang, D. D. (2010). A noncanonical mechanism of Nrf2 activation by autophagy deficiency: direct interaction between Keap1 and p62. Mol. Cell. Biol. 30, 3275-3285.

[0688] Lee, S., Greenlee, E. B., Amick, J. R., Ligon, G. F., Lillquist, J. S., Natoli, E. J., Jr, Hadari, Y., Alvarado, D., and Schlessinger, J. (2015). Inhibition of ErbB3 by a monoclonal antibody that locks the extracellular domain in an inactive configuration. Proc. Natl. Acad. Sci. U.S.A 112, 13225-13230.

[0689] Leiserson, M. D. M., Vandin, F., Wu, H.-T., Dobson, J. R., Eldridge, J. V., Thomas, J. L., Papoutsaki, A., Kim, Y., Niu, B., McLellan, M., et al. (2015). Pan-cancer network analysis identifies combinations of rare somatic mutations across pathways and protein complexes. Nat. Genet. 47, 106-114.

[0690] Li, H., Wawrose, J. S., Gooding, W. E., Garraway, L. A., Lui, V. W. Y., Peyser, N. D., and Grandis, J. R. (2014). Genomic Analysis of Head and Neck Squamous

Cell Carcinoma Cell Lines and Human Tumors: A Rational Approach to Preclinical Model Selection. Mol. Cancer Res. 12, 571-582.

[0691] Li, T., Wernersson, R., Hansen, R. B., Horn, H., Mercer, J., Slodkowicz, G., Workman, C. T., Rigina, O., Rapacki, K., Storfeldt, H. H., et al. (2016). A scored human protein-protein interaction network to catalyze genomic interpretation. Nat. Methods.

[0692] Liu, S., Knapp, S., and Ahmed, A. A. (2014). The structural basis of PI3K cancer mutations: from mechanism to therapy. Cancer Res. 74, 641-646.

[0693] Lobingier, B. T., Htittenhain, R., Eichel, K., Miller, K. B., Ting, A. Y., von Zastrow, M., and Krogan, N. J. (2017). An Approach to Spatiotemporally Resolve Protein Interaction Networks in Living Cells. Cell 169, 350-360. e12.

[0694] Luck, K., Kim, D.-K., Lambourne, L., Spirohn, K., Begg, B. E., Bian, W., Brignall, R., Cafarelli, T., Campos-Laborie, F. J., Charloteaux, B., et al. (2020). A reference map of the human binary protein interactome. Nature 580, 402-408.

[0695] Lui, V. W. Y., Hedberg, M. L., Li, H., Vangara, B. S., Pendleton, K., Zeng, Y., Lu, Y., Zhang, Q., Du, Y., Gilbert, B. R., et al. (2013). Frequent Mutation of the PI3K Pathway in Head and Neck Cancer Defines Predictive A Biomarkers. Cancer Discov. 3, 761-769.

[0696] MacLean, B., Tomazela, D. M., Shulman, N., Chambers, M., Finney, G. L., Frewen, B., Kern, R., Tabb, D. L., Liebler, D. C., and MacCoss, M. J. (2010). Skyline: an open source document editor for creating and analyzing targeted proteomics experiments. Bioinformatics 26, 966-968.

[0697] Mahalingam, M., Arvind, R., and Ida, H. (2008). ERK2 C D domain mutation from a human cancer cell line enhanced anchorage-independent cell growth and abnormality in *Drosophila*. Oncology.

[0698] Marinkovich, M. P. (2007). Tumour microenvironment: laminin 332 in squamous-cell carcinoma. Nat. Rev. Cancer 7, 370-380.

[0699] Martin, D., Abba, M. C., Molinolo, A. A., Vitale-Cross, L., Wang, Z., Zaida, M., Delic, N. C., Samuels, Y., Lyons, J. G., and Gutkind, J. S. (2014). The head and neck cancer cell oncogenome: a platform for the development of precision molecular therapies. Oncotarget 5, 8906-8923.

[0700] Miled, N., Yan, Y., Hon, W.-C., Perisic, O., Zvelebil, M., Inbar, Y., Schneidman-Duhovny, D., Wolfson, H. J., Backer, J. M., and Williams, R. L. (2007). Mechanism of two classes of cancer mutations in the phosphoinositide 3-kinase catalytic subunit. Science 317, 239-242.

[0701] Molinolo, A. A., Amornphimoltham, P., Squarize, C. H., Castilho, R. M., Patel, V., and Gutkind, J. S. (2009). Dysregulated molecular networks in head and neck carcinogenesis. Oral Oncol. 45, 324-334.

[0702] Nolte, H., MacVicar, T. D., Tellkamp, F., and Kruger, M. (2018). Instant Clue: A Software Suite for Interactive Data Visualization and Analysis. Sci. Rep. 8, 12648.

[0703] Oshita, A., Kishida, S., Kobayashi, H., Michiue, T., Asahara, T., Asashima, M., and Kikuchi, A. (2003). Identification and characterization of a novel Dvl-binding protein that suppresses Wnt signalling pathway. Genes Cells 8, 1005-1017.

[0704] Paczkowska, M., Barenboim, J., Sintupisut, N., Fox, N. S., Zhu, H., Abd-Rabbo, D., Mee, M. W., Boutros, P. C., PCAWG Drivers and Functional Interpretation Working Group, Reimand, J., et al. (2020). Integrative pathway enrichment analysis of multivariate omics data. Nat. Commun. 11, 735.

[0705] Park, J., Kim, J.-M., Park, J. K., Huang, S., Kwak, S. Y., Ryu, K. A., Kong, G., Park, J., and Koo, B. S. (2015). Association of p21-activated kinase-1 activity with aggressive tumor behavior and poor prognosis of head and neck cancer. Head Neck 37, 953-963.

[0706] Parvathy, M., Sreeja, S., Kumar, R., and Pillai, M. R. (2016). Potential role of p21 Activated Kinase 1 (PAKI) in the invasion and motility of oral cancer cells. BMC Cancer 16 Suppl 1, 293.

[0707] Paull, E. O., Carlin, D. E., Niepel, M., Sorger, P. K., Haussler, D., and Stuart, J. M. (2013). Discovering causal pathways linking genomic events to transcriptional states using Tied Diffusion Through Interacting Events (TieDIE). Bioinformatics 29, 2757-2764.

[0708] Perez-Riverol, Y., Csordas, A., Bai, J., Bernal-Llinares, M., Hewapathirana, S., Kundu, D. J., Inuganti, A., Griss, J., Mayer, G., Eisenacher, M., et al. (2019). The PRIDE database and related tools and resources in 2019: improving support for quantification data. Nucleic Acids Res. 47, D442-D450.

[0709] Pyndiah, S., Tanida, S., Ahmed, K. M., Cassimere, E. K., Choe, C., and Sakamuro, D. (2011). c-MYC Suppresses BIN1 to Release Poly(ADP-Ribose) Polymerase 1: A Mechanism by Which Cancer Cells Acquire Cisplatin Resistance. Sci. Signal. 4, ra19-ra19.

[0710] Reyna, M. A., Haan, D., Paczkowska, M., Verbeke, L. P. C., Vazquez, M., Kahraman, A., Pulido-Tamayo, S., Barenboim, J., Wadi, L., Dhingra, P., et al. (2020). Pathway and network analysis of more than 2500 whole A cancer genomes. Nat. Commun. 11, 729.

[0711] Riaz, N., Morris, L. G., Lee, W., and Chan, T. A. (2014). Unraveling the molecular genetics of head and neck cancer through genome-wide approaches. Genes Dis 1, 75-86.

[0712] Robinson, D., Van Allen, E. M., Wu, Y. M., Schultz, N., Lonigro, R. J., Mosquera, J. M., Montgomery, B., Taplin, M. E., Pritchard, C. C., Attard, G., et al. (2015). Integrative Clinical Genomics of Advanced Prostate Cancer. Cell 162, 454.

[0713] Rolland, T., Ta an, M., Charloteaux, B., Pevzner, S. J., Zhong, Q., Sahni, N., Y_i, S., Lemmens, I., Fontanillo, C., Mosca, R., et al. (2014). A Proteome-Scale Map of the Human Interactome Network. Cell 159, 1212-1226.

[0714] Rudd, M. L., Price, J. C., Fogoros, S., Godwin, A. K., Sgroi, D. C., Merino, M. J., and Bell, D. W. (2011). A unique spectrum of somatic PIK3C A (p110alpha) mutations within primary endometrial carcinomas. Clin. Cancer Res. 17, 1331-1340.

[0715] Salas, D., Stacey, R. G., Akinlaja, M., and Foster, L. J. (2020). Next-generation Interactomics: Considerations for the Use of Co-elution to Measure Protein Interaction Networks. Mol. Cell. Proteomics 19, 1-10.

[0716] Samavarchi-Tehrani, P., Samson, R., and Gingras, A.-C. (2020). Proximity dependent biotinylation: key enzymes and adaptation to proteomics approaches. Mol. Cell. Proteomics.

[0717] Schuler, M., Cho, B. C., Sayehli, C. M., Navarro, A., Soo, R. A., Richly, H., Cassier, P. A., Tai, D., Penel,

N., Nogova, L., et al. (2019). Rogaratinib in patients with advanced cancers selected by FGFR mRNA expression: a phase 1 dose-escalation and dose-expansion study. Lancet Oncol. 20, 1454-1466.

[0718] Shekar, S. C., Wu, H., Fu, Z., Yip, S.-C., Nagajyothi, Cahill, S. M., Girvin, M. E., and Backer, J. M. (2005). Mechanism of constitutive phosphoinositide 3-kinase activation by oncogenic mutants of the p85 regulatory subunit. J. Biol. Chem. 280, 27850-27855.

[0719] Shibata, T., Ohta, T., Tong, K. I., Kokubu, A., Odogawa, R., Tsuta, K., Asamura, H., Yamamoto, M., and Hirohashi, S. (2008). Cancer related mutations in NRF2 impair its recognition by Keap1-Cul3 E3 ligase and promote malignancy. Proc. Natl. Acad. Sci. U.S.A. 105, 13568-13573.

[0720] Songyang, Z., Shoelson, S. E., McGlade, J., Olivier, P., Pawson, T., Bustelo, X. R., Barbacid, M., Sabe, H., Hanafusa, H., and Y_i, T. (1994). Specific motifs recognized by the SH2 domains of Csk, 3BP2, fps/fes, GRB-2, HCP, SHC, Syk, and Vav. Mol. Cell. Biol. 14, 2777-2785.

[0721] Sowa, M. E., Bennett, E. J., Gygi, S. P., and Harper, J. W. (2009). Defining the Human Deubiquitinating Enzyme Interaction Landscape. Cell 138, 389-403.

[0722] Stephens, P. J., Tarpey, P. S., Davies, H., Van Loo, P., Greenman, C., Wedge, D. C., Nik-Zainal, S., Martin, S., Varela, I., Bignell, G. R., et al. (2012). The landscape of cancer genes and mutational processes in breast cancer. Nature 486, 400-404.

[0723] Stransky, N., Egloff, A. M., Tward, A. D., Kostic, A. D., Cibulskis, K., Sivachenko, A., Kryukov, G. V., Lawrence, M. S., Sougnez, C., McKenna, A., et al. (2011). The mutational landscape of head and neck squamous cell carcinoma. Science 333, 1157-1160.

[0724] Taguchi, K., and Yamamoto, M. (2017). The KEAP1-NRF2 System in Cancer. Front. Oncol. 7, 85.

[0725] Takahashi, Y., Coppola, D., Matsushita, N., Cualing, H. D., Sun, M., Sato, Y., Liang, C., Jung, J. U., Cheng, J. Q., Muld, J. J., et al. (2007). Bif-1 interacts with Beclin 1 through UVRAG and regulates autophagy and tumorigenesis. Nat. Cell Biol. 9, 1142-1151.

[0726] Taylor, C. A., 4th, Cormier, K. W., Keenan, S. E., Earnest, S., Stippec, S., Wichaidit, C., Juang, Y.-C., Wang, J., A Shvartsman, S. Y., Goldsmith, E. J., et al. (2019). Functional divergence caused by mutations in an energetic hotspot in ERK2. Proc. Natl. Acad. Sci. U.S.A. 116, 15514-15523.

[0727] Teo, G., Liu, G., Zhang, J., Nesvizhskii, A. I., Gingras, A.-C., and Choi, H. (2014). SAINTexpress: improvements and additional features in Significance Analysis of INTeractome software. J. Proteomics 100, 37-43.

[0728] Tsuruta, D., Kobayashi, H., Imanishi, H., Sugawara, K., Ishii, M., and Jones, J. C. R. (2008).

[0729] Laminin-332-integrin interaction: a target for cancer therapy? Curr. Med. Chem. 15, 1968-1975.

[0730] Vizcaíno, J. A., Deutsch, E. W., Wang, R., Csordas, A., Reisinger, F., Ríos, D., Dianes, J. A., Sun, Z., Farrah, T., Bandeira, N., et al. (2014). ProteomeXchange provides globally coordinated proteomics data submission and dissemination. Nat. Biotechnol. 32, 223-226.

[0731] Vogelstein, B., Bert, V., and Kinzler, K. W. (2004). Cancer genes and the pathways they control. Nat. Med. 10, 789-799.

[0732] Yu, K., Chen, B., Aran, D., Charalel, J., Yau, C., Wolf, D. M., van't Veer, L. J., Butte, A. J., Goldstein, T., and Sirota, M. (2019). Comprehensive transcriptomic analysis of cell lines as models of primary tumors across 22 tumor types. Nat. Commun. 10, 3574.

[0733] Zhao, L., and Vogt, P. K. (2008). Helical domain and kinase domain mutations in p110alpha of phosphatidylinositol 3-kinase induce gain of function by different mechanisms. Proc. Natl. Acad. Sci. U.S.A 105, 2652-2657.

[0734] Zhao, Y., Zhang, X., Chen, Y., Lu, S., Peng, Y., Wang, X., Guo, C., Zhou, A., Zhang, J., Luo, Y., et al. (2014). Crystal Structures of PI3Kα Complexed with PI103 and Its Derivatives: New Directions for Inhibitors Design. ACS Med. Chem. Lett. 5, 138-142.

[0735] Zheng, F., Tutuncuoglu, B., Ono, K., Swaney, D. L., Kim, M., Silva, E., Liu, S., Park, J., Kratz, A., Yu, M. K., et al. Convergence of cancer mutation on a hierarchy of protein systems. Submitted.

[0736] It will be apparent to those skilled in the art that various modifications and variations can be made in the present invention without departing from the scope or spirit of the invention. Other embodiments of the invention will be apparent to those skilled in the art from consideration of the specification and practice of the invention disclosed herein. It is intended that the specification and examples be considered as exemplary only, with a true scope and spirit of the invention being indicated by the following claims.

SEQUENCE LISTING

<160> NUMBER OF SEQ ID NOS: 16

<210> SEQ ID NO 1
<211> LENGTH: 393
<212> TYPE: PRT
<213> ORGANISM: Homo sapiens

<400> SEQUENCE: 1

```
Met Glu Glu Pro Gln Ser Asp Pro Ser Val Glu Pro Pro Leu Ser Gln
1               5                  10                  15

Glu Thr Phe Ser Asp Leu Trp Lys Leu Leu Pro Glu Asn Asn Val Leu
            20                  25                  30
```

-continued

```
Ser Pro Leu Pro Ser Gln Ala Met Asp Asp Leu Met Leu Ser Pro Asp
        35                  40                  45

Asp Ile Glu Gln Trp Phe Thr Glu Asp Pro Gly Pro Asp Glu Ala Pro
    50                  55                  60

Arg Met Pro Glu Ala Ala Pro Pro Val Ala Pro Ala Pro Ala Ala Pro
65                  70                  75                  80

Thr Pro Ala Ala Pro Ala Pro Ala Pro Ser Trp Pro Leu Ser Ser Ser
                85                  90                  95

Val Pro Ser Gln Lys Thr Tyr Gln Gly Ser Tyr Gly Phe Arg Leu Gly
            100                 105                 110

Phe Leu His Ser Gly Thr Ala Lys Ser Val Thr Cys Thr Tyr Ser Pro
        115                 120                 125

Ala Leu Asn Lys Met Phe Cys Gln Leu Ala Lys Thr Cys Pro Val Gln
    130                 135                 140

Leu Trp Val Asp Ser Thr Pro Pro Pro Gly Thr Arg Val Arg Ala Met
145                 150                 155                 160

Ala Ile Tyr Lys Gln Ser Gln His Met Thr Glu Val Val Arg Arg Cys
                165                 170                 175

Pro His His Glu Arg Cys Ser Asp Ser Asp Gly Leu Ala Pro Pro Gln
            180                 185                 190

His Leu Ile Arg Val Glu Gly Asn Leu Arg Val Glu Tyr Leu Asp Asp
        195                 200                 205

Arg Asn Thr Phe Arg His Ser Val Val Val Pro Tyr Glu Pro Pro Glu
    210                 215                 220

Val Gly Ser Asp Cys Thr Thr Ile His Tyr Asn Tyr Met Cys Asn Ser
225                 230                 235                 240

Ser Cys Met Gly Gly Met Asn Arg Arg Pro Ile Leu Thr Ile Ile Thr
                245                 250                 255

Leu Glu Asp Ser Ser Gly Asn Leu Leu Gly Arg Asn Ser Phe Glu Val
            260                 265                 270

Arg Val Cys Ala Cys Pro Gly Arg Asp Arg Arg Thr Glu Glu Glu Asn
        275                 280                 285

Leu Arg Lys Lys Gly Glu Pro His His Glu Leu Pro Pro Gly Ser Thr
    290                 295                 300

Lys Arg Ala Leu Pro Asn Asn Thr Ser Ser Ser Pro Gln Pro Lys Lys
305                 310                 315                 320

Lys Pro Leu Asp Gly Glu Tyr Phe Thr Leu Gln Ile Arg Gly Arg Glu
                325                 330                 335

Arg Phe Glu Met Phe Arg Glu Leu Asn Glu Ala Leu Glu Leu Lys Asp
            340                 345                 350

Ala Gln Ala Gly Lys Glu Pro Gly Gly Ser Arg Ala His Ser Ser His
        355                 360                 365

Leu Lys Ser Lys Lys Gly Gln Ser Thr Ser Arg His Lys Lys Leu Met
    370                 375                 380

Phe Lys Thr Glu Gly Pro Asp Ser Asp
385                 390


<210> SEQ ID NO 2
<211> LENGTH: 173
<212> TYPE: PRT
<213> ORGANISM: Unknown
<220> FEATURE:
<223> OTHER INFORMATION: Description of Unknown:
```

-continued

PIK3CA sequence

<400> SEQUENCE: 2

```
Met Gln Pro Phe Ser Ile Pro Val Gln Ile Thr Leu Gln Gly Ser Arg
1               5                   10                  15

Arg Arg Gln Gly Arg Thr Ala Phe Pro Ala Ser Gly Lys Lys Arg Glu
            20                  25                  30

Thr Asp Tyr Ser Asp Gly Asp Pro Leu Asp Val His Lys Arg Leu Pro
        35                  40                  45

Ser Ser Ala Gly Glu Asp Arg Ala Val Met Leu Gly Phe Ala Met Met
    50                  55                  60

Gly Phe Ser Val Leu Met Phe Phe Leu Leu Gly Thr Thr Ile Leu Lys
65                  70                  75                  80

Pro Phe Met Leu Ser Ile Gln Arg Glu Glu Ser Thr Cys Thr Ala Ile
                85                  90                  95

His Thr Asp Ile Met Asp Asp Trp Leu Asp Cys Ala Phe Thr Cys Gly
            100                 105                 110

Val His Cys His Gly Gln Gly Lys Tyr Pro Cys Leu Gln Val Phe Val
        115                 120                 125

Asn Leu Ser His Pro Gly Gln Lys Ala Leu Leu His Tyr Asn Glu Glu
    130                 135                 140

Ala Val Gln Ile Asn Pro Lys Arg Asp Val Thr Asp Cys Arg Val Lys
145                 150                 155                 160

Glu Lys Gln Thr Leu Thr Val Ser Asp Glu His Lys Gln
                165                 170
```

<210> SEQ ID NO 3
<211> LENGTH: 1068
<212> TYPE: PRT
<213> ORGANISM: Unknown
<220> FEATURE:
<223> OTHER INFORMATION: Description of Unknown:
PIK3CA sequence

<400> SEQUENCE: 3

```
Met Pro Pro Arg Pro Ser Ser Gly Glu Leu Trp Gly Ile His Leu Met
1               5                   10                  15

Pro Pro Arg Ile Leu Val Glu Cys Leu Leu Pro Asn Gly Met Ile Val
            20                  25                  30

Thr Leu Glu Cys Leu Arg Glu Ala Thr Leu Ile Thr Ile Lys His Glu
        35                  40                  45

Leu Phe Lys Glu Ala Arg Lys Tyr Pro Leu His Gln Leu Leu Gln Asp
    50                  55                  60

Glu Ser Ser Tyr Ile Phe Val Ser Val Thr Gln Glu Ala Glu Arg Glu
65                  70                  75                  80

Glu Phe Phe Asp Glu Thr Arg Arg Leu Cys Asp Leu Arg Leu Phe Gln
                85                  90                  95

Pro Phe Leu Lys Val Ile Glu Pro Val Gly Asn Arg Glu Glu Lys Ile
            100                 105                 110

Leu Asn Arg Glu Ile Gly Phe Ala Ile Gly Met Pro Val Cys Glu Phe
        115                 120                 125

Asp Met Val Lys Asp Pro Glu Val Gln Asp Phe Arg Arg Asn Ile Leu
    130                 135                 140

Asn Val Cys Lys Glu Ala Val Asp Leu Arg Asp Leu Asn Ser Pro His
```

-continued

```
145                 150                 155                 160

Ser Arg Ala Met Tyr Val Tyr Pro Pro Asn Val Glu Ser Ser Pro Glu
                165                 170                 175

Leu Pro Lys His Ile Tyr Asn Lys Leu Asp Lys Gly Gln Ile Ile Val
            180                 185                 190

Val Ile Trp Val Ile Val Ser Pro Asn Asn Asp Lys Gln Lys Tyr Thr
        195                 200                 205

Leu Lys Ile Asn His Asp Cys Val Pro Glu Gln Val Ile Ala Glu Ala
    210                 215                 220

Ile Arg Lys Lys Thr Arg Ser Met Leu Leu Ser Ser Glu Gln Leu Lys
225                 230                 235                 240

Leu Cys Val Leu Glu Tyr Gln Gly Lys Tyr Ile Leu Lys Val Cys Gly
                245                 250                 255

Cys Asp Glu Tyr Phe Leu Glu Lys Tyr Pro Leu Ser Gln Tyr Lys Tyr
            260                 265                 270

Ile Arg Ser Cys Ile Met Leu Gly Arg Met Pro Asn Leu Met Leu Met
        275                 280                 285

Ala Lys Glu Ser Leu Tyr Ser Gln Leu Pro Met Asp Cys Phe Thr Met
    290                 295                 300

Pro Ser Tyr Ser Arg Arg Ile Ser Thr Ala Thr Pro Tyr Met Asn Gly
305                 310                 315                 320

Glu Thr Ser Thr Lys Ser Leu Trp Val Ile Asn Ser Ala Leu Arg Ile
                325                 330                 335

Lys Ile Leu Cys Ala Thr Tyr Val Asn Val Asn Ile Arg Asp Ile Asp
            340                 345                 350

Lys Ile Tyr Val Arg Thr Gly Ile Tyr His Gly Gly Glu Pro Leu Cys
        355                 360                 365

Asp Asn Val Asn Thr Gln Arg Val Pro Cys Ser Asn Pro Arg Trp Asn
    370                 375                 380

Glu Trp Leu Asn Tyr Asp Ile Tyr Ile Pro Asp Leu Pro Arg Ala Ala
385                 390                 395                 400

Arg Leu Cys Leu Ser Ile Cys Ser Val Lys Gly Arg Lys Gly Ala Lys
                405                 410                 415

Glu Glu His Cys Pro Leu Ala Trp Gly Asn Ile Asn Leu Phe Asp Tyr
            420                 425                 430

Thr Asp Thr Leu Val Ser Gly Lys Met Ala Leu Asn Leu Trp Pro Val
        435                 440                 445

Pro His Gly Leu Glu Asp Leu Leu Asn Pro Ile Gly Val Thr Gly Ser
    450                 455                 460

Asn Pro Asn Lys Glu Thr Pro Cys Leu Glu Leu Glu Phe Asp Trp Phe
465                 470                 475                 480

Ser Ser Val Val Lys Phe Pro Asp Met Ser Val Ile Glu Glu His Ala
                485                 490                 495

Asn Trp Ser Val Ser Arg Glu Ala Gly Phe Ser Tyr Ser His Ala Gly
            500                 505                 510

Leu Ser Asn Arg Leu Ala Arg Asp Asn Glu Leu Arg Glu Asn Asp Lys
        515                 520                 525

Glu Gln Leu Lys Ala Ile Ser Thr Arg Asp Pro Leu Ser Glu Ile Thr
    530                 535                 540

Glu Gln Glu Lys Asp Phe Leu Trp Ser His Arg His Tyr Cys Val Thr
545                 550                 555                 560
```

-continued

```
Ile Pro Glu Ile Leu Pro Lys Leu Leu Leu Ser Val Lys Trp Asn Ser
                565                 570                 575

Arg Asp Glu Val Ala Gln Met Tyr Cys Leu Val Lys Asp Trp Pro Pro
            580                 585                 590

Ile Lys Pro Glu Gln Ala Met Glu Leu Leu Asp Cys Asn Tyr Pro Asp
        595                 600                 605

Pro Met Val Arg Gly Phe Ala Val Arg Cys Leu Glu Lys Tyr Leu Thr
    610                 615                 620

Asp Asp Lys Leu Ser Gln Tyr Leu Ile Gln Leu Val Gln Val Leu Lys
625                 630                 635                 640

Tyr Glu Gln Tyr Leu Asp Asn Leu Leu Val Arg Phe Leu Leu Lys Lys
                645                 650                 655

Ala Leu Thr Asn Gln Arg Ile Gly His Phe Phe Phe Trp His Leu Lys
            660                 665                 670

Ser Glu Met His Asn Lys Thr Val Ser Gln Arg Phe Gly Leu Leu Leu
        675                 680                 685

Glu Ser Tyr Cys Arg Ala Cys Gly Met Tyr Leu Lys His Leu Asn Arg
    690                 695                 700

Gln Val Glu Ala Met Glu Lys Leu Ile Asn Leu Thr Asp Ile Leu Lys
705                 710                 715                 720

Gln Glu Lys Lys Asp Glu Thr Gln Lys Val Gln Met Lys Phe Leu Val
                725                 730                 735

Glu Gln Met Arg Arg Pro Asp Phe Met Asp Ala Leu Gln Gly Phe Leu
            740                 745                 750

Ser Pro Leu Asn Pro Ala His Gln Leu Gly Asn Leu Arg Leu Glu Glu
        755                 760                 765

Cys Arg Ile Met Ser Ser Ala Lys Arg Pro Leu Trp Leu Asn Trp Glu
    770                 775                 780

Asn Pro Asp Ile Met Ser Glu Leu Leu Phe Gln Asn Asn Glu Ile Ile
785                 790                 795                 800

Phe Lys Asn Gly Asp Asp Leu Arg Gln Asp Met Leu Thr Leu Gln Ile
                805                 810                 815

Ile Arg Ile Met Glu Asn Ile Trp Gln Asn Gln Gly Leu Asp Leu Arg
            820                 825                 830

Met Leu Pro Tyr Gly Cys Leu Ser Ile Gly Asp Cys Val Gly Leu Ile
        835                 840                 845

Glu Val Val Arg Asn Ser His Thr Ile Met Gln Ile Gln Cys Lys Gly
    850                 855                 860

Gly Leu Lys Gly Ala Leu Gln Phe Asn Ser His Thr Leu His Gln Trp
865                 870                 875                 880

Leu Lys Asp Lys Asn Lys Gly Glu Ile Tyr Asp Ala Ala Ile Asp Leu
                885                 890                 895

Phe Thr Arg Ser Cys Ala Gly Tyr Cys Val Ala Thr Phe Ile Leu Gly
            900                 905                 910

Ile Gly Asp Arg His Asn Ser Asn Ile Met Val Lys Asp Asp Gly Gln
        915                 920                 925

Leu Phe His Ile Asp Phe Gly His Phe Leu Asp His Lys Lys Lys Lys
    930                 935                 940

Phe Gly Tyr Lys Arg Glu Arg Val Pro Phe Val Leu Thr Gln Asp Phe
945                 950                 955                 960
```

-continued

Leu Ile Val Ile Ser Lys Gly Ala Gln Glu Cys Thr Lys Thr Arg Glu
965 970 975

Phe Glu Arg Phe Gln Glu Met Cys Tyr Lys Ala Tyr Leu Ala Ile Arg
980 985 990

Gln His Ala Asn Leu Phe Ile Asn Leu Phe Ser Met Met Leu Gly Ser
995 1000 1005

Gly Met Pro Glu Leu Gln Ser Phe Asp Asp Ile Ala Tyr Ile Arg
1010 1015 1020

Lys Thr Leu Ala Leu Asp Lys Thr Glu Gln Glu Ala Leu Glu Tyr
1025 1030 1035

Phe Met Lys Gln Met Asn Asp Ala His His Gly Gly Trp Thr Thr
1040 1045 1050

Lys Met Asp Trp Ile Phe His Thr Ile Lys Gln His Ala Leu Asn
1055 1060 1065

<210> SEQ ID NO 4
<211> LENGTH: 3008
<212> TYPE: DNA
<213> ORGANISM: Unknown
<220> FEATURE:
<223> OTHER INFORMATION: Description of Unknown:
Akt1 sequence

<400> SEQUENCE: 4

taattatggg tctgtaacca ccctggactg ggtgctcctc actgacggac ttgtctgaac 60

ctctctttgt ctccagcgcc cagcactggg cctggcaaaa cctgagacgc ccggtacatg 120

ttggccaaat gaatgaacca gattcagacc ggcaggggcg ctgtggttta ggaggggcct 180

ggggtttctc ccaggaggtt tttgggcttg cgctggaggg ctctggactc ccgtttgcgc 240

cagtggcctg catcctggtc ctgtcttcct catgtttgaa tttctttgct ttcctagtct 300

ggggagcagg gaggagccct gtgccctgtc ccaggatcca tgggtaggaa caccatggac 360

agggagagca aacggggcca tctgtcacca ggggcttagg gaaggccgag ccagcctggg 420

tcaaagaagt caaaggggct gcctggagga ggcagcctgt cagctggtgc atcagaggct 480

gtggccaggc cagctgggct cggggagcgc cagcctgaga ggagcgcgtg agcgtcgcgg 540

gagcctcggg caccatgagc gacgtggcta ttgtgaagga gggttggctg cacaaacgag 600

gggagtacat caagacctgg cggccacgct acttcctcct caagaatgat ggcaccttca 660

ttggctacaa ggagcggccg caggatgtgg accaacgtga ggctcccctc aacaacttct 720

ctgtggcgca gtgccagctg atgaagacgg agcggccccg gcccaacacc ttcatcatcc 780

gctgcctgca gtggaccact gtcatcgaac gcaccttcca tgtggagact cctgaggagc 840

gggaggagtg gacaaccgcc atccagactg tggctgacgg cctcaagaag caggaggagg 900

aggagatgga cttccggtcg ggctcaccca gtgacaactc aggggctgaa gagatggagg 960

tgtccctggc caagcccaag caccgcgtga ccatgaacga gtttgagtac ctgaagctgc 1020

tgggcaaggg cactttcggc aaggtgatcc tggtgaagga gaaggccaca ggccgctact 1080

acgccatgaa gatcctcaag aaggaagtca tcgtggccaa ggacgaggtg gcccacacac 1140

tcaccgagaa ccgcgtcctg cagaactcca ggcacccctt cctcacagcc ctgaagtact 1200

ctttccagac ccacgaccgc ctctgctttg tcatggagta cgccaacggg ggcgagctgt 1260

tcttccacct gtcccgggag cgtgtgttct ccgaggaccg ggcccgcttc tatggcgctg 1320

-continued

agattgtgtc agccctggac tacctgcact cggagaagaa cgtggtgtac cgggacctca 1380

agctggagaa cctcatgctg gacaaggacg ggcacattaa gatcacagac ttcgggctgt 1440

gcaaggaggg gatcaaggac ggtgccacca tgaagacctt ttgcggcaca cctgagtacc 1500

tggcccccga ggtgctggag gacaatgact acggccgtgc agtggactgg tgggggctgg 1560

gcgtggtcat gtacgagatg atgtgcggtc gcctgccctt ctacaaccag gaccatgaga 1620

agctttttga gctcatcctc atggaggaga tccgcttccc gcgcacgctt ggtcccgagg 1680

ccaagtcctt gctttcaggg ctgctcaaga aggaccccaa gcagaggctt ggcgggggct 1740

ccgaggacgc caaggagatc atgcagcatc gcttctttgc cggtatcgtg tggcagcacg 1800

tgtacgagaa gaagctcagc ccacccttca agccccaggt cacgtcggag actgacacca 1860

ggtattttga tgaggagttc acggcccaga tgatcaccat cacaccacct gaccaagatg 1920

acagcatgga gtgtgtggac agcgagcgca ggccccactt cccccagttc tcctactcgg 1980

ccagcggcac ggcctgaggc ggcggtggac tgcgctggac gatagcttgg agggatggag 2040

aggcggcctc gtgccatgat ctgtatttaa tggtttttat ttctcgggtg catttgagag 2100

aagccacgct gtcctctcga gcccagatgg aaagacgttt ttgtgctgtg ggcagcaccc 2160

tcccccgcag cggggtaggg aagaaaacta tcctgcgggt tttaatttat ttcatccagt 2220

ttgttctccg ggtgtggcct cagccctcag aacaatccga ttcacgtagg gaaatgttaa 2280

ggacttctgc agctatgcgc aatgtggcat tgggggggccg ggcaggtcct gcccatgtgt 2340

cccctcactc tgtcagccag ccgccctggg ctgtctgtca ccagctatct gtcatctctc 2400

tggggccctg ggcctcagtt caacctggtg gcaccagatg caacctcact atggtatgct 2460

ggccagcacc ctctcctggg ggtggcaggc acacagcagc cccccagcac taaggccgtg 2520

tctctgagga cgtcatcgga ggctgggccc ctgggatggg accagggatg ggggatgggc 2580

cagggtttac ccagtgggac agaggagcaa ggtttaaatt tgttattgtg tattatgttg 2640

ttcaaatgca ttttgggggt ttttaatctt tgtgacagga aagccctccc ccttcccctt 2700

ctgtgtcaca gttcttggtg actgtcccac cgggagcctc cccctcagat gatctctcca 2760

cggtagcact tgacctttc gacgcttaac ctttccgctg tcgccccagg ccctccctga 2820

ctccctgtgg gggtggccat ccctgggccc ctccacgcct cctggccaga cgctgccgct 2880

gccgctgcac cacggcgttt ttttacaaca ttcaacttta gtatttttac tattataata 2940

taatatggaa ccttccctcc aaattcttca ataaaagttg cttttcaaaa aaaaaaaaaa 3000

aaaaaaaa 3008

<210> SEQ ID NO 5
<211> LENGTH: 1342
<212> TYPE: PRT
<213> ORGANISM: Unknown
<220> FEATURE:
<223> OTHER INFORMATION: Description of Unknown:
HER3 sequence

<400> SEQUENCE: 5

Met Arg Ala Asn Asp Ala Leu Gln Val Leu Gly Leu Leu Phe Ser Leu
1 5 10 15

Ala Arg Gly Ser Glu Val Gly Asn Ser Gln Ala Val Cys Pro Gly Thr
20 25 30

Leu Asn Gly Leu Ser Val Thr Gly Asp Ala Glu Asn Gln Tyr Gln Thr

-continued

```
        35                  40                  45

Leu Tyr Lys Leu Tyr Glu Arg Cys Glu Val Val Met Gly Asn Leu Glu
    50                  55                  60

Ile Val Leu Thr Gly His Asn Ala Asp Leu Ser Phe Leu Gln Trp Ile
65                  70                  75                  80

Arg Glu Val Thr Gly Tyr Val Leu Val Ala Met Asn Glu Phe Ser Thr
                85                  90                  95

Leu Pro Leu Pro Asn Leu Arg Val Val Arg Gly Thr Gln Val Tyr Asp
            100                 105                 110

Gly Lys Phe Ala Ile Phe Val Met Leu Asn Tyr Asn Thr Asn Ser Ser
        115                 120                 125

His Ala Leu Arg Gln Leu Arg Leu Thr Gln Leu Thr Glu Ile Leu Ser
    130                 135                 140

Gly Gly Val Tyr Ile Glu Lys Asn Asp Lys Leu Cys His Met Asp Thr
145                 150                 155                 160

Ile Asp Trp Arg Asp Ile Val Arg Asp Arg Asp Ala Glu Ile Val Val
                165                 170                 175

Lys Asp Asn Gly Arg Ser Cys Pro Pro Cys His Glu Val Cys Lys Gly
            180                 185                 190

Arg Cys Trp Gly Pro Gly Ser Glu Asp Cys Gln Thr Leu Thr Lys Thr
        195                 200                 205

Ile Cys Ala Pro Gln Cys Asn Gly His Cys Phe Gly Pro Asn Pro Asn
    210                 215                 220

Gln Cys Cys His Asp Glu Cys Ala Gly Gly Cys Ser Gly Pro Gln Asp
225                 230                 235                 240

Thr Asp Cys Phe Ala Cys Arg His Phe Asn Asp Ser Gly Ala Cys Val
                245                 250                 255

Pro Arg Cys Pro Gln Pro Leu Val Tyr Asn Lys Leu Thr Phe Gln Leu
            260                 265                 270

Glu Pro Asn Pro His Thr Lys Tyr Gln Tyr Gly Gly Val Cys Val Ala
        275                 280                 285

Ser Cys Pro His Asn Phe Val Val Asp Gln Thr Ser Cys Val Arg Ala
    290                 295                 300

Cys Pro Pro Asp Lys Met Glu Val Asp Lys Asn Gly Leu Lys Met Cys
305                 310                 315                 320

Glu Pro Cys Gly Gly Leu Cys Pro Lys Ala Cys Glu Gly Thr Gly Ser
                325                 330                 335

Gly Ser Arg Phe Gln Thr Val Asp Ser Ser Asn Ile Asp Gly Phe Val
            340                 345                 350

Asn Cys Thr Lys Ile Leu Gly Asn Leu Asp Phe Leu Ile Thr Gly Leu
        355                 360                 365

Asn Gly Asp Pro Trp His Lys Ile Pro Ala Leu Asp Pro Glu Lys Leu
    370                 375                 380

Asn Val Phe Arg Thr Val Arg Glu Ile Thr Gly Tyr Leu Asn Ile Gln
385                 390                 395                 400

Ser Trp Pro Pro His Met His Asn Phe Ser Val Phe Ser Asn Leu Thr
                405                 410                 415

Thr Ile Gly Gly Arg Ser Leu Tyr Asn Arg Gly Phe Ser Leu Leu Ile
            420                 425                 430

Met Lys Asn Leu Asn Val Thr Ser Leu Gly Phe Arg Ser Leu Lys Glu
        435                 440                 445
```

-continued

```
Ile Ser Ala Gly Arg Ile Tyr Ile Ser Ala Asn Arg Gln Leu Cys Tyr
    450                 455                 460

His His Ser Leu Asn Trp Thr Lys Val Leu Arg Gly Pro Thr Glu Glu
465                 470                 475                 480

Arg Leu Asp Ile Lys His Asn Arg Pro Arg Arg Asp Cys Val Ala Glu
                485                 490                 495

Gly Lys Val Cys Asp Pro Leu Cys Ser Ser Gly Gly Cys Trp Gly Pro
            500                 505                 510

Gly Pro Gly Gln Cys Leu Ser Cys Arg Asn Tyr Ser Arg Gly Gly Val
        515                 520                 525

Cys Val Thr His Cys Asn Phe Leu Asn Gly Glu Pro Arg Glu Phe Ala
    530                 535                 540

His Glu Ala Glu Cys Phe Ser Cys His Pro Glu Cys Gln Pro Met Glu
545                 550                 555                 560

Gly Thr Ala Thr Cys Asn Gly Ser Gly Ser Asp Thr Cys Ala Gln Cys
                565                 570                 575

Ala His Phe Arg Asp Gly Pro His Cys Val Ser Ser Cys Pro His Gly
            580                 585                 590

Val Leu Gly Ala Lys Gly Pro Ile Tyr Lys Tyr Pro Asp Val Gln Asn
        595                 600                 605

Glu Cys Arg Pro Cys His Glu Asn Cys Thr Gln Gly Cys Lys Gly Pro
    610                 615                 620

Glu Leu Gln Asp Cys Leu Gly Gln Thr Leu Val Leu Ile Gly Lys Thr
625                 630                 635                 640

His Leu Thr Met Ala Leu Thr Val Ile Ala Gly Leu Val Val Ile Phe
                645                 650                 655

Met Met Leu Gly Gly Thr Phe Leu Tyr Trp Arg Gly Arg Arg Ile Gln
            660                 665                 670

Asn Lys Arg Ala Met Arg Arg Tyr Leu Glu Arg Gly Glu Ser Ile Glu
        675                 680                 685

Pro Leu Asp Pro Ser Glu Lys Ala Asn Lys Val Leu Ala Arg Ile Phe
    690                 695                 700

Lys Glu Thr Glu Leu Arg Lys Leu Lys Val Leu Gly Ser Gly Val Phe
705                 710                 715                 720

Gly Thr Val His Lys Gly Val Trp Ile Pro Glu Gly Glu Ser Ile Lys
                725                 730                 735

Ile Pro Val Cys Ile Lys Val Ile Glu Asp Lys Ser Gly Arg Gln Ser
            740                 745                 750

Phe Gln Ala Val Thr Asp His Met Leu Ala Ile Gly Ser Leu Asp His
        755                 760                 765

Ala His Ile Val Arg Leu Leu Gly Leu Cys Pro Gly Ser Ser Leu Gln
    770                 775                 780

Leu Val Thr Gln Tyr Leu Pro Leu Gly Ser Leu Leu Asp His Val Arg
785                 790                 795                 800

Gln His Arg Gly Ala Leu Gly Pro Gln Leu Leu Leu Asn Trp Gly Val
                805                 810                 815

Gln Ile Ala Lys Gly Met Tyr Tyr Leu Glu Glu His Gly Met Val His
            820                 825                 830

Arg Asn Leu Ala Ala Arg Asn Val Leu Leu Lys Ser Pro Ser Gln Val
        835                 840                 845
```

-continued

```
Gln Val Ala Asp Phe Gly Val Ala Asp Leu Leu Pro Pro Asp Asp Lys
    850                 855                 860

Gln Leu Leu Tyr Ser Glu Ala Lys Thr Pro Ile Lys Trp Met Ala Leu
865                 870                 875                 880

Glu Ser Ile His Phe Gly Lys Tyr Thr His Gln Ser Asp Val Trp Ser
                885                 890                 895

Tyr Gly Val Thr Val Trp Glu Leu Met Thr Phe Gly Ala Glu Pro Tyr
            900                 905                 910

Ala Gly Leu Arg Leu Ala Glu Val Pro Asp Leu Leu Glu Lys Gly Glu
        915                 920                 925

Arg Leu Ala Gln Pro Gln Ile Cys Thr Ile Asp Val Tyr Met Val Met
    930                 935                 940

Val Lys Cys Trp Met Ile Asp Glu Asn Ile Arg Pro Thr Phe Lys Glu
945                 950                 955                 960

Leu Ala Asn Glu Phe Thr Arg Met Ala Arg Asp Pro Pro Arg Tyr Leu
                965                 970                 975

Val Ile Lys Arg Glu Ser Gly Pro Gly Ile Ala Pro Gly Pro Glu Pro
            980                 985                 990

His Gly Leu Thr Asn Lys Lys Leu  Glu Glu Val Glu Leu  Glu Pro Glu
        995                 1000                1005

Leu Asp  Leu Asp Leu Asp Leu  Glu Ala Glu Glu Asp  Asn Leu Ala
    1010                1015                1020

Thr Thr  Thr Leu Gly Ser Ala  Leu Ser Leu Pro Val  Gly Thr Leu
    1025                1030                1035

Asn Arg  Pro Arg Gly Ser Gln  Ser Leu Leu Ser Pro  Ser Ser Gly
    1040                1045                1050

Tyr Met  Pro Met Asn Gln Gly  Asn Leu Gly Glu Ser  Cys Gln Glu
    1055                1060                1065

Ser Ala  Val Ser Gly Ser Ser  Glu Arg Cys Pro Arg  Pro Val Ser
    1070                1075                1080

Leu His  Pro Met Pro Arg Gly  Cys Leu Ala Ser Glu  Ser Ser Glu
    1085                1090                1095

Gly His  Val Thr Gly Ser Glu  Ala Glu Leu Gln Glu  Lys Val Ser
    1100                1105                1110

Met Cys  Arg Ser Arg Ser Arg  Ser Arg Ser Pro Arg  Pro Arg Gly
    1115                1120                1125

Asp Ser  Ala Tyr His Ser Gln  Arg His Ser Leu Leu  Thr Pro Val
    1130                1135                1140

Thr Pro  Leu Ser Pro Pro Gly  Leu Glu Glu Glu Asp  Val Asn Gly
    1145                1150                1155

Tyr Val  Met Pro Asp Thr His  Leu Lys Gly Thr Pro  Ser Ser Arg
    1160                1165                1170

Glu Gly  Thr Leu Ser Ser Val  Gly Leu Ser Ser Val  Leu Gly Thr
    1175                1180                1185

Glu Glu  Glu Asp Glu Asp Glu  Glu Tyr Glu Tyr Met  Asn Arg Arg
    1190                1195                1200

Arg Arg  His Ser Pro Pro His  Pro Pro Arg Pro Ser  Ser Leu Glu
    1205                1210                1215

Glu Leu  Gly Tyr Glu Tyr Met  Asp Val Gly Ser Asp  Leu Ser Ala
    1220                1225                1230

Ser Leu  Gly Ser Thr Gln Ser  Cys Pro Leu His Pro  Val Pro Ile
```

-continued

```
    1235                1240                1245

Met Pro  Thr Ala Gly Thr Thr  Pro Asp Glu Asp Tyr  Glu Tyr Met
    1250                1255                1260

Asn Arg  Gln Arg Asp Gly Gly  Gly Pro Gly Gly Asp  Tyr Ala Ala
    1265                1270                1275

Met Gly  Ala Cys Pro Ala Ser  Glu Gln Gly Tyr Glu  Glu Met Arg
    1280                1285                1290

Ala Phe  Gln Gly Pro Gly His  Gln Ala Pro His Val  His Tyr Ala
    1295                1300                1305

Arg Leu  Lys Thr Leu Arg Ser  Leu Glu Ala Thr Asp  Ser Ala Phe
    1310                1315                1320

Asp Asn  Pro Asp Tyr Trp His  Ser Arg Leu Phe Pro  Lys Ala Asn
    1325                1330                1335

Ala Gln  Arg Thr
    1340


<210> SEQ ID NO 6
<211> LENGTH: 4721
<212> TYPE: DNA
<213> ORGANISM: Unknown
<220> FEATURE:
<223> OTHER INFORMATION: Description of Unknown:
      HER3 sequence

<400> SEQUENCE: 6

ctccgaggtg ggcaactctc aggcagtgtg tcctgggact ctgaatggcc tgagtgtgac     60

cggcgatgct gagaaccaat accagacact gtacaagctc tacgagaggt gtgaggtggt    120

gatggggaac cttgagattg tgctcacggg acacaatgcc gacctctcct tcctgcagtg    180

gattcgagaa gtgacaggct atgtcctcgt ggccatgaat gaattctcta ctctaccatt    240

gcccaacctc cgcgtggtgc gagggaccca ggtctacgat gggaagtttg ccatcttcgt    300

catgttgaac tataacacca actccagcca cgctctgcgc cagctccgct tgactcagct    360

caccgagatt ctgtcagggg gtgtttatat tgagaagaac gataagcttt gtcacatgga    420

cacaattgac tggagggaca tcgtgaggga ccgagatgct gagatagtgg tgaaggacaa    480

tggcagaagc tgtccccccc gtcatgaggt ttgcaagggg cgatgctggg gtcctggatc    540

agaagactgc cagacattga ccaagaccat ctgtgctcct cagtgtaatg gtcactgctt    600

tgggcccaac cccaaccagt gctgccatga tgagtgtgcc gggggctgct caggccctca    660

ggacacagac tgctttgcct gccggcactt caatgacagt ggagcctgtg tacctcgctg    720

tccacagcct cttgtctaca acaagctaac tttccagctg gaacccaatc cccacaccaa    780

gtatcagtat ggaggagttt gtgtagccag ctgtccccat aactttgtgg tggatcaaac    840

atcctgtgtc agggcctgtc ctcctgacaa gatggaagta gataaaaatg ggctcaagat    900

gtgtgagcct tgtgggggac tatgtcccaa agcctgtgag ggaacaggct ctgggagccg    960

cttccagact gtggactcga gcaacattga tggatttgtg aactgcacca agatcctggg   1020

caacctggac tttctgatca ccggcctcaa tggagacccc tggcacaaga tccctgccct   1080

ggacccagag aagctcaatg tcttccggac agtacgggag atcacaggtt acctgaacat   1140

ccagtcctgg ccgccccaca tgcacaactt cagtgttttt tccaatttga caaccattgg   1200

aggcagaagc ctctacaacc ggggcttctc attgttgatc atgaagaact tgaatgtcac   1260
```

-continued

atctctgggc ttccgatccc tgaaggaaat tagtgctggg cgtatctata taagtgccaa 1320

taggcagctc tgctaccacc actctttgaa ctggaccaag gtgcttcggg ggcctacgga 1380

agagcgacta gacatcaagc ataatcggcc gcgcagagac tgcgtggcag agggcaaagt 1440

gtgtgaccca ctgtgctcct ctgggggatg ctggggccca ggccctggtc agtgcttgtc 1500

ctgtcgaaat tatagccgag gaggtgtctg tgtgacccac tgcaactttc tgaatgggga 1560

gcctcgagaa tttgcccatg aggccgaatg cttctcctgc cacccggaat gccaacccat 1620

ggggggcact gccacatgca atggctcggg ctctgatact tgtgctcaat gtgcccattt 1680

tcgagatggg ccccactgtg tgagcagctg cccccatgga gtcctaggtg ccaagggccc 1740

aatctacaag tacccagatg ttcagaatga atgtcggccc tgccatgaga actgcaccca 1800

ggggtgtaaa ggaccagagc ttcaagactg tttaggacaa acactggtgc tgatcggcaa 1860

aacccatctg acaatggctt tgacagtgat agcaggattg gtagtgattt tcatgatgct 1920

gggcggcact tttctctact ggcgtgggcg ccggattcag aataaaaggg ctatgaggcg 1980

atacttggaa cggggtgaga gcatagagcc tctggacccc agtgagaagg ctaacaaagt 2040

cttggccaga atcttcaaag agacagagct aaggaagctt aaagtgcttg gctcgggtgt 2100

ctttggaact gtgcacaaag gagtgtggat ccctgagggt gaatcaatca agattccagt 2160

ctgcattaaa gtcattgagg acaagagtgg acggcagagt tttcaagctg tgacagatca 2220

tatgctggcc attggcagcc tggaccatgc ccacattgta aggctgctgg gactatgccc 2280

agggtcatct ctgcagcttg tcactcaata tttgcctctg ggttctctgc tggatcatgt 2340

gagacaacac cgggggggcac tggggccaca gctgctgctc aactggggag tacaaattgc 2400

caagggaatg tactaccttg aggaacatgg tatggtgcat agaaacctgg ctgcccgaaa 2460

cgtgctactc aagtcaccca gtcaggttca ggtggcagat tttggtgtgg ctgacctgct 2520

gcctcctgat gataagcagc tgctatacag tgaggccaag actccaatta agtggatggc 2580

ccttgagagt atccactttg ggaaatacac acaccagagt gatgtctgga gctatggtgt 2640

gacagtttgg gagttgatga ccttcggggc agagccctat gcagggctac gattggctga 2700

agtaccagac ctgctagaga agggggagcg gttggcacag ccccagatct gcacaattga 2760

tgtctacatg gtgatggtca agtgttggat gattgatgag aacattcgcc caacctttaa 2820

agaactagcc aatgagttca ccaggatggc ccgagaccca ccacggtatc tggtcataaa 2880

gagagagagt gggcctggaa tagcccctgg gccagagccc catggtctga caaacaagaa 2940

gctagaggaa gtagagctgg agccagaact agacctagac ctagacttgg aagcagagga 3000

ggacaacctg gcaaccacca cactgggctc cgccctcagc ctaccagttg gaacacttaa 3060

tcggccacgt gggagccaga gccttttaag tccatcatct ggatacatgc ccatgaacca 3120

gggtaatctt ggggggtctt gccaggagtc tgcagtttct gggagcagtg aacggtgccc 3180

ccgtccagtc tctctacacc caatgccacg gggatgcctg gcatcagagt catcagaggg 3240

gcatgtaaca ggctctgagg ctgagctcca ggagaaagtg tcaatgtgta gaagccggag 3300

caggagccgg agcccacggc cacgcggaga tagcgcctac cattcccagc gccacagtct 3360

gctgactcct gttaccccac tctccccacc cgggttagag gaagaggatg tcaacggtta 3420

tgtcatgcca gatacacacc tcaaaggtac tccctcctcc cgggaaggca ccctttcttc 3480

agtgggtctc agttctgtcc tgggtactga agaagaagat gaagatgagg agtatgaata 3540

-continued

catgaaccgg aggagaaggc acagtccacc tcatcccct aggccaagtt cccttgagga 3600

gctgggttat gagtacatgg atgtggggtc agacctcagt gcctctctgg gcagcacaca 3660

gagttgccca ctccaccctg tacccatcat gcccactgca ggcacaactc cagatgaaga 3720

ctatgaatat atgaatcggc aacgagatgg aggtggtcct gggggtgatt atgcagccat 3780

gggggcctgc ccagcatctg agcaagggta tgaagagatg agagcttttc aggggcctgg 3840

acatcaggcc ccccatgtcc attatgcccg cctaaaaact ctacgtagct tagaggctac 3900

agactctgcc tttgataacc ctgattactg gcatagcagg cttttcccca aggctaatgc 3960

ccagagaacg taactcctgc tccctgtggc actcagggag catttaatgg cagctagtgc 4020

ctttagaggg taccgtcttc tccctattcc ctctctctcc caggtcccag ccccttttcc 4080

ccagtcccag acaattccat tcaatctttg gaggctttta aacattttga cacaaaattc 4140

ttatggtatg tagccagctg tgcactttct tctctttccc aaccccagga aaggttttcc 4200

ttattttgtg tgctttccca gtcccattcc tcagcttctt cacaggcact cctggagata 4260

tgaaggatta ctctccatat cccttcctct caggctcttg actacttgga actaggctct 4320

tatgtgtgcc tttgtttccc atcagactgt caagaagagg aaagggagga aacctagcag 4380

aggaaagtgt aattttggtt tatgactctt aaccccctag aaagacagaa gcttaaaatc 4440

tgtgaagaaa gaggttagga gtagatattg attactatca taattcagca cttaactatg 4500

agccaggcat catactaaac ttcacctaca ttatctcact tagtccttta tcatccttaa 4560

aacaattctg tgacatacat attatctcat tttacacaaa gggaagtcgg gcatggtggc 4620

tcatgcctgt aatctcagca ctttgggagg ctgaggcaga aggattacct gaggcaagga 4680

gtttgagacc agcttagcca acatagtaag acccccatct c 4721

<210> SEQ ID NO 7
<211> LENGTH: 19
<212> TYPE: DNA
<213> ORGANISM: Artificial Sequence
<220> FEATURE:
<223> OTHER INFORMATION: Description of Artificial Sequence: Synthetic oligonucleotide
<220> FEATURE:
<223> OTHER INFORMATION: Description of Combined DNA/RNA Molecule: Synthetic oligonucleotide

<400> SEQUENCE: 7

ggaaccuguc uccacaaag 19

<210> SEQ ID NO 8
<211> LENGTH: 19
<212> TYPE: DNA
<213> ORGANISM: Artificial Sequence
<220> FEATURE:
<223> OTHER INFORMATION: Description of Artificial Sequence: Synthetic oligonucleotide
<220> FEATURE:
<223> OTHER INFORMATION: Description of Combined DNA/RNA Molecule: Synthetic oligonucleotide

<400> SEQUENCE: 8

gaagaaugca gguuuaaua 19

<210> SEQ ID NO 9
<211> LENGTH: 48
<212> TYPE: DNA

-continued

<213> ORGANISM: Artificial Sequence
<220> FEATURE:
<223> OTHER INFORMATION: Description of Artificial Sequence: Synthetic oligonucleotide
<220> FEATURE:
<221> NAME/KEY: CDS
<222> LOCATION: (1)..(48)

<400> SEQUENCE: 9

ggc ctg gag aag ctg ggt atc ttc gtc aag acc gtg acg gag ggt ggt 48
Gly Leu Glu Lys Leu Gly Ile Phe Val Lys Thr Val Thr Glu Gly Gly
1 5 10 15

<210> SEQ ID NO 10
<211> LENGTH: 16
<212> TYPE: PRT
<213> ORGANISM: Artificial Sequence
<220> FEATURE:
<223> OTHER INFORMATION: Description of Artificial Sequence: Synthetic peptide

<400> SEQUENCE: 10

Gly Leu Glu Lys Leu Gly Ile Phe Val Lys Thr Val Thr Glu Gly Gly
1 5 10 15

<210> SEQ ID NO 11
<211> LENGTH: 34
<212> TYPE: DNA
<213> ORGANISM: Artificial Sequence
<220> FEATURE:
<223> OTHER INFORMATION: Description of Artificial Sequence: Synthetic oligonucleotide

<400> SEQUENCE: 11

ggcctggaga agctgggtat tgacggaggg tggt 34

<210> SEQ ID NO 12
<211> LENGTH: 14
<212> TYPE: DNA
<213> ORGANISM: Artificial Sequence
<220> FEATURE:
<223> OTHER INFORMATION: Description of Artificial Sequence: Synthetic oligonucleotide

<400> SEQUENCE: 12

cttcgtcaag accg 14

<210> SEQ ID NO 13
<211> LENGTH: 46
<212> TYPE: DNA
<213> ORGANISM: Artificial Sequence
<220> FEATURE:
<223> OTHER INFORMATION: Description of Artificial Sequence: Synthetic oligonucleotide

<400> SEQUENCE: 13

ggcctggaga agctgggtat cttcgtcaag actgacggag ggtggt 46

<210> SEQ ID NO 14
<211> LENGTH: 47
<212> TYPE: DNA
<213> ORGANISM: Artificial Sequence
<220> FEATURE:
<223> OTHER INFORMATION: Description of Artificial Sequence: Synthetic oligonucleotide

-continued

<400> SEQUENCE: 14

ggcctggaga agctgggtat cttcgtcaag accggacgga gggtggt 47

<210> SEQ ID NO 15
<211> LENGTH: 11603
<212> TYPE: DNA
<213> ORGANISM: Artificial Sequence
<220> FEATURE:
<223> OTHER INFORMATION: Description of Artificial Sequence: Synthetic polynucleotide

<400> SEQUENCE: 15

tggaagggct aattcactcc caaagaagac aagatatcct tgatctgtgg atctaccaca 60

cacaaggcta cttccctgat tagcagaact acacaccagg gccaggggtc agatatccac 120

tgacctttgg atggtgctac aagctagtac cagttgagcc agataaggta gaagaggcca 180

ataaaggaga gaacaccagc ttgttacacc ctgtgagcct gcatgggatg gatgacccgg 240

agagagaagt gttagagtgg aggtttgaca gccgcctagc atttcatcac gtggcccgag 300

agctgcatcc ggagtacttc aagaactgct gatatcgagc ttgctacaag ggactttccg 360

ctggggactt tccagggagg cgtggcctgg gcgggactgg ggagtggcga gccctcagat 420

cctgcatata agcagctgct ttttgcctgt actgggtctc tctggttaga ccagatctga 480

gcctgggagc tctctggcta actagggaac ccactgctta agcctcaata aagcttgcct 540

tgagtgcttc aagtagtgtg tgcccgtctg ttgtgtgact ctggtaacta gagatccctc 600

agacccttttt agtcagtgtg gaaaatctct agcagtggcg cccgaacagg gacttgaaag 660

cgaaagggaa accagaggag ctctctcgac gcaggactcg gcttgctgaa gcgcgcacgg 720

caagaggcga ggggcggcga ctggtgagta cgccaaaaat tttgactagc ggaggctaga 780

aggagagaga tgggtgcgag agcgtcagta ttaagcgggg gagaattaga tcgcgatggg 840

aaaaaattcg gttaaggcca gggggaaaga aaaaatataa attaaaacat atagtatggg 900

caagcaggga gctagaacga ttcgcagtta atcctggcct gttagaaaca tcagaaggct 960

gtagacaaat actgggacag ctacaaccat cccttcagac aggatcagaa gaacttagat 1020

cattatataa tacagtagca accctctatt gtgtgcatca aaggatagag ataaaagaca 1080

ccaaggaagc tttagacaag atagaggaag agcaaaacaa aagtaagacc accgcacagc 1140

aagcggccgg ccgctgatct tcagacctgg aggaggagat atgagggaca attggagaag 1200

tgaattatat aaatataaag tagtaaaaat tgaaccatta ggagtagcac ccaccaaggc 1260

aaagagaaga gtggtgcaga gagaaaaaag agcagtggga ataggagctt tgttccttgg 1320

gttcttggga gcagcaggaa gcactatggg cgcagcgtca atgacgctga cggtacaggc 1380

cagacaatta ttgtctggta tagtgcagca gcagaacaat ttgctgaggg ctattgaggc 1440

gcaacagcat ctgttgcaac tcacagtctg gggcatcaag cagctccagg caagaatcct 1500

ggctgtggaa agatacctaa aggatcaaca gctcctgggg atttggggtt gctctggaaa 1560

actcatttgc accactgctg tgccttggaa tgctagttgg agtaataaat ctctggaaca 1620

gatttggaat cacacgacct ggatggagtg ggacagagaa attaacaatt acacaagctt 1680

aatacactcc ttaattgaag aatcgcaaaa ccagcaagaa aagaatgaac aagaattatt 1740

ggaattagat aaatgggcaa gtttgtggaa ttggtttaac ataacaaatt ggctgtggta 1800

tataaaatta ttcataatga tagtaggagg cttggtaggt ttaagaatag tttttgctgt 1860

-continued

actttctata gtgaatagag ttaggcaggg atattcacca ttatcgtttc agacccacct 1920

cccaaccccg aggggacccg acaggcccga aggaatagaa gaagaaggtg gagagagaga 1980

cagagacaga tccattcgat tagtgaacgg atctcgacgg tatcgccttt aaaagaaaag 2040

gggggattgg ggggtacagt gcaggggaaa gaatagtaga cataatagca acagacatac 2100

aaactaaaga actacaaaaa caaattacaa aaattcaaaa ttttcgggtt tattacaggg 2160

acagcagaga tccagtttat cgacttaact tgtttattgc agcttataat ggttacaaat 2220

aaggcaatag catcacaaat ttcacaaata aggcattttt ttcactgcat tctagttttg 2280

gtttgtccaa actcatcaat gtatcttatc atgtctggat ctcaaatccc tcggaagctg 2340

cgcctgtctt aggttggagt gatacatttt tatcactttt acccgtcttt ggattaggca 2400

gtagctctga cggccctcct gtcttaggtt agtgaaaaat gtcactctct tacccgtcat 2460

tggctgtcca gcttagctcg caggggaggt ggtctggatc cgccggcacc ggtgatcagt 2520

tatctagact acttgtcgtc gtcgtccttg tagtcgatgt cgtggtcctt gtagtcgccg 2580

tcgtggtcct tgtagtcggc gccaccgcct ccaaccactt tgtacaagaa agctgaacga 2640

gaaacgtaaa atgatataaa tatcaatata ttaaattaga ttttgcataa aaaacagact 2700

acataatact gtaaaacaca acatatccag tcactatgaa tcaactactt agatggtatt 2760

agtgacctgt agtcgactaa gttggcagca tcacccgacg cactttgcgc cgaataaata 2820

cctgtgacgg aagatcactt cgcagaataa ataaatcctg gtgtccctgt tgataccggg 2880

aagccctggg ccaacttttg gcgaaaatga gacgttgatc ggcacgtaag aggttccaac 2940

tttcaccata atgaaataag atcactaccg ggcgtatttt ttgagttatc gagattttca 3000

ggagctaagg aagctaaaat ggagaaaaaa atcactggat ataccaccgt tgatatatcc 3060

caatggcatc gtaaagaaca ttttgaggca tttcagtcag ttgctcaatg tacctataac 3120

cagaccgttc agctggatat tacggccttt ttaaagaccg taaagaaaaa taagcacaag 3180

ttttatccgg cctttattca cattcttgcc cgcctgatga atgctcatcc ggaattccgt 3240

atggcaatga aagacggtga gctggtgata tgggatagtg ttcacccttg ttacaccgtt 3300

ttccatgagc aaactgaaac gttttcatcg ctctggagtg aataccacga cgatttccgg 3360

cagtttctac acatatattc gcaagatgtg gcgtgttacg gtgaaaacct ggcctatttc 3420

cctaaagggt ttattgagaa tatgtttttc gtctcagcca atccctgggt gagtttcacc 3480

agttttgatt taaacgtggc caatatggac aacttcttcg cccccgtttt caccatgggc 3540

aaatattata cgcaaggcga caaggtgctg atgccgctgg cgattcaggt tcatcatgcc 3600

gtttgtgatg gcttccatgt cggcagaatg cttaatgaat tacaacagta ctgcgatgag 3660

tggcaggggg ggcgtaaacg ccgcgtggat ccggcttact aaaagccaga taacagtatg 3720

cgtatttgcg cgctgatttt tgcggtataa gaatatatac tgatatgtat acccgaagta 3780

tgtcaaaaag aggtatgcta tgaagcagcg tattacagtg acagttgaca gcgacagcta 3840

tcagttgctc aaggcatata tgatgtcaat atctccggtc tggtaagcac aaccatgcag 3900

aatgaagccc gtcgtctgcg tgccgaacgc tggaaagcgg aaaatcagga agggatggct 3960

gaggtcgccc ggtttattga aatgaacggc tcttttgctg acgagaacag gggctggtga 4020

aatgcagttt aaggtttaca cctataaaag agagagccgt tatcgtctgt ttgtggatgt 4080

acagagtgat attattgaca cgcccgggcg acggatggtg atccccctgg ccagtgcacg 4140

-continued

tctgctgtca gataaagtct cccgtgaact ttacccggtg gtgcatatcg gggatgaaag 4200

ctggcgcatg atgaccaccg atatggccag tgtgccggtc tccgttatcg gggaagaagt 4260

ggctgatctc agccaccgcg aaaatgacat caaaaacgcc attaacctga tgttctgggg 4320

aatataaatg tcaggctccc ttatacacag ccagtctgca ggtcgataca gtagaaatta 4380

cagaaacttt atcacgttta gtaagtatag aggctgaaaa tccagatgaa gccgaacgac 4440

ttgtaagaga aaagtataag agttgtgaaa ttgttcttga tgcagatgat tttcaggact 4500

atgacactag cgtatatgaa taggtagatg tttttatttt gtcacacaaa aaagaggctc 4560

gcacctcttt ttcttatttc tttttatgat ttaatacggc attgaggaca atagcgagta 4620

ggctggatac gacgattccg tttgagaaga acatttggaa ggctgtcggt cgactaagtt 4680

ggcagcatca cccgaagaac atttggaagg ctgtcggtcg actacaggtc actaatacca 4740

tctaagtagt tgattcatag tgactggata tgttgtgttt tacagtatta tgtagtctgt 4800

tttttatgca aaatctaatt taatatattg atatttatat cattttacgt ttctcgttca 4860

gctttttttgt acaaacttgt ggtaccggtg tatacgggaa ttctttacga gggtaggaag 4920

tggtacggaa agttggtata agacaaaagt gttgtggaat tgaagtttac tcaaaaaatc 4980

agcactcttt tataggcgcc ctggtttaca taagcaaagc ttatacgttc tctatcactg 5040

atagggagta aactggatat acgttctcta tcactgatag ggagtaaact gtagatacgt 5100

tctctatcac tgatagggag taaactggtc atacgttctc tatcactgat agggagtaaa 5160

ctccttatac gttctctatc actgataggg agtaaagtct gcatacgttc tctatcactg 5220

atagggagta aactcttcat acgttctcta tcactgatag ggagtaaact cgaggtgata 5280

attccacggg gttggggttg cgccttttcc aaggcagccc tgggtttgcg cagggacgcg 5340

gctgctctgg gcgtggttcc gggaaacgca gcggcgccga ccctgggtct cgcacattct 5400

tcacgtccgt tcgcagcgtc acccggatct tcgccgctac ccttgtgggc cccccggcga 5460

cgcttcctgc tccgccccta agtcgggaag gttccttgcg gttcgcggcg tgccggacgt 5520

gacaaacgga agccgcacgt ctcactagta ccctcgcaga cggacagcgc cagggagcaa 5580

tggcagcgcg ccgaccgcga tgggctgtgg ccaatagcgg ctgctcagca gggcgcgccg 5640

agagcagcgg ccgggaaggg gcggtgcggg aggcggggtg tggggcggta gtgtgggccc 5700

tgttcctgcc cgcgcggtgt tccgcattct gcaagcctcc ggagcgcacg tcggcagtcg 5760

gctccctcgt tgaccgaatc accgacctct ctccccaggg ggatcatcga attaccatgt 5820

ctagactgga caagagcaaa gtcataaact ctgctctgga attactcaat ggagtcggta 5880

tcgaaggcct gacgacaagg aaactcgctc aaaagctggg agttgagcag cctaccctgt 5940

actggcacgt gaagaacaag cgggccctgc tcgatgccct gccaatcgag atgctggaca 6000

ggcatcatac ccactcctgc cccctggaag gcgagtcatg gcaagacttt ctgcggaaca 6060

acgccaagtc ataccgctgt gctctcctct cacatcgcga cggggctaaa gtgcatctcg 6120

gcacccgccc aacagagaaa cagtacgaaa ccctggaaaa tcagctcgcg ttcctgtgtc 6180

agcaaggctt ctccctggag aacgcactgt acgctctgtc cgccgtgggc cactttacac 6240

tgggctgcgt attggaggaa caggagcatc aagtagcaaa agaggaaaga gagacaccta 6300

ccaccgattc tatgccccca cttctgaaac aagcaattga gctgttcgac cggcagggag 6360

ccgaacctgc cttccttttc ggcctggaac taatcatatg tggcctggag aaacagctaa 6420

-continued

agtgcgaaag cggcgggccg accgacgccc ttgacgattt tgacttagac atgctcccag 6480

ccgatgccct tgacgacttt gaccttgata tgctgcctgc tgacgctctt gacgattttg 6540

accttgacat gctccccggg taaacgcgcg aatgtgtgtc agttagggtg tggaaagtcc 6600

ccaggctccc cagcaggcag aagtatgcaa agcatgcatc tcaattagtc agcaaccagg 6660

tgtggaaagt ccccaggctc cccagcaggc agaagtatgc aaagcatgca tctcaattag 6720

tcagcaacca tagtcccgcc cctaactccg cccatcccgc ccctaactcc gcccagttcc 6780

gcccattctc cgccccatgg ctgactaatt ttttttattt atgcagaggc cgaggccgcc 6840

tcggcctctg agctattcca gaagtagtga ggaggctttt ttggaggcct aggcttttgc 6900

aaaacgcgac catgaccgag tacaagccca cggtgcgcct cgccacccgc gacgacgtcc 6960

cccgggccgt acgcaccctc gccgccgcgt tcgccgacta ccccgccacg cgccacaccg 7020

tcgacccgga ccgccacatc gagcgggtca ccgagctgca agaactcttc ctcacgcgcg 7080

tcgggctcga catcggcaag gtgtgggtcg cggacgacgg cgccgcggtg gcggtctgga 7140

ccacgccgga gagcgtcgaa gcgggggcgg tgttcgccga gatcggcccg cgcatggccg 7200

agttgagcgg ttcccggctg gccgcgcagc aacagatgga aggcctcctg gcgccgcacc 7260

ggcccaagga gcccgcgtgg ttcctggcca ccgtcggcgt ctcgcccgac caccagggca 7320

agggtctggg cagcgccgtc gtgctccccg gagtggaggc ggccgagcgc gccggggtgc 7380

ccgccttcct ggagacctcc gcgccccgca acctcccctt ctacgagcgg ctcggcttca 7440

ccgtcaccgc cgacgtcgag gtgcccgaag gaccgcgcac ctggtgcatg acccgcaagc 7500

ccggtgcctg aacgcgtctg gaacaatcaa cctctggatt acaaaatttg tgaaagattg 7560

actggtattc ttaactatgt tgctcctttt acgctatgtg gatacgctgc tttaatgcct 7620

ttgtatcatg ctattgcttc ccgtatggct ttcattttct cctccttgta taaatcctgg 7680

ttgctgtctc tttatgagga gttgtggccc gttgtcaggc aacgtggcgt ggtgtgcact 7740

gtgtttgctg acgcaacccc cactggttgg ggcattgcca ccacctgtca gctcctttcc 7800

gggactttcg ctttcccccc ccctattgcc acggcggaac tcatcgccgc ctgccttgcc 7860

cgctgctgga caggggctcg gctgttgggc actgacaatt ccgtggtgtt gtcggggaag 7920

ctgacgtcct ttccatggct gctcgcctgt gttgccacct ggattctgcg cgggacgtcc 7980

ttctgctacg tcccttcggc cctcaatcca gcggaccttc cttcccgcgg cctgctgccg 8040

gctctgcggc ctcttccgcg tcttcgcctt cgccctcaga cgagtcggat ctccctttgg 8100

gccgcctccc cgcctggaat taattctgca gtcgagacct agaaaaacat ggagcaatca 8160

caagtagcaa tacagcagct accaatgctg attgtgcctg gctagaagca caagaggagg 8220

aggaggtggg tttttccagt cacacctcag gtacctttaa gaccaatgac ttacaaggca 8280

gctgtagatc ttagccactt tttaaaagaa aagaggggac tggaagggct aattcactcc 8340

caacgaagac aagatatcct tgatctgtgg atctaccaca cacaaggcta cttccctgat 8400

tagcagaact acacaccagg gccaggggtc agatatccac tgacctttgg atggtgctac 8460

aagctagtac cagttgagcc agataaggta gaagaggcca ataaaggaga gaacaccagc 8520

ttgttacacc ctgtgagcct gcatgggatg gatgacccgg agagagaagt gttagagtgg 8580

aggtttgaca gccgcctagc atttcatcac gtggcccgag agctgcatcc ggagtacttc 8640

aagaactgct gatatcgagc ttgctacaag ggactttccg ctggggactt tccagggagg 8700

-continued

cgtggcctgg gcgggactgg ggagtggcga gccctcagat cctgcatata agcagctgct 8760

ttttgcctgt actgggtctc tctggttaga ccagatctga gcctgggagc tctctggcta 8820

actagggaac ccactgctta agcctcaata aagcttgcct tgagtgcttc aagtagtgtg 8880

tgcccgtctg ttgtgtgact ctggtaacta gagatccctc agacccttttt agtcagtgtg 8940

gaaaatctct agcagtagta gttcatgtca tcttattatt cagtatttat aacttgcaaa 9000

gaaatgaata tcagagagtg agaggccttg acattgctag cgttttaccg tcgacctcta 9060

gctagagctt ggcgtaatca tggtcatagc tgtttcctgt gtgaaattgt tatccgctca 9120

caattccaca caacatacga gccggaagca taaagtgtaa agcctggggt gcctaatgag 9180

tgagctaact cacattaatt gcgttgcgct cactgcccgc tttccagtcg ggaaacctgt 9240

cgtgccagct gcattaatga atcggccaac gcgcggggag aggcggtttg cgtattgggc 9300

gctcttccgc ttcctcgctc actgactcgc tgcgctcggt cgttcggctg cggcgagcgg 9360

tatcagctca ctcaaaggcg gtaatacggt tatccacaga atcaggggat aacgcaggaa 9420

agaacatgtg agcaaaaggc cagcaaaagg ccaggaaccg taaaaaggcc gcgttgctgg 9480

cgtttttcca taggctccgc ccccctgacg agcatcacaa aaatcgacgc tcaagtcaga 9540

ggtggcgaaa cccgacagga ctataaagat accaggcgtt tccccctgga agctccctcg 9600

tgcgctctcc tgttccgacc ctgccgctta ccggatacct gtccgccttt ctcccttcgg 9660

gaagcgtggc gctttctcat agctcacgct gtaggtatct cagttcggtg taggtcgttc 9720

gctccaagct gggctgtgtg cacgaacccc ccgttcagcc cgaccgctgc gccttatccg 9780

gtaactatcg tcttgagtcc aacccggtaa gacacgactt atcgccactg gcagcagcca 9840

ctggtaacag gattagcaga gcgaggtatg taggcggtgc tacagagttc ttgaagtggt 9900

ggcctaacta cggctacact agaagaacag tatttggtat ctgcgctctg ctgaagccag 9960

ttaccttcgg aaaaagagtt ggtagctctt gatccggcaa acaaaccacc gctggtagcg 10020

gtttttttgt ttgcaagcag cagattacgc gcagaaaaaa aggatctcaa gaagatcctt 10080

tgatcttttc tacggggtct gacgctcagt ggaacgaaaa ctcacgttaa gggattttgg 10140

tcatgagatt atcaaaaagg atcttcacct agatcctttt aaattaaaaa tgaagtttta 10200

aatcaatcta aagtatatat gagtaaacttt ggtctgacag ttaccaatgc ttaatcagtg 10260

aggcacctat ctcagcgatc tgtctatttc gttcatccat agttgcctga ctccccgtcg 10320

tgtagataac tacgatacgg gagggcttac catctggccc cagtgctgca atgataccgc 10380

gagacccacg ctcaccggct ccagatttat cagcaataaa ccagccagcc ggaagggccg 10440

agcgcagaag tggtcctgca actttatccg cctccatcca gtctattaat tgttgccggg 10500

aagctagagt aagtagttcg ccagttaata gtttgcgcaa cgttgttgcc attgctacag 10560

gcatcgtggt gtcacgctcg tcgtttggta tggcttcatt cagctccggt tcccaacgat 10620

caaggcgagt tacatgatcc cccatgttgt gcaaaaaagc ggttagctcc ttcggtcctc 10680

cgatcgttgt cagaagtaag ttggccgcag tgttatcact catggttatg gcagcactgc 10740

ataattctct tactgtcatg ccatccgtaa gatgcttttc tgtgactggt gagtactcaa 10800

ccaagtcatt ctgagaatag tgtatgcggc gaccgagttg ctcttgcccg gcgtcaatac 10860

gggataatac cgcgccacat agcagaactt taaaagtgct catcattgga aaacgttctt 10920

cggggcgaaa actctcaagg atcttaccgc tgttgagatc cagttcgatg taacccactc 10980

-continued

gtgcacccaa ctgatcttca gcatctttta ctttcaccag cgtttctggg tgagcaaaaa 11040

caggaaggca aaatgccgca aaaaagggaa taagggcgac acggaaatgt tgaatactca 11100

tactcttcct ttttcaatat tattgaagca tttatcaggg ttattgtctc atgagcggat 11160

acatatttga atgtatttag aaaaataaac aaataggggt tccgcgcaca tttccccgaa 11220

aagtgccacc tgacgtcgac ggatcgggag atcaacttgt ttattgcagc ttataatggt 11280

tacaaataaa gcaatagcat cacaaatttc acaaataaag catttttttc actgcattct 11340

agttgtggtt tgtccaaact catcaatgta tcttatcatg tctggatcaa ctggataact 11400

caagctaacc aaaatcatcc caaacttccc accccatacc ctattaccac tgccaattac 11460

ctagtggttt catttactct aaacctgtga ttcctctgaa ttattttcat tttaaagaaa 11520

ttgtatttgt taaatatgta ctacaaactt agtagttttt aaagaaattg tatttgttaa 11580

atatgtacta caaacttagt agt 11603

<210> SEQ ID NO 16
<211> LENGTH: 11612
<212> TYPE: DNA
<213> ORGANISM: Artificial Sequence
<220> FEATURE:
<223> OTHER INFORMATION: Description of Artificial Sequence: Synthetic polynucleotide

<400> SEQUENCE: 16

tggaagggct aattcactcc caaagaagac aagatatcct tgatctgtgg atctaccaca 60

cacaaggcta cttccctgat tagcagaact acacaccagg gccaggggtc agatatccac 120

tgacctttgg atggtgctac aagctagtac cagttgagcc agataaggta gaagaggcca 180

ataaaggaga gaacaccagc ttgttacacc ctgtgagcct gcatgggatg gatgacccgg 240

agagagaagt gttagagtgg aggtttgaca gccgcctagc atttcatcac gtggcccgag 300

agctgcatcc ggagtacttc aagaactgct gatatcgagc ttgctacaag ggactttccg 360

ctggggactt tccagggagg cgtggcctgg gcgggactgg ggagtggcga gccctcagat 420

cctgcatata agcagctgct ttttgcctgt actgggtctc tctggttaga ccagatctga 480

gcctgggagc tctctggcta actagggaac ccactgctta agcctcaata aagcttgcct 540

tgagtgcttc aagtagtgtg tgcccgtctg ttgtgtgact ctggtaacta gagatccctc 600

agacccttt agtcagtgtg gaaaatctct agcagtggcg cccgaacagg gacttgaaag 660

cgaaagggaa accagaggag ctctctcgac gcaggactcg gcttgctgaa gcgcgcacgg 720

caagaggcga ggggcggcga ctggtgagta cgccaaaaat tttgactagc ggaggctaga 780

aggagagaga tgggtgcgag agcgtcagta ttaagcgggg gagaattaga tcgcgatggg 840

aaaaaattcg gttaaggcca gggggaaaga aaaaatataa attaaaacat atagtatggg 900

caagcaggga gctagaacga ttcgcagtta atcctggcct gttagaaaca tcagaaggct 960

gtagacaaat actgggacag ctacaaccat cccttcagac aggatcagaa gaacttagat 1020

cattatataa tacagtagca accctctatt gtgtgcatca aaggatagag ataaaagaca 1080

ccaaggaagc tttagacaag atagaggaag agcaaaacaa aagtaagacc accgcacagc 1140

aagcggccgg ccgctgatct tcagacctgg aggaggagat atgagggaca attggagaag 1200

tgaattatat aaatataaag tagtaaaaat tgaaccatta ggagtagcac ccaccaaggc 1260

-continued

aaagagaaga gtggtgcaga gagaaaaaag agcagtggga ataggagctt tgttccttgg 1320

gttcttggga gcagcaggaa gcactatggg cgcagcgtca atgacgctga cggtacaggc 1380

cagacaatta ttgtctggta tagtgcagca gcagaacaat ttgctgaggg ctattgaggc 1440

gcaacagcat ctgttgcaac tcacagtctg gggcatcaag cagctccagg caagaatcct 1500

ggctgtggaa agatacctaa aggatcaaca gctcctgggg atttggggtt gctctggaaa 1560

actcatttgc accactgctg tgccttggaa tgctagttgg agtaataaat ctctggaaca 1620

gatttggaat cacacgacct ggatggagtg ggacagagaa attaacaatt acacaagctt 1680

aatacactcc ttaattgaag aatcgcaaaa ccagcaagaa aagaatgaac aagaattatt 1740

ggaattagat aaatgggcaa gtttgtggaa ttggtttaac ataacaaatt ggctgtggta 1800

tataaaatta ttcataatga tagtaggagg cttggtaggt ttaagaatag tttttgctgt 1860

actttctata gtgaatagag ttaggcaggg atattcacca ttatcgtttc agacccacct 1920

cccaaccccg aggggacccg acaggcccga aggaatagaa gaagaaggtg gagagagaga 1980

cagagacaga tccattcgat tagtgaacgg atctcgacgg tatcgccttt aaaagaaaag 2040

gggggattgg ggggtacagt gcaggggaaa gaatagtaga cataatagca acagacatac 2100

aaactaaaga actacaaaaa caaattacaa aaattcaaaa ttttcgggtt tattacaggg 2160

acagcagaga tccagtttat cgacttaact tgtttattgc agcttataat ggttacaaat 2220

aaggcaatag catcacaaat ttcacaaata aggcattttt ttcactgcat tctagttttg 2280

gtttgtccaa actcatcaat gtatcttatc atgtctggat ctcaaatccc tcggaagctg 2340

cgcctgtctt aggttggagt gatacatttt tatcactttt acccgtcttt ggattaggca 2400

gtagctctga cggccctcct gtcttaggtt agtgaaaaat gtcactctct tacccgtcat 2460

tggctgtcca gcttagctcg caggggaggt ggtctggatc cgccggcacc ggtgatcagt 2520

tatctagact aaaccacttt gtacaagaaa gctgaacgag aaacgtaaaa tgatataaat 2580

atcaatatat taaattagat tttgcataaa aaacagacta cataatactg taaaacacaa 2640

catatccagt cactatgaat caactactta gatggtatta gtgacctgta gtcgactaag 2700

ttggcagcat cacccgacgc actttgcgcc gaataaatac ctgtgacgga agatcacttc 2760

gcagaataaa taaatcctgg tgtccctgtt gataccggga agccctgggc caacttttgg 2820

cgaaaatgag acgttgatcg gcacgtaaga ggttccaact ttcaccataa tgaaataaga 2880

tcactaccgg gcgtattttt tgagttatcg agattttcag gagctaagga agctaaaatg 2940

gagaaaaaaa tcactggata taccaccgtt gatatatccc aatggcatcg taaagaacat 3000

tttgaggcat ttcagtcagt tgctcaatgt acctataacc agaccgttca gctggatatt 3060

acggcctttt taaagaccgt aaagaaaaat aagcacaagt tttatccggc ctttattcac 3120

attcttgccc gcctgatgaa tgctcatccg gaattccgta tggcaatgaa agacggtgag 3180

ctggtgatat gggatagtgt tcacccttgt tacaccgttt tccatgagca aactgaaacg 3240

ttttcatcgc tctggagtga ataccacgac gatttccggc agtttctaca catatattcg 3300

caagatgtgg cgtgttacgg tgaaaacctg gcctatttcc ctaaagggtt tattgagaat 3360

atgtttttcg tctcagccaa tccctgggtg agtttcacca gttttgattt aaacgtggcc 3420

aatatggaca acttcttcgc ccccgttttc accatgggca aatattatac gcaaggcgac 3480

aaggtgctga tgccgctggc gattcaggtt catcatgccg tttgtgatgg cttccatgtc 3540

-continued

ggcagaatgc ttaatgaatt acaacagtac tgcgatgagt ggcaggggcg gcgtaaacgc 3600

cgcgtggatc cggcttacta aaagccagat aacagtatgc gtatttgcgc gctgattttt 3660

gcggtataag aatatatact gatatgtata cccgaagtat gtcaaaaaga ggtatgctat 3720

gaagcagcgt attacagtga cagttgacag cgacagctat cagttgctca aggcatatat 3780

gatgtcaata tctccggtct ggtaagcaca accatgcaga atgaagcccg tcgtctgcgt 3840

gccgaacgct ggaaagcgga aaatcaggaa gggatggctg aggtcgcccg gtttattgaa 3900

atgaacggct cttttgctga cgagaacagg ggctggtgaa atgcagttta aggtttacac 3960

ctataaaaga gagagccgtt atcgtctgtt tgtggatgta cagagtgata ttattgacac 4020

gcccgggcga cggatggtga tccccctggc cagtgcacgt ctgctgtcag ataaagtctc 4080

ccgtgaactt tacccggtgg tgcatatcgg ggatgaaagc tggcgcatga tgaccaccga 4140

tatggccagt gtgccggtct ccgttatcgg ggaagaagtg gctgatctca gccaccgcga 4200

aaatgacatc aaaaacgcca ttaacctgat gttctgggga atataaatgt caggctccct 4260

tatacacagc cagtctgcag gtcgatacag tagaaattac agaaacttta tcacgtttag 4320

taagtataga ggctgaaaat ccagatgaag ccgaacgact tgtaagagaa aagtataaga 4380

gttgtgaaat tgttcttgat gcagatgatt ttcaggacta tgacactagc gtatatgaat 4440

aggtagatgt ttttatttttg tcacacaaaa aagaggctcg cacctctttt tcttatttct 4500

ttttatgatt taatacggca ttgaggacaa tagcgagtag gctggatacg acgattccgt 4560

ttgagaagaa catttggaag gctgtcggtc gactaagttg gcagcatcac ccgaagaaca 4620

tttggaaggc tgtcggtcga ctacaggtca ctaataccat ctaagtagtt gattcatagt 4680

gactggatat gttgtgtttt acagtattat gtagtctgtt ttttatgcaa aatctaattt 4740

aatatattga tatttatatc attttacgtt tctcgttcag ctttttttgta caaacttgtg 4800

gcgccaccgc ctcccttgtc gtcgtcgtcc ttgtagtcga tgtcgtggtc cttgtagtcg 4860

ccgtcgtggt ccttgtagtc catggtggcg gtaccggtgt atacgggaat tctttacgag 4920

ggtaggaagt ggtacggaaa gttggtataa gacaaaagtg ttgtggaatt gaagtttact 4980

caaaaaatca gcactctttt ataggcgccc tggtttacat aagcaaagct tatacgttct 5040

ctatcactga tagggagtaa actggatata cgttctctat cactgatagg gagtaaactg 5100

tagatacgtt ctctatcact gatagggagt aaactggtca tacgttctct atcactgata 5160

gggagtaaac tccttatacg ttctctatca ctgataggga gtaaagtctg catacgttct 5220

ctatcactga tagggagtaa actcttcata cgttctctat cactgatagg gagtaaactc 5280

gaggtgataa ttccacgggg ttggggttgc gccttttcca aggcagccct gggtttgcgc 5340

agggacgcgg ctgctctggg cgtggttccg ggaaacgcag cggcgccgac cctgggtctc 5400

gcacattctt cacgtccgtt cgcagcgtca cccggatctt cgccgctacc cttgtgggcc 5460

ccccggcgac gcttcctgct ccgcccctaa gtcgggaagg ttccttgcgg ttcgcggcgt 5520

gccggacgtg acaaacggaa gccgcacgtc tcactagtac cctcgcagac ggacagcgcc 5580

agggagcaat ggcagcgcgc cgaccgcgat gggctgtggc caatagcggc tgctcagcag 5640

ggcgcgccga gagcagcggc cgggaagggg cggtgcggga ggcggggtgt ggggcggtag 5700

tgtgggccct gttcctgccc gcgcggtgtt ccgcattctg caagcctccg gagcgcacgt 5760

cggcagtcgg ctccctcgtt gaccgaatca ccgacctctc tccccagggg gatcatcgaa 5820

-continued

ttaccatgtc tagactggac aagagcaaag tcataaactc tgctctggaa ttactcaatg 5880

gagtcggtat cgaaggcctg acgacaagga aactcgctca aaagctggga gttgagcagc 5940

ctaccctgta ctggcacgtg aagaacaagc gggccctgct cgatgccctg ccaatcgaga 6000

tgctggacag gcatcatacc cactcctgcc ccctggaagg cgagtcatgg caagactttc 6060

tgcggaacaa cgccaagtca taccgctgtg ctctcctctc acatcgcgac ggggctaaag 6120

tgcatctcgg cacccgccca acagagaaac agtacgaaac cctggaaaat cagctcgcgt 6180

tcctgtgtca gcaaggcttc tccctggaga acgcactgta cgctctgtcc gccgtgggcc 6240

actttacact gggctgcgta ttggaggaac aggagcatca agtagcaaaa gaggaaagag 6300

agacacctac caccgattct atgcccccac ttctgaaaca agcaattgag ctgttcgacc 6360

ggcagggagc cgaacctgcc ttccttttcg gcctggaact aatcatatgt ggcctggaga 6420

aacagctaaa gtgcgaaagc ggcgggccga ccgacgccct tgacgatttt gacttagaca 6480

tgctcccagc cgatgccctt gacgactttg accttgatat gctgcctgct gacgctcttg 6540

acgattttga ccttgacatg ctccccgggt aaacgcgcga atgtgtgtca gttagggtgt 6600

ggaaagtccc caggctcccc agcaggcaga agtatgcaaa gcatgcatct caattagtca 6660

gcaaccaggt gtggaaagtc cccaggctcc ccagcaggca gaagtatgca aagcatgcat 6720

ctcaattagt cagcaaccat agtcccgccc ctaactccgc ccatcccgcc cctaactccg 6780

cccagttccg cccattctcc gccccatggc tgactaattt tttttattta tgcagaggcc 6840

gaggccgcct cggcctctga gctattccag aagtagtgag gaggcttttt tggaggccta 6900

ggcttttgca aaacgcgacc atgaccgagt acaagcccac ggtgcgcctc gccacccgcg 6960

acgacgtccc ccgggccgta cgcaccctcg ccgccgcgtt cgccgactac cccgccacgc 7020

gccacaccgt cgacccggac cgccacatcg agcgggtcac cgagctgcaa gaactcttcc 7080

tcacgcgcgt cgggctcgac atcggcaagg tgtgggtcgc ggacgacggc gccgcggtgg 7140

cggtctggac cacgccggag agcgtcgaag cgggggcggt gttcgccgag atcggcccgc 7200

gcatggccga gttgagcggt tcccggctgg ccgcgcagca acagatggaa ggcctcctgg 7260

cgccgcaccg gcccaaggag cccgcgtggt tcctggccac cgtcggcgtc tcgcccgacc 7320

accagggcaa gggtctgggc agcgccgtcg tgctccccgg agtggaggcg gccgagcgcg 7380

ccggggtgcc cgccttcctg gagacctccg cgccccgcaa cctccccttc tacgagcggc 7440

tcggcttcac cgtcaccgcc gacgtcgagg tgcccgaagg accgcgcacc tggtgcatga 7500

cccgcaagcc cggtgcctga acgcgtctgg aacaatcaac ctctggatta caaaatttgt 7560

gaaagattga ctggtattct taactatgtt gctccttta cgctatgtgg atacgctgct 7620

ttaatgcctt tgtatcatgc tattgcttcc cgtatggctt tcattttctc ctccttgtat 7680

aaatcctggt tgctgtctct ttatgaggag ttgtggcccg ttgtcaggca acgtggcgtg 7740

gtgtgcactg tgtttgctga cgcaaccccc actggttggg gcattgccac cacctgtcag 7800

ctcctttccg ggactttcgc tttccccctc cctattgcca cggcggaact catcgccgcc 7860

tgccttgccc gctgctggac aggggctcgg ctgttgggca ctgacaattc cgtggtgttg 7920

tcggggaagc tgacgtcctt tccatggctg ctcgcctgtg ttgccacctg gattctgcgc 7980

gggacgtcct tctgctacgt cccttcggcc ctcaatccag cggaccttcc ttcccgcggc 8040

ctgctgccgg ctctgcggcc tcttccgcgt cttcgccttc gccctcagac gagtcggatc 8100

-continued

tccctttggg ccgcctcccc gcctggaatt aattctgcag tcgagaccta gaaaaacatg 8160

gagcaatcac aagtagcaat acagcagcta ccaatgctga ttgtgcctgg ctagaagcac 8220

aagaggagga ggaggtgggt ttttccagtc acacctcagg tacctttaag accaatgact 8280

tacaaggcag ctgtagatct tagccacttt ttaaaagaaa agaggggact ggaagggcta 8340

attcactccc aacgaagaca agatatcctt gatctgtgga tctaccacac acaaggctac 8400

ttccctgatt agcagaacta cacaccaggg ccaggggtca gatatccact gacctttgga 8460

tggtgctaca agctagtacc agttgagcca gataaggtag aagaggccaa taaaggagag 8520

aacaccagct tgttacaccc tgtgagcctg catgggatgg atgacccgga gagagaagtg 8580

ttagagtgga ggtttgacag ccgcctagca tttcatcacg tggcccgaga gctgcatccg 8640

gagtacttca agaactgctg atatcgagct tgctacaagg gactttccgc tggggacttt 8700

ccagggaggc gtggcctggg cgggactggg gagtggcgag ccctcagatc ctgcatataa 8760

gcagctgctt tttgcctgta ctgggtctct ctggttagac cagatctgag cctgggagct 8820

ctctggctaa ctagggaacc cactgcttaa gcctcaataa agcttgcctt gagtgcttca 8880

agtagtgtgt gcccgtctgt tgtgtgactc tggtaactag agatccctca gacccttta 8940

gtcagtgtgg aaaatctcta gcagtagtag ttcatgtcat cttattattc agtatttata 9000

acttgcaaag aaatgaatat cagagagtga gaggccttga cattgctagc gttttaccgt 9060

cgacctctag ctagagcttg gcgtaatcat ggtcatagct gtttcctgtg tgaaattgtt 9120

atccgctcac aattccacac aacatacgag ccggaagcat aaagtgtaaa gcctggggtg 9180

cctaatgagt gagctaactc acattaattg cgttgcgctc actgcccgct ttccagtcgg 9240

gaaacctgtc gtgccagctg cattaatgaa tcggccaacg cgcggggaga ggcggtttgc 9300

gtattgggcg ctcttccgct tcctcgctca ctgactcgct gcgctcggtc gttcggctgc 9360

ggcgagcggt atcagctcac tcaaaggcgg taatacggtt atccacagaa tcaggggata 9420

acgcaggaaa gaacatgtga gcaaaaggcc agcaaaaggc caggaaccgt aaaaaggccg 9480

cgttgctggc gtttttccat aggctccgcc cccctgacga gcatcacaaa aatcgacgct 9540

caagtcagag gtggcgaaac ccgacaggac tataaagata ccaggcgttt ccccctggaa 9600

gctccctcgt gcgctctcct gttccgaccc tgccgcttac cggatacctg tccgcctttc 9660

tcccttcggg aagcgtggcg ctttctcata gctcacgctg taggtatctc agttcggtgt 9720

aggtcgttcg ctccaagctg ggctgtgtgc acgaaccccc cgttcagccc gaccgctgcg 9780

ccttatccgg taactatcgt cttgagtcca acccggtaag acacgactta tcgccactgg 9840

cagcagccac tggtaacagg attagcagag cgaggtatgt aggcggtgct acagagttct 9900

tgaagtggtg gcctaactac ggctacacta gaagaacagt atttggtatc tgcgctctgc 9960

tgaagccagt taccttcgga aaaagagttg gtagctcttg atccggcaaa caaaccaccg 10020

ctggtagcgg ttttttttgtt tgcaagcagc agattacgcg cagaaaaaaa ggatctcaag 10080

aagatccttt gatcttttct acggggtctg acgctcagtg gaacgaaaac tcacgttaag 10140

ggattttggt catgagatta tcaaaaagga tcttcaccta gatcctttta aattaaaaat 10200

gaagttttaa atcaatctaa agtatatatg agtaaacttg gtctgacagt taccaatgct 10260

taatcagtga ggcacctatc tcagcgatct gtctatttcg ttcatccata gttgcctgac 10320

tccccgtcgt gtagataact acgatacggg agggcttacc atctggcccc agtgctgcaa 10380

-continued

```
tgataccgcg agacccacgc tcaccggctc cagatttatc agcaataaac cagccagccg  10440

gaagggccga gcgcagaagt ggtcctgcaa ctttatccgc ctccatccag tctattaatt  10500

gttgccggga agctagagta agtagttcgc cagttaatag tttgcgcaac gttgttgcca  10560

ttgctacagg catcgtggtg tcacgctcgt cgtttggtat ggcttcattc agctccggtt  10620

cccaacgatc aaggcgagtt acatgatccc ccatgttgtg caaaaaagcg gttagctcct  10680

tcggtcctcc gatcgttgtc agaagtaagt tggccgcagt gttatcactc atggttatgg  10740

cagcactgca taattctctt actgtcatgc catccgtaag atgcttttct gtgactggtg  10800

agtactcaac caagtcattc tgagaatagt gtatgcggcg accgagttgc tcttgcccgg  10860

cgtcaatacg ggataatacc gcgccacata gcagaacttt aaaagtgctc atcattggaa  10920

aacgttcttc ggggcgaaaa ctctcaagga tcttaccgct gttgagatcc agttcgatgt  10980

aacccactcg tgcacccaac tgatcttcag catcttttac tttcaccagc gtttctgggt  11040

gagcaaaaac aggaaggcaa aatgccgcaa aaaagggaat aagggcgaca cggaaatgtt  11100

gaatactcat actcttcctt tttcaatatt attgaagcat ttatcagggt tattgtctca  11160

tgagcggata catatttgaa tgtatttaga aaaataaaca aatagggtt ccgcgcacat  11220

ttccccgaaa agtgccacct gacgtcgacg gatcgggaga tcaacttgtt tattgcagct  11280

tataatggtt acaaataaag caatagcatc acaaatttca caaataaagc attttttca  11340

ctgcattcta gttgtggttt gtccaaactc atcaatgtat cttatcatgt ctggatcaac  11400

tggataactc aagctaacca aaatcatccc aaacttccca ccccataccc tattaccact  11460

gccaattacc tagtggtttc atttactcta aacctgtgat tcctctgaat tattttcatt  11520

ttaaagaaat tgtatttgtt aaatatgtac tacaaactta gtagttttta aagaaattgt  11580

atttgttaaa tatgtactac aaacttagta gt                                11612
```

1. A method of identifying a subject likely to respond to a hyperproliferative disorder treatment, the method comprising:

(a) compiling genetic data about a population of subjects that has a mutation candidate that causes a hyperproliferative disorder, wherein the population of subjects includes the subject;

(b) performing a mass spectrometry analysis on a sample associated with the hyperproliferative disorder to identify dysfunctional protein-protein interactions associated with the hyperproliferative disorder;

(c) obtaining a first set of rules that define dysfunctional protein-protein interactions as a function of a differential interaction score (DIS);

(c) calculating a differential interaction score (DIS);

(d) correlating the DIS with the likelihood that the dysfunctional protein-protein interaction is a causal agent of the hyperproliferative disorder by evaluating the DIS against the first set of rules, thereby generating a list of one or more causal agents to which a hyperproliferative disorder treatment for the subject should be targeted.

2.-**3**. (canceled)

4. The method of claim **1**, wherein the mass spectrometry analysis is performed on a plurality of samples.

5. (canceled)

6. The method of claim **1**, wherein the calculating comprises calculating one or more of a SAINTexpress algorithm score and a CompPASS algorithm score.

7. The method of claim **6**, wherein the SAINTexpress algorithm score is calculated by a formula:

$$P(X_{ij} \mid ?) = \pi_T P(X_{ij} \mid \lambda_{ij}) + (1 - \pi_T) P(X_{ij} \mid \kappa_{ij})) \quad (1)$$

? indicates text missing or illegible when filed

wherein X_{ij} is the spectral count for a prey protein i identified in a purification of bait j;

wherein λ_{ij} is the mean count from a Poisson distribution representing true interaction;

wherein κ_{ij} is the mean count from a Poisson distribution representing false interaction;

wherein π_T is the proportion of true interactions in the data; and

wherein dot notation represents all relevant model parameters estimated from the data for the pair of prey i and bait j.

8. (canceled)

9. The method of claim **1**, wherein the DIS is calculated by a first formula:

$$DIS_A(b, p) = S_{C1}(b, p) \times S_{C2}(b, p) \times [1 - S_{C3}(b, p)]$$

wherein DIS_A(b,p) is the DIS for each PPI (b, p) that is conserved in a first cell line and a second cell line, but not shared by a third cell line;

wherein S_{C1}(b,p) is the probability of a PPI being present in the first cell line;

wherein S_{C2}(b,p) is the probability of a PPI being present in the second cell line; and

wherein S_{c3}(b,p) is the probability of a PPI being present in the third cell line; and a second formula:

$$DIS_B(b, p) = [1 - S_{C1}(b, p)] \times [1 - S_{C2}(b, p)] \times S_{C3}(b, p$$

wherein DIS_B(b,p) is the DIS score for each PPI (b, p) that is conserved in the third cell line, but not shared by the first cell line and the second cell line;

wherein a (+) sign is assigned if $DIS_A(b,p) > DIS_B(b,p)$; and

wherein a (−) sign is assigned if $DIS_A(b,p) < DIS_B(b,p)$.

10. The method of claim **1**, wherein the DIS is an average of a SAINTexpress algorithm score and a CompPASS algorithm score.

11. The method of claim **1**, wherein the DIS is a SAINTexpress algorithm score.

12. (canceled)

13. The method of claim **1**, wherein a DIS of greater than 0.5 indicates that the dysfunctional protein-protein interaction is likely a causal agent of the hyperproliferative disorder: wherein a DIS of less than 0.5 indicates that the dysfunctional protein-protein interaction is not likely a causal agent of the hyperproliferative disorder.

14. (canceled)

15. The method of claim **1**, wherein the mass spectrometry analysis is performed on a plurality of samples, wherein calculating comprises calculating a SAINTexpress algorithm score for each sample, and averaging the SAINTexpress algorithm scores.

16. The method of claim **1**, wherein the hyperproliferative disorder is a cancer.

17-47. (canceled)

48. A method of identifying a subject likely to respond to a hyperproliferative disorder treatment, the method comprising:

a. calculating a differential interaction score (DIS); and

b. correlating the DIS with a likelihood that a dysfunctional protein-protein interaction is a causal agent of the hyperproliferative disorder,

wherein if the DIS score is above a first threshold, then the subject is likely to respond to a hyperproliferative disorder treatment based upon the causal agent, and

wherein if the DIS score is below the first threshold, then the subject is not likely to respond to the hyperproliferative disorder treatment based upon the causal agent.

49. The method of claim **0**, further comprising:

a. compiling genetic data about a population of subjects comprising the subject, wherein the population of subjects has a mutation candidate that causes the hyperproliferative disorder; and

b. performing a mass spectrometry analysis on a sample associated with the hyperproliferative disorder to identify dysfunctional protein-protein interactions associated with the hyperproliferative disorder.

50. A method of predicting a likelihood that a subject does or does not respond to a hyperproliferative disorder treatment, the method comprising:

a. compiling genetic data about a population of subjects that has a mutation candidate that causes a hyperproliferative disorder, wherein the population of subjects includes the subject;

b. performing a mass spectrometry analysis on a sample associated with the hyperproliferative disorder to identify dysfunctional protein-protein interactions associated with the hyperproliferative disorder;

c. calculating a differential interaction score (DIS);

d. correlating the DIS with the likelihood that the dysfunctional protein-protein interaction is the causal agent of the cancer; and

e. selecting a cancer treatment for the subject based upon the causal agent.

51. The method of claim **50**, further comprising:

(f) comparing the DIS score to a first threshold; and

(g) classifying the subject as being likely to respond to a hyperproliferative disorder treatment,

wherein each of steps (f) and (g) are performed after step (c), and

wherein the first threshold is calculated relative to a first control dataset.

52. A computer program product encoded on a computer-readable storage medium, wherein the computer program product comprises instructions for:

a. performing a mass spectrometry analysis on a sample from a subject that has a mutation candidate that causes a hyperproliferative disorder;

b. identifying dysfunctional protein-protein interactions associated with the hyperproliferative disorder; and

c. calculating a differential interaction score (DIS).

53. The computer program product of claim **52**, further comprising a step of correlating the DIS with the likelihood that the dysfunctional protein-protein interaction is a causal agent of the hyperproliferative disorder.

54. The computer program product of claim **53**, further comprising instructions for selecting a hyperproliferative treatment for the subject based upon the causal agent.

55. The computer program product of claim **52**, further comprising instructions for:

(d) comparing the DIS score to a first threshold; and

(e) classifying the subject as being likely to respond to a hyperproliferative disorder treatment,

wherein each of steps (d) and (e) are performed after step (c), and

wherein the first threshold is calculated relative to a first control dataset.

56. A system comprising the computer program product of any of claims **52** through **55**, and one or more of:

a. a processor operable to execute programs; and

b. a memory associated with the processor.

57.-61. (canceled)

62. A method of selecting a hyperproliferative disorder treatment for a subject in need thereof, the method comprising:

a. identifying genetic data from the subject in need of treatment;

b. comparing the genetic data from the subject to a compilation of genetic data from population of subjects that has a mutation candidate that causes a hyperproliferative disorder, wherein the population of subjects includes the subject in need thereof;

c. performing a mass spectrometry analysis on a sample from the subject associated with the hyperproliferative disorder to identify dysfunctional protein-protein interactions associated with the hyperproliferative disorder;

d. calculating a differential interaction score (DIS);

e. correlating the DIS with the likelihood that the dysfunctional protein-protein interaction is a causal agent of the hyperproliferative disorder; and

f. selecting a hyperproliferative disorder treatment for the subject based upon the causal agent.

63-65. (canceled)

* * * * *